PLASTIC POLLUTION

EDITED BY: François Galgani, Christopher K. Pham and Julia Reisser
PUBLISHED IN: Frontiers in Marine Science and Frontiers in Environmental Science

frontiers Research Topics

ISSN 1664-8714
ISBN 978-2-88945-330-6
DOI 10.3389/978-2-88945-330-6

About Frontiers

Frontiers is more than just an open-access publisher of scholarly articles: it is a pioneering approach to the world of academia, radically improving the way scholarly research is managed. The grand vision of Frontiers is a world where all people have an equal opportunity to seek, share and generate knowledge. Frontiers provides immediate and permanent online open access to all its publications, but this alone is not enough to realize our grand goals.

Frontiers Journal Series

The Frontiers Journal Series is a multi-tier and interdisciplinary set of open-access, online journals, promising a paradigm shift from the current review, selection and dissemination processes in academic publishing. All Frontiers journals are driven by researchers for researchers; therefore, they constitute a service to the scholarly community. At the same time, the Frontiers Journal Series operates on a revolutionary invention, the tiered publishing system, initially addressing specific communities of scholars, and gradually climbing up to broader public understanding, thus serving the interests of the lay society, too.

Dedication to Quality

Each Frontiers article is a landmark of the highest quality, thanks to genuinely collaborative interactions between authors and review editors, who include some of the world's best academicians. Research must be certified by peers before entering a stream of knowledge that may eventually reach the public - and shape society; therefore, Frontiers only applies the most rigorous and unbiased reviews.
Frontiers revolutionizes research publishing by freely delivering the most outstanding research, evaluated with no bias from both the academic and social point of view.
By applying the most advanced information technologies, Frontiers is catapulting scholarly publishing into a new generation.

What are Frontiers Research Topics?

Frontiers Research Topics are very popular trademarks of the Frontiers Journals Series: they are collections of at least ten articles, all centered on a particular subject. With their unique mix of varied contributions from Original Research to Review Articles, Frontiers Research Topics unify the most influential researchers, the latest key findings and historical advances in a hot research area! Find out more on how to host your own Frontiers Research Topic or contribute to one as an author by contacting the Frontiers Editorial Office: **researchtopics@frontiersin.org**

PLASTIC POLLUTION

Topic Editors:
François Galgani, French Research Institute for Exploitation of the Sea, France
Christopher K. Pham, University of the Azores, Portugal
Julia Reisser, The Ocean Cleanup, Netherlands

Lollipop sticks mixed after sampling a 100m long beach along the Seine estuary, France.

Image: L. Colasse.

The presence, at sea, of large amounts of plastic and microplastics, which are sometimes invisible and results from the fragmentation of larger debris, requires an in-depth knowledge of the nature of ocean debris, its transport mechanisms, life cycle and effects on the environment. This volume provides new insights in the topic of plastic pollution, an actual and important problem for the marine environment..

Citation: Galgani, F., Pham, C. K., Reisser, J., eds. (2017). Plastic Pollution. Lausanne: Frontiers Media. doi: 10.3389/978-2-88945-330-6

Table of Contents

frontiers in Marine Science

EDITORIAL
published: 22 September 2017
doi: 10.3389/fmars.2017.00307

Editorial: Plastic Pollution

François Galgani[1]*, *Christopher Kim Pham*[2] *and Julia Reisser*[3]

[1] French Research Institute for Exploitation of the Sea, Issy-les-Moulineaux, France, [2] Marine and Environmental Sciences Centre (MARE) and Institute of Marine Research (IMAR), University of the Azores, Horta, Portugal, [3] The Ocean Cleanup, Delft, Netherlands

Keywords: plastic, pollution, models, microplastics, degradation

Editorial on the Research Topic

Plastic Pollution

Our socioeconomic development models have led to an increased production of consumer goods of every type, facilitated by the petrochemical industry's ability to provide a range of cheap materials that are continuously becoming more varied. Introduced in the 1950s, plastics have continued to evolve for many purposes, and are currently used in all industrial sectors. A noteworthy application is packaging, which currently uses around 30–40% of the exponentially growing annual plastic production.

Plastics are a diverse group of synthetic materials composed of polymers (from the Greek poly = many, and meros = parts) predominantly derived from petrochemicals, such as petroleum and natural gas. Polyethylene, polypropylene, polystyrene, polycarbonates and polyamides, are all plastics manufactured from monomers with different chemical characteristics. They possess different properties (color, form, hardness, thickness, and degradability), which impart various fates once discarded in the environment. Unfortunately, some of the main plastic qualities sought by industry and consumers—lightness and resistance to degradation—are also leading to their negative impacts and persistence in natural habitats.

Marine litter is any directly or indirectly manufactured item thrown or abandoned voluntarily or involuntarily into the marine environment. It is well known that plastic is the main contributor to the growing amounts of litter accumulating in the world's oceans. Nonetheless, the marine plastic pollution research field is quite new, and more information about the nature, sources, transport, distribution and environmental effects of plastics is necessary for a better understanding of their biogeochemical cycles. Various studies have reported the existence of small plastic particles in pelagic and benthic environments that are often invisible to the naked eye. They are commonly referred to as "microplastics" (<5 mm) and can either be microparticles already manufactured in such small sizes or, more commonly, result from the fragmentation of larger plastic objects. The environmental implications of their presence at sea are still largely unknown.

Identifying sources and sinks of marine plastics can be difficult because pollution sources on land and at sea are often unknown and plastic particle transport and aging processes are highly dynamic and complex. Nonetheless, recent research suggest major sources are coastlines, rivers (Lebreton et al., 2017), and maritime (e.g., fishing) activities, with the presence of plastic accumulation zones being present in seafloor environments (Pham et al., 2014), beaches (Lavers and Bond, 2017), and surface waters of subtropical (Eriksen et al., 2014), Mediterranean (Cozar et al., 2015) and Arctic waters (Cozar et al., 2017). Over the past 15 years, plastic impacts in the seas have increased (Galgani, 2014), and the number of marine species known to be affected by this contaminant has gone from 247 to 680 (Gall and Thompson, 2015). A substantial portion of these impacts involves entanglement in fishing equipment and ingestion of debris, and occurs mainly in developing regions. The interaction of litter with marine organisms has been used as an approach to better map some of the risks (Wilcox et al., 2015; Darmon et al., 2017). The alteration of ecosystems caused by the transport of species over long distances also represents a major problem.

OPEN ACCESS

Edited by:
Hans Uwe Dahms,
Kaohsiung Medical University, Taiwan

Reviewed by:
Xiaoshou Liu,
Ocean University of China, China
Rodrigo Riera,
Atlantic Environmental Marine Center (CIMA SL), Spain

***Correspondence:**
François Galgani
Francois.Galgani@ifremer.fr

Specialty section:
This article was submitted to Marine Pollution, a section of the journal Frontiers in Marine Science

Received: *12 July 2017*
Accepted: *07 September 2017*
Published: *22 September 2017*

Citation:
Galgani F, Pham CK and Reisser J (2017) Editorial: Plastic Pollution. Front. Mar. Sci. 4:307. doi: 10.3389/fmars.2017.00307

Although there is mounting evidence that plastic pollution act as an important stressor for many marine organisms, we do not know how this is affecting the overall functioning of marine ecosystems and the services they provide. This research topic contributes to a better understanding of this type of marine contamination by presenting articles reporting observations and transport models of debris in the Adriatic Sea, Western Australian waters, Great Lakes, North West European seas, and Aegean Sea. There are also studies describing findings from (1) a statistical model that predicts areas of plastic accumulation in the Mediterranean, (2) a 6 months experiment that simulates the generation of microplastics from the fragmentation of Polyethylene films on beaches and at sea, (3) a review of transport models for marine plastics, and (4) models predicting the overlap between fin whales and plastic debris in a marine protected area.

AUTHOR CONTRIBUTIONS

All authors listed have made a substantial, direct and intellectual contribution to the work, and approved it for publication.

REFERENCES

Cozar, A., Martí, E., Duarte, C. M., García-de-Lomas, J., van Sebille, E., Ballatore, T. J., et al., (2017). The Arctic Ocean as a dead end for floating plastics in the North Atlantic branch of the Thermohaline Circulation. *Sci. Adv.* 3:e1600582. doi: 10.1126/sciadv.1600582

Cozar, A., Sanz-Martín, M., Martí E., González-Gordillo, J. I., Bárbara U., Gálvez, J. A., et al. (2015). Plastic Accumulation in the Mediterranean Sea. *PLoS ONE.* 10:e121762 doi: 10.1371/journal.pone.0121762

Darmon, G., Miaud, C., Claro, F., Doremus, G., and Galgani, F., (2017). Risk assessment reveals high exposure of sea turtles to marine debris in French Mediterranean and metropolitan Atlantic waters. *Deep Sea Res. II Top. Stud. Oceanogr.* 41, 319–328. doi: 10.1016/j.dsr2.2016.07.005

Eriksen, M., Lebreton, L. M., Carson, H. S., Thiel, M., Moore, C., Borerro, J. C., et al. (2014). Plastic pollution in the world's oceans: more than 5 trillion plastic pieces weighing over 250,000 tons afloat at sea. *PLOS ONE* 9:e111913. doi: 10.1371/journal.pone.0111913

Galgani, F. (2014). "Pollution by marine debris," in *Sea and Oceans, Book 3, The Land-Sea Interactions, ISTE Edition,* eds A. Monaco and P. Prouzet (HERMES Penton Publishing Ltd.), 195–236.

Gall, S. C., and Thompson, R. C. (2015). The impact of debris on marine life. *Mar. Pollut. Bull.* 92, 170–179. doi: 10.1016/j.marpolbul.2014.12.041

Lavers, J. L., and Bond, A. L. (2017). Exceptional and rapid accumulation of anthropogenic debris on one of the world's most remote and pristine islands. *Proc. Natl. Acad. Sci U.S.A.* 114, 6052–6055. doi: 10.1073/pnas.1619818114

Lebreton, L., van der Zwet, J., Damsteeg, J., Slat, B., Andrady, A., and Reisser, J. (2017). River plastic emissions to the World's Oceans. *Nat. Commun.* 8:15611. doi: 10.1038/ncomms15611

Pham, C. K., Ramirez-Llodra, E., Alt, C. H. S., Amaro, T., Bergmann, M., Canals, M., et al. (2014). Marine litter distribution and density in European Seas, from the shelves to deep basins. *PLoS ONE* 9:e95839. doi: 10.1371/journal.pone.0095839

Wilcox, C., Van Sebille, E., and Hardesty, B. D. (2015). Plastic pollution to seabirds is global, pervasive, and increasing. *Proc. Natl. Acad. Sci U.S.A.* 112, 11899–11904. doi: 10.1073/pnas.1502108112

Conflict of Interest Statement: The authors declare that the research was conducted in the absence of any commercial or financial relationships that could be construed as a potential conflict of interest.

frontiers in Marine Science

ORIGINAL RESEARCH
published: 26 May 2017
doi: 10.3389/fmars.2017.00135

Microplastics Baseline Surveys at the Water Surface and in Sediments of the North-East Atlantic

Thomas Maes[1,2], Myra D. Van der Meulen[3], Lisa I. Devriese[4], Heather A. Leslie[2], Arnaud Huvet[5], Laura Frère[6], Johan Robbens[4] and A. Dick Vethaak[3]*

[1] Lowestoft Laboratory, The Centre for the Environment, Fisheries and Aquaculture Science, Lowestoft, UK, [2] Department of Environment and Health, VU Amsterdam, Amsterdam, Netherlands, [3] Marine and Coastal Systems, Deltares, Delft, Netherlands, [4] Animal Science Unit—Aquatic Environment and Quality, Institute for Agricultural and Fisheries Research, Oostende, Belgium, [5] Ifremer, LEMAR UMR 6539 UBO-Centre National de la Recherche Scientifique-IRD-Ifremer, Plouzane, France, [6] Centre National de la Recherche Scientifique-Institute of Ecology and the Environment, Plouzane, France

Microplastic contamination was determined in sediments of the Southern North Sea and floating at the sea surface of North West Europe. Floating concentrations ranged between 0 and 1.5 microplastic/m^3, whereas microplastic concentrations in sediments ranged between 0 and 3,146 particles/kg dry weight sediment. In sediments, mainly fibers and spheres were found, whereas at the sea surface fragments were dominant. At the sea surface, concentrations of microplastics are lower and more variable than in sediments, meaning that larger sample sizes and water volumes are required to find detectable concentrations. We have calculated the widths of the confidence intervals (CI) for different sample sizes, to give a first indication of the necessary sample size for a microplastic survey at the water surface. Higher concentrations of floating microplastics were found near estuaries. In sediments, estuaries and areas with a high organic carbon content were likely hotspots. Standardization of monitoring methods within marine regions is recommended to compare and assess microplastics pollution over time.

Keywords: microplastics, marine litter, floating debris, sediment, Marine Strategy Framework Directive (MSFD), baseline

OPEN ACCESS

Edited by:
Julia Reisser, The Ocean Cleanup, Netherlands

Reviewed by:
Christos Ioakeimidis, United Nations Environment Programme Mediterranean Action Plan (UNEP/MAP), Greece
André Ricardo de Araújo Lima, Federal University of Pernambuco, Brazil

****Correspondence:***
Thomas Maes
thomas.maes@cefas.co.uk

Specialty section:
This article was submitted to Marine Pollution, a section of the journal Frontiers in Marine Science

Received: *01 February 2017*
Accepted: *24 April 2017*
Published: *26 May 2017*

Citation:
Maes T, Van der Meulen MD, Devriese LI, Leslie HA, Huvet A, Frère L, Robbens J and Vethaak AD (2017) Microplastics Baseline Surveys at the Water Surface and in Sediments of the North-East Atlantic. Front. Mar. Sci. 4:135. doi: 10.3389/fmars.2017.00135

INTRODUCTION

Marine litter accumulating in the marine environment may be one of the greatest threats facing the planet. The exact quantity of plastic in the ocean and volumes entering the ocean from waste generated on land is unknown. Recent studies estimate that 275 million metric tons (MT) of plastic waste was generated in 192 coastal countries in 2010, of which 4.8–12.7 million MT could have entered the ocean (Jambeck et al., 2015). It has been estimated there are 5.25 trillion pieces of plastic debris in the ocean, of that mass, 269,000-ton float on the sea surface (Cózar et al., 2014; Eriksen et al., 2014; van Sebille et al., 2015). Due to UV radiation and mechanical forces, this plastic slowly break down into smaller and smaller fragments below 5 mm, also known as microplastics (GESAMP, 2015). The origin of these fragments can be broken down fishing nets or lines, plastic films and bottles, remains of oxo-biodegradable plastic, industrial raw material like pellets, but also synthetic fibers from textiles as a result of washing clothes or other particular direct sources of microplastics, for example facial cleansers (Derraik, 2002; Arthur et al., 2009; Barnes et al., 2009; Fendall and Sewell, 2009; Browne et al., 2011; Leslie et al., 2011). In Norway, they found that

abrasion from tires and roadmarking was the biggest source of microplastics, followed by dust and particles from plastic based paint (Sundt et al., 2014). Next to breakdown, city storm water effluent and road runoff could thus be another major pathway for microplastics (Eriksen et al., 2013a; McCormick et al., 2014). Some of these microplastics will escape water treatment (Cheung and Fok, 2016) and can be transported via rivers downstream to estuaries and the marine environment (Moore et al., 2011; Lechner et al., 2014; Lima et al., 2014; Rech et al., 2014). In Brazil, the highest amount of microplastics was observed during the late rainy season, when the environment is under influence of the highest river flow, which induces the runoff of plastic fragments to the lower estuary (Lima et al., 2014). Microplastic fibers can even be deposited by atmospheric fallout (Dris et al., 2016).

A large proportion of plastics normally float on the surface being less dense than seawater, however the buoyancy and density of plastics depend on polymer type and may change during their residence at sea due to weathering and biofouling and therefore spread across surface, water column and sediments (Ye and Andrady, 1991; Morishige et al., 2007). Recent studies have demonstrated that pollution of microplastics, particles <5 mm, has spread at the surface of oceans, in the water column and in sediments, even in the deep sea (Woodall et al., 2014). Concentrations at the water surface range from thousands to hundred thousand of particles km^{-2}. Because of their size microplastics are available to a broad range of organisms and have already been shown to be ingested by several species (Cole et al., 2011). The ingestion of microplastics by species at the base of the food web causes human food safety concerns as little is known about their effects and transfer across trophic levels (Vethaak and Leslie, 2016). Moreover, plastics can leach toxic additives and accumulate persistent organic pollutants (POPs) while residing in the marine environment. Some of these POPs are known to have endocrine disruptive and carcinogenic effects (Rios Mendoza and Jones, 2015). Furthermore, plastic particles create habitats for micro-organisms and other species, allowing potential invasive species to transfer to new areas of the ocean (Gregory, 2009; Keswani et al., 2016).

International attention is focusing more and more on the problem of marine litter, including microplastics. In Europe, marine litter and microplastics are included in the Marine Strategy Framework Directive (MSFD), specific information in relation to trends in the amount, distribution and, where possible, composition of micro-particles (in particular microplastics) is requested (criterion 10.1.3 of the MSFD; Galgani et al., 2013). There are several other actions and measures directly related to microplastics and their sources e.g., microbead bans and thus baseline studies are urgently needed to produce appropriate regional baselines to monitor future amounts of microplastics and follow progress of action plans and where required assess potential impacts on the marine environment (Galgani et al., 2014).

This study presents the outcomes of two baseline studies, looking at microplastics in sediments of the Southern North Sea and floating at the water surface in seas of North West Europe. Samples from the surface layers of the North Sea, Irish Sea, Celtic Sea, and Channel Area were analyzed and compared with sediment samples in approximately the same region. Even though sampling locations do not overlap exactly in terms of spatio-temporal scale, it is the first study in the North Sea region in which results from both matrices are compared. Since sediment is thought to be a sink (Morét-Ferguson et al., 2010; Foekema et al., 2013; Van Cauwenberghe et al., 2013; Cózar et al., 2014) for microplastics, research on the occurrence and relationship between floating and deposited microplastics is paramount in understanding the physical processes acting on plastic particles and predicting hotspots for monitoring and clean-up (Gago et al., 2016).

MATERIALS AND METHODS

Sediment

Sampling took place on the Dutch continental shelf in 2014; on the Belgian continental shelf in 2013 and 2014; in the North Sea and English Channel area of the UK in 2013 and 2014 (**Figure 1**); and in the French part of the English Channel in 2014. In total, 27 locations were sampled (**Table 1**). The sample size differed per country; the UK had the smallest number of sampling stations (4 stations), whereas the Netherlands had the highest number of stations (11 stations).

Sediment samples were collected from shallow (wadable) locations using a scoop (FR) and from deeper locations with a van Veen grab (NL, BE, UK). At those deeper locations, three sediment grabs were taken from which the upper 5 cm layer of sediment was collected and pooled into one sample. Samples were collected in 1l glass jars with plastic lids and cooled (4°C). Any visible biota was removed. Upon arrival on shore, samples were frozen at −20°C until further analysis.

Samples were analyzed by the Institute for Environmental Studies (Amsterdam, the Netherlands). Sediment samples were thawed and homogenized, subsamples were taken for microplastic analysis and determination of dry weight. To extract microplastics from sediments, a modified method of Thompson et al. (2004) was followed. The sediment (25 g) was added to an Erlenmeyer with MilliQ water and a saturated NaCl solution (1.2 kg/L). The suspension was stirred for 2 min using a Teflon stirrer at the bottom of the Erlenmeyer flask. This allowed the sample material to suspend and enabled density separation of the sediment and particle material. Post-stirring, the suspension was left for 1 h, allowing the heavier sediment particles to sink while the lighter particles start to float on the saturated salt solution. The suspension was filtered over a 0.7 µm Whatman GF/C glass filter, followed by a rinsing step with hydrogen peroxide (30%) to remove any residual organic material. Alongside each batch of samples, two blanks, and two duplicate analyses were performed. The filters were examined using light microscopy and measured the length of the particles with MicroCamLab for Microsoft. Microplastics were counted and corrected for background levels determined by the blank samples. The dry weight of the sediments was determined gravimetrically after freeze-drying a 5 g subsample of the homogenized sample until a constant weight was observed. Microplastic concentrations were expressed as number of particles per kg of dry sediment and

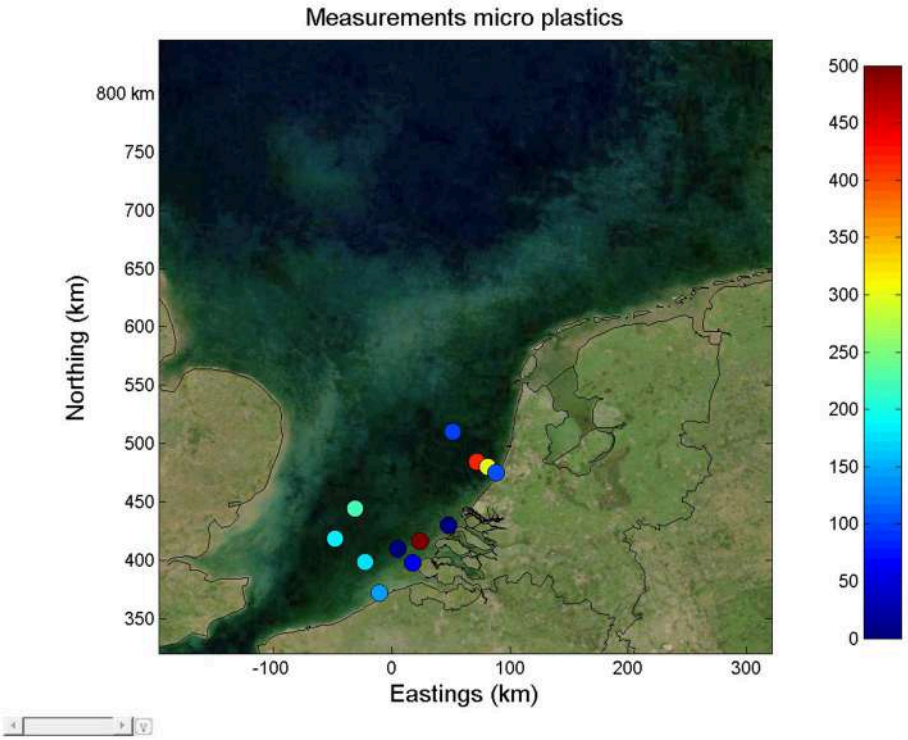

FIGURE 1 | Visual representation of amounts of microplastic particles found per location/kg dry weight sediment.

sorted into three categories "fibers/kg DW," "spheres/kg DW," and "fragments/kg DW."

Sediment organic matter or total organic carbon (TOC) on the upper layer sediment was measured using the "dichromate method" (Mebius, 1960). Carbonate content was measured on the same sediment fraction as "loss on ignition" (Dean, 1974). Grain size distribution was calculated using laser diffraction particle sizing. All samples were analyzed by means of a Malvern Mastersizer 2000G hydro version 5.40 (ISO 13320:2009)[1]. Grain size fractions were determined as volume percentages according to the Wentworth scale (Wentworth, 1922): clay (<4 μm), silt (4–63 μm), very fine sand (63–125 μm), fine sand (125–250 μm), medium sand (250–500 μm), coarse sand (500–1000 μm), very coarse sand (1–2 mm), and gravel (>2 mm). Throughout this study, the clay and silt fractions have been combined as clay/silt (<63 microns).

Sea Surface

Floating microplastic sampling was carried out during existing fisheries surveys in the UK Channel, North, and Celtic Sea area from January to March 2011 (**Figure 5**). Samples were collected from surface waters in between fisheries stations using a high-speed manta trawl with a rectangular opening 50 cm high by 15.5 cm wide, and a 4.5 m long 333 μm net with a 30 × 10 cm cylindrical collecting bag. Collection took place in winter time, when low biomass facilitated sampling, during the following three Cefas cruises: Cend3/11, Cend4/11, and Cend5/11 (**Table 3**). In the Atlantic Ocean the water flow is predominantly from west to east driven by the northern and southern branches of the North Atlantic Drift. In the shelf areas currents are predominately generated by tides and wind, but the main water flow is from south to north (Pollard et al., 1996). The sea state on the Beaufort Scale remained between 1 and 3 for all sample sites. Water surface samples were only collected during calm sea conditions with wave heights below 50 cm.

The sampled transects were not equidistant, but sampling periods were each 60 min long. Coordinates of start and stop positions were registered, along with the number of rotations of the flow meter inside the lower part of the mouth of the manta trawl. The area sampled was calculated firstly by calculating the distance between start and stop coordinates and secondly by using the onboard knotmeter, which takes into account the ground speed and measures the number of nautical miles traveled over a defined distance, to measure the actual length of sea surface trawled in the 60-min period. These tow lengths multiplied by the width of the trawl mouth provided the area sampled, allowing for the particle abundance per square kilometer to be calculated in two different ways. Next to this, we also calculated the total number of particles by volume sampled as indicated by the flowmeter. The lower part of the manta trawl opening was fitted with a GO environmental flowmeter (http://cce.lternet.edu/docs/data/methods/M2-1314e%20Mechanical%20flowmeter.pdf) with a standard speed rotor constant of 26,873 and 1 rotor revolution equaling 10 counts.

[1]https://www.iso.org/standard/44929.html

TABLE 1 | Overview of sampling details and number of microplastic particles at each location.

Location number	Country	Location name	IVM LIMS code	Latitude	Longitude	Sampling year	Total MPs/kg dry weight sediment
1	BE	MIC 1	14/0030	51°17.944	002°50.004	2013	252
2	BE	MIC 1	14/0031	51°17.944	002°50.004	2013	110
3	BE	MIC 3	14/0032	51°26.400	002°35.500	2013	54
4	BE	MIC 1	14/0562	51°17.944	002°50.004	2014	59
5	BE	WO2	14/0563			2014	330
6	BE	830	14/0564	51°42.54	2°27.03	2014	146
7	BE	OO harbor	14/0565	51°14.277	2°54.415	2014	3,146
8	UK	CSEMP475	14/0014	52.00	2.33	2013	0
9	UK	CSEMP536	14/0015	50.43	–3.12	2013	348
10	UK	CSEMP484	14/0016	50.97	1.03	2013	643
11	UK	CSEMP466	14/0017	51.50	1.00	2013	233
12	NL	NOORDWK70	14/1180	052°34′10.00″	003°31′53.00″	2014	96
13	NL	NOORDWK20	14/1179	052°20′30.00″	004°10′30.00″	2014	418
14	NL	NOORDWK10	14/1178	052°18′08.00″	004°18′09.00″	2014	301
15	NL	NOORDWK2	14/1177	052°15′41.00″	004°24′22.00″	2014	109
16	NL	GOERE2	14/1174	051°50′49.00″	003°50′05.00″	2014	0
17	NL	SCHOUWN10	14/1173	51,950	2,667	2014	176
18	NL	WALCRN70	14/1172	051°57′25.00″	002°40′45.00″	2014	225
19	NL	WALCRN20	14/1171	051°39′31.00″	003°13′14.00″	2014	0
20	NL	WALCRN2	14/1170	051°32′56.00″	003°24′39.00″	2014	62
21	NL	LOSWLN	14/1175			2014	499
22	NL	TERHEIJ2	14/1176	52,052	4,160	2014	561
23	FR	BR 3	14/0525	N 48°37′47.56	O 003°50′51.79	2014	194
24	FR	BR 4	14/0526	N 48°46′51.60	O 003°00′46.69	2014	138
25	FR	BR 5	14/0527	N 48°30′09.19	O 002°40′47.43	2014	140
26	FR	BR 6	14/0528	N 48°36′18.49	O 002°01′51.08	2014	425
27	FR	BR 7	14/0529	N 48°40′02.14	O 001°51′41.22	2014	1,509

The trawled distance in meters equals the count between rotation numbers multiplied by 26,873 divided by 999,999. Marks were made on the side of the high speed mantatrawl to visually estimate the depth of the opening during transects. The sample surface of the net is 15.5 by 50 cm but for the majority of the duration of the transects the net was only half submerged while operating as a result of the repetitive wave oscillation. Based on these observations, the net surface was calculated as 0.155 by 0.25 m. These assumptions allowed us to calculate the measured volume in cubic meters by multiplying the sample surface of the net in meters by the trawled distance obtained by the calculations above.

The manta net was rinsed from the outside with a hose to concentrate the sample in the cod end. The cod end was removed over a bucket, to prevent any spillage and the sample was transferred into a large bowl. The cod end was inverted and washed out from the outside using very little water. Leftovers were gently removed by using a long metal spoon which was rinsed into the bowl. Samples were put into a glass container and preserved in 10% formalin. A yellow waterproof label with the trawl number, date, and time was included in all containers. The lids were covered with aluminum foil and the lids labeled again with a waterproof marker from the outside of the sample container.

In the laboratory, samples were rinsed with filtered, distilled water and large floating plastic items were removed. The remaining items were separated on sieves in six size classes and stored in isopropyl alcohol. Size classes above 4.75 mm were hand picked out the sieve and the smaller fractions (>4.75) were sieved over five more sieves to retain ever smaller fractions (0.355–0.499, 0.500–0.709, 0.710–0.999, 1.00–2.79, 2.800–4.749 mm). The fractions were removed by gentle washing of the sieves and concentrated in Petri dishes. A dissecting microscope was used to sort through the remaining debris and organic material. Debris was sorted by category (plastics, non-plastics, plankton, and miscellaneous) and plastics were further categorized and counted (fragment, pellet, line, film, and foam). These size classes were then sorted and quantified into shape type (fragment, pellet, line, film, and foam). The color of each piece of plastic was also recorded (by size class) (BLACK/GRAY, BLUE/GREEN, BROWN/TAN, ORANGE/PINK/RED, TRANSPARENT/TRANSLUCENT, WHITE, YELLOW). Plastic, plankton, and plant material were weighed, then oven dried at 65°C for 24 h and weighed again. The selection of sieve sizes, plastic shapes, and color categories

was based on available literature and existing studies (Moore et al., 2005, 2011; Eriksen et al., 2013b).

Data Analysis

The statistical analysis and strength of correlations in the sediment microplastic data were calculated with a 2-tailed Pearson Correlation in SPSS (version 22). We analyzed the floating microplastic data and calculated the widths of CI for different sample sizes using the R package. The graphical representation of the sediment and floating data was produced with Microsoft Excel (2010), except for the histograms which were produced in R.

RESULTS

Sediment Samples

At all stations, apart from UK station (No. 74) and two Dutch station (No. 16 and 19), microplastic particles were found in the sediment. Both the highest and lowest number of microplastics were found in samples from Belgium, respectively at location 3 with 54 particles/kg DW sediment and location 7 with 3,146 particles/kg DW sediment. The overall average amount found across all areas was 421 particles/kg DW sediment. Remarkably, no plastic fragments, only spheres and fibers were observed at any of the locations. Furthermore, the amount of spheres/kg DW of sediment was higher on average across all stations compared to the amount of fibers.

The average amount of fibers/kg DW was the lowest (99 fibers) in the Dutch coastal sediment samples, whereas the highest average amount of fibers/kg DW was found in coastal sediment samples from Belgium (301 fibers). The sediment samples from the French coast of the English Channel had the highest amount of spheres/kg DW on average (350 spheres) while the Dutch samples had the lowest (123 spheres) amount of spheres/kg DW. In terms of the average number of total particles/kg DW, the highest amounts were found in marine sediments collected from coastal zones in Belgium (585 particles) and the lowest amounts in coastal zones from the Netherlands (222 particles). The average amounts of plastic particles/kg DW are in the same order of magnitude between the different countries, indicating that there are no marked differences between counties, however, more samples are required to obtain a clearer picture. In terms of percentage of dry weight of the sediment, samples from France had the lowest level (55%), and samples from the Netherlands had the highest level (76%). An overview of the results is given in **Table 2**.

An indication of a relationship between the percentage Total Organic Carbon (TOC) and the number of plastic particles/kg dry sediment ($R^2 = 0.616$, $p = 0.001$), signifies that there are more plastic particles present with higher concentrations of TOC in the sediment (**Figure 2**).

In all samples, an indication of a negative relationship between the median grain size of the sediment and the number

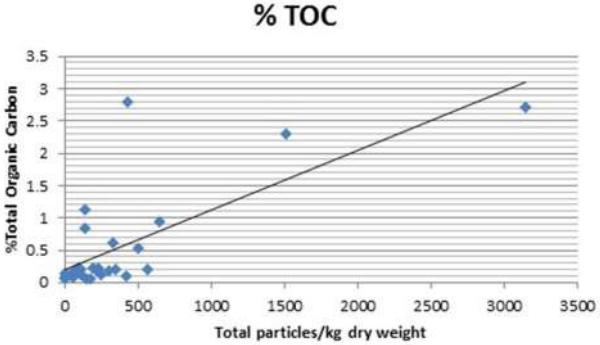

FIGURE 2 | Relationship between Total Organic Carbon (TOC) and the total plastics amount found.

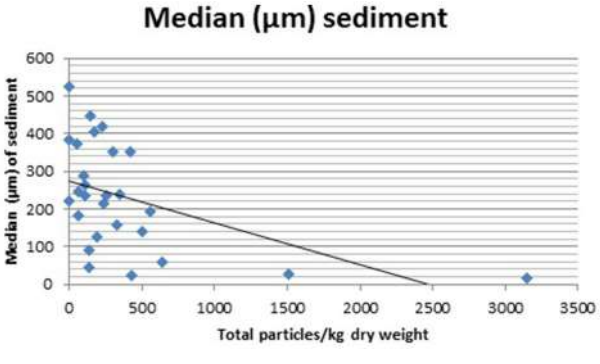

FIGURE 3 | Median size of the sediment grains (in µm) in relation to the total amount of particles found per location/kg dry weight.

TABLE 2 | Average amounts of microplastics found per country in terms of number of samples, average fibers/kg dry weight sediment, average spheres/kg dry weight sediment, average fragments/kg dry weight sediment, average total particles, dry weight (% of wet weight), average median grain size of the sediment.

Country	Number of stations samples	Average fibers/kg dry weight	Average spheres/kg dry weight	Average fragments/kg dry weight	Average total particles	Dw (% of ww)	Average median grain size (µm)
Belgium	7	301 (445)	283 (695)	0	585 (1,114)	69 (21)	245 (140)
France	5	131 (154)	350 (471)	0	481 (587)	55 (13)	62 (45)
Netherlands	11	99 (110)	123 (136)	0	222 (198)	76 (3)	291 (98)
UK	4	121 (144)	185 (150)	0	306 (267)	70 (13)	260 (194)

Values between brackets represent standard deviations.

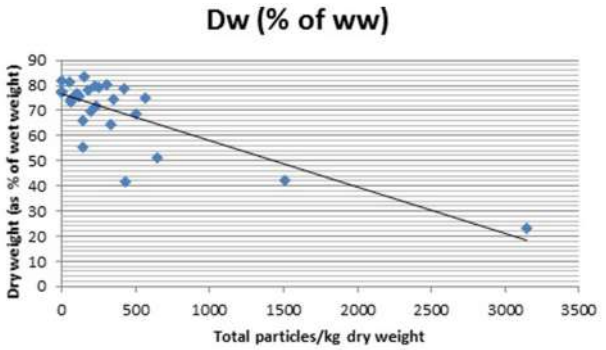

FIGURE 4 | Dry Weight (as % of wet weight) in relation to the total amount of particles found per location/kg dry weight.

TABLE 3 | Selected surveys for manta trawl sampling.

Time	Cruise name	Cruise type	No. of stations greater north Sea	No. of stations celtic Sea
Feb-11	Cend 3/11	Nutrient	15	9
Mar-11	Cend 4/11	Fisheries	0	48
Mar-11	Cend 5/11	Fisheries	65	15

of microplastic items was found ($R^2 = -0.492$, $p = 0.009$), signifying that at locations with a smaller grain size, more plastic particles can be found (**Figure 3**).

The microplastics particles make up a certain fraction in weight of the sediment. Here, the dry weight (DW) of the sediment was determined as a percentage of the wet weight. Similarly, an indication of a negative relationship can be found between DW and the total number of microplastics present ($R^2 = -0.796$, $p = 0.000$), indicating that at locations with a lower DW, more plastic particles can be found (**Figure 4**).

Water Samples

A total of 3,597 items were collected from 152 manta trawl transects in the Channel, North, and Celtic Sea with vessels speeds between 1.6 and 8.2 knots (**Table 3**). We were not able to sample the North-East part of the Channel and parts of the North Sea due to adverse weather conditions in 2011, leading to rough seas, complicating the sampling by manta trawl (**Figure 5**). Nevertheless, on almost all sampled locations, litter items were found, indicating a general presence of plastic items floating at the sea surface of both the North Sea and Celtic Sea.

Geographical variations in microplastic abundance at the sea surface were observed (**Figure 6**). The different type of distance measurements available, allowed us to calculate the number of plastic items in a few different ways. We calculated the number of items present per trawled surface area and per volume (**Table 4**).

From the three applied methods to measure distance, the flowmeter results were significantly different from the others ($p < 0.005$). Abundance ranged from 0 to 185,000 items per km^2 using the distance between coordinates, 0 to 157,000 items per km^2 when using the actual distance covered by the ship and 0–376,000 items per km^2 when using the distance as measured by the flow meter. Expressed as items per m^3, this equals to 0–0.7 items per m^3 for the coordinates method, 0–0.6 items per m^3 using the knotmeter and 0–1.5 items per m^3 using the flow meter readings.

The size class 1.00–2.79 mm accounted for the highest proportion of microplastics. In terms of shapes, the most abundant types found were fragments (63%), followed by thin film (14%), pellets (10%), foam (8%), line (5%). The most prominent color was white (33%), but also transparent (29%) and black (19%) The highest catch contained 283 items consisting out of 128 fragments, 28 pellets, 28 pieces of lines, 50 thin films, and 49 foamy items.

Our study did report wind data and indicates average wind speeds of 12.5 mph which only allows for a low amount of mixing (Kukulka et al., 2012). No correlation between the measured wind speed and the observed concentrations was found ($R = -0.1497$; **Figure 7**).

We have calculated the widths of the confidence intervals (CI) for different sample sizes so that the mean can be estimated with a certain precision of its value, giving a first indication of the necessary sample size for a microplastic survey at the water surface. From our 152 transects, only two returned with no microplastics. A histogram of the non-zero observations and the natural log of these values is shown in **Figure 7**. From this it seems reasonable to assume that the non-zero data follows an approximate lognormal distribution (i.e., that the natural log of the data is Gaussian). Thus, we modeled the data as a two-stage process. Firstly, we assumed that a proportion p (where p is estimated by 2/152 = 0.01316) of observations are zero and that the remaining data follows a lognormal distribution. N observations were simulated from this distribution and the width of the bootstrap 95% percentile confidence interval (using 1,000 replications) was calculated. The values of N were 20, 40, 60, 80, 100, 120, 140, 160, 180, 200. This whole process was repeated 500 times and a mean width was determined for each value of N. A plot of these mean widths against N is shown in the bottom left plot of **Figure 7**. This width represents the precision with which we have calculated the mean number of items per km^2. From the original data, the original mean was 19,237 items per km^2. Thus, with a sample size of $n = 200$, we achieve a confidence interval of width (8,000), almost 40% of this mean (**Figure 8**). Future monitoring programmes for microplastics at the sea surface in coastal waters of North West Europe should thus have a minimum of 200 stations so that the mean can be estimated with a precision of 40% of its value.

DISCUSSION

Microplastics in the Sediment

Microplastics particles were found in 89% of the sediments (24 out of 27) collected from locations in the North Sea and Channel area between BE, NL, FR, and the UK. No plastic fragments were found, most observed plastic particles were spheres, followed by fibers. In the sublittoral zone of the Belgian Continental Shelf, part of the North Sea, an average concentration of 97.2 microplastics particles/kg dry sediment was found (Claessens

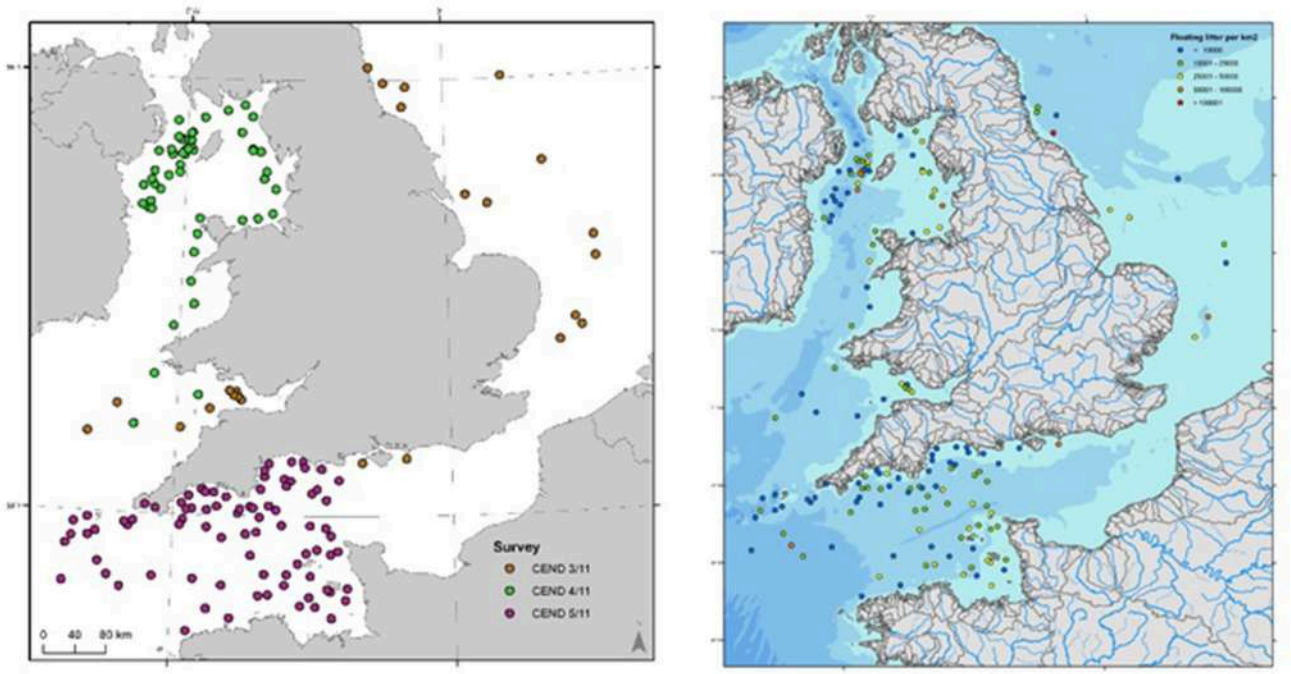

FIGURE 5 | Spatial overview of manta trawl stations (left) and microplastic concentrations (right).

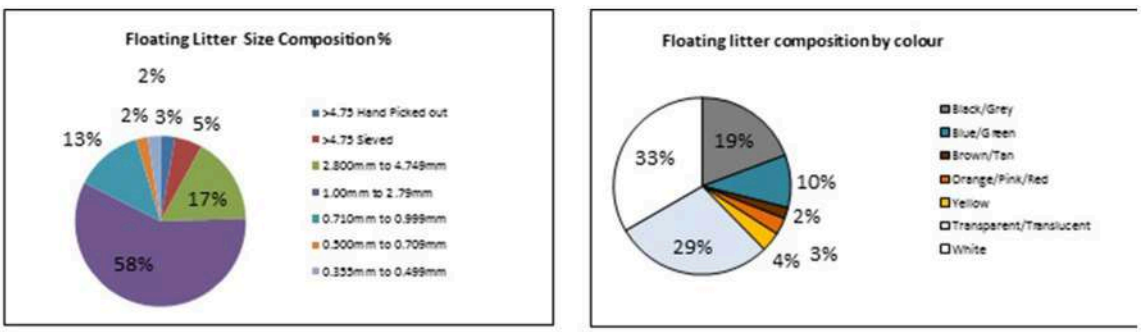

Number of Microplastics in UK waters	
Mean	19,237 items/km²
Median	11,881 items/km²
Max	15,6624 items/km²

FIGURE 6 | Floating marine litter concentrations along the European coasts, including a table with mean, median, and maximum values.

et al., 2011), lower than the findings in our study. In harbors, however, both studies found markedly higher amounts of microplastics compared with other locations (Claessens et al., 2011). The different amounts of microplastic particles reported by studies in nearby locations (**Table 5**) might be an indication of the heterogeneous nature of microplastics presence in marine sediments, temporal changes, and/or result from differences in the analysis (Filella, 2015), we filtered over a smaller pore size filter. Apart from the harbor station (nr. 7), results are still in the same order of magnitude and might thus give an indication for the accumulation rate of microplastics at those sites. Results from a tidal flat in Germany showed concentrations ranging between 36 and 136 microplastics per 10 g of sediment (Liebezeit and Dubaish, 2012), a result which falls within a similar range of

TABLE 4 | Number of microplastics per surface area and per volume using different types of observations.

Station	Abundance lat/long (items/m^2)	Abundance knotmeter (items/m^2)	Abundance flowmeter (items/m^2)	Concentrations lat/long (items/m^2)	Concentrations knotmeter (items/m^2)	Concentrations flowmeter (items/m^2)
MICROPLASTICS						
AVG	0.023360	0.019237	0.036623	0.093439	0.076947	0.146494
STDEV	0.029278	0.022878	0.045556	0.117114	0.091512	0.182225
MEDIAN	0.013146	0.011881	0.023183	0.052586	0.047525	0.092732
MIN	0.000000	0.000000	0.000000	0.000000	0.000000	0.000000
MAX	0.184727	0.156624	0.375854	0.738907	0.626498	1.503417

Lat/long, distance calculated based on coordinates; knotmeter, distance based on onboard equipment measuring speed; flowmeter, distance based on number of rotations.

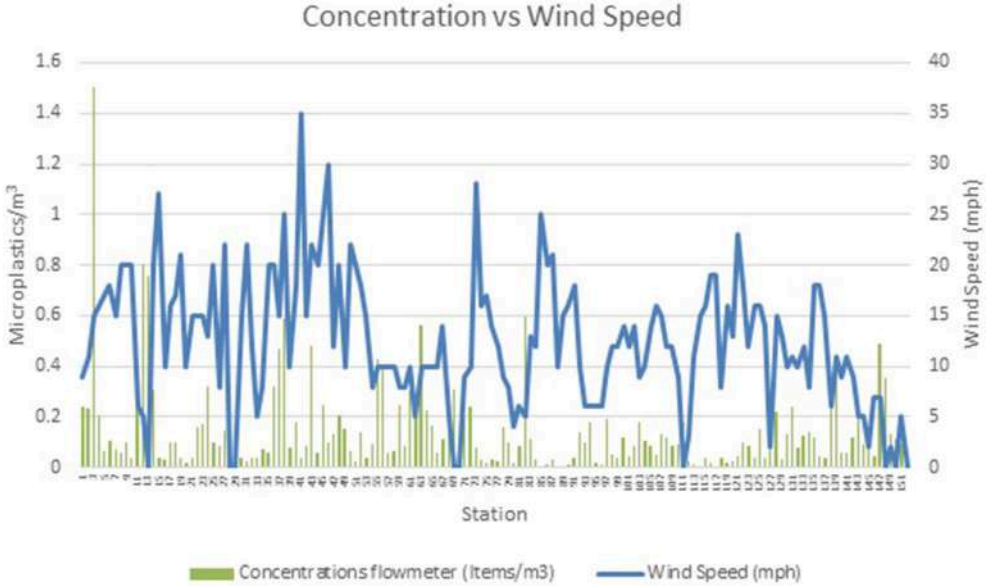

FIGURE 7 | The concentration of microplastics on the water surface compared with the wind speed.

our highest observations. In the sampled regions, however, due to the regular disturbance of the sediments by natural events such as storms (Carretero et al., 1998) and/or anthropogenic activities such as trawling and dredging (Schratzberger and Jennings, 2002; Allen and Clarke, 2007), the upper sediment layer is regularly mixed, making it difficult to link sedimentation rates with temporal microplastics accumulation (Van Cauwenberghe et al., 2013).

There is a large spread of values around the average, indicating a heterogeneous spread of microplastics in sea floor sediments. This inhomogeneity could mean that there are areas where microplastics settle in higher amounts. In the present study, we investigated if a correlation between sediment characteristics and microplastic abundance exists. Our research indicates a relationship between the amount of organic carbon and the amount of microplastics present in the sediment. This finding is supported by a Danish study (Strand et al., 2013) who found a correlation between the content of microplastics in marine sediments and %TOC. Although further research is required, similarities in densities and resulting sedimentation processes might be driving this correlation, %TOC could help to identify potential areas with high microplastic concentrations. From our findings, it seems sensible for future monitoring to target undisturbed patches of fine sediments.

Microplastics at the Sea Surface

The ubiquity of small floating litter items in the UK Channel, North and Celtic Sea is prominently illustrated in this study by the presence of microplastics in all samples except two. The abundance of microplastics appears to be still relatively low in surface waters of the North Sea and Celtic Sea compared to other regions e.g., Pacific gyre. We observed some higher concentrations of microplastics near the coast and river estuaries. This might indicate the relative importance of inputs through rivers (Cheung et al., 2016) or could be a result of higher inputs from industrialized and populated areas nearby (Browne et al., 2011; Naidoo et al., 2015). Nevertheless, plastic particles were also commonly found at the sea surface of the North and Celtic Sea far away from land or potential sources. This could be a result of atmospheric deposition of microplastics (Dris et al., 2016). Microplastic abundance at the sea surface has been shown to vary with wind speed due to vertical mixing (Kukulka et al., 2012;

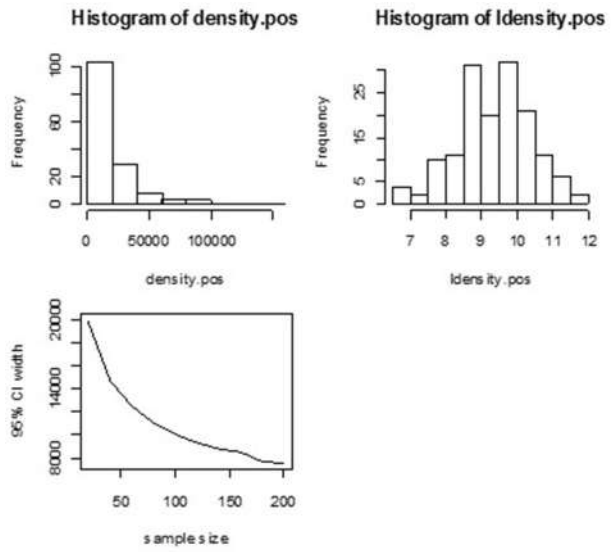

FIGURE 8 | Histograms of non-zero and ln non-zero data (top row), confidence interval widths (bottom row).

TABLE 5 | Comparison between microplastic numbers at the same stations between Claessens et al. (2011) and the findings in this study.

	Claessens et al., 2011	This study
Station	S5	MIC 1
Result (particles/kg dry sediment)	98.2	2013: 110–280 2014: 59
Station	S2	WO2
Result (particles/kg dry sediment)	115.8	330
Station	OO4	Ooh
Result (particles/kg dry sediment)	109.2	3,146

Reisser et al., 2015). Data from the eastern North Pacific suggest that the abundance of suspended plastic within 10–30 m of the sea surface averages two orders of magnitude less than that of surface (Ryan et al., 2009). We found no correlation between wind speed and microplastic concentrations.

The distances measured or calculated by different techniques such as coordinates, knot meter and flow meter result in large differences in reported microplastic concentrations. Our maximum values of 157,000 particles km^{-2}, calculated using the distance given by the onboard instrumentation, are similar to those reported on average in the Mediterranean (Collignon et al., 2012), 116,000 particles km^{-2} and well below those measured in the Pacific Gyre (Moore et al., 2001), who recorded densities of more than 300,000 particles km^{-2} in 1999. However, concentrations based on flowmeter data equaled maximum concentrations of 375,854 particles km^{-2}. This indicates the need for standardized marine litter protocols, methodologies and units worldwide. Internationally, various techniques, and principles have been applied to sample and analyse floating microplastics (Filella, 2015). Consequently, available studies have been reporting marine litter abundance in diverse dimensions

TABLE 6 | Comparison of the current study results with results from research in the same region (Morris and Hamilton, 1974; Lusher et al., 2013; Cole et al., 2014; Frias et al., 2014; Mintenig, 2014).

Location	Equipment	Particles/m^3	Sources
UK offshore waters	Manta trawl	0.14	Current Study
Offshore, Ireland	Underway sampling	2.46	Lusher et al., 2014
English Channel, UK	Plankton net	0.27	Cole et al., 2014
Bristol Channel, UK	Lowestoft Plankton Sampler	0–100	Morris and Hamilton, 1974
Portuguese coast	Neuston net/CPR	0.02–0.036	Frias et al., 2014
North Sea	Manta trawl	0–3.5	Mintenig, 2014

and scales, making direct comparisons extremely difficult, e.g., the number of microplastics by volume (particles/m^3) or by surface area (particles/km^2), smaller or bigger than 5 mm, analyzed with microscopes or spectroscopes (Galgani et al., 2015).

We showed above that even within the same study, several ways of expressing microplastic quantities can be used depending on the initial calculation of trawled distance. Only using coordinates could easily lead to errors as it doesn't consider ocean currents and factual sampling distance. When available, using onboard instruments to precisely measure the vessels groundspeed while sampling gives a more accurate estimate of the trawled distance. The flow meter determines the distance based on the water flow through the net. However, there were significant differences between the first two methods and the flowmeter method. The flow meter registered a smaller distance than what was obtained by using coordinates or onboard instrumentation. This could be due to the bow wave effect which has been previously observed when trawling nets at high speeds or a result of the chopping through waves (Chiang et al., 2011), meaning that a far lower volume will be filtered by the manta net compared to what one could calculate from less direct measurements such as coordinates and ship speed. Microplastics are vertically distributed within the upper water column due to wind and temperature driven mixing (Kukulka et al., 2012, 2016). This suggests that microplastic concentrations could be significantly underestimated by traditional surface measurements. To allow for comparison, it is therefore recommended to sample in comparable conditions of calm sea state with low wind and wave intensity. The authors also propose to use flow meters and to report both units, items per km^2 and items per m^3, in future microplastic studies at the sea surface.

We listed microplastic concentrations from within the same geographical area, using comparable equipment for sampling microplastics (**Table 6**). Our average value, 0.14 items per m^3 and maximum value of 1.5 items per m^3, based on the flow meter data, is comparable to previous microplastic studies with manta nets in this region.

Comparison Water and Sediment Matrices

Our results indicated that sediments were more contaminated with microplastics, by number of items per volume, than surface waters. The transport of small particles to the seafloor and

their deposition in the benthic sediments is facilitated by the colonization of the material by fouling organisms, which increase the density of the particles and force them to sink (Andrady, 2015). Plastics degrade very slowly resulting in high persistence of plastic litter especially at the seafloor (Andrady, 2015). Several microplastics of a few micron were found in marine sediments with a rapid-screening approach based on fluorescent tagging with Nile Red, highlighting the role of marine sediments as a sink (Maes et al., 2017). In our study, most of the microplastics found in the sediments were fibers and spheres, with spheres having the highest average amount/kg sediment. This is in contrast with the findings from the floating microplastics were mainly fragments were found. It seems that for the floating microplastic particles there is a potential influence from rivers. Rivers are both pathways and producers of microplastics (Thiel et al., 2011; Rech et al., 2014). A study on microplastics in European rivers indeed found that fragments (Po and Rhine) and fibers (Danube and Dalålven) were the largest part of the microplastics found (van der Wal et al., 2015). Plastic fragments are breakdown products of larger plastic items via mechanical and/or UV-weathering (Barnes et al., 2009), which occurs when exposed to the sun, wind and other mechanical stresses such as found in a river. Similarly, we observed thousands of fragments in the floating fraction in our study.

The fact that there are mostly spheres and fibers found in the sediments is not so surprising, many spheres and fibers are made from polystyrene and polyacrylamides which are often heavier then seawater and thus readily sink (Cheung and Fok, 2016). The shape of the particle and fiber could influence its settling velocity, however, few studies have been published on this topic. The high amounts of fibers in the sediments, could be a result of the degradation of fishing nets and dolly rope while dragging over the seafloor (Devriese et al., 2015), from the continuous input via sewage and laundry (Browne et al., 2011) or via the disposal of sewage sludge and dredged sediments (Browne et al., 2011). Also Brown shrimp, collected from the same study area, contained mainly fibers (Devriese et al., 2015). It is much more challenging to define the main sources of microplastics in sediment due to the wide variety of potential pathways (Andrady, 2015), including atmospheric depositions (Dris et al., 2016).

Due to wind and currents, floating microplastics are more mobile compared to those found in sediments (Kukulka et al., 2012), which act as a stable sink (Woodall et al., 2014). In this study, microplastic concentrations in different surface transects varied between a few tens to a few thousands. Due to this variability, large sample sizes, above 200 stations, are required to ensure that the mean can be estimated with a precision of 40% of its value. North West European seas in the North-East Atlantic are periodically impacted by geologically significant storms, which have a marked influence on water circulation but also affect terrigenous sediment supply, flood deposition, and long-term accumulation of fine-grained sediment on the continental shelf (Green et al., 1995). Also, fisheries activities disturb the sediment and homogenize the upper sediment layers by trawling (Schratzberger and Jennings, 2002). So far, there are no studies considering the impact of these physical processes on microplastic distribution in water or sediment samples. Our results indicated that the number of microplastics in sediment samples were less variable, especially at locations with high %TOC, in comparison to those found at the sea surface. To look at temporal trends, it seems sensible for future monitoring to target undisturbed patches of fine sediments with high %TOC. Such monitoring could be combined with the monitoring of hazardous substances, since these surveys are well established and targeting fine sediments (<64 microns) to monitor persistent organic pollutants (Davies et al., 2012).

Monitoring of Microplastics

This study is one of the first to determine baseline values for microplastics in North West European seas. Based on our findings, we see a potential for microplastics monitoring in combination with existing environmental surveys. Standardized methods resulted in a comparable outcome between the project partners of the Interreg 2 Seas MICRO IVa project (van der Meulen et al., 2015). The standardization of methods for collecting, processing, and analysis of samples is required to achieve comparable outcomes within one region. When counting microplastics, different types of equipment like regular microscopy or spectroscopy can be applied, causing under or over estimations which possibly influence the final numbers (Löder and Gerdts, 2015). To monitor and compare spatial and temporal trends of microplastics, simple, cost-effective and standardized protocols, capable of efficiently and accurately sampling, and enumerating microplastics in a variety of environmental matrices are recommended (Maes et al., 2017; Underwood et al., 2017). Without this it will remain impossible to make direct comparisons among studies and habitats, because such comparisons could be confounded with methods used (Underwood et al., 2017).

The results of this study demonstrate that microplastics were present at the sea surface and in sediments of the UK Channel, North Sea and Celtic Sea. Different shapes and types of plastics were found in both matrices. Monitoring of both matrices had certain advantages and disadvantages which must be considered when designing future monitoring programmes. Microplastic monitoring in sediments can easily be combined with existing contaminant surveys sampling fine sediments. Water column and sea surface monitoring might be more appropriate for determining effect concentrations for certain marine biota. Because the concentrations of microplastics in the water are lower and the variability is higher than in sediments, more water must be sampled to achieve a comparable sample size to sediments or other seafloor indicators. We recommend to install a flow meter near the lower edge of the manta net frame to give additional information on the number of items per cubic meter.

Areas with high concentrations of floating microplastics were found in the estuarine and coastal areas. For the sediment, we observed high concentrations of microplastics in estuarine areas and in organic sediments, supported by the correlation with high total organic carbon content. Hotspot areas are thus likely situated in areas with fine muds since these generally contain high concentrations of organic materials and are made up of smaller grain sizes. The settling of microplastics might be following similar sedimentation processes as those observed in

fine sediments. A previous study of microplastics in the deep sea suggested that aggregation of microplastics with organic matter, such as marine snow and fecal pellets of marine organisms, could play a role in the sinking processes (Van Cauwenberghe et al., 2013). This also indicates that benthic organisms burrowing and feeding in muddy environments, are likely exposed to higher concentrations of microplastics than benthic organisms in areas with a larger grain size and lower TOC. Pooled sampling, repeated over time, is advisable to determine trends while minimizing spatial heterogeneity. Determination of sediment characteristics will enlarge our understanding of underlying sedimentation processes and could help with the identification of potential microplastic hotspots. We suggest that future programs of monitoring continue to distinguish the type of microplastic particles as well as the sampled size fractions, and we advise to monitor microplastics in sediments with standard mesh sizes and equipment such as the van Veen grab to allow future spatio-temporal comparison of microplastic abundance across wider marine environments.

CONCLUSIONS

This study presents a baseline for the monitoring of microplastic in coastal sediments and surface waters of North West European seas. Floating concentrations ranged between zero and 1.5 microplastic per m^3, whereas microplastic concrentrations in sediments ranged between zero and a few thousands per kg dw sediment. In sediments, mainly fibers and spheres were found, whereas at the sea surface fragments were dominant. For the water phase concentrations of microplastics are lower and more variable than in sediments, meaning that larger sampled water volumes are required to find detectable concentrations. Future monitoring programmes for microplastics at the sea surface in coastal waters of North West Europe should have a minimum of 200 stations to estimate the mean with a precision of 40% of its value. Standardization of monitoring methods within OSPAR and EU is recommended to aid in the implementation of the MSFD and the assessment of the microplastics pollution of Northern European waters over time. High concentrations of microplastics in the water can be found in estuaries. For sediments, estuaries and areas with a high organic carbon content are likely hotspots.

AUTHOR CONTRIBUTIONS

TM: sediment and water sampling/analysis, and manuscript writing. MV: sediment sampling and manuscript writing. LD, AH, and LF: sediment sampling. HL: sediment analysis. JR: project administration. AV: sediment sampling, review and guidance.

ACKNOWLEDGMENTS

Support for this research came from the EU Interreg 2 Seas IVa project MICRO (MICRO 09-002-BE). This study was partly funded by Defra (UK) and the Dutch Ministry of Infrastructure and the Environment (NL). Shiptime on RV Simon Stevin was provided by VLIZ and DAB Vloot. Some floating litter data was collected on board of the RV Cefas Endeavour and funded by Defra (UK) project ME5415. Many thanks to Manuel Nicolaus (Cefas), Jon Barry (Cefas), and all researchers involved in the project, as well as the VU University Institute for Environmental Studies, the Cefas Plankton lab, and ILVO lab of chromatography.

REFERENCES

Allen, J. I., and Clarke, K. R. (2007). Effects of demersal trawling on ecosystem functioning in the North Sea: a modelling study. *Mar. Ecol. Prog. Ser.* 336, 63–75. doi: 10.3354/meps336063

Andrady, A. L. (2015). "Persistence of plastic litter in the oceans," in *Marine Anthropogenic Litter*, eds M. Bergmann, L. Gutow, and M. Klages (Cham: Springer International Publishing), 57–72. doi: 10.1007/978-3-319-16510-3_3

Arthur, C., Baker, J., and Bamford, H. (eds.). (2009). *Proceedings of the International Research Workshop on the Occurrence, Effects, and Fate of Microplastic Marine Debris.* NOAA Technical Memorandum NOS-OR&R-30. Available online at: https://marinedebris.noaa.gov/file/2192/download?token=5dvqb-YY

Barnes, D. K. A., Galgani, F., Thompson, R. C., and Barlaz, M. (2009). Accumulation and fragmentation of plastic debris in global environments. *Philos. Trans. R. Soc. Lond. B Biol. Sci.* 364, 1985–1998. doi: 10.1098/rstb.2008.0205

Browne, M. A., Crump, P., Niven, S. J., Teuten, E., Tonkin, A., Galloway, T., et al. (2011). Accumulation of microplastic on shorelines woldwide: sources and sinks. *Environ. Sci. Technol.* 45, 9175–9179. doi: 10.1021/es201811s

Carretero, J. C., Gomez, M., Lozano, I., De Elvira, A. R., Serrano, O., Iden, K., et al. (1998). Changing waves and storms in the Northeast Atlantic? *Bull. Am. Meteorol. Soc.* 79, 741–760. doi: 10.1175/1520-0477(1998)079<0741:CWASIT>2.0.CO;2

Cheung, P. K., and Fok, L. (2016). Evidence of microbeads from personal care product contaminating the sea. *Mar. Pollut. Bull.* 109, 582–585. doi: 10.1016/j.marpolbul.2016.05.046

Cheung, P. K., Cheung, L. T. O., and Fok, L. (2016). Seasonal variation in the abundance of marine plastic debris in the estuary of a subtropical macro-scale drainage basin in South China. *Sci. Total Environ.* 562, 658–665. doi: 10.1016/j.scitotenv.2016.04.048

Chiang, K.-P., Wu, C.-J., and Shin, C.-M. (2011). Does the mesh size of the plankton net affect the result of statistical analyses of the relationship between the copepod community and water masses? *Crustaceana* 84, 1069–1083. doi: 10.1163/001121611X586701

Claessens, M., De Meester, S., Van Landuyt, L., De Clerck, K., and Janssen, C. R. (2011). Occurrence and distribution of microplastics in marine sediments along the Belgian coast. *Mar. Pollut. Bull.* 62, 2199–2204. doi: 10.1016/j.marpolbul.2011.06.030

Cole, M., Lindeque, P., Halsband, C., and Galloway, T. S. (2011). Microplastics as contaminants in the marine environment: A review. *Mar. Pollut. Bull.* 62, 2588–2597. doi: 10.1016/j.marpolbul.2011.09.025

Cole, M., Webb, H., Lindeque, P. K., Fileman, E. S., Halsband, C., and Galloway, T. S. (2014). Isolation of microplastics in biota-rich seawater samples and marine organisms. *Sci. Rep.* 4:4528. doi: 10.1038/srep04528

Collignon, A., Hecq, J. H., Glagani, F., Voisin, P., Collard, F., and Goffart, A. (2012). Neustonic microplastic and zooplankton in the North Western Mediterranean Sea. *Mar. Pollut. Bull.* 64, 861–864. doi: 10.1016/j.marpolbul.2012.01.011

Cózar, A., Echevarría, F., González-Gordillo, J. I., Irigoien, X., Ubeda, B., Hernández-León, S., et al. (2014). Plastic debris in the open ocean. *Proc. Natl. Acad. Sci. U.S.A.* 111, 10239–10244. doi: 10.1073/pnas.1314705111

Davies, I. M., Gubbins, M., Hylland, K., Maes, T., Martinez-Gomez, C., Moffat, C., et al. (2012). *Guidelines for the Integrated Monitoring and Assessment of Contaminants and Their Effects.* Available online at: https://research.vu.nl/en/

publications/guidelines-for-the-integrated-monitoring-and-assessment-of-contam (Accessed April 7, 2017).

Dean, W. E. J. (1974). Determination of carbonate and organic matter in calcareous sediments and sedimentary rocks by loss on ignition: comparison with other methods. *J. Sediment. Petrol.* 44, 242–248.

Derraik, J. G. B. (2002). The pollution of the marine environment by plastic debris. *Mar. Pollut. Bull.* 44, 842–852. doi: 10.1016/S0025-326X(02)00220-5

Devriese, L. I., van der Meulen, M. D., Maes, T., Bekaert, K., Paul-Pont, I., Frère, L., et al. (2015). Microplastic contamination in brown shrimp (*Crangon crangon*, Linnaeus 1758) from coastal waters of the Southern North Sea and Channel area. *Mar. Pollut. Bull.* 98, 179–187. doi: 10.1016/j.marpolbul.2015.06.051

Dris, R., Gasperi, J., Saad, M., Mirande, C., and Tassin, B. (2016). Synthetic fibers in atmospheric fallout: a source of microplastics in the environment? *Mar. Pollut. Bull.* 104, 290–293. doi: 10.1016/j.marpolbul.2016.01.006

Eriksen, M., Lebreton, L. C. M., Carson, H. S., Thiel, M., Moore, C. J., Borerro, J. C., et al. (2014). Plastic pollution in the world's oceans: more than 5 trillion plastic pieces weighing over 250,000 tons afloat at sea. *PLoS ONE* 9:e111913. doi: 10.1371/journal.pone.0111913

Eriksen, M., Mason, S., Wilson, S., Box, C., Zellers, A., Edwards, W., et al. (2013a). Microplastic pollution in the surface waters of the Laurentian Great Lakes. *Mar. Pollut. Bull.* 77, 177–182. doi: 10.1016/j.marpolbul.2013.10.007

Eriksen, M., Maximenko, N., Thiel, M., Cummins, A., Lattin, G., Wilson, S., et al. (2013b). Plastic pollution in the South Pacific subtropical gyre. *Mar. Pollut. Bull.* 68, 71–76. doi: 10.1016/j.marpolbul.2012.12.021

Fendall, L. S., and Sewell, M. A. (2009). Contributing to marine pollution by washing your face: microplastics in facial cleansers. *Mar. Pollut. Bull.* 58, 1225–1228. doi: 10.1016/j.marpolbul.2009.04.025

Filella, M. (2015). Questions of size and numbers in environmental research on microplastics: methodological and conceptual aspects. *Environ. Chem.* 12, 527–538. doi: 10.1071/EN15012

Foekema, E. M., De Gruijter, C., Mergia, M. T., van Franeker, J. A., Murk, A. J., and Koelmans, A. A. (2013). Plastic in north sea fish. *Environ. Sci. Technol.* 47, 8818–8824. doi: 10.1021/es400931b

Frias, J. P. G. L., Otero, V., and Sobral, P. (2014). Evidence of microplastics in samples of zooplankton from Portuguese coastal waters. *Mar. Environ. Res.* 95, 89–95. doi: 10.1016/j.marenvres.2014.01.001

Gago, J., Galgani, F., Maes, T., and Thompson, R. C. (2016). Microplastics in Seawater: recommendations from the marine strategy framework directive implementation process. *Front. Mar. Sci.* 3:219. doi: 10.3389/fmars.2016.00219

Galgani, F., Hanke, G., and Maes, T. (2015). "Global distribution, composition and abundance of marine litter," in *Marine Anthropogenic Litter*, eds M. Bergmann, L. Gutow, and M. Klages (London: Springer), 29–56.

Galgani, F., Hanke, G., Werner, S., and De Vrees, L. (2013). Marine litter within the European marine strategy framework directive. *ICES J. Mar. Sci.* 70, 1055–1064. doi: 10.1093/icesjms/fst122

Galgani, F., Hanke, G., Werner, S., Oosterbaan, L., Nilsson, P., Fleet, D., et al. (2014). *Guidance on Monitoring of Marine Litter in European Seas*. JRC, 1–128. Available online at: http://publications.jrc.ec.europa.eu/repository/bitstream/JRC83985/lb-na-26113-en-n.pdf

GESAMP (2015). *Sources, Fate and Effects of Microplastics in the Marine Environment: A Global Assessment*. Available online at: http://www.gesamp.org/data/gesamp/files/media/Publications/Reports_and_studies_90/gallery_2230/object_2500_large.pdf

Green, M. O., Vincent, C. E., McCave, I. N., Dickson, R. R., Rees, J. M., and Pearsons, N. D. (1995). Storm sediment transport: observations from the British North Sea shelf. *Cont. Shelf Res.* 15, 889–912. doi: 10.1016/0278-4343(95)80001-T

Gregory, M. R. (2009). Environmental implications of plastic debris in marine settings–entanglement, ingestion, smothering, hangers-on, hitch-hiking and alien invasions. *Philos. Trans. R. Soc. Lond. B Biol. Sci.* 364, 2013–2025. doi: 10.1098/rstb.2008.0265

Jambeck, J. R., Geyer, R., Wilcox, C., Siegler, T. R., Perryman, M., Andrady, A., et al. (2015). Plastic waste inputs from land into the ocean. *Science* 347, 768–770. doi: 10.1126/science.1260352

Keswani, A., Oliver, D. M., Gutierrez, T., and Quilliam, R. S. (2016). Microbial hitchhikers on marine plastic debris: human exposure risks at bathing waters and beach environments. *Mar. Environ. Res.* 118, 10–19. doi: 10.1016/j.marenvres.2016.04.006

Kukulka, T., Law, K. L., and Proskurowski, G. (2016). Evidence for the influence of surface heat fluxes on turbulent mixing of microplastic marine debris. *J. Phys. Oceanogr.* 46, 809–815. doi: 10.1175/jpo-d-15-0242.1

Kukulka, T., Proskurowski, G., Morét-Ferguson, S., Meyer, D. W., and Law, K. L. (2012). The effect of wind mixing on the vertical distribution of buoyant plastic debris. *Geophys. Res. Lett.* 39:L07601. doi: 10.1029/2012gl051116

Lechner, A., Keckeis, H., Lumesberger-Loisl, F., Zens, B., Krusch, R., Tritthart, M., et al. (2014). The Danube so colourful: a potpourri of plastic litter outnumbers fish larvae in Europe's second largest river. *Environ. Pollut.* 188, 177–181. doi: 10.1016/j.envpol.2014.02.006

Leslie, H. A., van der Meulen, M. D., Kleissen, F. M., and Vethaak, A. D. (2011). *Microplastic Litter in the Dutch Marine Environment Providing Facts and Analysis for with Marine Microplastic Litter*. Deltares, 104.

Liebezeit, G., and Dubaish, F. (2012). Microplastics in beaches of the East Frisian Islands Spiekeroog and Kachelotplate. *Bull. Environ. Contam. Toxicol.* 89, 213–217. doi: 10.1007/s00128-012-0642-7

Lima, A. R. A., Costa, M. F., and Barletta, M. (2014). Distribution patterns of microplastics within the plankton of a tropical estuary. *Environ. Res.* 132, 146–155. doi: 10.1016/j.envres.2014.03.031

Löder, M. G. J., and Gerdts, G. (2015). "Methodology used for the detection and identification of microplastics—a critical appraisal," in *Marine Anthropogenic Litter*, eds M. Bergmann, L. Gutow, and M. Klages (London: Springer), 201–227.

Lusher, A. L., Burke, A., O'Connor, I., and Officer, R. (2014). Microplastic pollution in the Northeast Atlantic Ocean: validated and opportunistic sampling. *Mar. Pollut. Bull.* 88, 325–333. doi: 10.1016/j.marpolbul.2014.08.023

Lusher, A. L., McHugh, M., and Thompson, R. C. (2013). Occurrence of microplastics in the gastrointestinal tract of pelagic and demersal fish from the English Channel. *Mar. Pollut. Bull.* 67, 94–99. doi: 10.1016/j.marpolbul.2012.11.028

Maes, T., Jessop, R., Wellner, N., Haupt, K., and Mayes, A. G. (2017). A rapid-screening approach to detect and quantify microplastics based on fluorescent tagging with Nile Red. *Sci. Rep.* 7:44501. doi: 10.1038/srep44501

McCormick, A., Hoellein, T. J., Mason, S. A., Schluep, J., and Kelly, J. J. (2014). Microplastic is an abundant and distinct microbial habitat in an urban river. *Environ. Sci. Technol.* 48, 11863–11871. doi: 10.1021/es503610r

Mebius, L. J. (1960). A rapid method for the determination of organic carbon in soil. *Anal. Chim. Acta* 22, 120–124. doi: 10.1016/S0003-2670(00)88254-9

Mintenig, S. (2014). *Microplastic in Plankton of the North- and Baltic Sea. Epic*. Available online at: http://epic.awi.de/36907/#.WOgwPNsXQHk.mendeley&title=MicroplasticinplanktonoftheNorth-andBalticSea-ePIC (Accessed April 8, 2017).

Moore, C. J., Lattin, G. L., and Zellers, A. F. (2011). Quantity and type of plastic debris flowing from two urban rivers to coastal waters and beaches of Southern California. *Rev. Gestão Costeira Integr.* 11, 65–73. doi: 10.5894/rgci194

Moore, C. J., Moore, S. L., Leecaster, M. K., and Weisberg, S. B. (2001). A comparison of plastic and plankton in the north Pacific central gyre. *Mar. Pollut. Bull.* 42, 1297–1300. doi: 10.1016/S0025-326X(01)00114-X

Moore, C., Lattin, G., and Zellers, A. (2005). *Density of Plastic Particles Found in Zooplankton Trawls from Coastal Waters of California to the North Pacific Central Gyre. ..., Redon*. Beach, CA. Available online at: http://alguita.com/pdf/Density-of-Particles.pdf

Morét-Ferguson, S., Law, K. L., Proskurowski, G., Murphy, E. K., Peacock, E. E., and Reddy, C. M. (2010). The size, mass, and composition of plastic debris in the western North Atlantic Ocean. *Mar. Pollut. Bull.* 60, 1873–1878. doi: 10.1016/j.marpolbul.2010.07.020

Morishige, C., Donohue, M. J., Flint, E., Swenson, C., and Woolaway, C. (2007). Factors affecting marine debris deposition at French Frigate Shoals, Northwestern Hawaiian Islands Marine National Monument, 1990-2006. *Mar. Pollut. Bull.* 54, 1162–1169. doi: 10.1016/j.marpolbul.2007.04.014

Morris, A. W., and Hamilton, E. I. (1974). Polystyrene spherules in the Bristol Channel. *Mar. Pollut. Bull.* 5, 26–27. doi: 10.1016/0025-326X(74)90311-7

Naidoo, T., Glassom, D., and Smit, A. J. (2015). Plastic pollution in five urban estuaries of KwaZulu-Natal, South Africa. *Mar. Pollut. Bull.* 101, 473–480. doi: 10.1016/j.marpolbul.2015.09.044

Pollard, R. T., Griffttths, M. J., Cunningham, S. A., Read, J. F., Pérez, F. F., and Ríos, A. F. (1996). Vivaldi 1991–A study of the formation, circulation and ventilation of Eastern North Atlantic Central Water. *Prog. Oceanogr.* 37, 167–192. doi: 10.1016/S0079-6611(96)00008-0

Rech, S., Macaya-Caquilpán, V., Pantoja, J. F., Rivadeneira, M. M., Jofre Madariaga, D., and Thiel, M. (2014). Rivers as a source of marine litter–a study from the SE Pacific. *Mar. Pollut. Bull.* 82, 66–75. doi: 10.1016/j.marpolbul.2014.03.019

Reisser, J., Slat, B., Noble, K., Du Plessis, K., Epp, M., Proietti, M., et al. (2015). The vertical distribution of buoyant plastics at sea: an observational study in the North Atlantic Gyre. *Biogeosciences* 12, 1249–1256. doi: 10.5194/bg-12-1249-2015

Rios Mendoza, L. M., and Jones, P. R. (2015). Characterisation of microplastics and toxic chemicals extracted from microplastic samples from the North Pacific Gyre. *Environ. Chem.* 12, 611–617. doi: 10.1071/EN14236

Ryan, P. G., Moore, C. J., van Franeker, J. A., and Moloney, C. L. (2009). Monitoring the abundance of plastic debris in the marine environment. *Philos. Trans. R. Soc. Lond. B Biol. Sci.* 364, 1999–2012. doi: 10.1098/rstb.2008.0207

Schratzberger, M., and Jennings, S. (2002). Impacts of chronic trawling disturbance on meiofaunal communities. *Mar. Biol.* 141, 991–1000. doi: 10.1007/s00227-002-0895-5

Strand, J., Lassen, P., Shashoua, Y., and Andersen, J. (2013). "Microplastic particles in sediments from Danish waters," in *ICES Annual Science Conference (ASC).* Available online at: http://www.forskningsdatabasen.dk/en/catalog/2282206747 (Accessed January 31, 2017).

Sundt, P., Schultze, P.-E., and Syversen, F. (2014). *Sources of Microplastic Pollution to the Marine Environment.* Mepex Norwegian Environment Agency. 1–108. Report number: M-321/2015. Available online at: http://www.miljodirektoratet.no/Documents/publikasjoner/M321/M321.pdf

Thiel, M., Hinojosa, I. A., Joschko, T., and Gutow, L. (2011). Spatio-temporal distribution of floating objects in the German Bight (North Sea). *J. Sea Res.* 65, 368–379. doi: 10.1016/j.seares.2011.03.002

Thompson, R. C., Olsen, Y., Mitchell, R. P., Davis, A., Rowland, S. J., John, A. W., et al. (2004). Lost at sea: where is all the plastic? *Science* 304, 838. doi: 10.1126/science.1094559

Underwood, A. J., Chapman, M. G., Browne, M. A., Hobbs, G., Lednev, I. K., Kurtz, S. M., et al. (2017). Some problems and practicalities in design and interpretation of samples of microplastic waste. *Anal. Methods* 9, 1332–1345. doi: 10.1039/C6AY02641A

Van Cauwenberghe, L., Vanreusel, A., Mees, J., and Janssen, C. R. (2013). Microplastic pollution in deep-sea sediments. *Environ. Pollut.* 182, 495–499. doi: 10.1016/j.envpol.2013.08.013

van der Meulen, M. D., Devriese, L. I., Maes, T., Van Dalfsen, J. A., Huvet, A., Soudant, P., et al. (2015). *Socio-Economic Impact of Microplastics in the 2 Seas, Channel and France Manche Region*. Deltares. Available online at: http://archimer.ifremer.fr/doc/00287/39834/38359.pdf

van der Wal, M., Van der Meulen, M., Tweehuijsen, G., Peterlin, M., Palatinus, A., Kovač Viršek, M., et al. (2015). *Identification and Assessment of Riverine Input of (Marine) Litter*. JRC. Available online at: http://mcc.jrc.ec.europa.eu/document.py?code=201606244356&title=Final%20Report%20on%20Identification%20and%20Assessment%20of%20Riverine%20Input%20of%20(Marine)%20Litter

van Sebille, E., Wilcox, C., Lebreton, L., Maximenko, N., Hardesty, B. D., van Franeker, J. A., et al. (2015). A global inventory of small floating plastic debris. *Environ. Res. Lett.* 10:124006. doi: 10.1088/1748-9326/10/12/124006

Vethaak, A. D., and Leslie, H. A. (2016). Plastic Debris is a human health issue. *Environ. Sci. Technol.* 50, 6825–6826. doi: 10.1021/acs.est.6b02569

Wentworth, C. K. (1922). A scale of grade and class terms for clastic sediments. *J. Geol.* 30, 377–392. doi: 10.1086/622910

Woodall, L. C., Sanchez-Vidal, A., Canals, M., Paterson, G. L. J., Coppock, R., Sleight, V., et al. (2014). The deep sea is a major sink for microplastic debris. *R. Soc. Open Sci.* 1, 140317–140317. doi: 10.1098/rsos.140317

Ye, S., and Andrady, A. L. (1991). Fouling of floating plastic debris under Biscayne Bay exposure conditions. *Mar. Pollut. Bull.* 22, 608–613. doi: 10.1016/0025-326X(91)90249-R

Conflict of Interest Statement: The authors declare that the research was conducted in the absence of any commercial or financial relationships that could be construed as a potential conflict of interest.

frontiers in Marine Science

ORIGINAL RESEARCH
published: 31 May 2017
doi: 10.3389/fmars.2017.00167

Plastic Debris Occurrence, Convergence Areas and Fin Whales Feeding Ground in the Mediterranean Marine Protected Area Pelagos Sanctuary: A Modeling Approach

Maria Cristina Fossi[1], Teresa Romeo[2], Matteo Baini[1], Cristina Panti[1], Letizia Marsili[1], Tommaso Campani[1], Simonepietro Canese[2], François Galgani[3], Jean-Noël Druon[4], Sabina Airoldi[5], Stefano Taddei[6], Maria Fattorini[6,7], Carlo Brandini[6,7] and Chiara Lapucci[6,7]*

[1] Department of Physical, Earth and Environmental Sciences, University of Siena, Siena, Italy, [2] Laboratory of Milazzo, ISPRA, Institute for Environmental Protection and Research, Milazzo, Italy, [3] IFREMER, French Research Institute for Exploitation of the Sea, Immeuble Agostini, Corsica, France, [4] Unit D.02 Water and Marine Resources, European Commission, Joint Research Centre, Directorate D – Sustainable Resources, Ispra, Italy, [5] Thetys Research Institute, Milan, Italy, [6] LaMMA Consortium, Florence, Italy, [7] Institute of BioMeteorology, National Council of Research (CNR), Florence, Italy

OPEN ACCESS

Edited by:
Mario Barletta, Federal University of Pernambuco, Brazil

Reviewed by:
Mark Peter Simmonds, University of Bristol, United Kingdom
Sunwook Hong, Our Sea of East Asia Network, South Korea
Russell Christopher Leaper, University of Aberdeen, United Kingdom

***Correspondence:**
Cristina Panti
panti4@unisi.it

Specialty section:
This article was submitted to Marine Pollution, a section of the journal Frontiers in Marine Science

Received: *13 January 2017*
Accepted: *15 May 2017*
Published: *31 May 2017*

Citation:
Fossi MC, Romeo T, Baini M, Panti C, Marsili L, Campani T, Canese S, Galgani F, Druon J-N, Airoldi S, Taddei S, Fattorini M, Brandini C and Lapucci C (2017) Plastic Debris Occurrence, Convergence Areas and Fin Whales Feeding Ground in the Mediterranean Marine Protected Area Pelagos Sanctuary: A Modeling Approach. Front. Mar. Sci. 4:167. doi: 10.3389/fmars.2017.00167

The Mediterranean Sea is greatly affected by marine litter. In this area, research on the impact of plastic debris (including microplastics) on biota, particularly large filter-feeding species such as the fin whale (*Balaenoptera physalus*), is still in its infancy. We investigated the possible overlap between microplastic, mesoplastic and macrolitter accumulation areas and the fin whale feeding grounds in in a pelagic Specially Protected Area of Mediterranean Importance (SPAMI): the Pelagos Sanctuary. Models of ocean circulation and fin whale potential habitat were merged to compare marine litter accumulation with the presence of whales. Additionally, field data on microplastics, mesoplastics, and macrolitter abundance and cetacean presence were simultaneously collected. The resulting data were compared, as a multi-layer, with the simulated distribution of plastic concentration and the whale habitat model. These data showed a high occurrence of microplastics (mean: 0.082 items/m^2, STD ± 0.079 items/m^2) spatial distribution agreed with our modeling results. Areas with high microplastic density significantly overlapped with areas of high macroplastic density. The most abundant polymer detected in all the sampling sites was polyethylene (PE), suggesting fragmentation of larger packaging items as the primary source. To our knowledge, this is the first study in the Pelagos Sanctuary in which the simulated microplastic distribution has been confirmed by field observations. The overlap between the fin whale feeding habitat and the microplastic hot spots is an important contribution for risk assessment of fin whale exposure to microplastics.

Keywords: floating plastic debris, microplastics, Mediterranean Sea, convergence areas, modeling, fin whales, Marine Protected Area

INTRODUCTION

In the Mediterranean Sea, marine litter has recently been confirmed as a critical issue (Eriksen et al., 2014; Cózar et al., 2015; UNEP/MAP, 2015; Suaria et al., 2016). The highest fraction (∼80%) of marine litter comprises plastic, particularly small sized plastic. This is exacerbated by the basin's limited water exchanges as well as by the presence of densely populated and trafficked coastal areas. An increasing number of studies have investigated the interactions of marine fauna with marine debris in the Mediterranean basin, covering a vast array of species affected by marine litter, such as invertebrates, fish, reptiles and birds (Campani et al., 2013; Codina-García et al., 2013; Deudero and Alomar, 2015; Romeo et al., 2015; Alomar et al., 2016). On the other hand, research on the impact of microplastics (plastic fragments smaller than 5 mm) and mesoplastics (plastic fragments smaller than 25 mm) on large filter-feeding species such fin whale (*Balaenoptera physalus*) is a largely unexplored topic.

Fin whale is the only resident mysticete in the Mediterranean and aggregates during the summer in the feeding grounds of the north-western Mediterranean Sea (Panigada et al., 2011; Druon et al., 2012). Fin whales potentially ingest microplastics during their feeding activity and might undergo the accumulation of plastic additives in their tissues, leached by plastic particles ingested (Fossi et al., 2012). The same authors investigated the interaction between free-ranging fin whales and microplastics by comparing populations living in two semi-enclosed basins, the Mediterranean Sea and the Gulf of California (Mexico) (Fossi et al., 2016). In these studies, high concentrations of microplastics and plastic additives (phthalates) were detected in neustonic samples collected in the Pelagos Sanctuary for Mediterranean Marine Mammals (hereafter Pelagos Sanctuary). Pelagos Sanctuary is the only pelagic Marine Protected Area in the Mediterranean Sea, designated as one of the Specially Protected Areas of Mediterranean Importance (SPAMI). This marine area, located in the north-western Mediterranean Sea, is characterized by high offshore productive frontal features that attract a variety of large marine vertebrates including eight cetacean species (Coll et al., 2012). This exceptional biodiversity coexists with high human pressure (Fossi et al., 2013; Pinzone et al., 2015), including plastic pollution (Collignon et al., 2012; Fossi et al., 2012; Cózar et al., 2015).

Using observations and models, a number of authors have reported the existence of five large-scale accumulation regions of floating plastic debris in the oceans corresponding to each of the subtropical gyres located on either side of the Equator (Cózar et al., 2014; Eriksen et al., 2014; Law et al., 2014; van Sebille et al., 2015). As for the Mediterranean sea, the average concentration found is comparable to the high values found in subtropical gyres (Cózar et al., 2015; Suaria et al., 2016). This high concentration is in part explainable considering the retention of floating debris facilitated by a limited surface outflow toward the Atlantic ocean (Lebreton et al., 2012). Moreover, within the Mediterranean, there is a marked variability of hydrodynamic circulation features, mainly induced by a strongly variable atmospheric forcing that can also lead to particularly high concentrations corresponding to specific structures, such as fronts and eddies (Zambianchi et al., 2014).

Marine litter drift in the Mediterranean was simulated at a climatological level by ocean circulation models with the main objective of determining the possible existence of permanent, or at least long-term, accumulation areas. Long-term accumulation areas of marine litter in the Mediterranean were not found (Mansui et al., 2015), although floating items may be retained and eventually redistributed by meso-scale structures in a timescale of a few weeks or months. These long-term simulations can be used to derive general trends of marine litter distribution on climatological time scales (years or decades), although such model data are not directly comparable to observations, since the distribution derived from field surveys is limited to short specific periods.

In addition, the dynamics of fronts and gyres are complex and are associated with convergence and divergence areas, in which floating items such as microplastics tend to concentrate. Moreover, the dynamics of mesoscale oceanic features, which generate upwelling (divergence) and downwelling (convergence), are likely to drive both the concentration of floating particles and the presence of favorable feeding habitats for several species, including fin whales (D'Amico et al., 2003), as the spatial and temporal scales of the distribution of these feeding habitats are connected to the variability of combined biogeochemical/hydrodynamical covariates distributed over the area.

Since plastic particles are not uniformly distributed in the Mediterranean Sea, like elsewhere, the possible overlap between plastic debris accumulation areas and charismatic mega-fauna feeding grounds, is a challenging research task. Data from hydrodynamic models and field observation are needed to define accumulation areas of plastic fragments and to assess the risk of exposure of Mediterranean fauna.

In this paper, we present the results of the Plastic Pelagos survey aimed to investigate, using a multi-layer multidisciplinary approach, whether the fin whale feeding grounds and the areas of high floating plastic debris concentration can overlap and create critical conditions for fin whales exposed to plastic in the Pelagos Sanctuary. For this reason, data on microplastics, mesoplastic, macrolitter distribution, cetacean sightings and whale preferred feeding habitat in the north-western Mediterranean Sea were merged.

The novelty of the approach was the use of a sub-seasonal (≈15–30 days) timescale, instead of a climatological one, where models and field data have similar time-scales of variability, which allowed an evaluation of the risk to marine organisms living in the area.

METHODS

Plastic Pelagos Survey and Sampling

The Plastic Pelagos survey was carried out for 10 days (8–18 September 2014) with the Research Vessel ASTREA (ISPRA) across the whole Pelagos Sanctuary. The research cruise was planned for several research activities, such as: (a) microplastic and mesoplastic sampling in potential accumulation

areas identified by ocean models and satellite data, (b) macroplastics survey and (c) cetacean survey (in particular fin whales). The experimental design and the selection of the sampling sites was determined using the hydrodynamic forecast produced by LaMMA (http://www.lamma.rete.toscana.it/en/currents-lamma-roms-model), satellite data (SST, chlorophyll-a and altimetry), and the operational model of fin whale potential habitat (Druon et al., 2012). During the Plastic Pelagos survey, a total of 967 nautical miles were traveled, 21 zooplankton/microplastic samples were collected, (Figure 1SM) and, simultaneously, 78 miles were monitored for marine litter.

Sampling of Microplastics

All zooplankton-neustonic/microplastic samples were collected during daylight hours and under calm weather and sea conditions. The samples were collected with a High Speed Manta Trawl (mouth opening: 25 × 50 cm; 330 μm mesh size) equipped with a flow meter to measure the volume of filtered water. The GPS coordinates were noted at the beginning and the end of the sampling station. The net was towed horizontally in surface waters at a speed of approximately 3–4 knots for 30 min. The net was washed on board, to collect particles and zooplankton and to avoid contamination, and the resulting materials preserved in a 4% formaldehyde-seawater buffered solution for subsequent analyses of plastic particles and further analysis of zooplankton.

Counting and Characterization of Microplastics and Mesoplastics

For the analysis of plastic particles, the samples were observed under a stereomicroscope Stereo Zoom NBS (mod. NBS-STMDLX-T) with a LED light and micrometer ocular lens. During the laboratory procedure, care was taken to prevent airborne contamination of samples by performing sample analysis in a clean air flow room. Each plastic particle was characterized and classified by: (a) color: white, black, red, blue, transparent, green, other color and (b) size: ≤0.5; 0.51–1.0; 1.01–2.5, 2.51–5.0 mm for microplastics and 5.01–25 mm for mesoplastics. The microplastics and mesoplastics were also isolated, dried at 60°C for 24 h and weighed on a petri dish. The weight was measured at least three times until a stable value was obtained.

Micro and mesoplastics collected with the manta trawl (number of items and weight) were normalized to the total water surface filtered and expressed as items/m^2 and mg/m^2. All data were corrected according to weather and sea conditions considering the possible "wind stress" effect, considering the wind speed (m/s) and wave height (m) applying the correction factors adopted by Kooi et al. (2016) and Kukulka et al. (2012).

Polymer Identification: Fourier Transform Infrared Spectroscopy

Plastic polymers were identified using the Fourier Transform Infrared (FT-IR) spectroscopy technique (Hummel, 2002) in 10% of the total microplastic items and 50% of mesoplastic items detected in each sampling site. For each plastic fragment, depending on its heterogeneity (including degradation status and fouling presence), three measurements were carried out. The samples were compressed in a diamond anvil compression cell and infrared spectra were acquired using an Agilent Cary 630 FTIR spectrophotometer. Spectra were collected in transmission mode in 16 scans, with a resolution of 4 cm^{-1}. Agilent Micro Lab FTIR software was used for output spectra elaboration. For the identification of polymers, a similarity algorithm was used searching in three different Agilent polymer spectral databases, followed by a visual analysis comparison of characteristic bands in the reference spectrum. Only spectra matching more than 80% with reference polymers were accepted; this minimum hit quality is greater than the one adopted by Lusher (Lusher et al., 2013).

Quantification and Monitoring of Floating Macrolitter

During the Plastic Pelagos survey, for the first time in the Mediterranean Sea, a monitoring of floating macrolitter (items larger than 2.5 cm) was simultaneously carried out with the microplastic and mesoplastic sampling. The methodology used for the quantification and monitoring of floating marine debris was visual observation from the vessel. The protocol is based on the experience acquired from the National Oceanic and Atmospheric Administration (NOAA) in previous studies on floating marine litter that includes the computation of density of marine litter within the transect area (Arthur et al., 2009). The classification system used is consistent with the one reported in Descriptor 10 of the European Marine Strategy Framework Directive (MSFD Technical Subgroup on Marine Litter, 2013). The observations were made from the bow of the boat and only in optimum sea and weather conditions (calm seas and good visibility). Only floating litter observed without binocular within 20 meters from the boat was taken into account. Observers were changed every 30 min to avoid fatigue. The data were then processed in terms of quantity, size and quality. The density of macrolitter was calculated using the formula (Hinojosa and Thiel, 2009): $D = N/(W \times L)$; where N is the number of observed plastic debris, W is the maximum distance (0.02 km in the present study) perpendicular to the transect and L is the total length (in km) of the transect.

Statistical Analysis

The plastic data set was processed using non-parametric tests. The normality of the data was checked by a Pearson omnibus normality test. The non-parametric Kruskal-Wallis analysis of variance was used. Correlation between micro-, meso-, and macroplastics was performed with the Spearman correlation ($p < 0.05$). All the statistical analyses were conducted using STATISTICA 10 (StartSoft) software.

Cetacean Survey

The vessel tracks were not designed to obtain an even coverage of the study area but rather to maximize the encounter rate with whales (based on previous experience and modeling information). During the searching effort, two observers were positioned, one at each side of the vessel, scanning the sea surface looking for cetaceans using 7 × 50 magnification binoculars equipped with a compass. Observations were made preferentially in favorable conditions, i.e., with daylight and good visibility

and sea state ≤3 Beaufort. The sea state was recorded every 60 min, or more frequently if changes in conditions occurred (Panigada et al., 2005). The transect was interrupted once a cetacean was located for further approach to record geographic position, movements, group size, behavior, and to assess the presence or absence of calves and sub-adults. The species of interest in the project was the fin whale *(B. physalus*) (details on the species in Supplementary Material). *Stenella coeruleolba*, *Tursiops truncatus* and *Grampus griseus* were also investigated during the cruise (see Figure 2SM).

Model of Potential Fin Whale Habitat

The chosen modeling approach of potential fin whale habitat relies on the niche theory, which links environmental with ecological processes to select a limited set of predictors and improve model interpretability. The potential feeding habitat of fin whales (Druon et al., 2012) (FHO - Feeding Habitat Occurrence), was mainly traced by the occurrence of productive oceanic fronts which are perceived as features sufficiently stable to sustain zooplankton production. By relating the proximity of over 10 years of fin whale sighting locations (n = 1,451) in the Western Mediterranean Sea to concurrent remotely sensed oceanic fronts of chlorophyll-a, the habitat model is able to efficiently detect and map the fin whale's preferred feeding habitat on a daily time scale.

Compared with habitat modeling (Druon et al., 2012) the favorable feeding habitat was identified here by sea surface chlorophyll-a (Chl-a) fronts only and not in combination with satellite-derived SST fronts. Indeed, infrared data was found to be more unstable from day-to-day than optical data (Chl-a). Overall, the potential feeding habitat was derived on a daily basis using a) the productive frontal features (Chl-a fronts), b) a preferred range of surface Chl-a concentration and c) a minimum water depth. The optimized set of parameters that was used to define the fin whale's preferred habitat had the following values (using Chl-a data from the MODIS-Aqua sensor): linear increase of daily habitat value from 0.3 to 1 in the range of Chl-a horizontal gradient from 0.00086 to 0.0052 mgChl-a.m^{-3}.km^{-1}, and 1 above the latter value,- 0.11 < Chl-a concentration < 0.50 mg.m^{-3}- water depth > 90 m.

Ocean Circulation Model and Satellite Data

In the period of the sampling cruise (September 2014), the circulation in the North Tyrrhenian and Ligurian Sea was deduced by a joint analysis of satellite and modeling data: sea level anomaly (SLA), absolute dynamic topography (ADT), sea surface temperature (SST), chlorophyll a concentration (Chl-a), and hydrodynamic models at both basin scale (re-analysis of the Copernicus Marine Environment Monitoring Service, CMEMS) and at regional scale (Tyrreno-ROMS).

The Tyrreno-ROMS model is a regional implementation of the Regional Ocean Modelling System (ROMS) currently operational at the LaMMA consortium for ocean forecast. The model is implemented in a domain covering the Tyrrhenian Sea, the Ligurian Sea, and the western portion of the Mediterranean Sea to the east of the Gulf of Lyon, with a horizontal resolution of 2 km. ROMS has a generalized vertical, terrain-following, coordinate system (Shchepetkin and McWilliams, 2005), so-called s-coordinates, in our case implemented through 30 s-levels. Initial and boundary conditions are taken from the CMEMS. Turbulent fluxes on the ocean/atmosphere interface, estimated by the bulk flux formulation (Fairall et al., 1996), are derived from an implementation of the WRF-ARW (Weather Research and Forecasting-Advanced Research) model over the central Mediterranean area at 3 km resolution and using European Center Medium Weather Forecast (ECMWF) data as initial and boundary conditions. Regarding satellite data, weekly updated delayed maps of sea level anomaly (SLA), Ssalto/Duacs altimeter products, mean dynamic topography (MDT), and the resulting absolute dynamic topography (ADT) maps (Iacono et al., 2013) were selected and distributed by the CMEMS. As for SST, the CMEMS sea surface temperature nominal operational product for the Mediterranean Sea, daily gap-free maps (L4) at 1 km horizontal resolution (Buongiorno Nardelli et al., 2013) were chosen. Chl-a concentrations were estimated by the OC5 algorithm (Gohin et al., 2002) on NASA MODIS AQUA reflectances, 1 km space resolution, as this algorithm presents intrinsic robustness in the waters of the Ligurian and North Tyrrhenian Seas (Lapucci et al., 2012; more details in Supplementary Material).

Modeling Marine Litter Distribution

The marine litter transport at the sea surface has been modeled using virtual particles, advected as Lagrangian tracers in our numerical circulation model. To identify areas where floating particles can be concentrated, the tendency to accumulation/dispersion from homogenous initial conditions can be estimated through the parameter

$$C_t = \frac{N_t}{N_0}$$

where C_t is the dimensionless concentration of floating debris at time t, N_0 is the number of simulated floating particles in an area equal to the size of the model resolution at the initial time (in our case, in open sea conditions, 10^2 uniformly distributed particles for each square element), and N_t is the number of floating particles in the same element area at time t. This is motivated by the lack of global information describing the distribution of floating debris (Mansui et al., 2015).

We simulated the hydrodynamic conditions for the entire period of the survey by using the Tyrreno-ROMS regional model, initialized every day with the CMEMS analysis data. Every simulation obtained by the regional hydrodynamic model was stopped after 15 days because of the progressive decay of its reliability after 1–2 weeks of simulation. Hydrodynamic simulations started 15 days before the beginning of the survey, and were performed up to 15 days after the end, so that a total of 40 simulations have been realized. At the beginning of each simulation, an uniform release of particles in the study area, by using the virtual Lagrangian floats available in ROMS, was performed in order to simulate the 15-days evolution of floating items.

Due to the uncertainties in the hydrodynamic fields, instantaneous concentrations computed with the present method

may be progressively unreliable with increasing simulation time. At the same time, the concentration of a passive tracer (such as floating debris) at the mesoscale depends on previous hydrodynamic history, and too short of a simulation time does not allow particles to concentrate or to disperse on significant hydrodynamic structures such as fronts and gyres. Therefore, to calculate the value of the dimensionless concentration, or relative density, C_t, best correlated with observations, we made averages of C_t corresponding to different model simulations. Each averaged concentration is estimated from instantaneous concentrations, as for instance the mean value $< C_3 >$ is obtained with the instantaneous values C_3, computed after 3 days of each different simulation, taken over different time periods of 48, 144, and 336 h centered at the time of observation. As a consequence, the accumulation/dispersion of the plastic particles was assumed to be due to hydrodynamic structures that have a persistence longer than 1 day. This average was centered to consider possible uncertainty in the presence of the hydrodynamical structures over time. In fact, we see that a time shift of the position of the averaging window does not significantly change our results.

Statistical correlations between observed surface microplastic concentration and both the instantaneous C_t and the mean values $<C_t>$ were computed. Considering only instantaneous concentrations, this comparison showed a progressive decrease of correlation with increasing simulation time. On the contrary, $<C_t>$ show a much stronger correlation.

RESULTS

During the Plastic Pelagos survey, floating marine litter (micro-,meso- and macroplastic) sampling and cetacean survey were conducted to verify the possible overlap between the marine litter accumulation areas and preferred fin whale feeding ground identified by regional hydrodynamic circulation and fin whale potential habitat models, in the Pelagos Sanctuary. This multi-layer approach (models and field data sets) allowed identifying areas of higher risk of exposure to plastic ingestion for fin whale and other cetacean species in the SPAMI.

Microplastics Abundance, Characterization and Spatial Distribution

Data revealed a high occurrence of microplastics (mean: 0.082 items/m^2, STD ± 0.079 items/m^2) (**Figure 1A**) in the investigated surface neustonic/planktonic samples. The samples collected close to Genoa harbor (PP5, PP6) and in the proximity of Capraia Island (PP11) (**Figure 1A**), showed the highest values of the whole dataset. The average concentration of plastic particles is similar to the one previously shown by other authors in the Pelagos Sanctuary (Collignon et al., 2012; Fossi et al., 2016). These data are consistent and slightly higher than those measured in the Mediterranean Sea by Faure and collaborators in 2015. The Tuscan Archipelago area (Capraia Island) was also found to be one of the site with highest concentration values and weight of microplastics, as also recently highlighted (Suaria et al., 2016).

Microplastic size analysis is in line with (Panti et al., 2015) with 47% of microplastics in the size range between 1 and 2.5 mm (**Figure 1B**). Characterization in terms of color and dimension in the different sampling sites is reported in **Figure 1C**. Fragment is the most frequent shape and transparent and white the predominant colors. A more detailed analysis was performed on the 10% of the total microplastics isolated during the analytical procedure. The most abundant polymer detected in all of the sampling site was polyethylene (PE), suggesting the potential origin of the microplastic analyzed by fragmentation of packaging items (Plastics Europe, 2015). PE and polypropylene

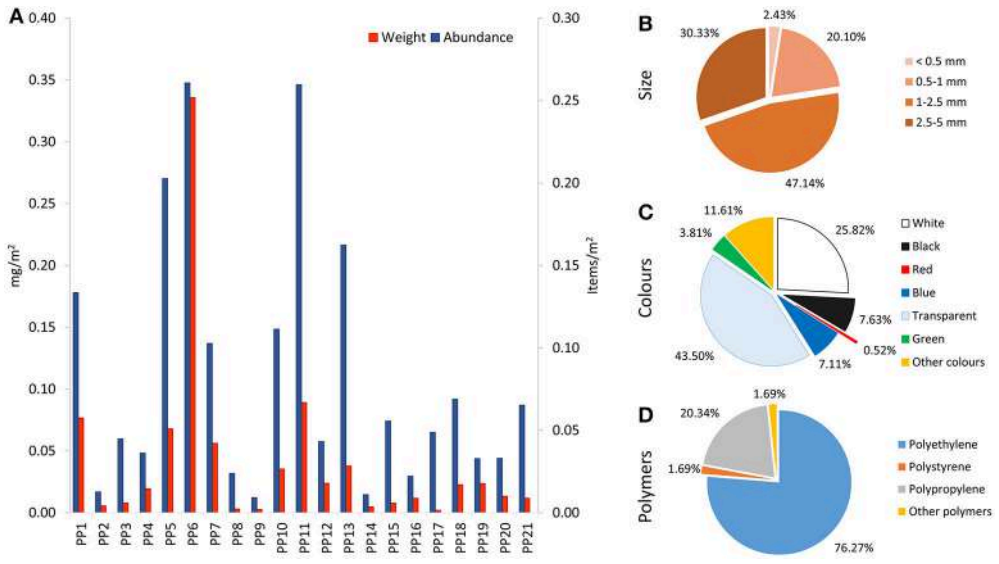

FIGURE 1 | Microplastic abundance and characterization in the Pelagos Sanctuary. **(A)** Microplastic abundance (items/m^2) and weight (mg/m^2) in the different sampling sites; **(B)** microplastic size; **(C)** microplastic color; **(D)** microplastic polymers.

(PP) represent 76 and 20% of the total plastic polymers measured, respectively (**Figure 1D**).

Mesoplastics Abundance, Characterization and Spatial Distribution

Mesoplastics were present in 19 out of the 21 samples, ranging from 0 to 0.037 items/m^2, (mean: 0.0126 items/m^2, STD ± 0.0118 items/m^2) (**Figure 2A**). The data are in the same order of magnitude as found by Faure and collaborators in 2015, where the maximum value is 0.021 items/m^2. Transparent was the predominant color (**Figure 2B**). The polymer analysis was performed on 50% of the total mesoplastics isolated during the analytical procedure. Similarly to microplastics, PE and PP were also the most abundant polymers for this size class (**Figure 2C**).

Microliter Abundance, Characterization and Spatial Distribution

Simultaneously with manta trawl sampling, a survey of floating macrolitter was carried out, for the first time in the Mediterranean Sea (**Figure 3**) in order to explore the correlation between these two data. The analysis was performed on the total floating macrolitter, considering all objects defined as marine litter according to NOAA. A more specific analysis was made on plastic objects (macroplastics), which represent 83.5% of total floating litter composed mainly by fragments of larger plastic items, bottles/packaging items and fishing gears. Seventy-eight miles were monitored during the cruise for a total of 1.6 km^2 (**Figure 3**) with an average value of 175.24 macroplastics/km^2. Again, the areas close to the Genoa harbor and in proximity to the Capraia Island showed the highest values for macroplastics, confirming both areas as hot spots for plastic debris in the Pelagos Sanctuary. In a similar survey across the Mediterranean Sea, Suaria and Aliani (Suaria and Aliani, 2014) found a lower mean value of floating debris (6.9 items/km^2) with a maximum value of 194.6 items/km^2. Finally, in the investigated areas of the Pelagos Sanctuary, a significant correlation between micro-, meso- and macroplastic debris was found (**Figure 4**).

Cetacean Survey

Four different cetacean species were identified during the sampling cruise (Bp = *B. physalus,* Sc = *S. coeruleolba*, Tt = *T. truncatus*, Gg = *G. griseus*) in the Pelagos Sanctuary with a total of 14 sightings and 44 specimens. The respective sighting sites and numbers of individuals are reported in **Table 1** and in Figure S2.

Ocean Circulation in the Pelagos Area During the Survey

In general, ocean circulation in the Pelagos area appears to be associated with a prevailing transport from South to North. This dominant circulation feature is in turn modulated by intense mesoscale activity characterized by ocean eddies (cyclonic and anticyclonic), meandering currents and fronts. The spatial and temporal resolution of the Tyrreno-ROMS allows the simulation of all such phenomena. Along the western and eastern Corsica coast two branches of ascending currents (Eastern and Western Corsica currents) converge and give a fundamental contribution to generation of the North Mediterranean current (**Figure 5A**). The Mean Kinetic Energy (MKE) has been used as a proxy for the velocity field (**Figure 6B**) in order to highlight the main circulation (Mansui et al., 2015). The currents generating the North Mediterranean current are associated with a wide cyclonic area with a counter current to the East, which generates a considerable negative sea level anomaly as well as relatively low SST levels and a high level of Chl-a. The satellite observations reported in **Figure 5B** of MADT, SST and Chl-a, for August

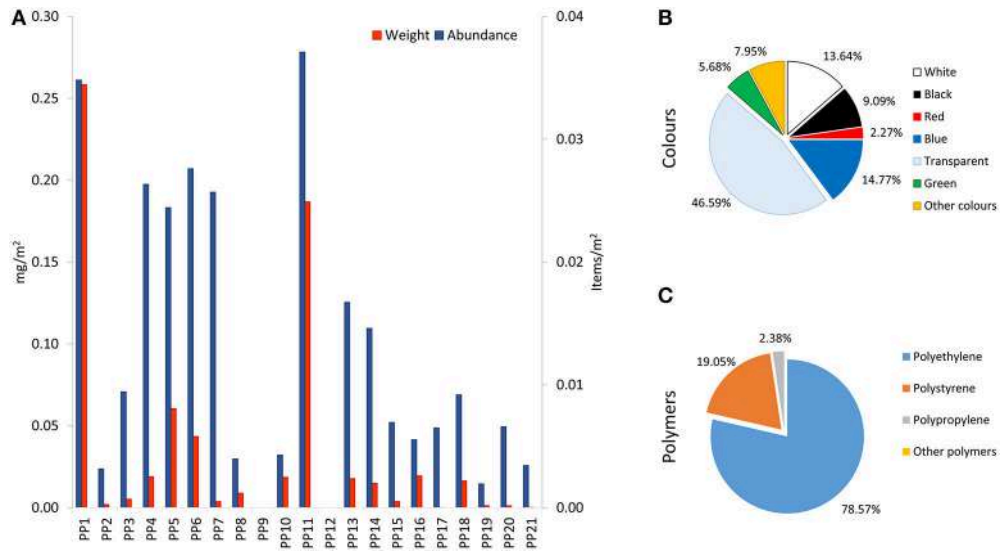

FIGURE 2 | Mesoplastic abundance and characterization in the Pelagos Sanctuary. **(A)** Mesoplastic abundance (items/m^2) and weight (mg/m^2) in the different sampling sites; **(B)** mesoplastic color; **(C)** mesoplastic polymers.

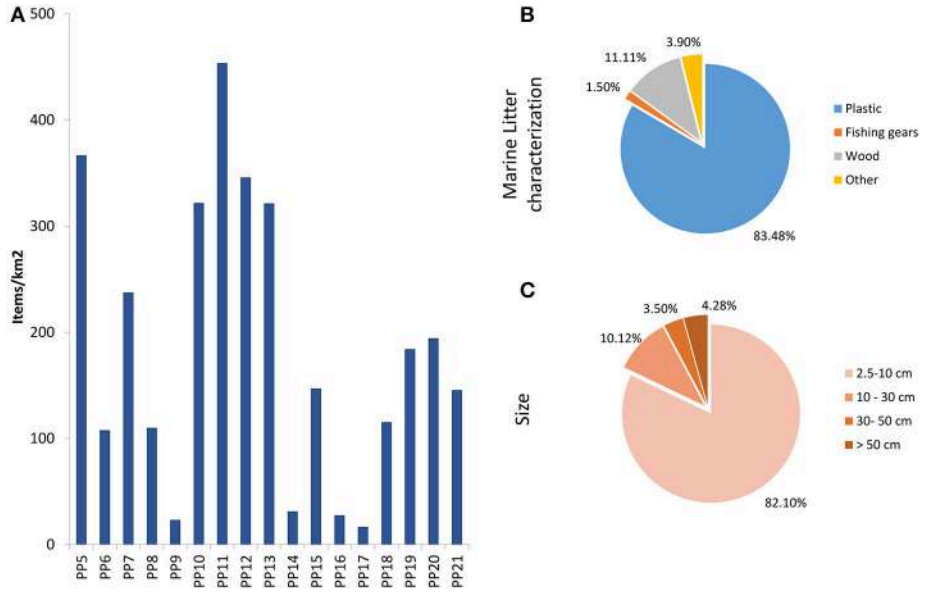

FIGURE 3 | Macrolitter abundance and characterization in the Pelagos Sanctuary. **(A)** macrolitter abundance in the different samplig sites (items/Km^2); **(B)** macrolitter characterization; **(C)** macrolitter size.

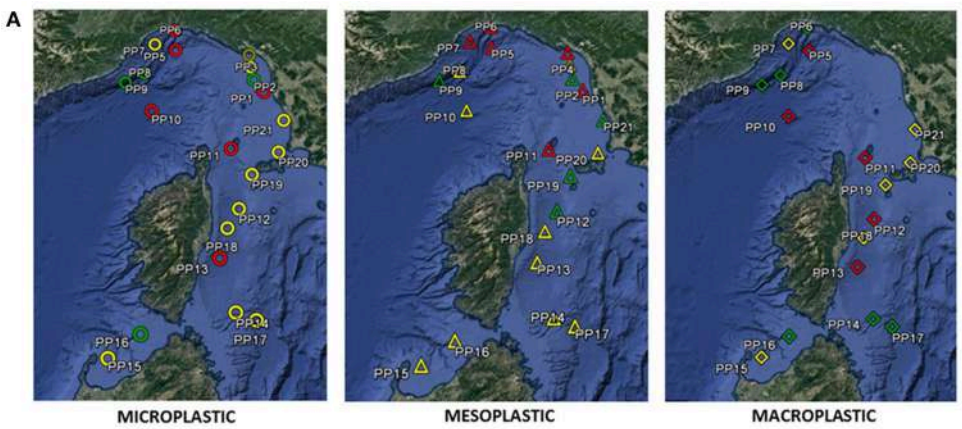

	Microplastc item/m^2	Mesoplastc item/m^2	Macroplastc items/Km^2
	0.264-0.111	0.033-0.012	453.399-237.143
	0.110-0.022	0.012-0.003	237.143-70.822
	0.022-0.009	0.003-0.000	70.822-16.264

B

	Microplastics/m^2	Mesoplastics/m^2	Macroplastics/km^2
Microplastics/m2	1	0.63	0.61
Mesoplastics/m2	0.63	1	0.22
Macroplastics/km2	0.61	0.22	1

FIGURE 4 | Spatial distribution of microplastics, mesoplastics and macroplastics in the Pelagos Sanctuary during the Plastic Pelagos survey. **(A)** The different colors of the sampling sites represent the relative concentration of items/m^2 (microplastics and mesoplastics) and items/km^2 (macroplastics). Red symbols are values ≥75th percentile; yellow are values <75th and ≥25th percentile; green are values <25th percentile; map produced using the Google Earth version 7.1.5.1557 open source software; **(B)** Correlation between micro-, meso-, and macroplastic in the Pelagos Sanctuary.

TABLE 1 | Cetaceans sightings in the Pelagos Sanctuary during the Plastic Pelagos survey.

Species	Date	No individuals	Latitude	Longitude	Hour
Tursiops truncatus	08/09/2014	8	43°46.927N	10°00.725E	15:25
	09/09/2014	2	44°04.223N	09°29.083E	10:40
Stenella coeruleoalba	09/09/2014	10	44°04.400N	09°07.588E	12:00
	10/09/2014	4	43°40.734N	07°59.913E	11:30
Grampus griseus	10/09/2014	9	43°40.288N	08°08.933E	17:00
Balaenoptera physalus	11/09/2014	4	43°33.038N	08°01.032E	09:52
	12/09/2014	2	42°57.868N	09°48.809E	15:30
	14/09/2014	5	41°21.231N	10°04.243E	12:40

24th 2014, supports the presence of hydrodynamic structures in accordance with the circulation model results. The mesoscale anticyclonic eddy structure located around Capraia Island (Structure A in **Figure 5A**) is outlined by the regional Tyrreno-ROMS model and confirmed by satellite data, showing a relative maximum of MADT, typical of downwelling dynamics.

This "Capraia gyre," as a potential accumulation area of marine debris, was already observed (Schroeder et al., 2011), although it is still not completely characterized in its seasonal variability. The well-marked cyclonic gyre in the northern Tyrrhenian Sea (Structure B in **Figure 5A**), or northern Tyrrhenian gyre (Artale et al., 1994), is also shown on satellite data through relative minimum levels of SSTs, relative maximum levels of MADT, and higher Chl-a levels at the center of the gyre, possibly due to the upwelling associated with cyclonic dynamics.

Comparison between Microplastic Field and Model Data

To compare model data with *in situ* measurements, we computed the statistical correlation between the observed surface microplastic concentration and the simulated values of the relative density parameter C_t (or its mean values $<C_t>$). This comparison showed: (a) a progressive decrease of correlation of instantaneous values C_t from 3 to 15 days that is likely due to the reliability decay in the regional hydrodynamic model for increasing simulation times (**Table 2**); and (b) a significant increase of correlation of mean values $<C_t>$, with t ranging from 3 to 15 days and using time windows of 144 and 366 h, as shown in **Table 3**.

Taking an appropriate average of instantaneous value, the simulation results confirm that concentration levels are strongly dependent on the hydrodynamic history. The mean values $<C_t>$, computed over the different time windows, can be utilized as a tool to highlight the persistence of hydrodynamic structures that may have contributed accumulating or dispersing the floating particles in a given area.

The strong statistical correlation (**Table 3**) between the field data and the mean relative density, $<C_t>$, computed by the regional model, allows to convert the dimensionless concentration into physical concentrations expressed in terms of standard units (e.g., items/m^2). A bias and a factor for unit conversion were estimated using a linear fit between the modeled and observed concentrations. Hence the dimensionless concentration or relative density, $<C_t>$, can be transformed into a dimensional concentration of floating plastic debris, $<C>$, by a linear relationship of this type:

$$<C>\ [\text{items/m}^2] \ = \ A \times <C_t>[\text{a.u.}] \ + \ B.$$

In particular, for our best case (hence the relative mean density $<C_{15}>$ computed over 336 h, as in **Table 3**), the linear fit gives the values: $A = 3.42$ and $B = -1.51$ (**Figure 7A**). Although the values of correlation obtained are quite high, the number of samples reported in **Figure 7A** is not large enough to obtain a more significant correlation. This could be achieved by a more extended study.

The estimated concentrations expressed in terms of standard units can be plotted on the map, as reported in **Figure 8**, where modeled microplastic concentrations were averaged for the whole month of September 2014. The highest microplastic concentration value, found close to Capraia Island (PP11, Structure A in **Figure 5A**), is very well reproduced by the regional model simulation (**Figures 7B**, **8**). The most prominent hydrodynamic characteristic of this point is the stable anticyclonic circulation for the investigated period (mid-August – mid-September). In other areas, characterized by strong hydrodynamic features, concentration values from our modeling are very similar to those measured at sea, such as point PP17 (**Figures 4**, **7B**) which is the closest to the most relevant cyclonic feature of the area (the Northern Tyrrhenian gyre, Structure B in **Figure 5A**), and point PP10 (**Figures 4**, **7B**) in the middle of the cyclonic circulation over the Ligurian sea (Structure C in **Figure 5A**). In general, most of the observed variations can be explained in terms of prominent hydrodynamic features (observed and modeled) in the period of interest, with the remarkable exception of coastal areas in which local inputs can affect abundances and distributions of floating debris, for instance, points PP5, PP6, PP7 close to the Ligurian coast (e.g., Genoa) (**Figures 4**, **7B**).

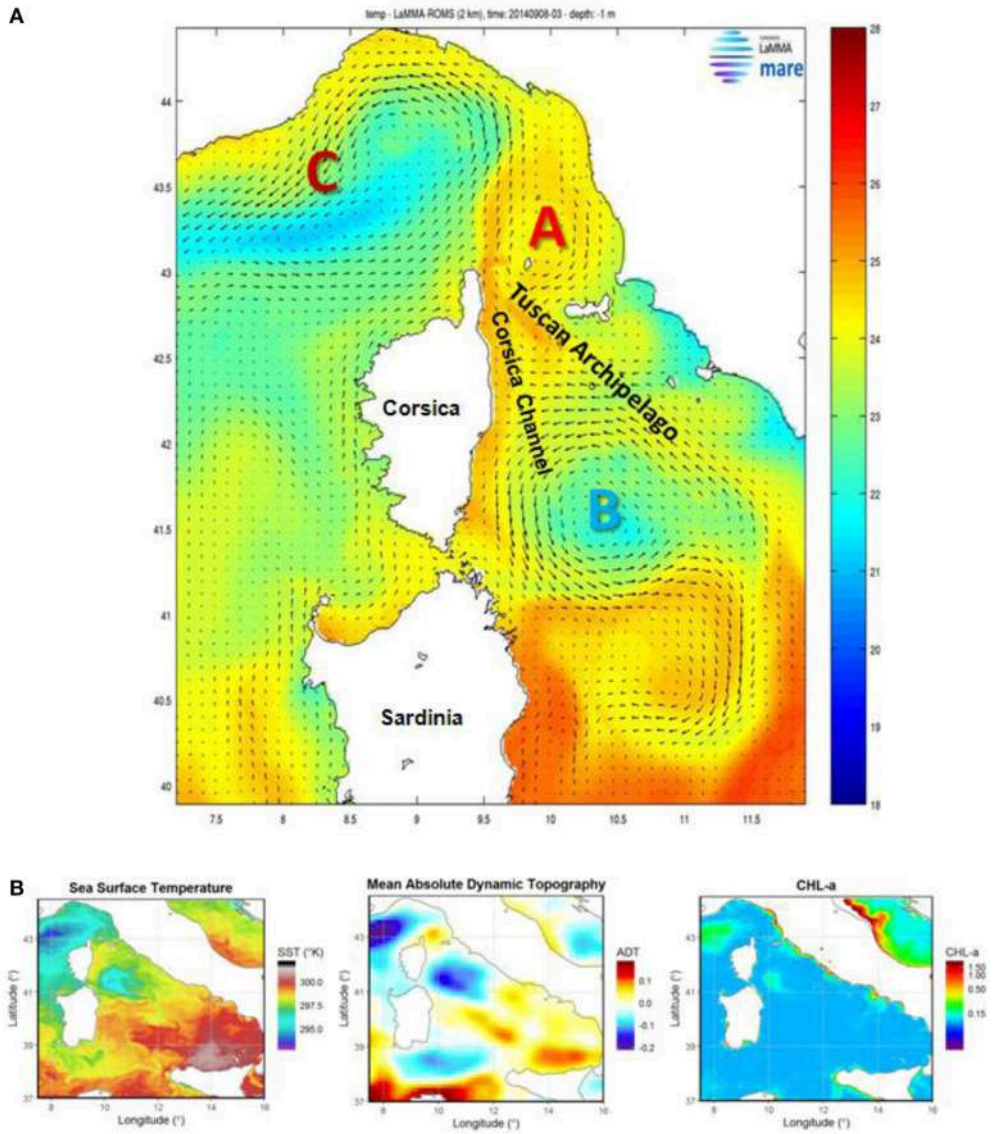

FIGURE 5 | Relevant hydrodynamic structures in the Pelagos Sanctuary area. **(A)** Anticyclonic circulation of the "Capraia Gyre" (Structure A), Northern Tyrrhenian Cyclone (Structure B), Ligurian current (Structure C); map produced using the Matlab Release 14 software; **(B)** SST, MADT, and Chla maps, 28th August 2014; maps produced using the IDL 5.6 with Rgdal R package version 1.1-3 software, and the SeaDAS 7.2 26 and R library 27 open-source software.

Microplastic Convergence Areas and Fin Whale Feeding Grounds

The overlap of preferred feeding habitat for planktivorous species with high concentrations of microplastic areas can increase the probability of plastic ingestion by these marine species. Because the FHO index can point out the presence of favorable feeding habitats in a certain area (Druon et al., 2012), we can compare its related maps (**Figure 9A**) with the simulated microplastic concentration (**Figure 9B**) to give an estimation of the potential impact of floating plastic on fin whale in the Pelagos Sanctuary.

The results of the model simulations show that some upwelling areas associated to cyclonic circulation, where FHO is particularly high, correspond to relatively low levels of microplastic concentration (**Figures 9A2,B2**). Instead the areas characterized by anticyclonic circulation, associated with downwelling (for example the Capraia gyre), despite their high values of plastic concentration, can be less favorable for whale feeding (**Figures 9A1,B1**). On the other hand, there is a possible overlap of feeding habitats and areas of high microplastic concentration in the external part of both cyclonic and anticyclonic structures. With cyclonic structures, the major contribution to the ingestion risk could be due to the high probability of feeding determined by the proximity to highly trophic upwelling areas. In the case of anticyclonic structures, the contribution of relatively high concentration of plastic could play a major role even with more oligotrophic conditions.

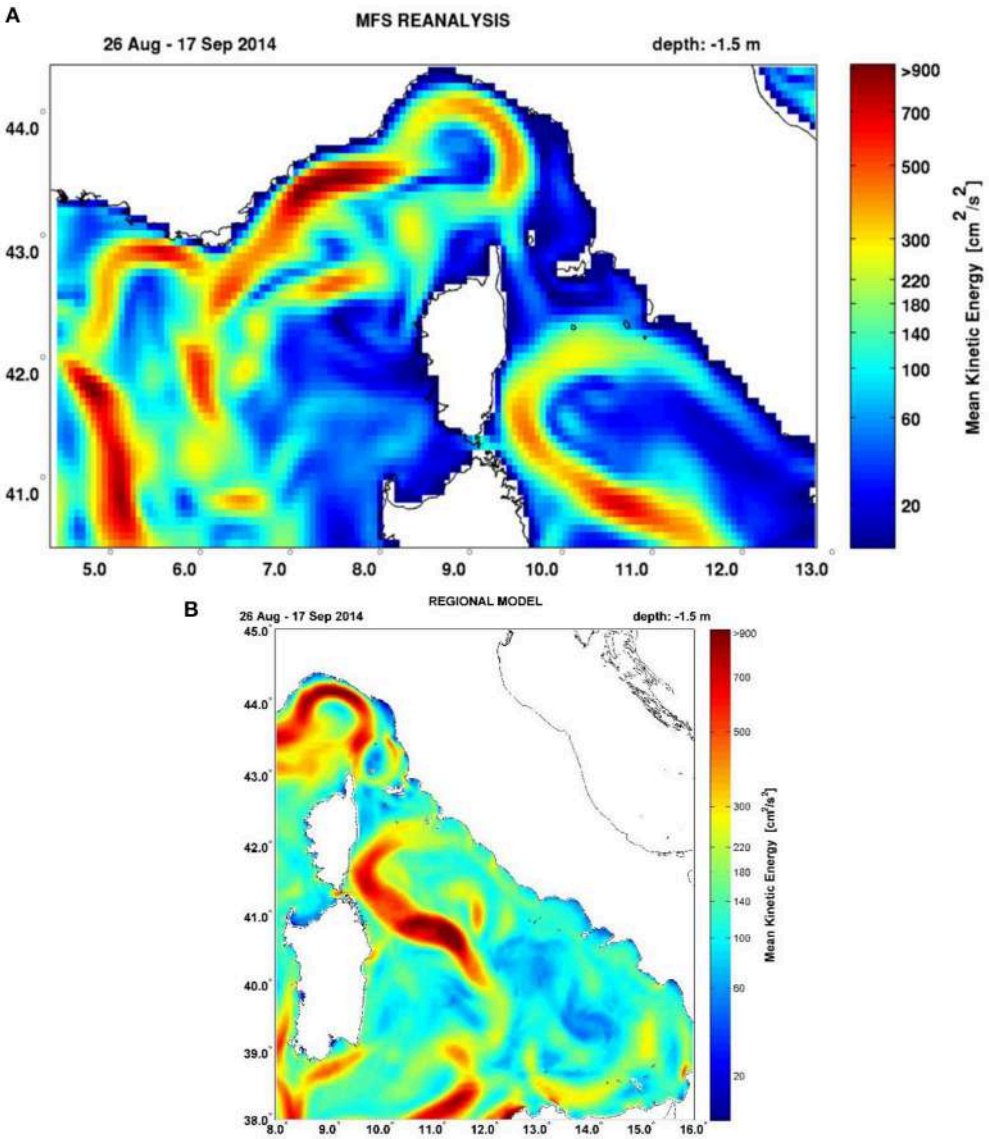

FIGURE 6 | Ocean circulation model and satellite data. **(A)** Mean Kinetic Energy (MKE) distribution from CMEMS, for the period 26 August-17 September 2014, which highlights the most energetic circulation patterns; **(B)** Mean MKE result from the Tyrreno-ROMS circulation model for the same period. Major differences between the Mediterranean CMEMS and the Tyrreno-ROMS model consist in improved representation of small scale hydrodynamic features.

TABLE 2 | Correlations obtained by using instantaneous values C_t of model concentrations.

	C_3	C_7	C_{15}
R	0.36	−0.04	−0.07
p-value	0.205	0.90	0.816

Besides the comparison with the feeding habitat model, it is important to consider the cetaceans sighting data obtained during the cruise. In particular, some of the direct whale observations are close to the areas with a high FHO index and many of them are in the areas with high estimated microplastic concentrations (**Figures 9A,B**). It is worth noting that two whale sightings are inside the area of highest plastic concentration, related to the anticyclonic Capraia gyre (**Figures 9A1,B1**).

Moreover, three other cetacean species (*S. coeruleolba*, *T. truncatus* and *G. griseus*) were identified during the sampling cruise for a total of 44 specimens. The striped dolphin and Risso's dolphin sightings (see Figure 2SM) overlap with the pelagic areas of high microplastic occurrence. This preliminary observation suggests a potential exposure also for odontocete cetaceans that prey preferentially on cephalopods and fish, in particular myctophidae (lanternfish). Myctophidae are a key trophic component of the marine food chain and are known to present high levels of microplastic ingestion worldwide (Lusher

TABLE 3 | Correlations obtained by using mean values $<C_t>$ of model concentrations.

$<C_t>$		48 h average	144 h average	336 h average
$<C_3>$	*R*	0.37	0.38	0.29
	p-value	0.197	0.185	0.309
$<C_7>$	*R*	0.04	0.33	0.32
	p-value	0.891	0.254	0.265
$<C_{15}>$	*R*	0.18	0.60	0.73
	p-value	0.545	0.024	0.003

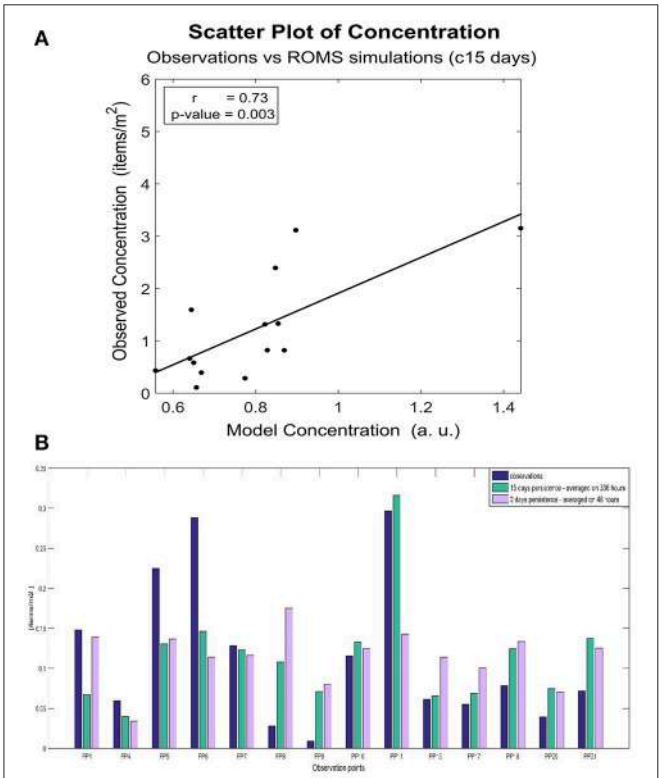

FIGURE 7 | Comparison of microplastic concentrations observed and the model estimations. **(A)** Scatter plot of microplastic concentrations: observation vs. ROMS simulation (15-days centered average case), **(B)** Histogram of microplastic concentrations observed and modeled.

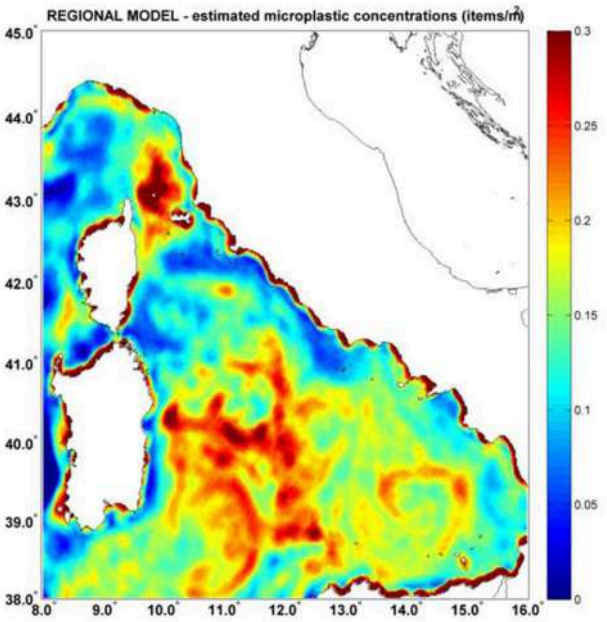

FIGURE 8 | Modeling marine litter distribution. Estimated concentrations of microplastics (items/m^2) in the period September-October 2014; map produced using the Matlab Release 14 software (https://www.mathworks.com/).

et al., 2016; Romeo et al., 2016). These fish species could be a potential vector of microplastic intake for odontocete species inhabiting this protected area.

DISCUSSION

The data obtained during the Plastic Pelagos survey confirm that floating plastic debris and particularly microplastics are widespread in the north-western Mediterranean Sea including the Pelagos Sanctuary (Collignon et al., 2012, 2014; Fossi et al., 2012, 2016; Cózar et al., 2014; Faure et al., 2015; Suaria et al., 2016). The most abundant polymer detected in the study area was polyethylene (76%), suggesting the main origin of the microplastics and mesoplastics analyzed was from fragmentation of larger packaging items. Polyethylene was found to be the most common plastic polymer among the plastic debris in the Mediterranean Sea and other oceans worldwide (Hidalgo-Ruz et al., 2012; Cózar et al., 2014). The data on floating plastic abundance confirm the high concentration found by other authors in the Mediterranean Sea (Cózar et al., 2015), identified as the sixth accumulation area for marine litter together with the main five oceanic gyres, as also predicted by global models (Eriksen et al., 2014).

The assessment of the potential exposure of fin whale to plastic was obtained comparing empirical data with a model of the fin whale feeding habitat and a model estimating the concentration of floating debris for the SPAMI Pelagos Sanctuary. The latter model was calibrated using observations, so it allows to spatialize an initially sparse dataset. This approach can give an important contribution to the preliminary risk assessment of the fin whales exposure to microplastics and could be extended to other marine species exposed to plastic ingestion if appropriate model for the feeding habitat of a given species is available.

Compared to other studies that use a simulation-based approach to describe the impact of spatial debris distributions on species such as sea turtles (Schuyler et al., 2016) or sea birds (Wilcox et al., 2015), we used high-resolution operational models to identify the variability of floating litter concentrations induced by hydrodynamic features. Using real data from aerial surveys performed in the Channel, the Atlantic and the Mediterranean regions, Darmon and collaborators (Darmon et al., in press) identified the exposure areas of loggerhead sea turtles (*Caretta*

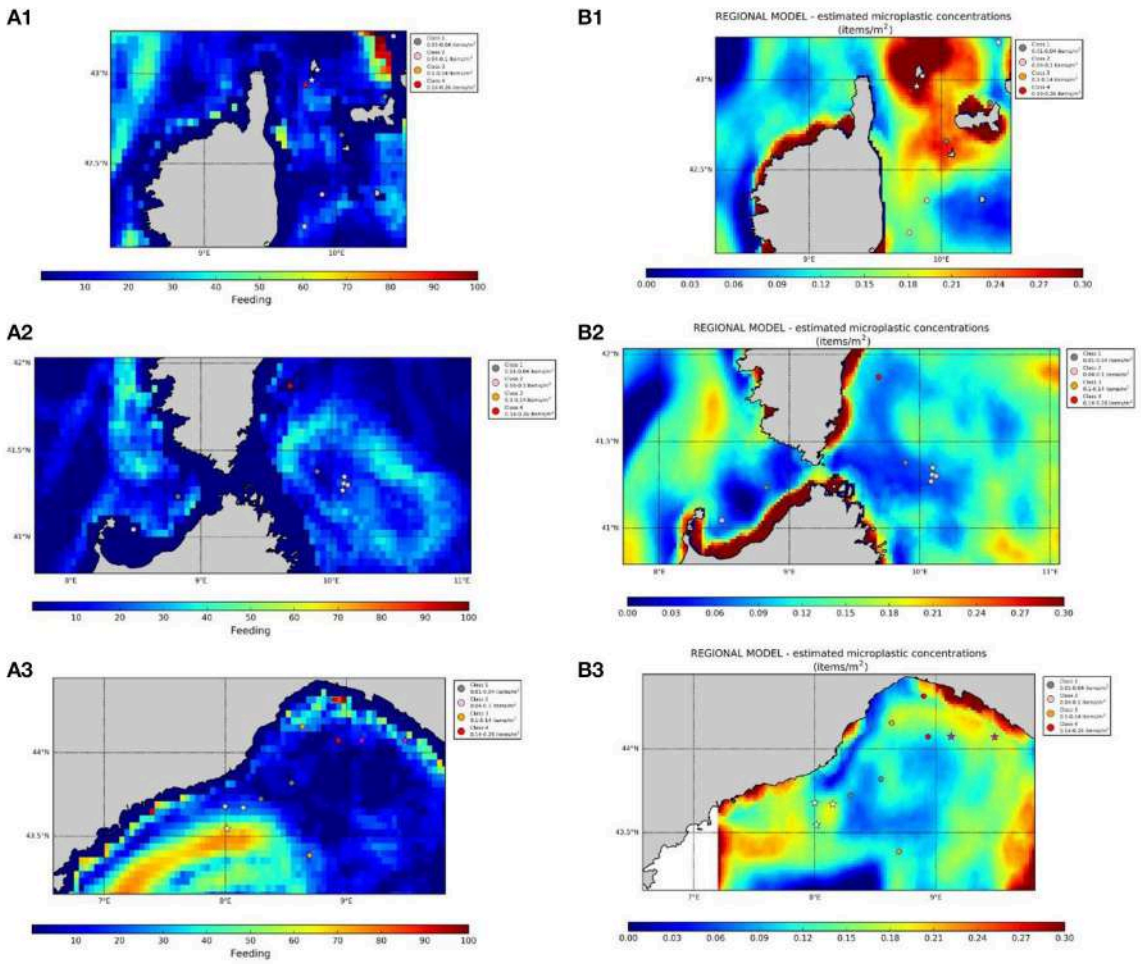

FIGURE 9 | Fin whale habitat maps (Feeding Habitat Occurrence) **(A1–A3)** and simulated distribution of microplastics (items/m2) **(B1–B3)** in north-western Mediterranean Sea. Microplastic concentrations (circle), and cetacean sighting data (white star: *Balaenoptera physalus*, pink star: *Stenella coeruleolba*, *Tursiops truncatus*, *Grampus griseus*) plotted in the two maps. Maps were produced using Matlab software (Release 14) and Python 2.7.12 for Linux 64-bit.

caretta) and magnitude in terms of spatial overlap, encounter probability and density of surrounding debris at various spatial scales. A modeling approach, calibrated with *in-situ* data, as used in the Plastic Pelagos survey, can be better extended to identify exposure areas and ingestion risk at various spatial and temporal scales.

Although permanent and stable circulation structures similar to the main ocean gyres do not occur in the north-western Mediterranean Sea, temporary accumulation patterns can be induced by seasonal circulation features. Local upwelling features, which are highly productive areas, could not coincide with the strongest observed accumulation areas mostly generated by anticyclonic circulation. On the other hand, several dynamical aspects as the proximity of the accumulation patterns to fronts and feeding habitats could largely increase the risk of plastic ingestion by several marine species, including fin whale. These findings indicate that fin whales can be exposed to microplastic ingestion in specific areas of Pelagos Sanctuary, especially in the summer, when the whale population is concentrated there (Druon et al., 2012). The effects related to this exposure was previously observed. Higher concentrations of persistent, bioaccumulative and toxic chemicals, plastic additives, and biomarker responses in the biopsies of Mediterranean whales were found in whales compared to whales inhabiting the less polluted Sea of Cortez (Mexico) (Fossi et al., 2016). In the same paper, a temporal increase in toxicological stress in whales, from the beginning to the end of the summer feeding period, suggests that exposure to microplastic contamination increases over the span of permanence in the summer feeding grounds in the Pelagos Sanctuary.

In addition, seven phthalate esters (plastic additives) were detected in microplastic/neustonic samples and in skin biopsies of several cetacean species collected in the same protected areas (Baini et al., 2017), confirming the occurrence of associated plastic chemicals and their related risk to the inhabiting fauna.

In conclusion, to our knowledge, this is the first study in which simulated plastic distributions show a quantitative agreement with the distributions derived from a floating litter data set. The overlap of microplastic convergence areas with the fin whale feeding grounds can serve as a provisional model for estimating hazard to marine biota in this and other SPAMI areas. The methodology proposed is promising, although a larger dataset, both for plastics debris (abundance and characterization) and marine species distribution, is necessary for a more comprehensive risk assessment. In particular, future works should include in the simulation model the potential sources of marine litter (as for instance ports, rivers and ship routes) to better characterize the origin of marine litter in the Pelagos Sanctuary to establish targeted conservation/mitigation actions based, for instance, on the characterization of the polymer plastic items, for instance PE and PP, which mainly derives from packaging and fisheries activity, respectively. The actions should promote instruments and incentives to reduce the use of disposable single-use and other items and identifying measures to address key waste items from the fishing industry and aquaculture, as underlined in the UNEP/MAP Regional Plan on Marine Litter (UNEP/MAP, 2015).

ETHICS STATEMENT

The paper does not include any sampling and laboratory analysis on cetaceans but only data based on observations from a boat platform. Therefore, ethics approval was not required as per institutional and national guidelines. Moreover, the field activities were carried out under the Italian Ministry for Environment authorization Prot. 0017880/PNM.

AUTHOR CONTRIBUTIONS

MCF designed the study, conducted the field sampling, and wrote the manuscript. TR organized the field sampling. MB carried out the field sampling, processed microplastics samples, performed data analysis and edited the manuscript. CP carried out the field sampling, processed microplastics samples, performed data analysis, and commented on and edited the manuscript. LM carried out the field sampling. TC carried out the field sampling and performed marine litter data analysis. SC organized and carried out the field sampling. FG carried out the field sampling, contributed to design the study and commented on the manuscript. JD commented on the manuscript and provided the model of whale feeding ground. SA contributed to design cetacean survey. ST performed the model of marine litter distribution and helped write the manuscript. MF performed the model of marine litter distribution. CB contributed to design the field study, performed the model of marine litter distribution, and helped write the manuscript. CL contributed to design the field study, helped in the field sampling, performed the model of marine litter distribution, and helped write the manuscript.

FUNDING

This project (Plastic Pelagos) was partially supported by the Italian Ministry of Environment, Territory and Sea (prot n° CUP F65I14000120001).

ACKNOWLEDGMENTS

We would like to thanks the technical staff of R/V ASTREA (ISPRA), Dr. Luca Bittau, Dr. Françoise Clarò and Ms. Laura Carletti, for the support during the sampling cruise.

SUPPLEMENTARY MATERIAL

The Supplementary Material for this article can be found online at: http://journal.frontiersin.org/article/10.3389/fmars.2017.00167/full#supplementary-material

REFERENCES

Alomar, C., Estarellas, F., and Deudero, S. (2016). Microplastics in the Mediterranean Sea: deposition in coastal shallow sediments, spatial variation and preferential grain size. *Mar. Environ. Res.* 115, 1–10. doi: 10.1016/j.marenvres.2016.01.005

Artale, V., Astraldi, M., Buffoni, G., and Gasparini, G. P. (1994). Seasonal variability of gyre-scale circulation in the northern Tyrrhenian Sea. *J. Geophys. Res.* 99, 14127. doi: 10.1029/94JC00284

Arthur, C., Baker, J., and Bamford, H. (2009). "Effects, and fate of microplastic marine debris," in *Proceedings of the International Research Workshop on the Occurrence* (Tacoma, WA: NOAA Technical Memorandum NOS-OR&R-30).

Baini, M., Martellini, T., Cincinelli, A., Campani, T., Minutoli, R., Panti, C., et al. (2017). First detection of seven phthalate esters (PAEs) as plastic tracers in superficial neustonic/planktonic samples and cetacean blubber. *Anal. Methods* 9, 1512–1520. doi: 10.1039/C6AY02674E

Buongiorno Nardelli, B., Tronconi, C., Pisano, A., and Santoleri, R. (2013). High and Ultra-High resolution processing of satellite Sea Surface Temperature data over Southern European Seas in the framework of MyOcean project. *Remote Sens. Environ.* 129, 1–16. doi: 10.1016/j.rse.2012.10.012

Campani, T., Baini, M., Giannetti, M., Cancelli, F., Mancusi, C., Serena, F., et al. (2013). Presence of plastic debris in loggerhead turtle stranded along the Tuscany coasts of the Pelagos Sanctuary for Mediterranean Marine Mammals (Italy). *Mar. Pollut. Bull.* 74, 225–230. doi: 10.1016/j.marpolbul.2013.06.053

Codina-García, M., Militão, T., Moreno, J., and González-Solís, J. (2013). Plastic debris in Mediterranean seabirds. *Mar. Pollut. Bull.* 77, 220–226. doi: 10.1016/j.marpolbul.2013.10.002

Coll, M., Piroddi, C., Albouy, C., Ben Rais Lasram, F., Cheung, W. W. L., Christensen, V., et al. (2012). The Mediterranean Sea under siege: spatial overlap between marine biodiversity, cumulative threats and marine reserves: the Mediterranean Sea under siege. *Glob. Ecol. Biogeogr.* 21, 465–480. doi: 10.1111/j.1466-8238.2011.00697.x

Collignon, A., Hecq, J.-H., Galgani, F., Collard, F., and Goffart, A. (2014). Annual variation in neustonic micro- and meso-plastic particles and zooplankton in the Bay of Calvi (Mediterranean–Corsica). *Mar. Pollut. Bull.* 79, 293–298. doi: 10.1016/j.marpolbul.2013.11.023

Collignon, A., Hecq, J.-H., Glagani, F., Voisin, P., Collard, F., and Goffart, A. (2012). Neustonic microplastic and zooplankton in the North Western Mediterranean Sea. *Mar. Pollut. Bull.* 64, 861–864. doi: 10.1016/j.marpolbul.2012.01.011

Cózar, A., Echevarria, F., Gonzalez-Gordillo, J. I., Irigoien, X., Ubeda, B., Hernandez-Leon, S., et al. (2014). Plastic debris in the open ocean. *Proc. Natl. Acad. Sci. U.S.A.* 111, 10239–10244. doi: 10.1073/pnas.1314705111

Cózar, A., Sanz-Martín, M., Martí, E., González-Gordillo, J. I., Ubeda, B., Gálvez, J. Á., et al. (2015). Plastic accumulation in the Mediterranean Sea. *PLOS ONE* 10:e0121762. doi: 10.1371/journal.pone.0121762

D'Amico, A., Bergamasco, A., Zanasca, P., Carniel, S., Nacini, E., Portunato, N., et al. (2003). Qualitative correlation of marine mammals with physical and biological parameters in the ligurian sea. *IEEE J. Ocean. Eng.* 28, 29–43. doi: 10.1109/JOE.2002.808206

Darmon, G., Miaud, C., Claro, F., Doremus, G., and Galgani, F. (in press). Risk assessment reveals high exposure of sea turtles to marine debris in French Mediterranean and metropolitan Atlantic waters. *Deep Sea Res. II Top. Stud. Oceanogr.* doi: 10.1016/j.dsr2.2016.07.005

Deudero, S., and Alomar, C. (2015). Mediterranean marine biodiversity under threat: reviewing influence of marine litter on species. *Mar. Pollut. Bull.* 98, 58–68. doi: 10.1016/j.marpolbul.2015.07.012

Druon, J., Panigada, S., David, L., Gannier, A., Mayol, P., Arcangeli, A., et al. (2012). Potential feeding habitat of fin whales in the western Mediterranean Sea: an environmental niche model. *Mar. Ecol. Prog. Ser.* 464, 289–306. doi: 10.3354/meps09810

Eriksen, M., Lebreton, L. C. M., Carson, H. S., Thiel, M., Moore, C. J., Borerro, J. C., et al. (2014). Plastic Pollution in the World's Oceans: more than 5 Trillion Plastic Pieces Weighing over 250,000 Tons Afloat at Sea. *PLoS ONE* 9:e111913. doi: 10.1371/journal.pone.0111913

Fairall, C. W., Bradley, E. F., Godfrey, J. S., Wick, G. A., Edson, J. B., and Young, G. S. (1996). Cool-skin and warm-layer effects on sea surface temperature. *J. Geophys. Res. Oceans* 101, 1295–1308. doi: 10.1029/95JC03190

Faure, F., Saini, C., Potter, G., Galgani, F., Alencastro, L. F., de, and Hagmann, P. (2015). An evaluation of surface micro- and mesoplastic pollution in pelagic ecosystems of the Western Mediterranean Sea. *Environ. Sci. Pollut. Res.* 22, 12190–12197. doi: 10.1007/s11356-015-4453-3

Fossi, M. C., Marsili, L., Baini, M., Giannetti, M., Coppola, D., Guerranti, C., et al. (2016). Fin whales and microplastics: the Mediterranean Sea and the Sea of Cortez scenarios. *Environ. Pollut.* 209, 68–78. doi: 10.1016/j.envpol.2015.11.022

Fossi, M. C., Panti, C., Guerranti, C., Coppola, D., Giannetti, M., Marsili, L., et al. (2012). Are baleen whales exposed to the threat of microplastics? A case study of the Mediterranean fin whale (Balaenoptera physalus). *Mar. Pollut. Bull.* 64, 2374–2379. doi: 10.1016/j.marpolbul.2012.08.013

Fossi, M. C., Panti, C., Marsili, L., Maltese, S., Spinsanti, G., Casini, S., et al. (2013). The Pelagos Sanctuary for Mediterranean marine mammals: Marine Protected Area (MPA) or marine polluted area? The case study of the striped dolphin (Stenella coeruleoalba). *Mar. Pollut. Bull.* 70, 64–72. doi: 10.1016/j.marpolbul.2013.02.013

Gohin, F., Druon, J. N., and Lampert, L. (2002). A five channel chlorophyll concentration algorithm applied to SeaWiFS data processed by SeaDAS in coastal waters. *Int. J. Remote Sens.* 23, 1639–1661. doi: 10.1080/01431160110071879

Hidalgo-Ruz, V., Gutow, L., Thompson, R. C., and Thiel, M. (2012). Microplastics in the marine environment: a review of the methods used for identification and quantification. *Environ. Sci. Technol.* 46, 3060–3075. doi: 10.1021/es2031505

Hinojosa, I. A., and Thiel, M. (2009). Floating marine debris in fjords, gulfs and channels of southern Chile. *Mar. Pollut. Bull.* 58, 341–350. doi: 10.1016/j.marpolbul.2008.10.020

Hummel, D. O. (2002). Atlas of *Plastics Additives: Analysis* by *Spectrometric Methods*. Berlin; New York, NY: Springer.

Iacono, R., Napolitano, E., Marullo, S., Artale, V., and Vetrano, A. (2013). Seasonal variability of the Tyrrhenian Sea surface geostrophic circulation as assessed by altimeter data. *J. Phys. Oceanogr.* 43, 1710–1732. doi: 10.1175/JPO-D-12-0112.1

Kooi, M., Reisser, J., Slat, B., Ferrari, F. F., Schmid, M. S., Cunsolo, S., et al. (2016). The effect of particle properties on the depth profile of buoyant plastics in the ocean. *Sci. Rep.* 6:33882. doi: 10.1038/srep33882

Kukulka, T., Proskurowski, G., Morét-Ferguson, S., Meyer, D. W., and Law, K. L. (2012). The effect of wind mixing on the vertical distribution of buoyant plastic debris. *Geophys. Res. Lett.* 39:L07601. doi: 10.1029/2012GL051116

Lapucci, C., Ampolo Rella, M., Brandini, C., Ganzin, N., Gozzini, B., Maselli, F., et al. (2012). Evaluation of empirical and semi-analytical chlorophyll algorithms in the Ligurian and North Tyrrhenian Seas. *J. Appl. Remote Sens.* 6, 063565–063561. doi: 10.1117/1.JRS.6.063565

Law, K. L., Morét-Ferguson, S. E., Goodwin, D. S., Zettler, E. R., DeForce, E., Kukulka, T., et al. (2014). Distribution of Surface Plastic Debris in the Eastern Pacific Ocean from an 11-Year Data Set. *Environ. Sci. Technol.* 48, 4732–4738. doi: 10.1021/es4053076

Lebreton, L. C.-M., Greer, S. D., and Borrero, J. C. (2012). Numerical modelling of floating debris in the world's oceans. *Mar. Pollut. Bull.* 64, 653–661. doi: 10.1016/j.marpolbul.2011.10.027

Lusher, A. L., McHugh, M., and Thompson, R. C. (2013). Occurrence of microplastics in the gastrointestinal tract of pelagic and demersal fish from the English Channel. *Mar. Pollut. Bull.* 67, 94–99. doi: 10.1016/j.marpolbul.2012.11.028

Lusher, A. L., O'Donnell, C., Officer, R., and O'Connor, I. (2016). Microplastic interactions with North Atlantic mesopelagic fish. *ICES J. Mar. Sci. J. Cons.* 73, 1214–1225. doi: 10.1093/icesjms/fsv241

Mansui, J., Molcard, A., and Ourmières, Y. (2015). Modelling the transport and accumulation of floating marine debris in the Mediterranean basin. *Mar. Pollut. Bull.* 91, 249–257. doi: 10.1016/j.marpolbul.2014.11.037

MSFD Technical Subgroup on Marine Litter (2013). *Guidance on Monitoring of Marine Litter in European Seas*. Luxembourg: Publications Office.

Panigada, S., Lauriano, G., Burt, L., Pierantonio, N., and Donovan, G. (2011). Monitoring winter and summer abundance of cetaceans in the pelagos sanctuary (Northwestern Mediterranean Sea) through aerial surveys. *PLoS ONE* 6:e22878. doi: 10.1371/journal.pone.0022878

Panigada, S., Notarbartolo di Sciara, G., Zanardelli, M., Airoldi, S., Borsani, J. F., and Jahoda, M. (2005). Fin whales summering in the Ligurian Sea: distribution, encounter rate, mean group size and relation to physiographic variables. *J. Cetacean Res. Manag.* 7, 137–145.

Panti, C., Giannetti, M., Baini, M., Rubegni, F., Minutoli, R., and Fossi, M. C. (2015). Occurrence, relative abundance and spatial distribution of microplastics and zooplankton NW of Sardinia in the Pelagos Sanctuary Protected Area, Mediterranean Sea. *Environ. Chem.* 12:618. doi: 10.1071/EN14234

Pinzone, M., Budzinski, H., Tasciotti, A., Ody, D., Lepoint, G., Schnitzler, J., et al. (2015). POPs in free-ranging pilot whales, sperm whales and fin whales from the Mediterranean Sea: influence of biological and ecological factors. *Environ. Res.* 142, 185–196. doi: 10.1016/j.envres.2015.06.021

Plastics Europe (2015). *Plastics – the Facts 2015 An Analysis of European Plastics Production, Demand and Waste Data*. Bruxelles: Plastics Europe

Romeo, T., Pedà, C., Fossi, M. C., Andaloro, F., and Battaglia, P. (2016). First record of plastic debris in the stomach of Mediterranean lanternfishes [Prvi zapis o plastičnim krhotinama u želucu mediteranskih riba žaboglavki (Myctophidae). *Acta Adriat.* 57, 115–124.

Romeo, T., Pietro, B., Pedà C., Consoli, P., Andaloro, F., and Fossi, M. C. (2015). First evidence of presence of plastic debris in stomach of large pelagic fish in the Mediterranean Sea. *Mar. Pollut. Bull.* 95, 358–361. doi: 10.1016/j.marpolbul.2015.04.048

Schroeder, K., Haza, A. C., Griffa, A., Özgökmen, T. M., Poulain, P. M., Gerin, R., et al. (2011). Relative dispersion in the Liguro-Provençal basin: from sub-mesoscale to mesoscale. *Deep Sea Res. Part I: Oceanogr. Res. Pap.* 58, 209–228. doi: 10.1016/j.dsr.2010.11.004

Schuyler, Q. A., Wilcox, C., Townsend, K. A., Wedemeyer-Strombel, K. R., Balazs, G., van Sebille, E., et al. (2016). Risk analysis reveals global hotspots for marine debris ingestion by sea turtles. *Glob. Change Biol.* 22, 567–576. doi: 10.1111/gcb.13078

Shchepetkin, A. F., and McWilliams, J. C. (2005). The regional oceanic modeling system (ROMS): a split-explicit, free-surface, topography-following-coordinate oceanic model. *Ocean Model.* 9, 347–404. doi: 10.1016/j.ocemod.2004.08.002

Suaria, G., and Aliani, S. (2014). Floating debris in the Mediterranean Sea. *Mar. Pollut. Bull.* 86, 494–504. doi: 10.1016/j.marpolbul.2014.06.025

Suaria, G., Avio, C. G., Mineo, A., Lattin, G. L., Magaldi, M. G., Belmonte, G., et al. (2016). The Mediterranean Plastic Soup: synthetic polymers in Mediterranean surface waters. *Sci. Rep.* 6:37551. doi: 10.1038/srep37551

UNEP/MAP (2015). *Marine Litter Assessment in the Mediterranean*. Athens: UNEP/MAP.

van Sebille, E., Wilcox, C., Lebreton, L., Maximenko, N., Hardesty, B. D., van Franeker, J. A., et al. (2015). A global inventory of small floating plastic debris. *Environ. Res. Lett.* 10:124006. doi: 10.1088/1748-9326/10/12/124006

Wilcox, C., Sebille, E. V., and Hardesty, B. D. (2015). Threat of plastic pollution to seabirds is global, pervasive, and increasing. *Proc. Natl. Acad. Sci. U.S.A.* 112, 11899–11904. doi: 10.1073/pnas.1502108112

Zambianchi, E., Iermano, I., Suaria, G., and Aliani, S. (2014). "Marine litter in the Mediterranean Sea: an oceanographic perspective," in *Marine litter in the Mediterranean and Black Seas. CIESM Workshop Monograph n° 46, Edition,* ed F. Briand (Tirana: CIESM Publisher), 180.

Conflict of Interest Statement: The authors declare that the research was conducted in the absence of any commercial or financial relationships that could be construed as a potential conflict of interest.

frontiers in Marine Science

ORIGINAL RESEARCH
published: 10 March 2017
doi: 10.3389/fmars.2017.00063

Plastic Pollution Patterns in Offshore, Nearshore and Estuarine Waters: A Case Study from Perth, Western Australia

Sara Hajbane[1,2]* *and Charitha B. Pattiaratchi*[1]

[1] School of Civil, Environmental and Mining Engineering, and UWA Oceans Institute, University of Western Australia, Crawley, WA, Australia, [2] School of Earth and Environment, University of Western Australia, Crawley, WA, Australia

Plastic pollution in marine surface waters is prone to high spatial and temporal variability. As a result increases in pollution over time are hard to detect. Selecting areas, based on variable oceanographic and climatological drivers, rather than distance-based approaches, is proposed as a means to better understand the dynamics of this confounding variability in coastal environments. A pilot study conducted in Perth metropolitan waters aimed to explore the applicability of this approach, whilst quantifying levels of plastic pollution in an understudied part of the world. Pollution ranged from 950 to 60,000 pieces km^{-2} and was dominated by fishing line. Offshore concentrations were highest with strongest Leeuwin Current flow, in the estuary immediately after rainfall, and increased in the nearshore after estuarine outfall. Results elucidated significant relationships between physical drivers and concentration changes and therefore their roles in increasing or decreasing local plastic pollution. Such observations can form the basis for predicting peak pollution periods and inform targeted mitigation.

Keywords: plastic pollution, spatiotemporal variability, coastal oceanography, Western Australia, mitigation, fishing line

OPEN ACCESS

Edited by:
Francois Galgani, French Research Institute for Exploitation of the Sea, France

Reviewed by:
Sunwook Hong, Our Sea of East Asia Network, South Korea
Nicolas Kalogerakis, Technical University of Crete, Greece

***Correspondence:**
Sara Hajbane
sara.hajbane@gmail.com

Specialty section:
This article was submitted to Marine Pollution, a section of the journal Frontiers in Marine Science

Received: *30 November 2016*
Accepted: *20 February 2017*
Published: *10 March 2017*

Citation:
Hajbane S and Pattiaratchi CB (2017) Plastic Pollution Patterns in Offshore, Nearshore and Estuarine Waters: A Case Study from Perth, Western Australia. Front. Mar. Sci. 4:63. doi: 10.3389/fmars.2017.00063

INTRODUCTION

Plastic pollution in the surface of the ocean has become an issue of growing concern since it was first observed and documented in the open ocean in the early 1970s (Carpenter and Smith, 1972; Andrady, 2011). Large-scale and long-term studies with the aim of quantifying concentrations and distributions are growing rapidly to further our knowledge on the state of plastic pollution (Hidalgo-Ruz et al., 2012; do Sul and Costa, 2014). Various gyre-wide and multi-year comparisons have been conducted in the last decade to understand the spread and increase in pollution at sea (Thompson et al., 2004; Law et al., 2010; Eriksen et al., 2013). Whilst subtropical gyres as major accumulation zones for buoyant plastic debris are now widely studied in the northern hemisphere, multi-year analysis have so far yielded no clear temporal trends, leaving sources and sinks of plastic pollution poorly understood (Thompson et al., 2004; Law et al., 2010). High concentrations have also been recorded near coastal population centers with the consensus being, that they are the main source of marine plastic debris (Corcoran et al., 2009; Jambeck et al., 2015). An often cited statistic proposes that 80% of all marine plastic pollution is sourced directly from land-based sources, particularly from urban areas (Vegter et al., 2014; Jambeck et al., 2015). This shifted the focus more

recently toward studies of the state of pollution in localized coastal waters (Thompson et al., 2004; Yamashita and Tanimura, 2007; Doyle et al., 2011; Thiel et al., 2013; Isobe et al., 2015). A recent literature review by 26 expert researchers has highlighted two priorities for coastal plastic pollution studies. Firstly, a lack of studies focused on identifying sources of rather than quantifying the state of plastic pollution, and secondly a dire necessity for studies at management-relevant scales, such as catchments and coastal zones (Vegter et al., 2014).

So far, studies that have physically measured and analyzed concentrations in coastal waters were equally unable to detect significant changes or increasing trends over multi-decadal time frames (see Gilfillan et al., 2009; Goldstein et al., 2013). Two possible statistical considerations may explain why increases in plastic production and waste outputs to sea are not reflected in field measurements to date. The first one is very high spatial and temporal variability (Gilfillan et al., 2009). Goldstein et al. (2013) postulate that very large sample sizes are needed to detect spatial changes in concentrations, due to statistic design considerations. The second reason may be experimental design: spatial analyses in coastal areas to date were conducted with respect to distance from shore (see also: Yamashita and Tanimura, 2007). No studies so far have compared areas of interest to determine statistical difference or change over time in a coastal setting. Various studies have addressed individual driving forces for plastic accumulation, such as surface currents and Ekman drift (Kubota, 1994; Martinez et al., 2009), rainfall (Carson et al., 2013), and winds (Kukulka et al., 2012). Carson et al. (2013) indicated that nearshore and tidal dynamics might have important and variable effects on pollution retention in coastal areas. Therefore, selecting areas characteristic of various physical drivers may create a better understanding of high variability over short time scales and inform approaches for successful long-term comparisons. Understanding both the scale and source of variability of plastic pollution is necessary to understand potential ecosystem threats.

The major threats that pelagic plastics pose to marine life are entanglement, ingestion, and introduction of invasive rafting communities living on the plastic surface (Gregory, 2009; Andrady, 2011). Hydrophobic plastic fragments also leach contaminants and attract additional lipid soluble pollutants, such as persistent organic pollutants (POPs), aqueous metals, and endocrine disrupting chemicals (Derraik, 2002; Cole et al., 2011; Rochman et al., 2014; Rochman, 2015). These can biomagnify up marine food chains when ingested by biota, and pose a threat to human health through our collective dependence on marine food sources (Erren et al., 2015; Seltenrich, 2015). The threats associated with organic pollutants are perceived to be particularly high in small plastics, because their surface area to volume ratio facilitates considerably higher pollutant concentration, than larger fragments (Cole et al., 2011). Lower trophic-level organisms can ingest microplastics easily due to their small size thus releasing adsorbed chemicals into the base of the food chain and exacerbating biomagnification (Avio et al., 2015). Therefore, it is important to measure length or size ranges for plastics recovered and employ sampling methods that are able to collect small plastics reliably (Hidalgo-Ruz et al., 2012; Vegter et al., 2014).

Synthetic polymers do not naturally decompose, but break down into ever-smaller fragments or so-called secondary microplastics (SMPs) (Barnes et al., 2009; Andrady, 2011). Varying definitions still exist for the size range of a microplastic, but a common definition denominates microplastics as being $\leq$5 mm in maximum length (Hidalgo-Ruz et al., 2012). This denomination is followed herein. As plastics fragment into smaller pieces over time, smaller SMPs are suspected to have spent longer time at sea than their larger counter parts or complete items (Morét-Ferguson et al., 2010; Reisser et al., 2013; Cózar et al., 2014). Primary microplastics (PMPs) on the other hand, are polymer products that have been intentionally produced in the nominal size range of $\leq$5 mm, such as cosmetic microbeads, some pre-production pellets, and synthetic sandblasting media (Cole et al., 2011). SMPs are often the most dominant type of plastic found in marine environments (Shaw and Day, 1994; Morét-Ferguson et al., 2010; Reisser et al., 2013). Therefore, another rationale why increases of microplastic concentrations in oceanic surface waters over time have not been recorded yet, is due to nano-fragmentation to size ranges below current limits of detection (Andrady, 2011). As a result, progressive fragmentation models are being tested and new methods for the acquisition of nano-plastics trialed (Cózar et al., 2014; Enders et al., 2015). The specific mechanisms for breakdown are poorly understood to date, however breakdown or removal rates must be higher than input rates to explain the lack of detectable increases in plastic concentration over time (Cózar et al., 2014). One proposed mechanism for such breakdown is wave activity, particularly along shorelines (Corcoran et al., 2009; Andrady, 2011).

Additionally, studies have shown that material in marine environments is lost depending on characteristics (Shaw and Day, 1994; Cózar et al., 2014). Therefore, plastic color and type (e.g., hard, film, pellet, line etc.) are commonly recorded attributes of plastics found in marine environments (see Hidalgo-Ruz et al., 2012). These characteristics have identified significant temporal change in plastic assemblages, where concentrations alone yielded no conclusive results (Shaw and Day, 1994; Vlietstra and Parga, 2002). This type- and color-dependent variability has been ascribed to predator selectivity when plastics are mistaken for food (Shaw and Day, 1994; Schuyler et al., 2012), but may also be due to type-dependent density changes and chemical degradation causing discoloration and bleaching (Pérez et al., 2010). Studies that report plastic type and colors, found the dominant proportion of SMPs in the open ocean to be white or clear in color, and composed of hard plastic fragments (Shaw and Day, 1994; Morét-Ferguson et al., 2010; Reisser et al., 2013). Recording characteristics of type and color has also been highlighted as a means for global comparisons (Morét-Ferguson et al., 2010). Therefore, it may be an additional source of informing variability not only globally, but also between areas of interest at a more localized and manageable scale.

Primarily this study aimed to quantify pollution in local waters and test if physical drivers can predict short-term variability of plastic pollution at management-relevant scale through strategic

selection of areas for comparison. An increased focus on a variety of physical drivers influencing ocean surface dynamics may be a valuable new approach to understanding variability of plastic pollution concentrations in the long-term and may be used to discuss future predictions. To this end this case study set out to sample plastic pollution over a timeframe that spanned summer and winter months, visiting the same areas repeatedly. Secondly, this study aimed to demonstrate that variability of sizes and characteristics of plastic debris can shed a light on specific sources to local waters and recommend potential mitigating measures. To this end all material collected during this study was recorded in depth. The objectives toward this are 3-fold: (1) Determine concentrations of plastic pollution and test whether they increase during the austral winter months in accordance with their respective physical drivers. (2) Investigate variations in particle sizes between areas to infer proximity to source and new pollution being introduced with rainfall from local sources during austral winter months. (3) Compare characteristics of plastics between areas to test for a more heterogeneous assemblage closer to source in the estuary with the offshore being comparable to previous finds around Australian waters and in international waters.

MATERIALS AND METHODS

Study Areas

All sampling for this study was conducted in metropolitan waters of Perth, Western Australia between February and July 2015 during four recurring transits. No special permits were required, since sample collection was limited to inanimate debris. The West Australian coast is home to a number of unique and highly seasonal oceanic and climatic drivers. The characteristics of these drivers are well described in the scientific literature and we propose that they can be used to predict and understand the variability and concentrations of plastic pollution in local surface waters. The key drivers that were used to determine areas of interest for this study are the poleward flowing Leeuwin Current, the opposing alongshore Capes current, and rainfall. Highlighted in **Figure 1** are the three selected sampling areas [hereafter referred to as "offshore" (OS), "nearshore" (NS) and "estuarine" (EST)].

Leeuwin Current in the Offshore

The Leeuwin Current (LC) presents one of the key drivers of local oceanography and climatology in Western Australia. It is an anomalous eastern boundary current that flows poleward against prevailing equatorward winds (Godfrey and Ridgway, 1985). The LC is driven by an alongshore geopotential gradient created by warm, nutrient-poor Pacific Ocean waters spilling into the Indian Ocean with the Indonesian Through-flow (ITF) (Pearce and Phillips, 1988; Fieux et al., 2005). While most of the ITF contributes to the westward flowing Indian Ocean Equatorial current, some of it flows into the Holloway current along the North West shelf of Australia and extends further south where it contributes to the LC (Pearce and Phillips, 1988; Yit Sen Bull and van Sebille, 2016). Seasonal variability of the LC creates strongest transport during the austral winter months, as opposing winds weaken (Godfrey and Ridgway, 1985; Feng et al., 2003). A peak in LC strength within the study area is observed from May to June each year, when the alongshore pressure gradient peaks (Morrow and Birol, 1998). While interannual peaks are driven by Pacific sea level variations, Ridgway and Godfrey (2015) have proposed a monsoonal sea level pulse as the driver of seasonal variations. This post-monsoon pulse explains maximum flow in the South West of Western Australia from May to June (Feng et al., 2003). Transport of international plastic pollutants to the area is facilitated through entrainment of Indian Ocean surface waters and the ITF, which extends into the Holloway and then Leeuwin Current, capable of transporting water down the coast from Asia (Meyers et al., 1995; Pattiaratchi and Woo, 2009). ITF waters are hereby modeled to make up the highest proportion of water transported in the LC (Yit Sen Bull and van Sebille, 2016). Importantly, the three countries with the highest estimated influx of mismanaged plastic waste to the ocean—namely China, Indonesia and the Philippines—are directly connected to Western Australia by these surface currents (Jambeck et al., 2015). Therefore, it is hypothesized that the highest concentrations of plastic pollution in the offshore will occur during strongest Leeuwin current flow in May.

Rainfall and Estuarine-sourced Debris

The Perth metropolitan coast is a micro-tidal environment with a diurnal tide of approximately 0.6 m (Ruiz-Montoya and Lowe, 2014). The Swan River estuary is a predominantly tidally driven, seasonally reversing estuary. Over the past decades, the area has been experiencing increasingly long droughts during the summer months (Gallant et al., 2013), with the bulk of rainfall occurring in the austral winter (Smith et al., 2000). Recent decades have seen a decrease in rainfall in addition to increasingly concentrated rainfall patterns during the early austral winter (May–July), as opposed to an even spread into the later winter months (August–October) (Smith et al., 2000). With a sampling protocol that targets Swan River effluent during ebb tides, it is expected that the highest amounts of estuarine-sourced pollution will be recorded directly after concentrated rainfall events during the early winter months, from May through to July.

Coastal Current Dominating the Nearshore

The coastal current (CC) is a northward alongshore current flowing strongest during the austral summer when southerly winds are strongest (Ruiz-Montoya and Lowe, 2014). It has been suggested to be an extension of the Capes Current flowing between Cape Leeuwin and Cape Naturaliste in the southwest of Western Australia (Pearce and Pattiaratchi, 1999), The nearshore circulation pattern of the coastal current in PMW during summer is highly variable and responds quickly to changes in wind, but is mostly driven northward by the dominant southerly sea breeze (Pattiaratchi et al., 1997; Ruiz-Montoya and Lowe, 2014). In the presence of predominantly southerly winds concentrations in the nearshore are therefore expected to be highest after periods of rain, as estuarine outfall can be accumulated against the shore, with the LC creating a boundary preventing offshore transport of plastic particles.

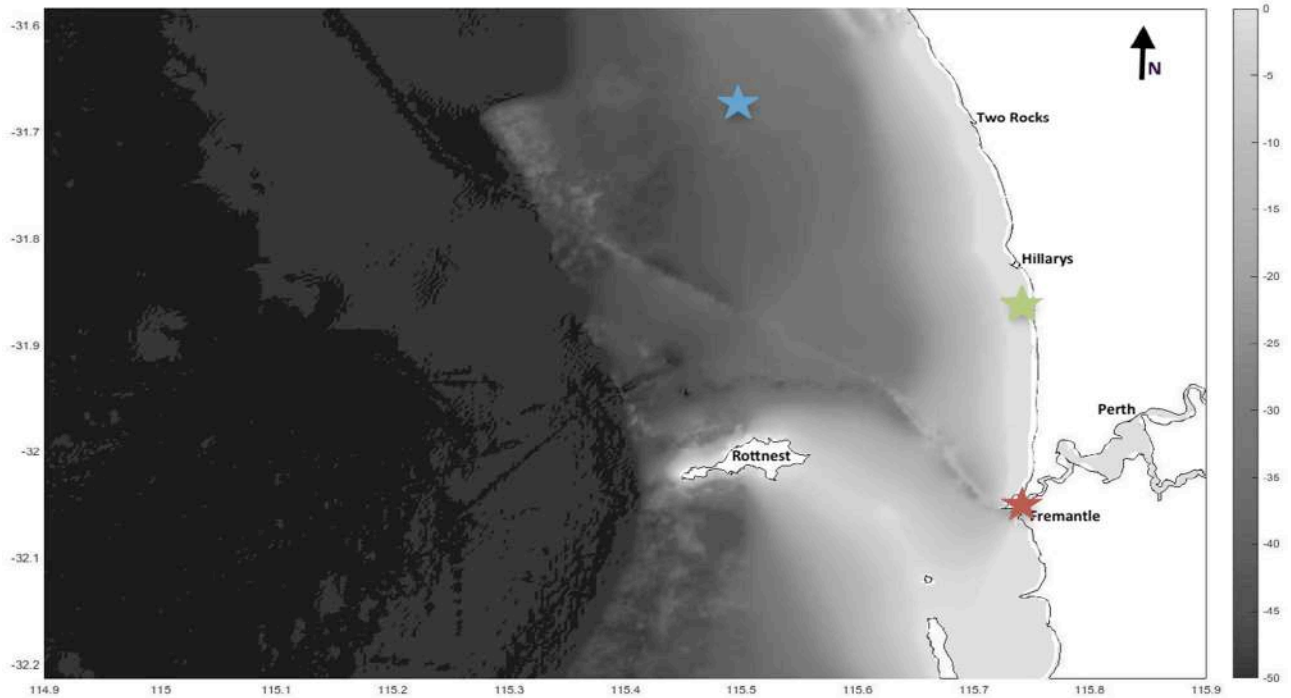

FIGURE 1 | Study site with bathymetry. Offshore (blue), nearshore (green) and estuarine (red) areas are highlighted as stars.

Data Collection

All plastic sampled was collected using a manta net (1 × 0.17 m, 333 micron mesh), designed and manufactured by Oceans Instruments, San Diego (Brown and Cheng, 1981; Goldstein et al., 2013; Reisser et al., 2013). One station in each of the three areas of interest was sampled on four occasions during the study period (**Table 1**). At each station the net was towed through the sea-surface interface in three consecutive replicate tows of 15 min (NOAA, 2015). All collected material was transferred from the cod-ends of the manta net to a transfer container (Reisser et al., 2013). The net and cod-end were carefully rinsed and plastics refloated in seawater within it. The transfer containers were then immediately and thoroughly examined visually for plastic pieces, placed into a graduated dish with forceps, individually counted, and transported to the lab in vials (similar procedures utilized by Morét-Ferguson et al., 2010; Cózar et al., 2014). Sampling was not conducted during high wind conditions, due to potential dangers of instrument deployment in rough seas and rapid decline in plastic detectability in the surface layer at high wind speeds (Kukulka et al., 2012; Reisser et al., 2014). Wind speed and tides were consulted in fieldwork planning and recorded throughout sampling. Planning ensured sampling of the estuarine sites occurred only during ebb tides, when flotsam is exiting out the estuary, and that dangerous seas were avoided. Rainfall, wind speed, and wind direction time-series data was obtained from the Bureau of Meteorology (2015), from measurements taken on Rottnest Island in 30-min intervals. Significant wave height data is based on a localized surf forecast by Wandres (2015) based on the ERA –Interim model reanalysis (Dee et al., 2011).

TABLE 1 | Reference table for levels of sampling procedure.

Levels	Site	Area	Station	Replicate
Number within	1 Perth metro-politan waters	3 nearshore, offshore, estuarine	12 3 areas on 4 days: 25/2/2015 (Feb); 27/3/2015 (Mar); 26/5/215 (May)& 3/7/2015 (July)	35 of originally 36–3 per station

Data Recording

To estimate surface concentrations at all stations the total numbers of plastics were standardized to pieces per km^2 (Law et al., 2010). Surface area was calculated using tow length × net width for each replicate tow. The concentrations are reported as a mean in pieces/km^2 and presented as an averaged value from the replicate tows at each station and their standard deviation (Reisser et al., 2013; NOAA, 2015). Tow length was measured with a General Oceanics analog flow meter, fixed inside the manta net frame (Brown and Cheng, 1981; Goldstein et al., 2013), and cross-validated with GPS measurements of the sampled transects (Reisser et al., 2013). Whilst Kukulka et al. (2012) have demonstrated that wind speeds can have a significant effect on the detectability of plastics in the surface layer, and proposed a one-dimensional column model for estimation of wind integrated plastic surface concentrations, this model was not used in this study. Since the maximum depth at any sampling site was 34 m, a well-mixed water column was expected, which was confirmed in the detection of a small number of non-buoyant plastics during sampling.

TABLE 2 | Mean plastic pollution concentrations in pieces/km^2 in PMW.

Concentration Mean pcs/km^2	Offshore 4,957	Nearshore 21,598	Estuarine 16,461
February	**1,518** (± 156/190)	**17,717** (± 3,646/4,253)	**14,036** (± 8,585/9,951)
March	**948** (± 276/300)	**1,199** (± 1,144/1,370)	**2,461**(± 1,404/1,567)
May	**15,042** (± 4,715/5,528)	**7,846** (± 6,177/7,297)	**47,164**(± 2,170/2,170)
July	**2,319** (± 1,222/1,496)	**59,631** (± 32,892/40,270)	**12,417** (± 5,015/5,864)

Bold values show the mean concentration in pcs/km^2 and numbers in brackets denote standard errors and the interquartile range.

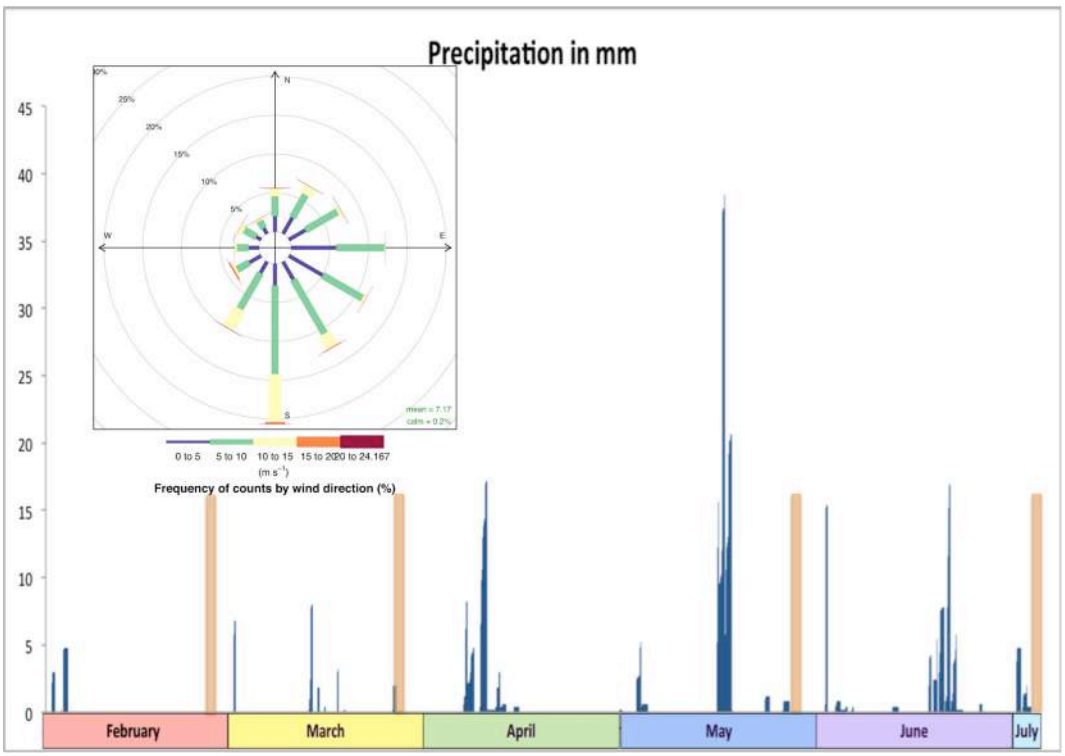

FIGURE 2 | Histogram of precipitation in mm (blue bars) over the study period (Source: Bureau of Meteorology, 2015). Sampling days marked by orange bars and inset is a wind rose of wind speeds and direction. For the wind rose colors denote: blue = 0–5, green = 5–10, yellow 10–15, orange 15–20, red 20–24.17 m s^{-1} (R openair package: Carslaw and Ropkins, 2012).

TABLE 3 | Dunn's test results for differences in concentration by area and month.

Kruskal-Wallis rank sum with Dunn's test by area		Estuarine	Nearshore
	Nearshore	$p = 0.4353$	–
	Offshore	$\mathbf{p = 0.0166}$	$\mathbf{p = 0.0221}$
By Month	February	July	March
July	$p = 0.3394$	–	–
March	$\mathbf{p = 0.0050}$	$\mathbf{p = 0.0014}$	–
May	$p = 0.1853$	$p = 0.3107$	$\mathbf{p = 0.0003}$

Significant p-values marked in bold.

After sampling all plastics were air dried at room temperature for at least 24 h. All plastics were measured along their maximum length and recorded to the nearest 0.5 mm using a millimeter ruler. For plastics that were larger than 30 cm a measuring tape was used. Particles between the minimum limit of detection, 0.33 mm, and 1 mm were conservatively recorded as 0.8 mm to allow for statistical analysis of continuous data (Eriksen et al., 2014). The collected plastics were then categorized into several types—namely hard/sheet, soft/film, line, styrofoam, rubber, cellulose, and microbeads—and their color recorded. Such characterizations are important for geographic and temporal comparisons (Shaw and Day, 1994; Morét-Ferguson et al., 2010). Yet, no uniform characterization approach exists. All common categories identified in a recent review of the relevant

TABLE 4 | *Post-hoc* Dunn's test of concentrations.

Dunn's test for concentrations	EST Feb	NS Feb	OS Feb	EST July	NS July	OS July	EST Mar	NS Mar	OS Mar	EST May	NS May
NS-Feb	0.38										
OS-Feb	0.05	**0.03**									
EST-July	0.45	0.33	0.07								
NS-July	0.14	0.22	**0.0**	0.12							
OS-July	0.06	**0.03**	0.47	0.08	**0.0**						
EST-Mar	0.07	**0.04**	0.44	0.09	**0.01**	0.47					
NS-Mar	**0.02**	**0.01**	0.35	**0.03**	**0.0**	0.32	0.29				
OS-Mar	**0.01**	**0.0**	0.26	**0.02**	**0.0**	0.24	0.21	0.41			
EST-May	0.16	0.24	**0.01**	0.14	0.49	**0.01**	**0.01**	**0.00**	**0.00**		
NS-May	0.26	0.17	0.16	0.3	**0.04**	0.18	0.20	0.08	0.05	0.06	
OS-May	0.44	0.44	**0.04**	0.4	0.18	**0.04**	0.07	**0.02**	**0.01**	0.2	0.2

Significant p-values marked in bold and colors show direct comparisons between same areas over time with red, estuarine; green, nearshore; blue, offshore (Dunn, 1964; Dinno, 2015).

literature were used, with the exception of preproduction pellets, since none were found in the study site (Hidalgo-Ruz et al., 2012). Further, infrared Raman spectroscopy was applied to a randomly selected, representative subsample from all areas and replicate tows (total $n = 116$) (Allen et al., 1999; Cózar et al., 2014). For Raman spectroscopy the non-destructive confocal Raman instrument WiTec Alpha 300 was used. The instrument was pre-calibrated with a silicon wafer (Murray and Cowie, 2011), and spectra recorded under a 200 μm scan stage with 532 nm excitation lengths. Raman spectrometry served to confirm that all plastics collected were in fact synthetic polymers (Allen et al., 1999), since visual analysis alone might be prone to human errors and accuracy of results otherwise questionable (Hidalgo-Ruz et al., 2012; Lenz et al., 2015).

TABLE 5 | Dunn's test results for spatial and temporal differences in size.

Kruskal-Wallis rank sum with Dunn's test by area*		Estuarine (6 mm, 17)	Nearshore (5 mm/11)
Nearshore		$p = 0.0018$	
Offshore (2.5 mm/2.5)		$p = 0.0000$	$p = 0.0001$
By month	February	July	March
July	$p = 0.0000$	–	–
March	$p = 0.4404$	$p = 0.0165$	–
May	$p = 0.0000$	$p = 0.4002$	$p = 0.0216$

**Numbers in brackets indicate median sizes and the interquartile range. Significant p-values are bold.*

Statistical Analyses

Preliminary plotting of data obtained for both concentrations and sizes showed a highly skewed distribution and heteroskedasticity in model residuals even after log transformations. As a result, non-parametric analyses were performed in the RStudio package. To test for significant differences in plastic concentrations between areas and over time, firstly, a nonparametric Kruskal-Wallis analysis of variance (KW-ANOVA) was used (Kruskal and Wallis, 1952). The KW-ANOVA determines if at least one of the areas or months is statistically different, without elucidating which ones specifically differ (Kruskal and Wallis, 1952; Dunn, 1964). After establishing if at least one population was significantly different, a *post-hoc* Dunn's (1964) rank sum test was run to see where exactly the differences occurred (Dinno, 2015). The Dunn's test is a convenient joint ranking method, applicable to test the null hypothesis that concentrations and sizes are identically distributed in populations—or in this case areas and months (Sherman, 1965). Significant *p*-values after the Dunn's test show which exact areas and months differ. To determine variations in characteristics between areas all recorded data was manually transformed into counts in Microsoft Excel™. Chi-square tests were used to determine if the proportion of types and colors varied between areas overall for comparison with other studies. To analyze differences in the characteristics between areas and size groups, data were visualized using non-metric multidimensional scaling (nMDS) based on Bray-Curtis dissimilarity in R (Oksanen et al., 2015). Bray Curtis is stable to the many zeros present in count data sets. Despite the fact that some counts were very high, no transformations were applied to the data, since our questions were mainly quantitative and would not merit from emphasizing less common types and colors. To test if the differences in characteristics were statistically significant between areas a permutational analysis of variance (PERMANOVA with 999 permutations) was applied with the effects of area, month, rainfall, wind speed and wind direction as independent and random factors. Pairwise comparisons of random factors are rarely logical in PERMANOVA approaches and therefore no tests were performed for interactions in this analysis (Anderson et al., 2008).

RESULTS

Concentrations

A total of 716 pieces of plastic were found. Material was found at all sites during all sampling times, and only one replicate tow produced no plastic fragments. Importantly, all plastics from the subsample ($n = 116$) were confirmed to be plastics by Raman spectrometry, giving confidence in the overall concentration estimates. The most common type of plastic overall was fishing line (38%), especially in the nearshore and estuarine areas, closely followed by hard plastic fragments (35%), which dominated in the offshore. Primary microplastics, all in the form of cosmetic microbeads, made up 6% ($n = 42$) of the overall sample and were most common in the nearshore area, but present in all areas. The highest concentrations of plastic pollution were detected in the nearshore environment during sampling in early July, and in the estuary and offshore in late May (**Table 2**). These concentrations confirmed hypotheses about predictable high concentrations in accordance with their respective drivers. In the offshore the highest concentration is in line with seasonally increased Leeuwin current flow. In May plastics were sampled within days of the first major rain event (**Figure 2**). This is reflected in the high concentration of estuarine plastics. Yet the nearshore showed much higher concentrations in early July than directly after the rainfall event in May.

Unexpectedly low concentrations for all areas were detected in March. Consecutive days of offshore winds were recorded prior to sampling in March. In some cases, standard deviations and interquartile ranges were found to be nearly as high as concentrations; evidence of immense spatial variability even between replicate tows (distance $\sim$ 1 nm).

The KWANOVA results showed a significant result for the interaction of area, month and rainfall in predicting concentrations ($p = 0.0026$). Spatial Dunn's test results show that both the estuary and the nearshore where significantly different form the offshore, but not from each other (**Table 3**). Temporal comparison of concentrations by month showed that March was significantly different form all other months and overpowered other significant differences. Detailed spatiotemporal results show that the offshore differed from all other months in May, and the estuarine only differed between March and May (**Table 4**). For the nearshore, significant differences were recorded for March and July compared to other months.

Plastic Size and Characteristics

KWANOVA identified a highly significant interaction of area, time and rainfall ($p < 0.005$) in determining plastic particle size. Dunn's test showed that size differed between all areas, and between but not within austral summer and winter months

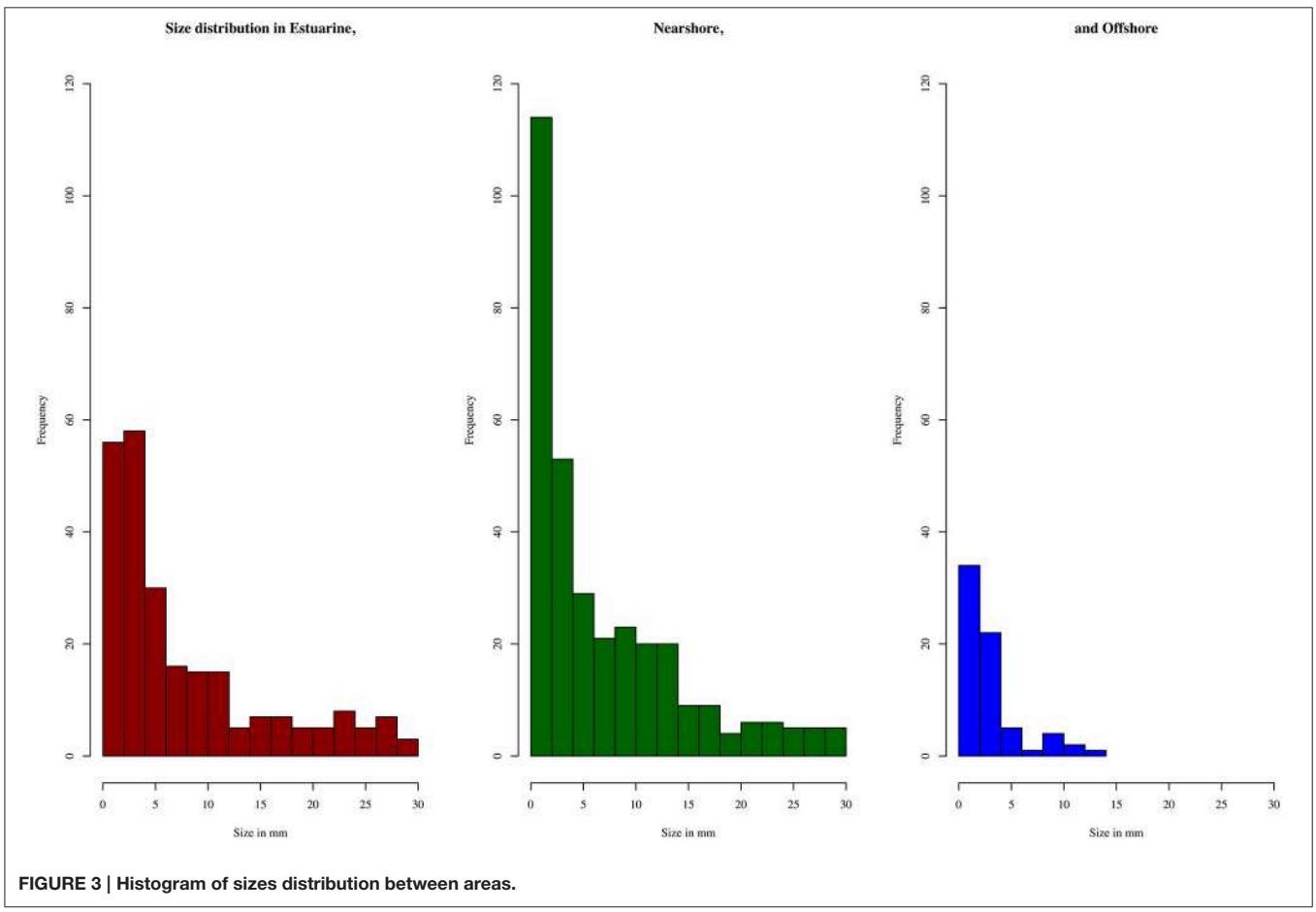

FIGURE 3 | Histogram of sizes distribution between areas.

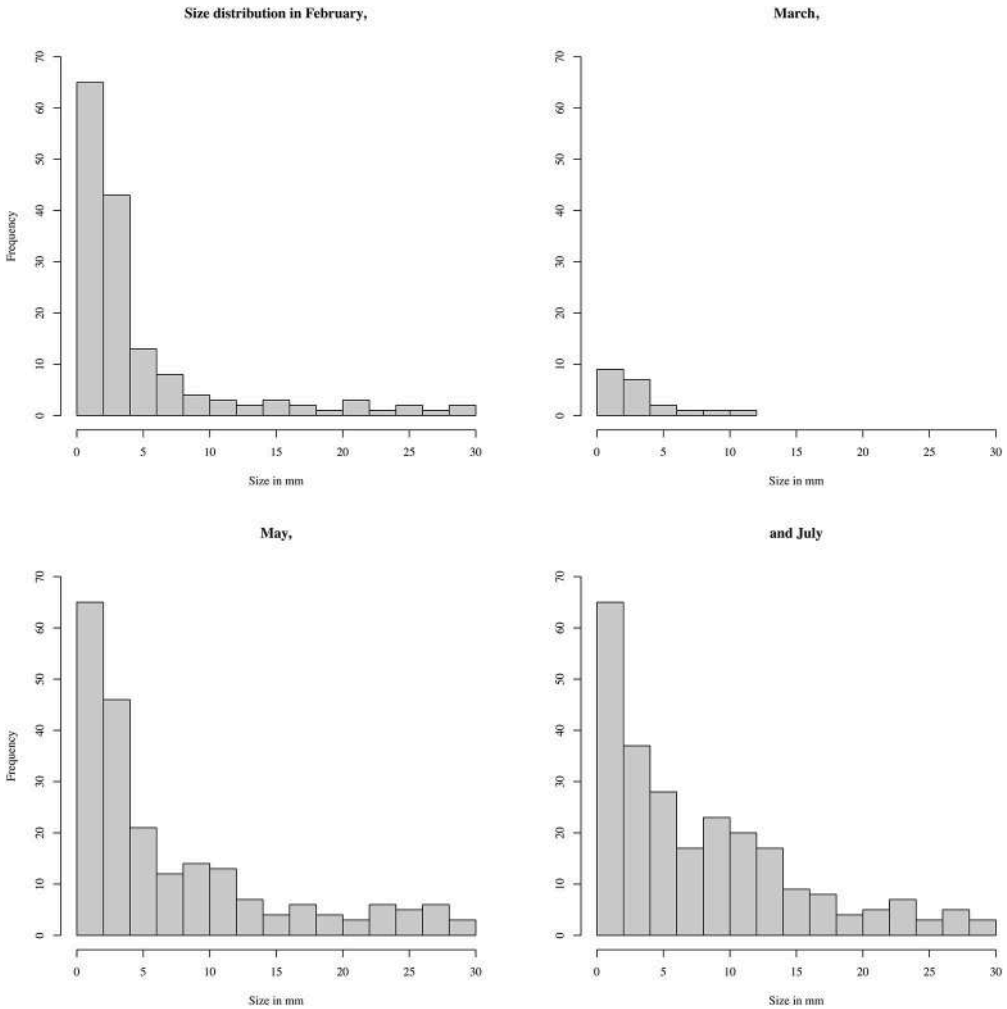

FIGURE 4 | Histogram of sizes over the duration of the study.

(**Table 5**). Offshore plastics were smallest and least variable, while estuarine had the largest fragments and interquartile ranges. Histograms of sizes reflect this and show the increased frequency of counts for larger sizes during May and July (**Figures 3**, **4**). Plastics in the smallest size categories were the most common in all areas and at all times. Sizes for the histograms presented were capped at 20 mm to be comparable to other studies (Hidalgo-Ruz et al., 2012), and to minimize one tailed skew.

Using chi-square tests showed a highly significant difference for the proportions of type (levels = 7, $p < 0.005$) and color (levels 13, $p = 0.013$) for the offshore from other areas, but no significant difference between the estuarine and nearshore areas. Offshore samples were dominated by hard plastics (fragments and microbeads adding to 70%) and estuarine and nearshore were predominantly fishing line (38 and 44% respectively, **Figure 5**). In terms of color, offshore plastics were predominantly white and clear in color (44 and 17%, **Figure 6**). In contrast, plastics from the nearshore and estuary showed a more heterogeneous array of colors with white making up only 25% in both. This difference can also be seen in the clustering of offshore samples in the nMDS that is distinct from the wide spread of nearshore and estuarine scaling (**Figures 7**, **8**). For the offshore, a deviation from the otherwise tight cluster can be seen in May. This indicates that along with higher concentrations reported earlier a wider variety of plastics types and colors are arriving with increased LC flow. PERMANOVA results show that main effects of area, month, rainfall and wind direction were significant in driving differences for type ($p = 0.039$, 0.002, 0.001, 0.003 respectively) and color ($p = 0.002$, 0.002, 0.001, 0.006 respectively), but wind speed was not (p type $= 0.362$, p color $= 0.313$).

DISCUSSION

Concentrations and Drivers of Variability

Australia has one of the largest exclusive economic zones in the world and 59,700 km of coastline, with a vast majority of the population living in coastal areas. Prior to this study, sampling

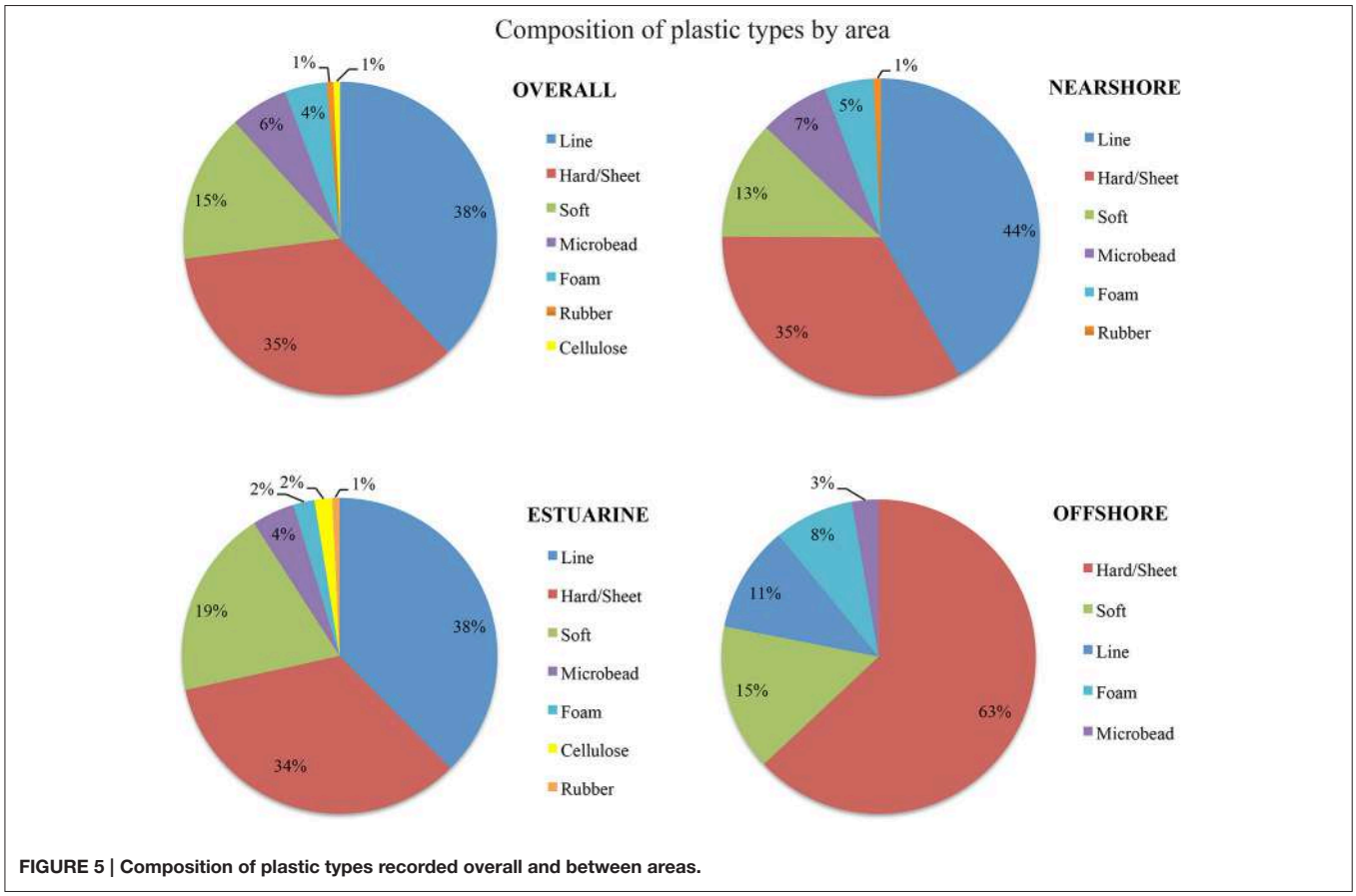

FIGURE 5 | Composition of plastic types recorded overall and between areas.

of buoyant plastics in Australian waters had been limited to approximately 60 sampling locations all around the continent (Reisser et al., 2013; Cózar et al., 2014). This study shows that concentrations of plastic pollution varied both between areas of interest and over time. Particularly the offshore area diverged widely from the estuarine and nearshore samples. The mean offshore concentration of 4,957 pieces per km^{-2} is comparable to previously recorded concentrations of 4256.4 pieces per km^{-2} in waters around the Australian continent by Reisser et al. (2013). However, temporal comparison showed that this figure could increase by an order of magnitude with increased LC flow (**Figure 2**). This increased figure is still substantially lower than high concentrations reported in subtropical gyres of up to 3.309×10^4 and 5.8×10^5 pieces/km^{-2} in the eastern North Pacific and North Atlantic respectively (Law et al., 2010, 2014). Yet, PMW average concentrations are higher than in other coastal seas, such as the Caribbean Sea ($1{,}414 \pm 112$) or the Gulf of Maine ($1{,}534 \pm 200$) (Law et al., 2010), and historical records from the Sargasso Sea (Carpenter and Smith, 1972), but lower than in comparable coastal current systems such as the Kuroshio Current (Yamashita and Tanimura, 2007). While quantification of plastics per unit of area is the most commonly used (Hidalgo-Ruz et al., 2012), differential recording of plastic concentrations as pieces per volume or in weight limits further direct comparisons (Gilfillan et al., 2009; Doyle et al., 2011).

The statistical test results showed that temporal and spatial variation could be mutually confounding, as evident in significant interaction effects for both concentrations and size. Law et al. (2014) have previously pointed this out. However by using detailed pairwise comparisons a clearer picture could be gained in this study. The confounding effects of offshore winds in March could thus be recognized without statistically overwhelming important differences between other months and areas. Previous studies have tried to navigate variability by comparing samples within spatial bins and over multiple time frames (Gilfillan et al., 2009; Morét-Ferguson et al., 2010), or spatial scales (Doyle et al., 2011; Goldstein et al., 2013), but without clearly addressing variability of physical drivers. This study had added the understanding that a focus on physical drivers—which are highly variable in space and time—rather than one large-scale feature (coastlines or gyres), can inform on the particular dynamics of interest. Furthermore, using areas for comparison rather than distance based approaches may effectively cut down sample size requirements for spatiotemporal analyses (Goldstein et al., 2013). A continuation and extension of this research design is recommended to address the utility of this approach for multi-year and decadal changes, since the sampling for this study was limited by time constraints. In those areas were historical data of plastic pollution exists measured concentrations can be coupled with historical field measurements

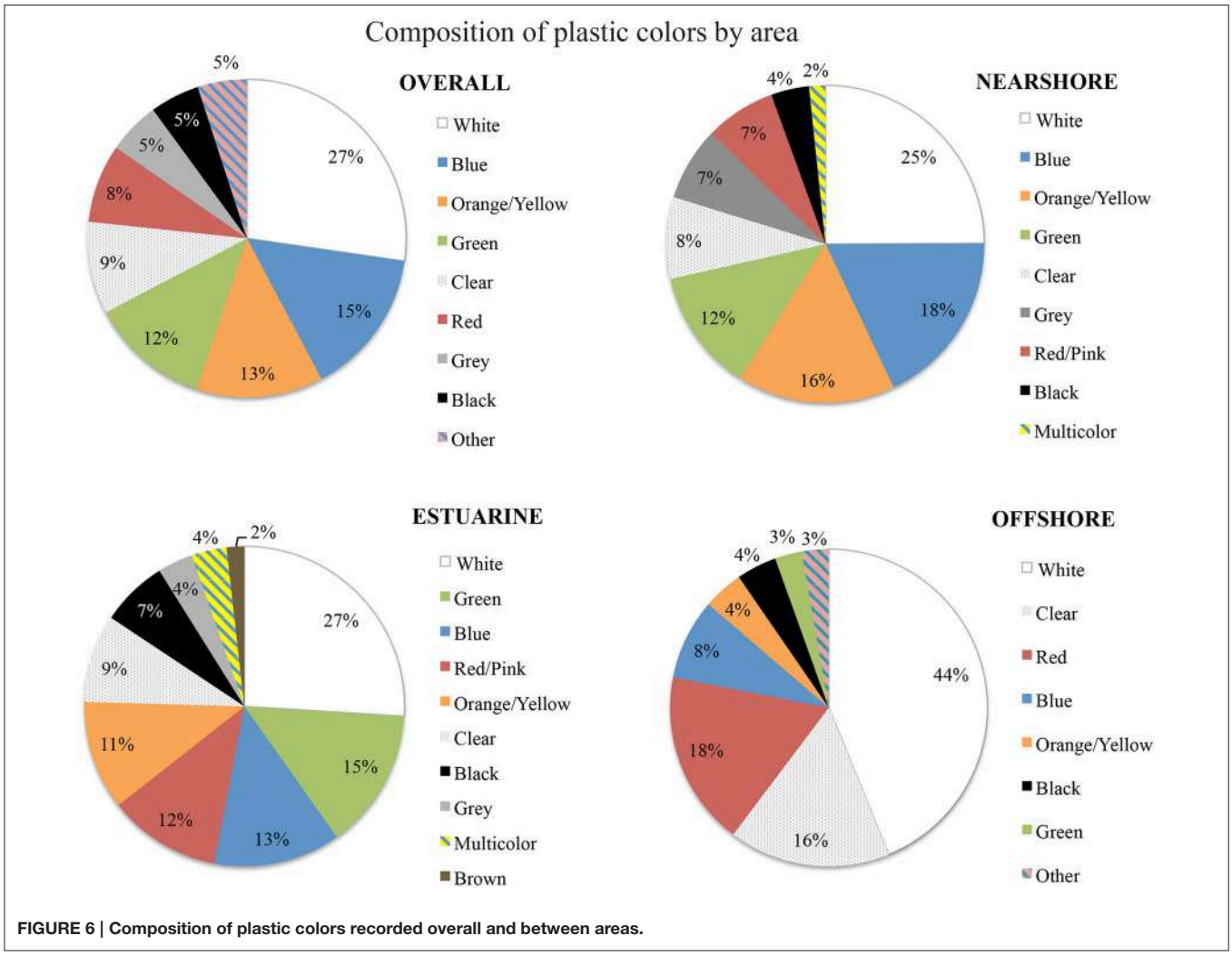

FIGURE 6 | Composition of plastic colors recorded overall and between areas.

or numerical models of physical drivers to select informed areas for comparison (Thompson et al., 2004; Gilfillan et al., 2009; Morét-Ferguson et al., 2010). This way more information may be gleaned about and from variability, which was previously not easily explained in multi-decadal or multi-year analyses.

Some preliminary predictions can be discussed to inform future research from the observed short-term variability of areas in accordance with their physical drivers. This study found that offshore microplastics, introduced to the study site with the Leeuwin current, increased with strength of flow in May. Both the ITC and Australian Monsoon driving LC variability are susceptible to changes based on El Niño Southern Oscillation (ENSO) (Pearce and Phillips, 1988; Jourdain et al., 2013). Therefore, concentrations may be significantly higher during non-ENSO years and La Nina episodes (Pearce and Phillips, 1988). With climate change driven rises in sea surface temperatures, the geostrophic Leeuwin flow is likely to increase, regardless of ENSO, and may bring with it higher concentrations of plastic fragments to local waters. This would present an additional stressor to the Western Australian marine environment that suffers significant heat stresses as a result of strong La Nina periods (Pearce et al., 2011). On the other hand, previous research has shown that ENSO periods lead to a weakening of large-scale subtropical gyre circulation and results in less concentrated debris within the center (Martinez et al., 2009). Therefore, an alternative theory would be that debris from the inner Indian Ocean subtropical gyre, spreading across the basin during El Niño episodes, might become more easily entrained into the Leeuwin current through geostrophic flow. These are some questions that can be answered through ongoing research and field sampling in the future.

Rain-induced estuarine and coastal concentrations were very high in comparison to other coastal areas, such as the Gulf of Maine and the Caribbean (**Table 2**; Law et al., 2010). A positive finding is that the dynamics of effluent from the estuary and delayed concentration along the shore was highly predictable and concentrated in time and space. This predictability may create opportunities for cost-effective cleanup initiatives. Technologies for pelagic plastic cleanups are currently being developed and trialed (Slat, 2015). Continuous study and improved understanding of the dynamics of estuarine and nearshore pollution can inform potential installations of clean

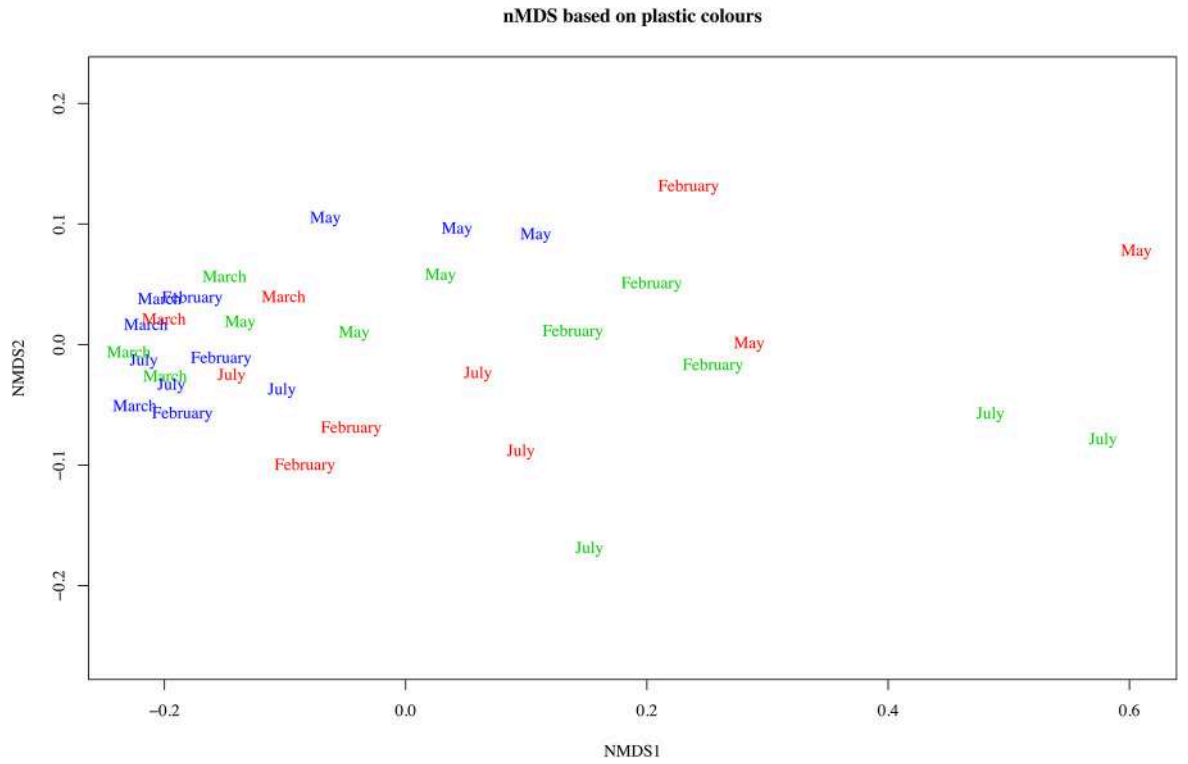

FIGURE 7 | Non-metric multidimensional scaling of Bray Curtis dissimilarity matrix computed from type counts for Perth metropolitan plastics. Color of text indicates the area of interest: blue, offshore; green, nearshore; red, estuarine.

up arrays. Well-timed, short-term installations could perceivably minimize impacts on marine life and shipping whilst reducing maintenance costs. Allan and Haylock (1993) found a strong relationship between declining rainfall along the Southwestern Australian coast and sea level pressure. With reduced and more concentrated rainfall patterns, pollution retention may become an increasing problem in the Swan River Estuary in decades to come.

Size of Plastic Fragments in PMW

As expected, the smallest fragments of plastic products were found in the offshore, and the largest in the estuary. Therefore, results presented here support the assumption that smaller plastics are "older" or have had longer residence times at sea, as long as the differentiation between SMPs and PMPs is made. The ubiquity of plastics in the smallest size category across all areas at all times raises concern about toxic effects of local pollution. The amplified hydrophilic potential of smaller fragments in the local environment may make for an underestimated impact on marine biota, when concentrations alone are considered. This study showed that small fragments are present, and likely moving in and out of the tide dominated Swan Estuary, where a large harbor is located (**Figure 1**). The most recent report by the Swan River Trust shows that environmental targets are not being met and water quality is deteriorating (Swan River Trust, 2016). If this trend continues, threat to marine and estuarine biota through plastic ingestion may be significant and increasing. As such monitoring of plastic pollution and additional studies on pollutant loads are recommended (Murray and Cowie, 2011; Rochman, 2015).

The skewedness of size distributions also suggests that a substantial amount of material below the manta net's limit of detection (333 micron) is present in local waters. The strong sea breeze in the area increases incident wave energy (Pattiaratchi et al., 1997). This may result in rapid mechanical breakdown of plastic particles trapped in the nearshore. New methods for the quantification of smaller size ranges are being developed and tested (for example: Enders et al., 2015). Further testing of such methods and comparative analysis with more standard approaches (such as presented here) is warranted to determine a viable method for the quantification of nano-plastics and their chemical loads and toxicity.

Types and Colors of Plastic Fragments

A significant difference between the types of plastics found in nearshore and estuary vs. the offshore gives some indication about local discard practices, which can be addressed through educational initiatives. The large amount of fishing line found exiting the estuary and in the nearshore points at substantial pollution from recreational fishing activities. Implementing initiatives to address this source and monitoring future trends can become one form of Key Performance Indicator for local environmental management. Offshore samples in PMW, on the other hand, seem to have a comparably more "oceanic signature."

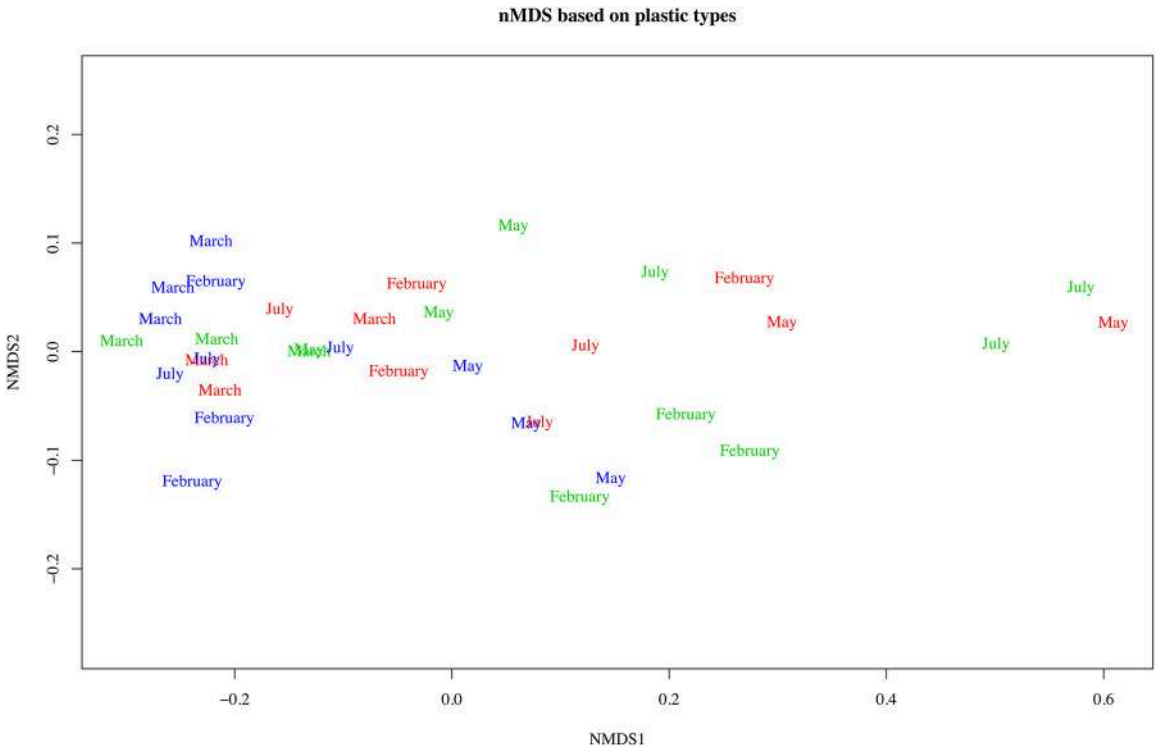

FIGURE 8 | Non-metric multidimensional scaling of Bray-Curtis dissimilarity matrix computed from color counts for Perth metropolitan plastics. Color of text indicates the area of interest: blue, offshore; green, nearshore; red, estuarine.

They are similar in type and colors to what has previously been recorded in deeper waters around Australia, the North Pacific and the North Atlantic: Reisser et al. (2013) reported 75% of plastics found around Australia were hard fragments, while Shaw and Day (1994) and Morét-Ferguson et al. (2010) reported 60–90% for the Pacific, and 50–90% for the Atlantic respectively. Furthermore, white or clear plastics made up 85% of fragments in Australian waters and 75% in the North Pacific Ocean. Previous studies have shown that these characteristics can inform on changes over time and between size classes (Shaw and Day, 1994; Vlietstra and Parga, 2002; Morét-Ferguson et al., 2010). Results presented here indicated some change occurring in the offshore with increased LC flow even over the limited time frame of this pilot study. Therefore, continuing to record this information is encouraged, for detailed detection of change in the future, to firstly better understand predator selectivity, and secondly enable comparisons with other studies globally.

CONCLUSIONS

One of the major finds of this case study is that statistically significant differences in concentrations of plastic pollution between areas over the short-term duration of the project were largely predictable. Where oceanic drivers were not predictive of the resulting concentrations, deviations could be explained through recorded climatic conditions, in this case wind direction. On one hand, this raises questions about the feasibility of extrapolation from single time-frame measurements as being representative of a full year for inter-annual comparison. On the other hand, it provides some insights to sources and dynamics of interest in similar environments globally. This case study provides an approach that may be more reliable in detecting trends and changes at multi-year or multi-decadal scales in the future. Using pairwise comparisons of previously defined areas may also yield better results in future studies, due to a reduced sample size needed for comparison and greater focus on oceanographic and climatic data explaining variability. This study adds to the very limited body of information for pelagic plastic pollution in Australian waters and compares local concentrations and characteristics with global data. A number of preliminary predictions were made, which will need to be tested in future research. In terms of findings that can be implemented for mitigation, the data shows that the majority of pollution is from local sources and dominated by fishing line in small size fractions. This indicates a clear fishing-related primary source of pollution. While further research will be invaluable in directing management recommendations to tackle this pervasive environmental problem over time, addressing the specific sources and behaviors leading to of plastic pollution is an important first step. This shows the benefits of qualitative analyses of plastic characteristics, which have the potential inform sources, rather than purely quantitative studies focusing on the state of pollution.

AUTHOR CONTRIBUTIONS

All authors listed, have made substantial, direct and intellectual contribution to the work, and approved it for publication.

ACKNOWLEDGMENTS

This work was funded by the Australian Integrated Marine Observing System's (IMOS) Australian National Facility for Ocean Gliders (ANFOG) at The University of Western Australia and the PADI Foundation (grant number CGA# 11311), CA. The authors acknowledge the facilities, and the scientific and technical assistance of the Australian Microscopy & Microanalysis Research Facility at the Centre for Microscopy, Characterisation & Analysis (CMCA), The University of Western Australia, a facility funded by the University, State and Commonwealth Governments. We would like to thank Dennis Stanley of ANFOG, and L. Kirilak & T. Becker of CMCA in particular for their technical assistance and recommendations.

REFERENCES

Allan, R. J., and Haylock, M. R. (1993). Circulation features associated with the winter rainfall decrease in southwestern Australia. *J. Clim.* 6, 1356–1367.

Allen, V., Kalivas, J. H., and Rodriguez, R. G. (1999). Post-consumer plastic identification using Raman spectroscopy. *Appl. Spectrosc.* 53, 672–681.

Anderson, M., Gorley, R., and Clarke, K. (2008). *PERMANOVA1 for PRIMER: Guide to Software and Statistical Methods*. Plymouth: PRIMER-E.

Andrady, A. L. (2011). Microplastics in the marine environment. *Mar. Pollut. Bull.* 62, 1596–1605. doi: 10.1016/j.marpolbul.2011.05.030

Avio, C. G., Gorbi, S., Milan, M., Benedetti, M., Fattorini, D., d'Errico, G., et al. (2015). Pollutants bioavailability and toxicological risk from microplastics to marine mussels. *Environ. Pollut.* 198, 211–222. doi: 10.1016/j.envpol.2014.12.021

Barnes, D. K., Galgani, F., Thompson, R. C., and Barlaz, M. (2009). Accumulation and fragmentation of plastic debris in global environments. *Philos. Trans. R. Soc. B. Biol. Sci.* 364, 1985–1998. doi: 10.1098/rstb.2008.0205

Brown, D., and Cheng, L. (1981). New net for sampling the ocean surface. *Mar. Ecol. Prog. Ser.* 5, 224–227.

Bureau of Meteorology (2015). *Latest Weather Observations for Rottnest Island*. Canberra, ACT: Bureau of Meteorology, Commonwealth of Australia.

Carpenter, E. J., and Smith, K. (1972). Plastics on the Sargasso Sea surface. *Science* 175, 1240–1241.

Carslaw, D. C., and Ropkins, K. (2012). Openair—an R package for air quality data analysis. *Environ. Model Softw.* 27, 52–61. doi: 10.1016/j.envsoft.2011.09.008

Carson, H. S., Lamson, M. R., Nakashima, D., Toloumu, D., Hafner, J., Maximenko, N., et al. (2013). Tracking the sources and sinks of local marine debris in Hawai'i. *Mar. Environ. Res.* 84, 76–83. doi: 10.1016/j.marenvres.2012.12.002

Cole, M., Lindeque, P., Halsband, C., and Galloway, T. S. (2011). Microplastics as contaminants in the marine environment: a review. *Mar. Pollut. Bull.* 62, 2588–2597. doi: 10.1016/j.marpolbul.2011.09.025

Corcoran, P. L., Biesinger, M. C., and Grifi, M. (2009). Plastics and beaches: a degrading relationship. *Mar. Pollut. Bull.* 58, 80–84. doi: 10.1016/j.marpolbul.2008.08.022

Cózar, A., Echevarría, F., González-Gordillo, J. I., Irigoien, X., Úbeda, B., Hernández-León, S., et al. (2014). Plastic debris in the open ocean. *Proc. Natl. Acad. Sci. U.S.A.* 111, 10239–10244. doi: 10.1073/pnas.1314705111

Dee, D., Uppala, S., Simmons, A., Berrisford, P., Poli, P., Kobayashi, S., et al. (2011). The ERA-Interim reanalysis: configuration and performance of the data assimilation system. *Q. J. R. Meteorol. Soc.* 137, 553–597. doi: 10.1002/qj.828

Derraik, J. G. B. (2002). The pollution of the marine environment by plastic debris: a review. *Mar. Pollut. Bull.* 44, 842–852. doi: 10.1016/S0025-326X(02)00220-5

Dinno, A. (2015). *dunn.test: Dunn's Test of Multiple Comparisons Using Rank Sums,* R Package Version 1.3. Available online at: http://CRAN.R-project.org/package=dunn.test

do Sul, J. A. I., and Costa, M. F. (2014). The present and future of microplastic pollution in the marine environment. *Environ. Pollut.* 185, 352–364. doi: 10.1016/j.envpol.2013.10.036

Doyle, M. J., Watson, W., Bowlin, N. M., and Sheavly, S. B. (2011). Plastic particles in coastal pelagic ecosystems of the Northeast Pacific ocean. *Mar. Environ. Res.* 71, 41–52. doi: 10.1016/j.marenvres.2010.10.001

Dunn, O. J. (1964). Multiple comparisons using rank sums. *Technometrics* 6, 241–252.

Enders, K., Lenz, R., Stedmon, C. A., and Nielsen, T. G. (2015). Abundance, size and polymer composition of marine microplastics $\geq$ 10μm in the Atlantic Ocean and their modelled vertical distribution. *Mar. Pollut. Bull.* 100, 70–81. doi: 10.1016/j.marpolbul.2015.09.027

Eriksen, M., Lebreton, L. C., Carson, H. S., Thiel, M., Moore, C. J., Borerro, J. C., et al. (2014). Plastic pollution in the World's Oceans: more than 5 trillion plastic pieces weighing over 250,000 tons Afloat at Sea. *PLoS ONE* 9:e111913. doi: 10.1371/journal.pone.0111913

Eriksen, M., Maximenko, N., Thiel, M., Cummins, A., Lattin, G., Wilson, S., et al. (2013). Plastic pollution in the South Pacific subtropical gyre. *Mar. Pollut. Bull.* 68, 71–76. doi: 10.1016/j.marpolbul.2012.12.021

Erren, T. C., Groß, J. V., Steffany, F., and Meyer-Rochow, V. B. (2015). "Plastic ocean": what about cancer? *Environ. Pollut.* 207, 436–437. doi: 10.1016/j.envpol.2015.05.025

Feng, M., Meyers, G., Pearce, A., and Wijffels, S. (2003). Annual and interannual variations of the Leeuwin current at 32 S. *J. Geophys. Res. Oceans* 108:3355. doi: 10.1029/2002JC001763

Fieux, M., Molcard, R., and Morrow, R. (2005). Water properties and transport of the Leeuwin current and eddies off Western Australia. *Deep Sea Res. Part I* 52, 1617–1635. doi: 10.1016/j.dsr.2005.03.013

Gallant, A. J. E., Reeder, M. J., Risbey, J. S., and Hennessy, K. J. (2013). The characteristics of seasonal-scale droughts in Australia, 1911–2009. *Int. J. Climatol.* 33, 1658–1672. doi: 10.1002/ joc.3540

Gilfillan, L. R., Ohman, M. D., Doyle, M. J., and Watson, W. (2009). Occurrence of plastic micro-debris in the southern California current system. *Cal. Coop. Ocean. Fish.* 50, 123–133. Available online at: http://137.110.142.7/publications/CR/2009/2009Gilf.pdf

Godfrey, J., and Ridgway, K. (1985). The large-scale environment of the poleward-flowing Leeuwin current, Western Australia: longshore steric height gradients, wind stresses and geostrophic flow. *J. Phys. Oceanogr.* 15, 481–495. doi: 10.1175/1520-0485(1985)015<0481:TLSEOT>2.0.CO;2

Goldstein, M. C., Titmus, A. J., and Ford, M. (2013). Scales of spatial heterogeneity of plastic marine debris in the northeast Pacific Ocean. *PLoS ONE* 8:e80020. doi: 10.1371/journal.pone.0080020

Gregory, M. R. (2009). Environmental implications of plastic debris in marine settings—entanglement, ingestion, smothering, hangers-on, hitch-hiking and alien invasions. *Philos. Trans. R. Soc. B. Biol. Sci.* 364, 2013–2025. doi: 10.1098/rstb.2008.0265

Hidalgo-Ruz, V., Gutow, L., Thompson, R. C., and Thiel, M. (2012). Microplastics in the marine environment: a review of the methods used for identification and quantification. *Environ. Sci. Technol.* 46, 3060–3075. doi: 10.1021/es2031505

Isobe, A., Uchida, K., Tokai, T., and Iwasaki, S. (2015). East Asian seas: a hot spot of pelagic microplastics. *Mar. Pollut. Bull.* 101, 618–623. doi: 10.1016/j.marpolbul.2015.10.042

Jambeck, J. R., Geyer, R., Wilcox, C., Siegler, T. R., Perryman, M., Andrady, A., et al. (2015). Plastic waste inputs from land into the ocean. *Science* 347, 768–771. doi: 10.1126/science.1260352

Jourdain, N. C., Gupta, A. S., Taschetto, A. S., Ummenhofer, C. C., Moise, A. F., and Ashok, K. (2013). The Indo-Australian monsoon and its relationship to ENSO and IOD in reanalysis data and the CMIP3/CMIP5 simulations. *Clim. Dyn.* 41, 3073–3102. doi: 10.1007/s00382-013-1676-1

Kruskal, W. H., and Wallis, W. A. (1952). Use of ranks in one-criterion variance analysis. *J. Am. Stat. Assoc.* 47, 583–621.

Kubota, M. (1994). A mechanism for the accumulation of floating marine debris north of Hawaii. *J. Phys. Oceanogr.* 24, 1059–1064.

Kukulka, T., Proskurowski, G., Morét-Ferguson, S., Meyer, D. W., and Law, K. L. (2012). The effect of wind mixing on the vertical distribution of buoyant plastic debris. *Geophys. Res. Lett.* 39:L07601. doi: 10.1029/2012GL051116

Law, K. L., Morét-Ferguson, S. E., Goodwin, D. S., Zettler, E. R., DeForce, E., Kukulka, T., et al. (2014). Distribution of surface plastic debris in the Eastern Pacific Ocean from an 11-year data set. *Environ. Sci. Technol.* 48, 4732–4738. doi: 10.1021/es4053076

Law, K. L., Morét-Ferguson, S., Maximenko, N. A., Proskurowski, G., Peacock, E. E., Hafner, J., et al. (2010). Plastic accumulation in the North Atlantic subtropical gyre. *Science* 329, 1185–1188. doi: 10.1126/science.1192321

Lenz, R., Enders, K., Stedmon, C. A., Mackenzie, D. M. A., and Nielsen, T. G. (2015). A critical assessment of visual identification of marine microplastic using Raman spectroscopy for analysis improvement. *Mar. Pollut. Bull.* 100, 82–91. doi: 10.1016/j.marpolbul.2015.09.026

Martinez, E., Maamaatuaiahutapu, K., and Taillandier, V. (2009). Floating marine debris surface drift: convergence and accumulation toward the South Pacific subtropical gyre. *Mar. Pollut. Bull.* 58, 1347–1355. doi: 10.1016/j.marpolbul.2009.04.022

Meyers, G., Bailey, R., and Worby, A. (1995). Geostrophic transport of Indonesian throughflow. *Deep Sea Res. Part I.* 42, 1163–1174.

Morét-Ferguson, S., Law, K. L., Proskurowski, G., Murphy, E. K., Peacock, E. E., and Reddy, C. M. (2010). The size, mass, and composition of plastic debris in the western North Atlantic Ocean. *Mar. Pollut. Bull.* 60, 1873–1878. doi: 10.1016/j.marpolbul.2010.07.020

Morrow, R., and Birol, F. (1998). Variability in the southeast Indian Ocean from altimetry: forcing mechanisms for the Leeuwin current. *J. Geophys. Res. Oceans* 103, 18529–18544. doi: 10.1029/98JC00783

Murray, F., and Cowie, P. R. (2011). Plastic contamination in the decapod crustacean Nephrops norvegicus (Linnaeus, 1758). *Mar. Pollut. Bull.* 62, 1207–1217. doi: 10.1016/j.marpolbul.2011.03.032

NOAA (2015). *How to Do a Manta Tow*. Available online at: https://swfsc.noaa.gov/textblock.aspx?Division=FRD&id=1342

Oksanen, J., Blanchet, F. G., Kindt, R., Legendre, P., Minchin, P. R., O'Hara, R. B., et al. (2015). *vegan: Community Ecology Package*, R package version 2.2-1. Available online at: http://CRAN.R-project.org/package=vegan

Pattiaratchi, C., Hegge, B., Gould, J., and Eliot, I. (1997). Impact of sea-breeze activity on nearshore and foreshore processes in southwestern Australia. *Cont. Shelf Res.* 17, 1539–1560. doi: 10.1016/S0278-4343(97)00016-2

Pattiaratchi, C., and Woo, M. (2009). The mean state of the Leeuwin current system between North West Cape and Cape Leeuwin. *J. R. Soc. West. Aust.* 92, 221–241. Available online at: http://www.rswa.org.au/publications/Journal/92(2)/ROY%20SOC%2092.2%20LEEUWIN%20221-241.pdf

Pearce, A., Lenanton, R., Jackson, G., Moore, J., Feng, M., and Gaughan, D. (2011). "The "Marine heat wave" off Western Australia during the summer of 2010/11," in *Fisheries Research Report No. 222.* Department of Fisheries, (Western Australia, WA).

Pearce, A., and Pattiaratchi, C. (1999). The Capes Current: a summer countercurrent flowing past Cape Leeuwin and Cape Naturaliste, Western Australia. *Cont. Shelf Res.* 19, 401–420. doi: 10.1016/S0278-4343(98)00089-2

Pearce, A., and Phillips, B. (1988). ENSO events, the Leeuwin Current, and larval recruitment of the western rock lobster. *J. du Conseil: ICES J. Mar. Sci.* 45, 13–21. doi: 10.1093/icesjms/45.1.13

Pérez, J. M., Vilas, J. L., Laza, J. M., Arnáiz, S., Mijangos, F., Bilbao, E., et al. (2010). Effect of reprocessing and accelerated ageing on thermal and mechanical polycarbonate properties. *J. Mater. Process. Technol.* 210, 727–733. doi: 10.1016/j.jmatprotec.2009.12.009

Reisser, J., Shaw, J., Wilcox, C., Hardesty, B. D., Proietti, M., Thums, M., et al. (2013). Marine plastic pollution in waters around Australia: characteristics, concentrations, and pathways. *PLoS ONE* 8:e80466. doi: 10.1371/journal.pone.0080466

Reisser, J., Slat, B., Noble, K., du Plessis, K., Epp, M., Proietti, M., et al. (2014). The vertical distribution of buoyant plastics at sea. *Biogeosci. Discuss.* 11, 16207–16226. doi: 10.5194/bg-12-1249-2015

Ridgway, K., and Godfrey, J. (2015). The source of the Leeuwin Current seasonality. *J. Geophys. Res. Oceans* 120, 6843–6864. doi: 10.1002/2015JC011049

Rochman, C. M. (2015). "The complex mixture, fate and toxicity of chemicals associated with plastic debris in the marine environment," in *Marine Anthropogenic Litter*, eds M. Bergmann, L. Gutow, and M. Klages (Cham: Springer International Publishing), 117–140. doi: 10.1007/978-3-319-16510-3

Rochman, C. M., Kurobe, T., Flores, I., and Teh, S. J. (2014). Early warning signs of endocrine disruption in adult fish from the ingestion of polyethylene with and without sorbed chemical pollutants from the marine environment. *Sci. Total Environ.* 493, 656–661. doi: 10.1016/j.scitotenv.2014.06.051

Ruiz-Montoya, L., and Lowe, R. (2014). Summer circulation dynamics within the Perth coastal waters of southwestern Australia. *Cont. Shelf Res.* 77, 81–95. doi: 10.1016/j.csr.2014.01.022

Schuyler, Q., Hardesty, B. D., Wilcox, C., and Townsend, K. (2012). To eat or not to eat? Debris selectivity by marine turtles. *PLoS ONE* 7:e40884. doi: 10.1371/journal.pone.0040884

Seltenrich, N. (2015). New link in the food chain? Marine plastic pollution and seafood safety. *Environm. Health Perspect.* 123:A34. doi: 10.1289/ehp.123-A34

Shaw, D. G., and Day, R. H. (1994). Colour-and form-dependent loss of plastic micro-debris from the North Pacific Ocean. *Mar. Pollut. Bull.* 28, 39–43.

Sherman, E. (1965). A note on multiple comparisons using rank sums. *Technometrics* 7, 255–256.

Slat, B. (ed.). (2015). *World's First Ocean Cleaning System to be Deployed in 2016.* T.O.C. Team. Available online at: http://www.theoceancleanup.com/blog/show/item/worlds-first-ocean-cleaning-system-to-be-deployed-in-2016.html

Smith, I., McIntosh, P., Ansell, T., Reason, C., and McInnes, K. (2000). Southwest Western Australian winter rainfall and its association with Indian Ocean climate variability. *Int. J. Climatol.* 20, 1913–1930. doi: 10.1002/1097-0088(200012)20:15<1913::AID-JOC594>3.0

Swan River Trust (2016). *Final Report 2015–2016, Government of Western Australia*. Available online at: https://swanrivertrust.dpaw.wa.gov.au/images/documents/annual_reports/37714_Swan_River_Trust_Annual_Report_2015-16_k2c_FNL2small.pdf

Thiel, M., Hinojosa, I., Miranda, L., Pantoja, J., Rivadeneira, M., and Vásquez, N. (2013). Anthropogenic marine debris in the coastal environment: a multi-year comparison between coastal waters and local shores. *Mar. Pollut. Bull.* 71, 307–316. doi: 10.1016/j.marpolbul.2013.01.005

Thompson, R. C., Olsen, Y., Mitchell, R. P., Davis, A., Rowland, S. J., John, A. W. G., et al. (2004). Lost at Sea: where is all the plastic? *Science* 304, 838. doi: 10.1126/science.1094559

Vegter, A. C., Barletta, M., Beck, C., Borrero, J., Burton, H., Campbell, M., et al. (2014). Global research priorities to mitigate plastic pollution impacts on marine wildlife. *Endanger. Species Res.* 25, 225–247. doi: 10.3354/esr00623

Vlietstra, L. S., and Parga, J. A. (2002). Long-term changes in the type, but not amount, of ingested plastic particles in short-tailed shearwaters in the southeastern Bering Sea. *Mar. Pollut. Bull.* 44, 945–955. doi: 10.1016/S0025-326X(02)00130-3

Wandres, M. (2015). *Perth surfing Forecast*. Available online at: online: http://perthsurfing.com/

Yamashita, R., and Tanimura, A. (2007). Floating plastic in the Kuroshio current area, western North Pacific Ocean. *Mar. Pollut. Bull.* 54, 485–488. doi: 10.1016/j.marpolbul.2006.11.012

Yit Sen Bull, C., and van Sebille, E. (2016). Sources, fate, and pathways of Leeuwin current water in the Indian Ocean and great Australian Bight: a Lagrangian study in an eddy-resolving ocean model. *J. Geophys. Res. Oceans* 121, 1626–1639. doi: 10.1002/2015JC011486

Conflict of Interest Statement: The authors declare that the research was conducted in the absence of any commercial or financial relationships that could be construed as a potential conflict of interest.

frontiers in Marine Science

TECHNOLOGY REPORT
published: 28 March 2017
doi: 10.3389/fmars.2017.00086

Toward a Harmonized Approach for Monitoring of Riverine Floating Macro Litter Inputs to the Marine Environment

Daniel González-Fernández and Georg Hanke*

Directorate-General Joint Research Centre, Directorate D – Sustainable Resources, European Commission, Ispra, Italy

A high percentage of the litter entering the marine environment is assumed to come from land-based sources, but freshwater litter inputs have not been quantified. The lack of data and knowledge on fluxes of riverine litter to the sea, i.e., quantities and sources, hinders implementation of appropriate environmental regulations and mitigation measures. Estimations of riverine litter inputs require a consistent and harmonized approach to gather comparable data. The visual observation of floating litter on rivers has been selected as a simple and robust methodology for litter monitoring. A collaborative network of 36 institutions has been set-up for large spatial coverage. Currently 58 rivers are being observed regularly. A tablet computer application has been developed for the monitoring of floating macro litter (>2.5 cm) to harmonize the visual observations. The application allows recording of the observed items, their size and geo-position data during monitoring sessions. A common agreed list of litter items and size ranges is used, providing a common harmonized approach for data collection and reporting.

Keywords: litter, plastics, floating debris, environmental monitoring, pollution, marine litter, Riverine input

OPEN ACCESS

Edited by:
Julia Reisser,
The Ocean Cleanup, Netherlands

Reviewed by:
Francois Galgani,
French Research Institute for Exploitation of the Sea, France
Monica F. Costa,
Federal University of Pernambuco, Brazil
Cristina Panti,
University of Siena, Italy

****Correspondence:***
Daniel González-Fernández
daniel.gonzalez@ec.europa.eu

Specialty section:
This article was submitted to Marine Pollution, a section of the journal Frontiers in Marine Science

Received: *22 December 2016*
Accepted: *13 March 2017*
Published: *28 March 2017*

Citation:
González-Fernández D and Hanke G (2017) Toward a Harmonized Approach for Monitoring of Riverine Floating Macro Litter Inputs to the Marine Environment. Front. Mar. Sci. 4:86. doi: 10.3389/fmars.2017.00086

INTRODUCTION

Marine pollution by anthropogenic litter is a global environmental issue, as recognized by international organizations and environmental policy frameworks in recent years. The European Marine Strategy Framework Directive (MSFD) (European Commission, 2008) provides for the assessment of Marine Litter as one Descriptor of Good Environmental Status: Descriptor 10, properties and quantities of marine litter do not cause harm to the coastal and marine environment. Therefore, assessment of marine litter is a requirement for the 23 European Union Member States (EU MSs) involved in the implementation of the MSFD. Further, the United Nations identify Marine Litter as a factor in the Sustainable Development Goal 14 and the G7 countries have declared commitment to avoid and reduce marine litter, in particular plastics from land-based sources, during the G7 Ise-Shima Summit (26–27 May 2016).

Plastics floating in the oceans have been estimated to count over 5 trillion pieces and weigh more than a quarter million tons globally, with microplastics (as pieces <4.75 mm) being about 92% of total counts and meso+macro plastics (as pieces >4.75 mm) comprising with ca. 87% the bulk of total litter weight (Eriksen et al., 2014). This large amount of meso+macro plastic is exposed to degradation and fragmentation processes, thus being a secondary source of micro plastic (Barnes et al., 2009; GESAMP, 2015). Jambeck et al. (2015) estimated that 4.8–12.7 million tons of plastics could be entering the marine environment from land-based sources yearly, with prediction

of a significant increase of this input in the near future if actions are not taken. However, these estimations are based on limited field data and subject to substantial lack of knowledge on litter behavior and transport, therefore significant uncertainties are present.

Floating macro litter, once it has reached the sea, can have a long term residence in the surface waters, which increases the probability of causing harm to marine animals (fish, marine mammals, reptiles, and birds) through ingestion and entanglement (EC JRC, 2016b). Moreover, floating litter fraction has a high mobility and can be transported from inland to remote areas in the oceans, even at global scale.

Although estimations have been made indicating that a high percentage of the marine litter comes directly from land-based sources, quantitative data on freshwater inputs of macro litter are not available. In order to prioritize prevention and reduction measures and to identify sources of litter input to the marine environment, appropriate attention should be given to riverine litter pathways. Consequently, quantitative data on riverine inputs are needed in order to identify hotspots, quantify loads and characterize sources. This information can support the implementation of environmental regulations to reduce marine litter.

In the marine environment, methodologies and protocols for visual observation at sea have been proposed by several institutions and scientific research groups such as UNEP (Cheshire et al., 2009), Hinojosa and Thiel (2009), European Commission (EC JRC, 2013), NOAA Marine Debris Program (NOAA, 2013), Ryan (2013), DeFishGear (2014) and UNEP/MAP (2016). These methodologies can serve as a basis for harmonization of approaches for the establishment of international monitoring programs. Regarding the freshwater environment, no specific monitoring programs have been developed at international level and harmonized approaches are lacking for litter monitoring in rivers (EC JRC, 2016c). Only recently have a few research efforts been dedicated to studying riverine litter and its inputs to the marine environment, mostly focused on micro plastic (Surfrider Foundation Europe, 2014; Hohenblum et al., 2015; van der Wal et al., 2015). In general, approaches lack maturity or do not exist, requiring further development and agreement on basic definitions and methodologies, as e.g., for micro plastics sampling and analytical procedures (Dris et al., 2015). The estimation of riverine litter inputs requires a consistent and harmonized approach in order to gather comparable data. Harmonization is required to facilitate the development of robust databases and eventually allow the use of models to account for spatial and temporal variability.

This paper presents a harmonized collaborative approach for the estimation of floating macro litter inputs to the marine environment. The approach involves a large geographical scale field monitoring network that has been set-up by the European Commission Joint Research Centre (EC JRC) within the RIMMEL project (EC JRC, 2016a). The network uses a tablet computer application, the JRC Floating Litter Monitoring Application (App), for collection of data in river estuaries. The methodology is based on visual observations, using a common agreed list of litter items and size categories. The App allows real time data acquisition during monitoring sessions, thus providing a tool for data collection and reporting.

RIVERINE LITTER OBSERVATION NETWORK–THE APPROACH

Within the JRC exploratory research project RIMMEL: RIverine and Marine floating macro litter Monitoring and Modeling of Environmental Loading (EC JRC, 2016a), a Riverine Litter Observation Network has been set up for acquisition of data on floating macro litter inputs to the sea. The network is a collaborative activity of 36 Scientific Institutes, Authorities, SMEs and NGOs covering 17 countries (**Table 1**). They provide the observations as an add-on to the scientific or monitoring activities they are involved in. Information exchange with and among project partners is achieved through a dedicated communication platform.

Monitoring is performed in 58 rivers and is expected to increase, with geographical distribution in the four European marine shared basins (Mediterranean Sea, Black Sea, North East Atlantic Ocean and Baltic Sea).

At MSFD scale, floating macro litter monitoring refers to items >2.5 cm that, due to their buoyancy properties, are floating or suspended in the water surface layer. In the marine environment, visual observation has been employed in different geographical areas (Galgani et al., 2015), and currently the only method with wider use. Other methodologies such as aerial surveys and automated camera systems would require further development in order to become practical for monitoring programs (EC JRC, 2013). The quantitative physical collection of litter items, which would provide the best information about litter flux and item identity cannot be employed in a large number of sites at a high frequency. While the observation of the water surface has shortcomings, e.g., submerged floating items cannot be seen in turbid rivers and items can only be identified in the short time they float by, it appears to be the only option for low cost and high frequency monitoring at a large number of sites. It is assumed that, to obtain comparative litter flux estimates, it provides a proxy which fulfills the needs. Therefore, the Riverine Litter Observation Network has selected the visual observation methodology as a practical option to collect data on floating macro litter (items >2.5 cm) as a simple and direct methodology that can be used at relevant geographical scale to provide an initial proxy in the short term.

Similarly to monitoring at sea, the visual observation methodology has limitations as litter detection is affected by: weather conditions, sun orientation, the eight of the observation site and characteristics of the litter items (color, size, shape, and floatability); but also by the observer's ability, experience, concentration, and fatigue (Ryan, 2013; Suaria and Aliani, 2014). In rivers, additional factors such as surface water speed and turbulence will be important for litter detection. The height of the selected observation site (vertical distance between observer's eyes and river surface) should allow detection of litter items down to 2.5 cm (lower limit for macro litter), but use of binoculars

TABLE 1 | List of participants in the riverine litter observation network.

Country	City	Institution
Albania	Tirana	Agricultural University of Tirana
France	Perpignan	CEFREM (UMR CNRS 5110)
France	Marseille	Mediterranean Institute of Oceanography (MIO)
France	Biarritz	SurfRider Foundation Europe
Georgia	Tbisili	Scientific Research Firm GAMMA
Georgia	Tbisili	Tbilisi State University
Germany	Wilhelmshaven	ICBM-Terramare, Carl von Ossietzky University
Greece	Anavissos	Hellenic Centre for Marine Research - Department of Inland Waters
Greece	Heraklion	terraSolutions m.e.r.
Ireland	Galway	iSea conservation of aquatic ecosystems (Greece)
Israel	Haifa	IOLR
Italy	La Spezia	CNR-ISMAR
Italy	Fiumicino	Accademia del Leviatano
Italy	Pisa	CNR - Biophysics Institute
Poland	Sopot	Institute of Oceanology, Polish Academy of Sciences (IO PAN)
Portugal	Vila Nova de Gaia	Águas de Gaia Em, SA
Portugal	Lisbon	Instituto Hidrográfico – Marinha
Portugal	Porto	LEPABE - Faculty of Engineering, University of Porto
Portugal	Coimbra	MARE - Marine and Environmental Sciences Centre
Portugal	Castro Marim	Odiana Association
Russia	Rostov-on-Don	Azov Scientific Institute of fishery industry (AzNIIRH)
Russia	Gelendzhik	South Branch P.P. Shirshov Institute of Oceanology of Russian Academy of Sciences
Spain	Barcelona	IDAEA-CSIC
Spain	St. Carles de la Ràpita	IRTA, Aquatic Ecosystems Program
Spain	Madrid	Paisaje limpio
Spain	Barcelona	Universidad de Barcelona
Spain	Puerto Real	Universidad de Cadiz
Spain	Vigo	Universidade de Vigo
The Netherlands	Amsterdam	Plastic Soup Foundation
The Netherlands	Maastricht, Lelystad	Rijkswaterstaat
The Netherlands	Utrecht	Deltares
Tunisia	Tunis	OR Ltd
Turkey	Mersin	Institute of Marine Sciences, Middle East Technical University
Turkey	Istanbul	Turkish Marine Research Foundation (TÜDAV)
UK	London	Thames21
Ukraine	Odessa	Ukrainian Scientific Center of Ecology of the Sea (UkrSCES)

could help with identification if necessary. Regarding observers' capabilities, training and experience in visual observation can improve data quality, as described in different disciplines (Parsons et al., 2009; Bernard et al., 2013).

The methodological approach considers regular short monitoring sessions (30–60 min) in the estuarine section of the river to account for inputs to the sea, using the tablet computer application described in Section The JRC Floating Litter Monitoring Application to perform visual observations from an elevated position (e.g., bridges, piers, pontoons, and others). As in visual observations in other research fields, e.g., cetaceans (Harwood and Joynt, 2009; Richman et al., 2014), marine birds (Titmus and David Hyrenbach, 2011) or jellyfish (Doyle et al., 2007), duration of monitoring sessions is limited in order to avoid observer's fatigue (EC JRC, 2013; Suaria and Aliani, 2014). Observation of the water from above allows an improved view into the surface water layer for identification of floating litter items. It is recommended to perform the observations facing upstream in order to have an unobstructed view of the arriving water surface (**Figure 1**). Observers will have to select the appropriate time of day for monitoring, considering light conditions (e.g., to reduce light reflections or shades). Depending on the geographical region (e.g., North East Atlantic Ocean region), tidal cycle should be considered to schedule the monitoring during ebb tide (ensuring a downstream flow in the river). Definition of observation track width (section where the observer focuses for identification of items) will allow estimation of litter fluxes in relation to the river section total width (distance

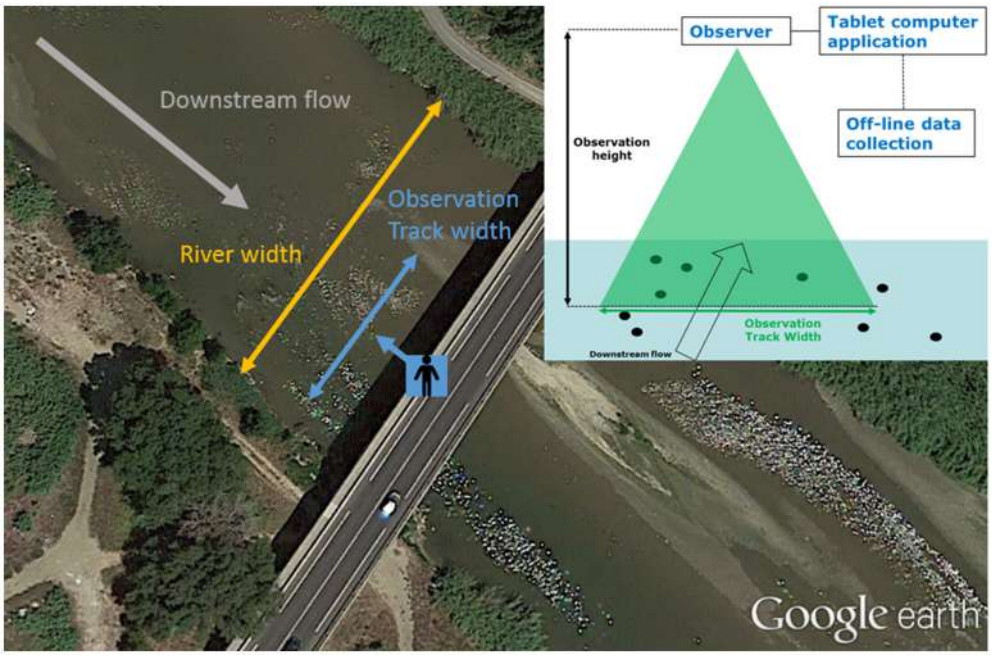

FIGURE 1 | Setup of visual observation from a bridge over a river.

between the two margins at the monitoring site) (**Figure 1**). In addition, the river surface water speed is also considered for surface flux calculation. Monitoring frequency is crucial to account for the expected high temporal variability in litter loads, thus most of the institutions in the network perform weekly or bi-weekly observation sessions.

The network was launched in September 2016 and foresees data collection over 1 year. Monitoring data files are sent to a JRC functional mailbox. Data files are imported into a common database, which is managed by JRC under Microsoft SQL Server 2014. It will be the first ever international database on floating macro litter inputs to the European marine basins. Collected data will be processed to elaborate results and build a statistical inverse model of litter loading based on the characteristics of the catchments. The call to join the monitoring network will remain open until the reporting phase.

THE JRC FLOATING LITTER MONITORING APPLICATION

In this initiative, the key to a harmonized approach for data collection and reporting is the use of the JRC Floating Litter Monitoring Application (App). The App is a dedicated common tool for real time documentation of floating macro litter data acquired during visual observation sessions. In the development of the App, provisions established in the "Guidance on Monitoring of Marine Litter in European Seas" document (EC JRC, 2013) have been considered and adapted to provide the required features and functionalities for floating litter monitoring. The "Guidance on Monitoring of Marine Litter in European Seas" discusses a list of observation parameters based on the assessment of existing approaches for visual ship-based observations, including: HELMEPA (2008), UNEP (Cheshire et al., 2009), Hinojosa and Thiel (2009), NOAA (Arthur et al., 2011), and Ryan (2013); and proposes a protocol for visual monitoring of floating litter within the MSFD implementation process. Additionally, a survey on available portable apps for marine litter monitoring was done, examining the features and functions included in: Marine Debris Tracker for beach and floating litter monitoring (http://www.marinedebris.engr.uga.edu/), Marine LitterWatch for beach litter monitoring (http://www.eea.europa.eu/themes/coast_sea/marine-litterwatch) and Ocean Cleanup Survey App for floating litter monitoring (https://www.theoceancleanup.com/). No published apps were dedicated to the issue of riverine floating litter.

The App concept (monitoring parameters, features, and functions) was designed by EC JRC after evaluation of existing options. Analogies to ship-based visual observations were made for selection of monitoring parameters, using a fixed observation track width to align the approach with MSFD guidance, as described in EC JRC (2013). The software was programmed by an external consultant (Atos IT Solutions and Services Sp. z o.o.), following an iterative testing process (including field work) between EC JRC scientists and the software developers, to fix bugs and make the App functional. **Figure 2** shows the main features and functions of the App.

The App allows selection of "sea" or "river" litter monitoring modes to start a session (**Figure 2A**). Both monitoring modes have similarities and it is important that riverine and sea monitoring consider the same litter attributes for coherence;

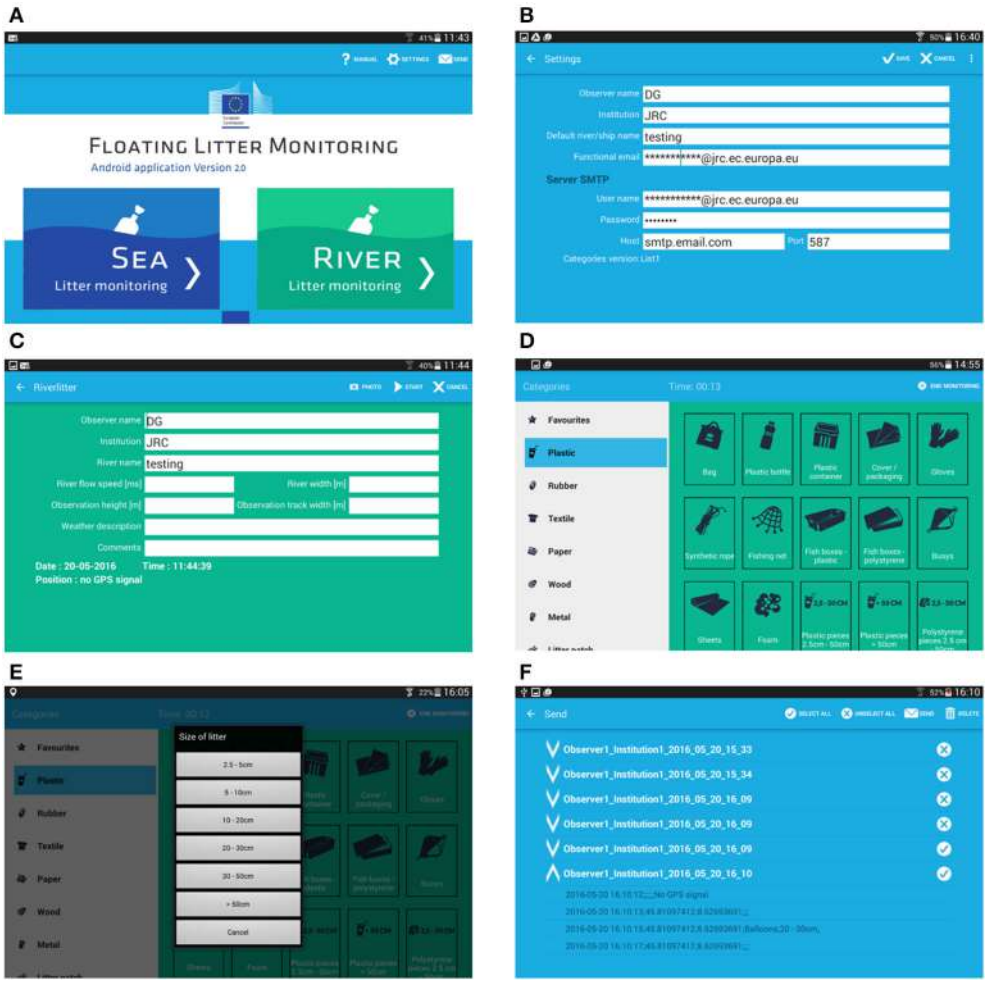

FIGURE 2 | Floating Litter Monitoring Application. Main features and functions: **(A)** start menu, **(B)** general settings, **(C)** river monitoring mode settings, **(D)** monitoring session-litter items categories, **(E)** monitoring session – size categories, **(F)** sending files menu.

however, the sea monitoring mode is not within the scope of this publication and will not be further described.

When the river monitoring mode is selected, a metadata settings menu is accessed (**Figure 2C**), where specific information about the observation set-up, e.g., river and observation site characteristics are entered before starting the session. Other basic information, such as observer name and institution affiliation is retrieved from general settings entered during the device set-up (**Figure 2B**). All details are recorded in the corresponding session data file. During the monitoring (**Figure 2D**), a list of floating macro litter items is available on a menu with icons, organized by materials. This list of items and materials is based on the "Master List of Categories of Litter Items" from the "Guidance on Monitoring of Marine Litter in the European Seas" (EC JRC, 2013), and includes all items that have been described as floating litter. It is also possible to create a list of favorite items to allow faster access to the most common items found in the monitoring area. The item list can be updated through loading of a new official category master list file, e.g., after a revision done by the MSFD Technical Group on Marine Litter. When an icon is selected, a secondary menu pops up for selection of size range classes (**Figure 2E**). Item and size details are registered along with GPS position and time into the data file. The size range classes have been harmonized with the "Guidance on Monitoring of Marine Litter in European Seas" document (EC JRC, 2013).

After ending a monitoring session, the data are saved in an individual.csv file and stored in the tablet computer memory. Data files can be sent directly from the App to a functional mailbox (**Figure 2F**) or copied manually to a PC (e.g., via USB connection). The use of a simple harmonized data format allows importation of the data into the project database.

The monitoring of floating macro litter requires reporting metadata that are crucial to understand the observation conditions and elaborate results. These conditions have been included based on existing MSFD protocol for visual observations at sea (EC JRC, 2013) and field experience gained during the development/testing of the App. For river litter

monitoring, observation height and observation track width are required, along with the river section total width. The river flow speed at the water surface is needed for surface flux calculations. Weather description is required and should include state of river water surface (e.g., turbulence and presence of natural foam), wind, cloud/rain, light conditions (e.g., reflections, direction of the sun and shades) and visibility (e.g., fog). There is also the option to register comments, where any other relevant information can be included.

The App (version 2.0) has been developed for tablet computers with an Android operating system. The tablet computer must have GPS functionality to allow position tracking. The App is further developed, based on incoming feedback through the observation network.

CONCLUSIONS

Using a common monitoring tool for data reporting (the JRC Floating Litter Monitoring Application), the riverine litter observation network will provide the first large scale assessment of riverine litter input to the marine environment, following a harmonized approach. This approach considers the monitoring of floating macro litter as a proxy for riverine litter inputs to the marine environment. The observation network includes both EU and non-EU partners in the European marine basins, with potential to grow as additional partners can still join. Through the participation of scientists and experienced observers, the observation procedure is improved in an iterative way, resulting in an observation protocol for future use. Collected data will be processed to elaborate results and build a statistical inverse model of litter loading based on the characteristics of the catchments, providing support to implementation of appropriate environmental regulations and mitigation measures. Results may show geographical differences in litter loads and help in identifying hotspots, meaning mitigation actions could be developed for and applied in specific areas. Additionally, acquired data will provide a list of the most frequent litter items, bringing important information for prioritization of measures to abate plastic pollution in aquatic ecosystems, e.g., identification of consumer products could have an impact on the EU strategy for plastics in a circular economy (http://ec.europa.eu/environment/circular-economy/index_en.htm). Furthermore, the experience in the observation network will be used to revise the MSFD Master List of Litter Categories, which is the official list used in marine litter monitoring by the 23 EU MSs involved in the implementation of the directive. Currently, the approach is open to participation of partners from EU and non-EU countries in the shared marine basins, as marine litter is a transboundary issue. A harmonized monitoring protocol, the App and RIMMEL database will be publicly available after the project has delivered final results. The acquired experience and developed tools will have a potential use worldwide.

AUTHOR CONTRIBUTIONS

DG and GH designed the work and wrote the article.

FUNDING

This work has been funded by the European Commission DG Joint Research Centre-Horizon 2020 EC programme–DG JRC exploratory research project RIMMEL (RIverine and Marine floating macro litter Monitoring and Modeling of Environmental Loading).

ACKNOWLEDGMENTS

The authors would like to acknowledge all participants in the Riverine Litter Observation Network featured in **Table 1** and the project EMBLAS (Environmental Monitoring in the Black Sea). We thank Martha B. Dunbar for proofreading the manuscript.

REFERENCES

Arthur, C., Murphy, P., Opfer, S., and Morishige, C. (2011). "Bringing together the marine debris community using "ships of opportunity" and a Federal marine debris information clearinghouse," in *Technical Proceedings of the Fifth International Marine Debris Conference. March 20–25, (2009). NOAA Technical Memorandum NOS-OR& R-38* (Honolulu, HI), 449–453.

Barnes, D. K., Galgani, F., Thompson, R. C., and Barlaz, M. (2009). Accumulation and fragmentation of plastic debris in global environments. *Philos. Trans. R. Soc. Lond. B Biol. Sci.* 364, 1985–1998. doi: 10.1098/rstb.2008.0205

Bernard, A. T. F., Götz, A., Kerwath, S. E., and Wilke, C. G. (2013). Observer bias and detection probability in underwater visual census of fish assemblages measured with independent double-observers. *J. Exper. Marine Biol. Ecol.* 443, 75–84. doi: 10.1016/j.jembe.2013.02.039

Cheshire, A. C., Adler, E., Barbière, J., Cohen, Y., Evans, S., Jarayabhand, S., et al. (2009). *UNEP/IOC Guidelines on Survey and Monitoring of Marine Litter.* UNEP Regional Seas Reports and Studies, No. 186; IOC Technical Series No. 83: xii + 120.

DeFishGear (2014). *Methodology for Monitoring Marine Litter on the Sea Surface - Visual Observation*. Available online at: http://www.defishgear.net/images/download/monitoring_surveys_/Floating_litter_monitoring_methodology_complete.pdf.

Doyle, T. K., Houghton, J. D. R., Buckley, S. M., Hays, G. C., and Davenport, J. (2007). The broad-scale distribution of five jellyfish species across a temperate coastal environment. *Hydrobiologia* 579, 29–39. doi: 10.1007/s10750-006-0362-2

Dris, R., Imhof, H., Sanchez, W., Gasperi, J., Galgani, F., Tassin, B., et al. (2015). Beyond the ocean: contamination of freshwater ecosystems with (micro-)plastic particles. *Environ. Chem.* 12, 539–550. doi: 10.1071/EN14172

EC JRC (2013). *European Commission Joint Research Centre, 2013. MSFD Technical Subgroup on Marine Litter (TSG-ML). Guidance on Monitoring of Marine Litter in European Seas. EUR 26113 EN - Joint Research Centre.* Available online at: https://ec.europa.eu/jrc/sites/default/files/lb-na-26113-en-n.pdf

EC JRC (2016a). *European Commission, Joint Research Center.* Exploratory Research Project: RIMMEL (RIverine and Marine floating macro litter Monitoring and Modeling of Environmental Loading). Available online at: http://mcc.jrc.ec.europa.eu/dev.py?N=simple&O=380&titre_page=RIMMEL&titre_chap=JRC%20Projects

EC JRC (2016b). *European Commission, Joint Research Centre, 2016. MSFD Technical Group on Marine Litter (TG-ML). Harm caused by Marine Litter. EUR 28317 EN.* Luxembourg: Publications Office of the European Union; 2016.

EC JRC (2016c). *European Commission, Joint Research Centre, 2016. MSFD Technical Group on Marine Litter (TG-ML). Monitoring of Riverine Litter - Options and Recommendations. EUR 28307 EN.* Luxembourg: Publications Office of the European Union; 2016. JR C104194.

Eriksen, M., Lebreton, L. C. M., Carson, H. S., Thiel, M., Moore, C. J., Borerro, J. C., et al. (2014). Plastic Pollution in the World's Oceans: more than 5 Trillion Plastic Pieces Weighing over 250,000 Tons Afloat at Sea. *PLoS ONE* 9:e111913. doi: 10.1371/journal.pone.0111913

European Commission (2008). *European Commission, 2008. Directive 2008/56/EC of the European Parliament and of the Council of 17 June 2008, Establishing a Framework for Community Action in the Field of Marine Environmental Policy (Marine Strategy Framework Directive).* Available online at: http://eur-lex.europa.eu/legal-content/EN/TXT/?uri=CELEX:32008L.0056

Galgani, F., Hanke, G., and Maes, T. (2015). "Global distribution, composition and abundance of marine litter," in *Marine Anthropogenic Litter* eds M. Bergmann, L. Gutow and M. Klages (Cham: Springer International Publishing), 29–56.

GESAMP (2015). *Sources, Fate and Effects of Microplastics in the Marine Environment: A Global Assessment (Kershaw, P. J., ed.). (IMO/FAO/UNESCO-IOC/UNIDO/WMO/IAEA/UN/UNEP/UNDP Joint Group of Experts on the Scientific Aspects of Marine Environmental Protection).* Rep. Stud. GESAMP No. 90, 96

Harwood, L. A., and Joynt, A. (2009). Factors influencing the effectiveness of Marine Mammal Observers on seismic vessels, with examples from the Canadian Beaufort Sea. *DFO Can. Sci. Advis. Sec. Res. Doc.* 2009/048. doi: 10.13140/RG.2.1.2166.2325

HELMEPA (2008). *Hellenic Marine Environment Protection Association (HELMEPA).* Marine Litter Observation Sheet. Available online at: http://www.helmepa.gr/zip/marine-litter-observation-sheet-en.pdf

Hinojosa, I. A., and Thiel, M. (2009). Floating marine debris in fjords, gulfs and channels of southern Chile. *Marine Pollut. Bull.* 58, 341–350. doi: 10.1016/j.marpolbul.2008.10.020

Hohenblum, P., Frischenschlager, H., Reisinger, H., Konecny, R., Uhl, M., Mühlegger, S., et al. (2015). *Plastik in der Donau.* Available online at: http://www.umweltbundesamt.at/fileadmin/site/publikationen/REP0547.pdf

Jambeck, J. R., Geyer, R., Wilcox, C., Siegler, T. R., Perryman, M., Andrady, A., et al. (2015). Plastic waste inputs from land into the ocean. *Science* 347, 768–771. doi: 10.1126/science.1260352

NOAA (2013). *Marine Debris Monitoring and Assessment*, Transl. by S. Lippiatt, S. Opfer, and C. Arthur. NOAA Technical Memorandum NOS-OR&R-46.

Parsons, E. C., Dolman, S. J., Jasny, M., Rose, N. A., Simmonds, M. P., and Wright, A. J. (2009). A critique of the UK's JNCC seismic survey guidelines for minimising acoustic disturbance to marine mammals: best practise? *Marine Poll. Bull.* 58, 643–651. doi: 10.1016/j.marpolbul.2009.02.024

Richman, N. I., Gibbons, J. M., Turvey, S. T., Akamatsu, T., Ahmed, B., Mahabub, E., et al. (2014). To see or not to see: investigating detectability of ganges river dolphins using a combined visual-acoustic survey. *PLoS ONE* 9:e96811. doi: 10.1371/journal.pone.0096811

Ryan, P. G. (2013). A simple technique for counting marine debris at sea reveals steep litter gradients between the Straits of Malacca and the Bay of Bengal. *Marine Pollut. Bull.* 69, 128–136. doi: 10.1016/j.marpolbul.2013.01.016

Suaria, G., and Aliani, S. (2014). Floating debris in the Mediterranean Sea. *Marine Pollut. Bull.* 86, 494–504. doi: 10.1016/j.marpolbul.2014.06.025

Surfrider Foundation Europe (2014). *Riverine Input Project*. Available online at: http://www.surfrider.eu/missions-environnement-education/proteger-oceans-mers-pollution/dechets-aquatiques/riverine-input/#

Titmus, A. J., and David Hyrenbach, K. (2011). Habitat associations of floating debris and marine birds in the North East Pacific Ocean at coarse and meso spatial scales. *Marine Pollut. Bull.* 62, 2496–2506. doi: 10.1016/j.marpolbul,0.2011.08.007

UNEP/MAP (2016). "Integrated monitoring and assessment guidance," in *19th Ordinary Meeting of the Contracting Parties to the Convention for the Protection of the Marine Environment and the Coastal Region of the Mediterranean and its Protocols Athens*, *9-12 February 2016. UNEP(DEPI)/MED IG.22/Inf.7* (Athens: UNEP/MAP).

van der Wal, M., van der Meulen, M., Tweehuijsen, G., Peterlin, M., Palatinus, A., Kovač Viršek, M., et al. (2015). *SFRA0025: Identification and Assessment of Riverine Input of (Marine) Litter.* Available online at: http://ec.europa.eu/environment/marine/good-environmental-status/descriptor-10/pdf/iasFinal%20Report.pdf

Conflict of Interest Statement: The authors declare that the research was conducted in the absence of any commercial or financial relationships that could be construed as a potential conflict of interest.

frontiers in Marine Science

ORIGINAL RESEARCH
published: 28 March 2017
doi: 10.3389/fmars.2017.00084

Microplastics Generation: Onset of Fragmentation of Polyethylene Films in Marine Environment Mesocosms

Nicolas Kalogerakis[1], Katerina Karkanorachaki[1], G. Calypso Kalogerakis[1], Elisavet I. Triantafyllidi[1], Alexandros D. Gotsis[2], Panagiotis Partsinevelos[2] and Fabio Fava[3]*

[1] School of Environmental Engineering, Technical University of Crete, Chania, Greece, [2] School of Mineral Resources Engineering, Technical University of Crete, Chania, Greece, [3] Department of Civil, Chemical, Environmental and Materials Engineering (DICAM), Alma Mater Studiorum—University of Bologna, Bologna, Italy

The fragmentation of high-density polyethylene (HDPE) films from single-use supermarket plastic bags to microplastics under laboratory-simulated onshore and nearshore conditions was investigated for a period of 6 months. The weathering process of the plastic strips either on beach sand or in seawater under direct natural sunlight was monitored by tensile strength, molecular weight measurements, FTIR, weight loss, and image processing of photographs of the plastic strips before and after mild mechanical stress was applied. The latter represents a novel method proposed for determining the *onset of fragmentation* through the application of mild mechanical stress on the weathered plastic samples emulating the action of sand and wind on a beach. It was found that 12 h of application of mild mechanical stress in rotating glass bottles filled partially with sand was sufficient time to reach the maximum degree of fragmentation that could occur for the weathered plastics samples being tested. For example, applied mechanical stress yielded an area loss of almost 14% for samples weathered for a period of 5 months and about 16.7% after 5.5 months. While tensile strength tests and molecular weight measurements were rather inconclusive till the very last month when the onset of fragmentation was identified; FTIR measurements revealed that samples under ultraviolet irradiation were gradually modified chemically until fragmentation commenced. After 6 months of weathering, molecular weight measurements showed a 60% reduction for sample SMB-1 whereas for sample SMB-2 the measurement was not possible due to extensive fragmentation. The onset of fragmentation for SMB-1 and SMB-2 samples occurred at a cumulative luminance of 5.3×10^6 lux•d and in the presence of atmospheric oxygen whereby the polymer films broke down partially to microplastics. When the UV exposure reached 7.2×10^6 lux•d the weathered plastic strips broke down fully to microplastics with the application of a mild mechanical stress. Samples placed in seawater proved to be resistant to fragmentation compared to those on sand over the 6-month period of the weathering experiment. The direct implication of this work is that beached macroplastic debris should be regularly collected from the seashore before they are weathered by sunlight and returned to the sea as microplastics by the action of high waves or strong winds.

Keywords: microplastics, plastics, fragmentation, polyethylene, HDPE, weathering

OPEN ACCESS

Edited by:
Francois Galgani, French Research Institute for Exploitation of the Sea, France

Reviewed by:
Fabienne Lagarde, University of Maine, France
Christos Ioakeimidis, United Nations Environment Programme Mediterranean Action Plan (UNEP/MAP), Greece

****Correspondence:***
Nicolas Kalogerakis
nicolas.kalogerakis@enveng.tuc.gr

Specialty section:
This article was submitted to Marine Pollution, a section of the journal Frontiers in Marine Science

Received: *30 December 2016*
Accepted: *13 March 2017*
Published: *28 March 2017*

Citation:
Kalogerakis N, Karkanorachaki K, Kalogerakis GC, Triantafyllidi EI, Gotsis AD, Partsinevelos P and Fava F (2017) Microplastics Generation: Onset of Fragmentation of Polyethylene Films in Marine Environment Mesocosms. Front. Mar. Sci. 4:84. doi: 10.3389/fmars.2017.00084

INTRODUCTION

Marine litter is any persistent, manufactured, or processed solid material discarded, disposed of or abandoned in the marine or coastal environment. In general it consists of man-made items that have been deliberately discarded or unintentionally lost in the sea or on beaches, and it includes materials transported from land by rivers, draining or sewage systems, or winds (Cheshire et al., 2009). Globally, the annual input of marine debris in the marine environment has been estimated to be nearly 6.4 million tons (Gregory, 2009), while 103,247,609 items were collected between 1989 and 2007 in 12 marine regions worldwide (Cheshire et al., 2009). Considering the low degradation rates, the effects of accumulation can be observed on both marine life and the human well-being (Barnes et al., 2009). Floating debris patches can act as a means of alien species dispersal in marine ecosystems, while debris ingestion and entanglement of marine organisms in debris, especially plastics, has caused injuries and even death to a multitude of species (Gregory, 2009). Apart from the aesthetic nature of marine litter pollution, it has also been reported to be the cause of injuries and other health concerns besides adverse economic and social impacts (Depledge et al., 2013; Brower, 2016).

Although, marine litter is found in all marine compartments, from surface waters and beaches to deep seas, their composition and quantity varies greatly among locations, due to hydrographic, geomorphologic, and anthropogenic factors (Pham et al., 2014). In the English Channel, 10 to more than 100 items/km^2 of debris could be observed floating on the water surface, while in the Atlantic and Pacific oceans concentrations of 0–20 items/km^2 and up to 36 items/km^2, have been reported accordingly. The values noted for the Mediterranean Sea are much lower, between 1.5 and 25 items/km^2. Seafloor densities were much higher, ranging from 50 items/km^2 in Indonesia to 1935 items/km^2 in the northwestern Mediterranean. Coastline data revealed concentrations of 15–29,000 items per km of shore (Cheshire et al., 2009; UNEP, 2014).

The most abundant of components of marine litter is plastic, and due to the ease with which it can be transferred, it can be found among litter collected from even the remotest locations (Ryan et al., 2009). Enclosed areas, such as the Mediterranean Sea, and oceanic gyres appear to be more heavily polluted, while plastic pollution has been detected even in the Antarctic. Uncontrollable discard of plastics and landfill leaks have been recognized as the most contributing land-based sources of marine pollution (Barnes et al., 2009; Ryan et al., 2009), while less contributing marine-based sources are related to professional activities related to the sea (fishing, offshore oil production, recreational activities, etc.) and to population accumulation in coastal areas. Lost, abandoned, or otherwise discarded fishing gear is the result of a variety of fishing activities both commercial and recreational. Derelict fishing gear, the so-called "ghost-nets" have been identified as a serious environmental problem, due to its negative impact on marine biota (Watson et al., 2006; Cheshire et al., 2009).

Accounting for almost 30% of the yearly demand for plastics in the European Union, Polyethylene is the most widely used type of plastic. Based on density, it can be found in two forms; Low Density Polyethylene (LDPE), used for the production of reusable bags, trays, containers, agricultural film and food packaging film, and High Density Polyethylene (HDPE), used as a manufacturing material for films, toys, bottles, pipes, house-ware, etc. (PlasticsEurope, 2015). It also represents 79% of the polymers in microplastics sampled at sea or in the marine environment (Hidalgo-Ruz and Thiel, 2013). Plastic carrier bags, usually composed of PE, represent a substantial portion of plastic pollution. In the EU alone, 98.6 billion plastic bags were used, corresponding to 198 plastic bags per citizen annually. A devastating 89% of plastic carrier bags are characterized as single-use, with half of the discarded bags ending up in landfills. Throughout the EU, measures have been taken by individual members for the reduction of single use plastic carrier bags, while the Commission policy will enforce pricing of plastic carrier bags, in order to discourage their use. This measure has been proven effective during its effect in member states such as Ireland, France, Portugal, and Spain (Directive of the European Parliament and of the Council Amending Directive, 2013; Martinho et al., 2017).

There is substantial bibliographic evidence of large debris accumulation in European seas, sea floors, and coasts. More specifically, carrier bags accounted for 73% of plastic waste collected of the coast of Tuscany and 70% of total debris collected around French cities, while in the UK, one plastic bag was sampled every 23 m of beach (Directive of the European Parliament and of the Council Amending Directive, 2013). Apart from the effects that marine debris can have on marine life discussed above, plastic bags pose an even greater threat. The effect of environmental factors such as radiation, heat and mechanical stress, leads to fragmentation into small pieces known as secondary microplastics (Andrady, 2011). In the most popular definition of microplastics, they are referred as plastic items with a maximum dimension smaller than 5 mm (Arthur et al., 2009). Besides the secondary microplastics, primary microplastics are also found in the marine environment and represent all polymer products that have been produced at a nominal size <5 mm. Primary microplastics include pellets as raw polymeric materials, cosmetic micro-beads, sandblasting plastic micro-beads (Cole et al., 2011). Secondary microplastics are the most dominant type of plastic found in marine environments and are usually made of polyethylene, with sizes ranging from 0.01 to 1 μm (UNEP, 2015; da Costa et al., 2016).

The generation of microplastics through fragmentation of larger pieces of plastic debris in the marine environment is a complex process, depending on numerous factors, such as luminance, temperature, oxygen level, as well as characteristics inherent to the nature of the degrading material including molecular weight distribution and the presence of additives. It is very important to have estimates of fragmentation rates of the plastics present in the marine environment if we wish to develop reliable models for predicting the future environmental status of our oceans and seas. However, fragmentation rates cannot be described by classical chemical kinetics; as the plastic is weathered, it remains intact while polymer chains are broken and oxygen is incorporated through oxidation. It is

only after sufficient weathering that the onset of fragmentation is reached when small fragments start breaking off with the application of mild mechanical stress. As weathering proceeds further, a higher portion of the original piece of plastic is turned into microplastics. The weathering of polyethylene has been previously studied in both real and simulated marine and coastal environments, utilizing mechanical stress and chemical techniques for the testing of degradation. Several studies have shown changes in mechanical properties, although their results are often contradicting. Structural modifications and brittleness, although a usual observation, do not always correspond to mechanical strength and molecular weight changes (Andrady, 1990; Jabarin and Lofgren, 1994; Tidjani, 2000; Carrasco et al., 2001). O'Brine and Thompson (2010) observed statistically significant decreases of tensile strength for four different types of plastic carrier bags in marine conditions. Area loss reported from the same team was insignificant (2%) for standard PE bags, while compostable bag samples had totally deteriorated after 16 weeks. Weight loss of almost 40% has been observed in plastics buried in soil (Accinelli et al., 2012), while Müller et al. (2012) estimated degradation rates between 3 and 9% for biodegradable bags in simulated sea turtle gastrointestinal conditions. Microorganisms have also been used for the biodegradation of weathered plastics (Shah et al., 2008), including polyethylene (Artham et al., 2009; Restrepo-Flórez et al., 2014; Kumar Sen and Raut, 2015).

Yet as of today, no published work has identified the onset of fragmentation. In this paper we determine experimentally the onset of fragmentation as well as the level of weathering that leads to complete fragmentation of PE films of specific thickness. Among the various plastics, we focused on high-density polyethylene (HDPE) films used in single-use supermarket carrier bags where both these weathering thresholds are identified. The study utilized standard techniques, such as tensile strength measurements, molecular weight measurements, FTIR, combined with weight loss and an optical quantification method of fragmentation through image analysis. An innovative protocol to determine the onset of fragmentation by the application of mild mechanical stress is also proposed.

MATERIALS AND METHODS

Experimental Setup

Plastic bags from two local supermarket stores were used to investigate their fragmentation to microplastics, as such carrier bags represent a usual macroplastic debris found on sandy beaches. The supermarket bags, SMB-1 and SMB-2, consisted of HDPE and had a thickness of 0.1 mm. This is the typical thickness of single-use supermarket plastic bags. Additional samples from bags with a thickness of 0.7 mm were also examined but no fragmentation could be observed after 6 months of irradiation. The results for these samples can be found in the Supplementary Material. All chosen bags were cut into strips of similar dimensions (1 × 20 cm) with an industrial concrete cutter kindly provided by Plastika Kritis SA (Heraklion, Crete, Greece).

Each supermarket bag (SMB) underwent four treatments, each representing different environmental conditions: *Treatment A*, an indoor sand bed (depth 35 cm, diameter 130 cm), representing the control for the weathering of plastics on a beach shore, with no exposure to UV light. *Treatment B* consisted of 2 similar sand beds placed outdoors and under direct sunlight emulating the conditions on a sandy beach. In parallel, three aquarium tanks filled with equal quantities of seawater and equipped with air pumps for mixing and oxygenation purposes, were used to observe potential fragmentation in seawater. One tank (the control) was placed indoors (*Treatment C*), while two were placed outdoors (*Treatment D*) under direct sunlight. All the sand beds contained the same quantity of sand, circa 188 kg and the tanks were filled with seawater 30 cm deep. About 50 plastic strips from both types of SMB were placed in each sand bed and seawater tank (shown in **Figure 1**). The experiment lasted 6 months in total, from 6/2/2015 to 2/8/2015. Samplings were performed on a biweekly basis, removing 5 samples per treatment for further examination. Monthly samplings were taken for the molecular weight and FTIR measurements.

The environmental conditions (temperature and sunlight intensity) were monitored in 5 min intervals, throughout the duration of the experiment, using one HOBO Temperature Light 3,500 DP Logger per treatment. The data from the loggers were collected monthly and processed, using MS Excel.

Experimental Procedures

Tensile Strength Measurements

Both new and weathered strips underwent tensile strength measurements, using an INSTRON (Norwood, MA, USA) apparatus, enabling the calculation (details given in

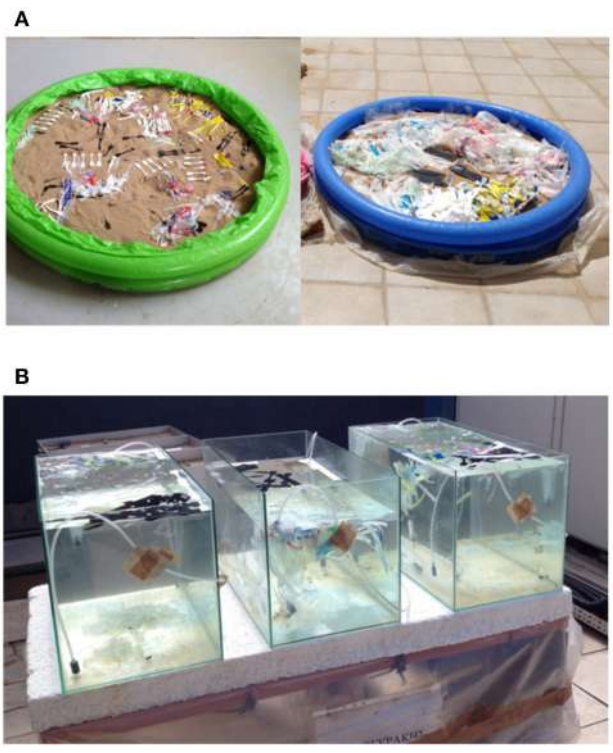

FIGURE 1 | Experimental setup. (A) Simulation of coastal conditions indoors (treatment A) and outdoors (treatment B), **(B)** simulation of marine conditions outdoors (treatment D).

Supplementary Materials, Figure S1) of the Young's Modulus (E), the Yield Strength (σ_y), and the Ultimate Elongation (ε_u). For this procedure, an initial length $L_o = 2$ cm was used, instead of the whole length of the plastics strips. The end part of each sample strip was first wrapped with paper, preventing slipping to occur during the testing (later, instead of using paper, the sample ends were covered with Teflon to avoid of slipping), and then attached to a mechanism of revolving screws applying the tensile forces. Tensile test samples followed the specific process every time and the velocity of the instrument was set at 0.005 mm/s. Each test was repeated five times and the values of E, σ_y, and ε_u were determined using the classical stress strain diagram (Figure S1).

Molecular Weight Estimation—Melt Index

An extrusion plastometer/melt flow index (MFI) tester (ZWICK ROELL, Ulm, Germany) was used to calculate the relative changes in the molecular weight of the samples. Operating conditions, such as temperature, the time required to complete each measurement, and the amount of plastic sample exiting the line were used in combination with basic methodologies (shear flow curve, molecular weight distribution, and melting of polyethylene) to produce the estimates. The procedure consists of the melting of the plastic sample at specific temperature, depending mainly on the type of the polymer tested, followed by extrusion. The measurement required 7 g samples and is repeated 5 times. The extruded plastic mass is measured with a 0.001 g precision scale. The temperature used for all samples was 190°C and the melt flow time was 10 min.

The assessment of the changes in the molecular weight (MW) were obtained indirectly through viscosity measurements and in particular through the MFI computed as the mass of the melt flow over a period of 10 min. From the fundamental equation relating viscosity to MW:

$$\eta = (K \cdot MW)^{3.4}$$

The viscosity (η) is inversely proportional to the MFI:

$$\eta = \frac{K}{MFI}$$

The MFI is essentially the mass of the melt (m) passing through over a period of 10 min, and hence, by considering the above equations for samples taken at time 0 and at time t:

$$\left(\frac{MFI_t}{MFI_0}\right)^{\frac{1}{3.4}} = \frac{MW_t}{MW_0}$$

Finally, the change in molecular weight is estimated from the measured melt mass initially (time 0) and at the requested point in time:

$$\frac{MW_t}{MW_0} = \left(\frac{m_t}{m_0}\right)^{\frac{1}{3.4}}$$

where m_t is the average mass of the initial sample (at time 0) from 5 replicates and m_0 is the average mass of the sample tested (at time t) from 5 replicates.

Fourier Transform Infrared Spectroscopy (FTIR)

In FTIR, infrared radiation is passed through the sample for the generation of the absorbance or transmittance spectrum. FTIR is preferred in this case due to the measurement of the whole wavelength range at once. Infrared frequency identical to the vibrational frequency of a bond results in absorption, creating a spectrum acting as a molecular "fingerprint" of the sample. The position, shape, and intensity of peaks in this spectrum reveal details about the molecular structure of the sample. All samples were washed twice in ultrasound for 5 min with ultra-pure water and left to dry naturally for 1 day. The spectrum range for the analysis was the middle infrared, 4,000 to 400 cm^{-1}; the spectral resolution was set at 4.0 cm^{-1} with a step of 2.0 cm^{-1} every 20 ns. Particular attention was paid for absorbance at 1,471 cm^{-1} over time where the oxidation of polyethylene is indicated.

Image Processing to Monitor Fragmentation and "Invisible" Plastics

Protocol for image processing of microscope images of new and weathered plastics

Image processing allows for a more detailed observation of the fragmentation, disintegration, and the overall deterioration of the surface of the plastic samples. Inspired by the image analysis performed by O'Brine and Thompson (2010) on weathered plastic bags, a protocol was developed that enables the confirmation and quantification of weathering (i.e., loss of material due to fragmentation or biodegradation) of intact pieces of plastic. The removed pieces due to fragmentation correspond to the so-called "invisible plastics" (maximum length <100 μm), as they are not degraded however they cannot be readily seen with naked eye. Certain samples can even be presented in three-dimensional form. The sample images are stored in a defined folder, also containing a set of initial variables, defined or automatically inferred from a MATLAB-based algorithm, including the gray scale and the size threshold over which pixels are classified as deterioration (i.e., removal of plastic due to fragmentation). The algorithm automatically acquires each image and proceeds to thresholding, in order to acquire deteriorated sections. A cleaning of "salt and pepper" type minor thresholded sections is followed by exclusion of microscope image borders. The overall area of deterioration and the number of deterioration sections are quantitatively measured for each image and finally the average deterioration area and the number of sections for all samples included in the folder are quantitatively estimated. Furthermore, the algorithm computes the degree of deterioration (%) as the ratio of deteriorated area to the total area, and the number of fragments in case distinct pieces of plastic can be identified in the picture, based on the identified area of deterioration. A selected sample (strip of supermarket plastic bag) exposed to sunlight outdoors on a sand bed for a period of 5 months compared to the initial condition when the samples were placed outdoors is shown in **Figure 2**.

The MATLAB-based algorithm used in this study can be found in the Supplementary Materials.

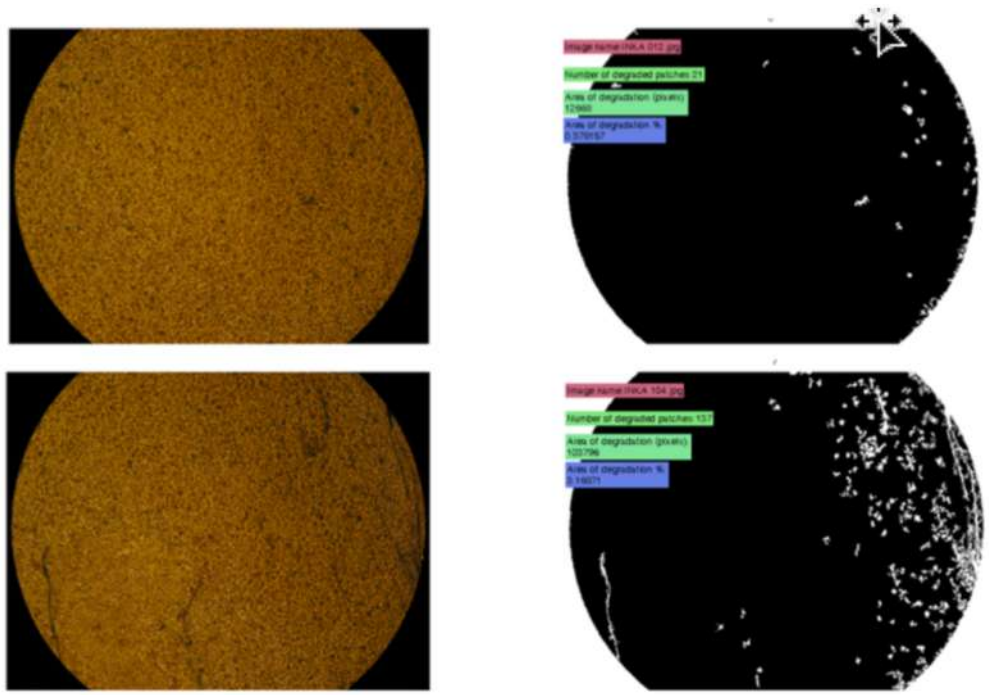

FIGURE 2 | New sample, initial image vs. processed image (above) and older sample, after 5 months of weathering, initial image vs. processed image (below).

Protocol for image processing of fragmented plastic strips to quantify fragmentation

After a longer weathering period, loss of plastic material could be visually observed especially at the loose edges of the plastic samples (strips). Additionally, the color of the samples often faded away and they became more brittle. The proposed protocol commences with the measurement of the weathered samples from a specific distance from the edge and continues with weighing using a six decimal precision (i.e., 0.000001 g) scale. Parallel placing of the strips on a piece of black paper is followed by the placement of a non-reflecting glass panel, allowing the photographing of the samples with a digital camera. Following that, the images are processed in a manner similar to the one used for the microscopic images. Sample strips or chunks are isolated during image thresholding, followed by noise removal and quantification of the area decrease for each sample over the initial intact sample and quantification of number of pieces (visible fragments) per sample. The algorithm performs the aforementioned steps for samples, strips, or even larger pieces of plastic. The image processing of the photograph of the weather plastic strips (locations 2, 3, and 4) and the initial plastic (location 1) are shown in **Figure 3**. The missing surface compared to strip in location 1 provides an estimate of the decrease and hence, it can be related to material loss.

Novel Method to Determine the Onset of Fragmentation—Application of Mild Mechanical Stress on Weathered Plastics

Weathering of plastics due to exposure to UV light in the presence of atmospheric oxygen results in the breakage of the polymer chains, which ultimately results in fragmentation of the plastic into many pieces; however, in the field, the breakage into pieces is observed following the application of mild mechanical stress by the prevailing winds, movement of the sand, or wave action. If the later is not applied, the plastic looks intact and the fragmentation cannot be quantified. Here we propose for the first time, a simple method for estimating the *onset of fragmentation,* namely the degree of weathering of the plastic material beyond which visually observed fragmentation takes place. We propose the application of *mild mechanical stress* to determine if a plastic strip will fragment into smaller pieces. This can be done in many different ways. In our case, we used the following procedure: plastic strips are placed in roller bottles filled 50% with sand, turning at a constant temperature and rotational speed. In our laboratory, we used 250 mL culture bottles that were placed in a Hybridization Incubator (Model#7601, Gesellschaft manufacturer für Labortechnik, Burgwedel, Germany), where the bottles were secured horizontally at specific positions and were left rotating for 24 h at 30°C and rotating at 13 rpm. This particular device holds up to 8 bottles, allowing the simultaneous testing of multiple samples. After 24 h of mild mechanical stress, the weathered samples were removed from the bottles and emptied in an aluminum tray, where all *visible plastic pieces* created during this procedure were collected with forceps. Care was taken so that any pieces of plastic adhering to the bottle cap were also collected. The plastic pieces were then weighed with a high precision balance and placed on black hardboard paper to be photographed. The weight difference between the original strip prior to weathering and the weight of the collected fragments provided an estimate of the amount of "*invisible*" plastics, namely

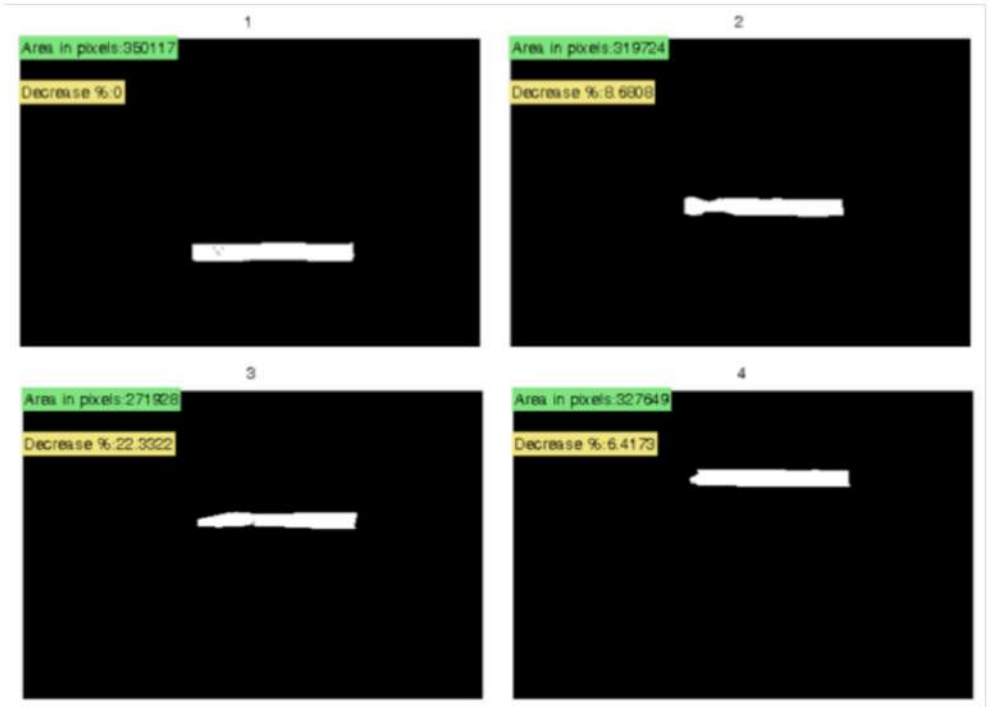

FIGURE 3 | Plastic strips along with area in pixels, and percent (%) area decrease of initial sample.

microplastics that are small enough not to be visible by naked eye (typically <0.1 mm). A MATLAB algorithm similar to the one used earlier, thresholds the digitally processed photographs for the isolation of sample strips or chunks and removes the noise from the images. A classification process follows, grouping the isolated chunks for each sample, based on a directional erosion process, so that the area decrease for each sample over the initial intact sample and quantification of number of pieces (visible fragments) can be conducted.

In an effort to minimize the time allocated for the application of mild mechanical stress, a series of experiments were conducted with additional HDPE samples (carrier bags and pure HDPE films) which were irradiated with artificial UV-A (wavelength 315–400 nm) for a period of 6 months, then rotated in the incubator for 4, 8, 12, and 24 h, respectively. This experiment revealed the minimum period of time that rotation should take place in order to reach the maximum fragmentation of the plastic samples for the given degree of weathering was 12 h. Hence, a 12 h period is proposed for future experiments.

RESULTS

Environmental Conditions

Temperature variations were observed over time during the experiment and they were due to seasonal temperature changes (winter to summer period). The mean, minimum, and maximum daily temperatures during sunlight exposure times for the periods between samplings and the cumulative luminance exposure on sampling days for all four treatments are shown in **Table 1**. The mean indoor temperatures (control treatments A and C) are consistently lower than the outdoors (treatments B and D). The minimum temperatures for both indoors control treatments were quite similar, ranging from 4.9 to 20.1°C for treatment A (on sand) and from 5.4 to 20.1°C for treatment C (in seawater). The outdoor samples on beach sand (Treatment B) experienced greater temperature fluctuations, with minimum temperatures from 1.0 to 33.1°C, while the smallest range was observed for the outdoor aquarium tank (treatment D), from 2.6 to 17.4°C. Correspondingly, maximum temperatures of 19.6 to 33.0°C and 17.1 to 28.6°C were measured for treatments A and C (indoors), while the outdoors maximum temperatures for treatment B (33.1–65.3°C) were nearly double those of treatment D (16.1–39.5°C).

As expected, both control treatments A and C were exposed to significantly less irradiation (0.15–0.45%) compared to the outdoors treatments B and D, respectively (**Table 1**). Furthermore, among the outdoor treatments, on 30/6/2015 treatment B (samples placed on beach sand) had a cumulative luminance of 5.37×10^6 lux•d whereas treatment D (samples placed in seawater) had a cumulative luminance of 9.59×10^5 lux•d which is about 18% of the value measured in treatment B. By 2/8/2015 the corresponding values were 7.18×10^6 and 1.51×10^6, respectively as seen in **Table 1**.

Tensile Strength Tests

Tensile strength tests were performed, in order to determine whether the weathering of the samples could be linked to changes in their mechanical properties. Results obtained for SMB-1 and

TABLE 1 | Mean, minimum, and maximum temperature during exposure time and cumulative luminance exposure values for all treatments as a function of time.

TREATMENT																			
Sampling no.	Sampling date	Time (d)	Minimum temperature (°C)				Mean temperature (°C)				Maximum temperature (°C)				Cumulative luminance exposure (lux*d)			
			A	B	C	D	A	B	C	D	A	B	C	D	A	B	C	D
0	6/2/2015	0	19.6	33.1	17.6	16.1	19.6	33.1	17.6	16.1	19.6	33.1	17.6	16.1	0	0	0	0
1	23/2/2015	17	4.9	1.0	5.4	2.6	10.7	10.4	10.1	9.7	23.1	39.0	20.6	23.0	9.6×10^2	3.36×10^5	1.9×10^2	6.91×10^4
2	5/3/2015	27	12.3	9.1	12.5	9.5	14.9	14.5	14.1	14.0	20.0	38.7	17.1	27.2	1.5×10^3	6.01×10^5	3.8×10^2	1.24×10^5
3	20/3/2015	42	11.0	7.3	11.4	7.3	13.9	12.9	13.4	13.1	20.8	36.9	17.8	24.2	2.3×10^3	8.20×10^5	5.9×10^2	1.87×10^5
4	10/4/2015	63	10.1	6.5	10.0	7.1	16.2	17.3	15.4	16.2	22.6	43.6	26.7	30.5	3.1×10^3	1.54×10^6	1.0×10^3	2.60×10^5
5	24/4/2015	77	12.0	8.5	11.2	9.3	18.4	22.8	17.2	19.7	26.2	52.3	22.7	34.5	3.9×10^3	2.31×10^6	1.5×10^3	3.93×10^5
6	8/5/2015	91	17.0	15.6	17.0	14.0	21.9	28.7	20.5	23.0	30.1	64.7	26.6	36.7	4.9×10^3	3.04×10^6	1.9×10^3	5.09×10^5
7	22/5/2015	105	18.2	14.6	17.9	15.7	21.8	28.2	20.7	22.9	26.4	62.1	23.1	34.9	6.1×10^3	3.11×10^6	2.6×10^3	6.43×10^5
8	8/6/2015	122	18.6	16.0	18.3	15.5	21.9	27.7	21.0	23.1	26.6	56.0	23.6	35.1	7.5×10^3	4.03×10^6	3.1×10^3	7.37×10^5
9	30/6/2015	144	20.1	16.7	20.1	17.4	25.3	32.1	23.9	26.8	33.0	65.3	28.6	39.5	9.4×10^3	5.37×10^6	4.2×10^3	9.59×10^5
10	15/7/2015	159	23.5	21.0	23.1	19.9	26.4	33.8	24.9	28.0	32.1	63.8	28.4	39.8	10.7×10^3	6.16×10^6	5.0×10^3	1.18×10^6
11	2/8/2015	177	24.3	21.5	–	20.8	26.9	36.1	–	29.7	30.5	66.5	–	41.2	13.9×10^3	7.18×10^6	–	1.51×10^6
12	18/8/2015	193	24.9	21.8	–	21.6	26.8	33.1	–	29.1	28.9	61.6	–	41.3	17.3×10^3	7.93×10^6	–	2.15×10^6

SMB-2 were similar as shown in **Figures 4–6**. More specifically, Young's modulus (E) changes over time (**Figure 4**) do not show a statistically significant difference between treatments A and B or C and D at all sampling times; namely, the weathering of the plastic film indoors and outdoors did not affect significantly Young's modulus in both media (on sand and in seawater). Similar results can be observed for the yield strength in **Figure 5** and the ultimate elongation in **Figure 6**. Yet, one can make an interesting observation for treatments A and B (on beach sand). The values of ultimate elongation for treatment B are not statistically different; however, they are consistently lower than the control (treatment A), namely 8 out of 10 measurements for SMB-1 and 10 out of 10 for SMB-2. Using arguments from statistical process control, it is noticed that even though there is no significant difference between the data at each sampling time, the overall behavior is statistically significant. For example, under the null hypothesis for SMB-2 that there is no difference in the values of ultimate elongation between the two treatments, the probability of observing 10 times treatment A 10 to be higher than treatment B is $(1/2)^{10} \approx 0.00098$ which is highly improbable (i.e., in an industrial production process an alarm would have been set much earlier). Similar arguments apply for Young's modulus measurements as well (**Figure 4**). This means that there is a definite decrease in values of ultimate elongation and in Young's modulus due to weathering, however, it is very difficult to reliably observe it with very few measurements; only if many measurements are considered together, one may observe a statistically significant reduction in these two parameters. The measurements in seawater (treatments C and D) do not show any trend. This is due to the lower degree of weathering of the plastic samples that took place in seawater where a significant amount of UV light is absorbed by the seawater. Finally, it should be noted that samples could not be analyzed in the last month of the experiment for treatment B due to breakage during sample handling as the strips became very brittle.

Molecular Weight Changes

Molecular weight is a weathering indicator of great significance. Only samples from the most heavily weathered treatment (B) were analyzed and the results are shown in **Figure 7**. As seen, extensive UV exposure leads to reduction in molecular weight over time for both SMB-1 and SMB-2, due to breakage of the polymer chains. In the last month the MW of SMB-1 was reduced to 60% of its initial value whereas SMB-2 could not be measured as it fragmented into pieces and several were lost by the wind action and it was not feasible to collect the 7 g of material required for the test.

FTIR Spectra

The characteristic peaks for PE detection with FTIR are 2,923, 2,849, 1,471, and 719 cm^{-1}. Increase in absorption at 1,471 cm^{-1} over time indicates increased oxidation of the polymer chains. A gradual increase of absorption at 1,471 cm^{-1} was observed in all samples exposed to solar radiation (Treatment B), implying gradual oxidation of the polymer with time. The spectra for SMB-1 can be observed in **Figures 8–10**. The characteristic peak for PE at 1,471 cm^{-1} was found to be higher with increasing weathering

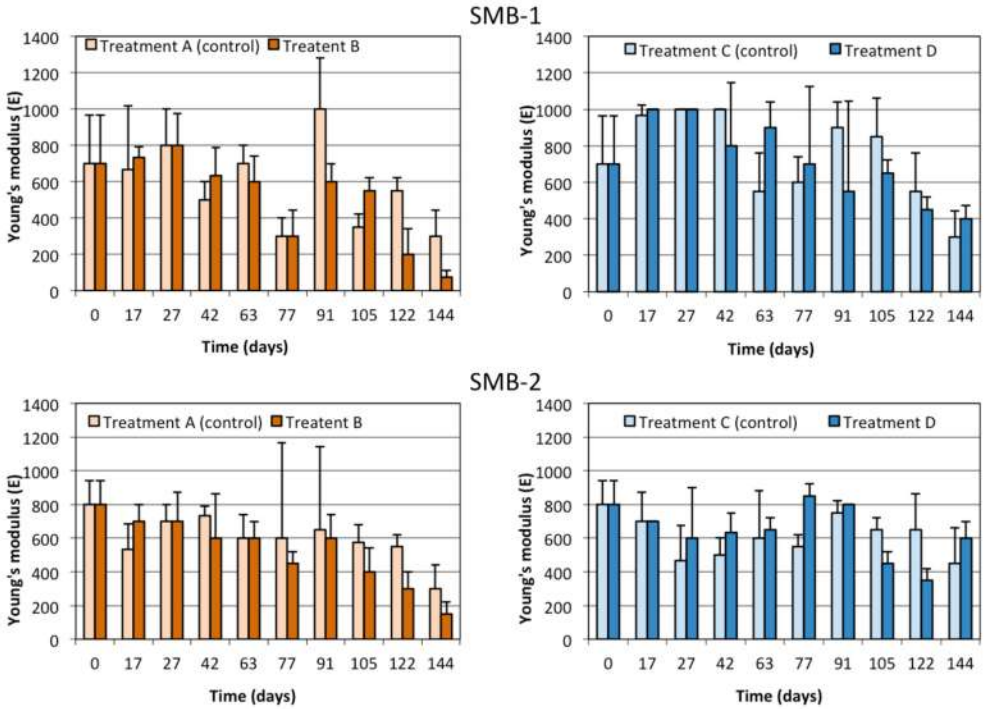

FIGURE 4 | Young's modulus for SMB-1 and SMB-2 in Treatments A, B, C, and D.

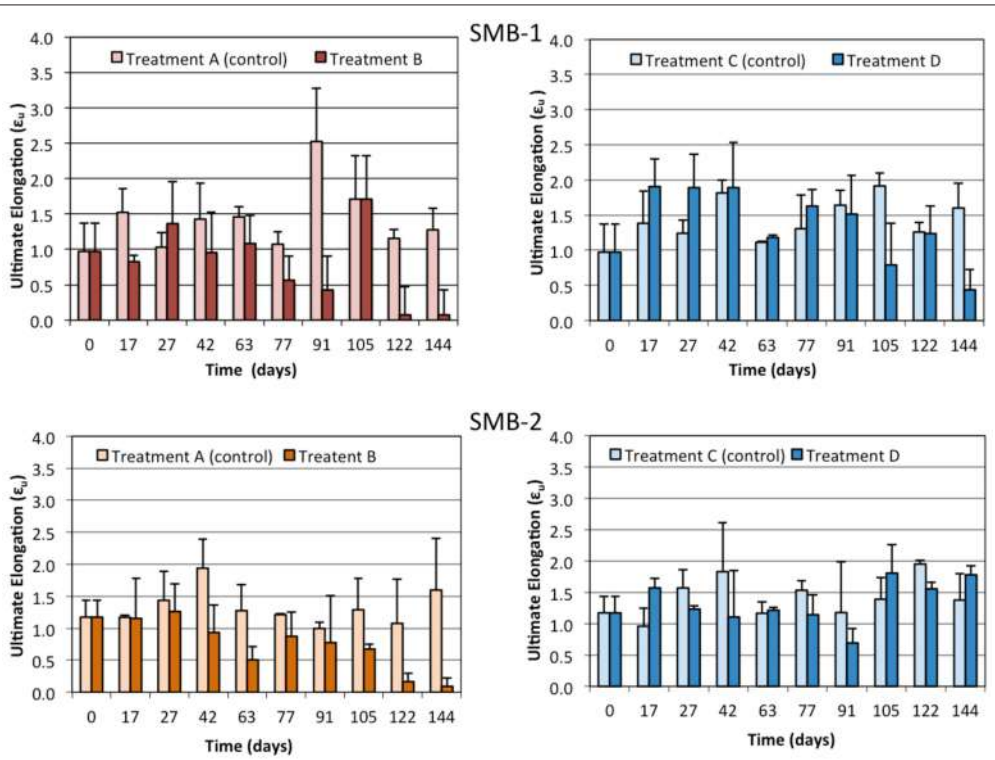

FIGURE 5 | Ultimate elongation (ε_u) for SMB-1 and SMB-2 in treatments A, B, C, and D.

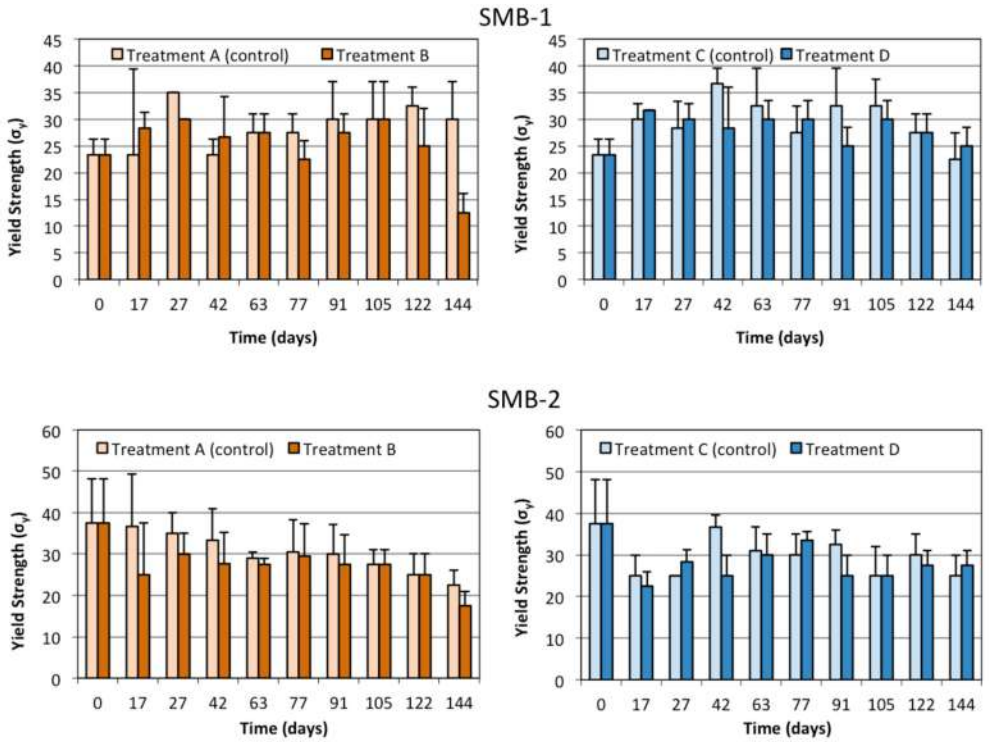

FIGURE 6 | Yield strength (σ_y) for SMB-1 and SMB-2 in Treatments A, B, C, and D.

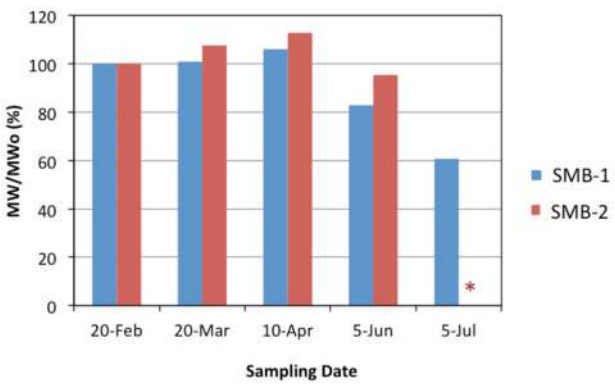

FIGURE 7 | Molecular weight changes (%) of SMB-1 and SMB-2 over time for Treatment B (*measurement could not be done due to excessive fragmentation of sample SMB-2).

in all treatments and samples. A difference can be observed even after a short period time of 30 days (**Figures 8**, **9**). Combination with absorption data from samples left in seawater both indoors and outdoors for the same period of time (**Figure 10**), reveals that the oxidation process is much more pronounced when the samples have been left outside (Treatment B) rather than inside (Treatment A), and the water absorbs a significant amount of UV radiation, thus limiting significantly the weathering process. In addition, the reduced availability of oxygen as dissolved oxygen in seawater compared to atmospheric oxygen also limits the oxidation to process via UV irradiation (i.e., peaks for Treatments A and B are higher than those for Treatments C and D).

Determination of the Onset of Fragmentation

The quantification of fragmentation cannot be effectively represented by a usual kinetic rate equation for fragmentation rates. It is obvious by the aforementioned tensile strength tests, molecular weight measurements, and FTIR analysis that although the weathering process proceeds, the fragmentation rates cannot be quantified as no fragmentation occurs. Only when the degree of weathering is above a certain threshold that can be quantified by the cumulative exposure to UV light, the polymer starts to break down to microplastics. Upon further exposure to UV light, the polymer films become very brittle and break down to "invisible" microplastics.

For modeling purposes, it is vital to be able to identify the *onset of fragmentation*, which represents the degree of weathering after which fragmentation to microplastics occurs. When the onset of fragmentation has been reached, only a minimal amount of mechanical stress is required for fragmentation of a portion of the polymer film. The procedure to apply mild mechanical stress was specifically designed for the determination of the actual moment when the fragmentation process commences.

Following the application of mild mechanical stress to weathered strips (treatment B) in bottles containing 125

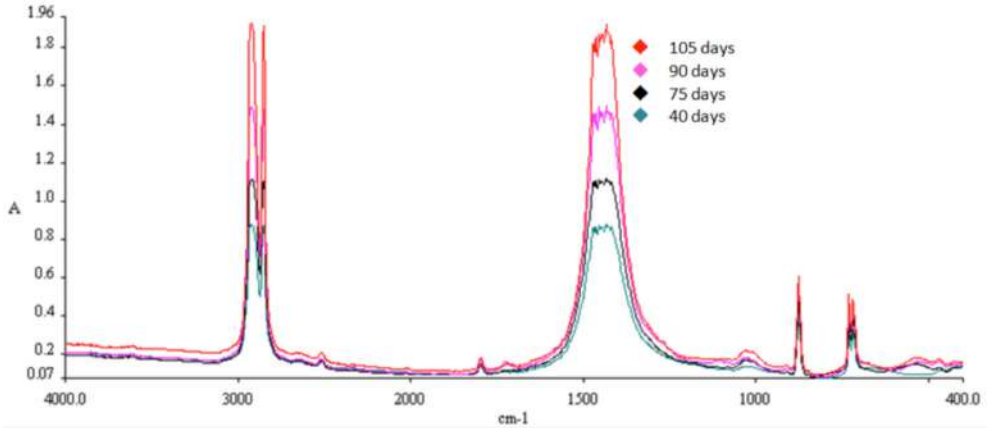

FIGURE 8 | Absorption spectrum for SMB-1 in Treatment B as a function of weathering time.

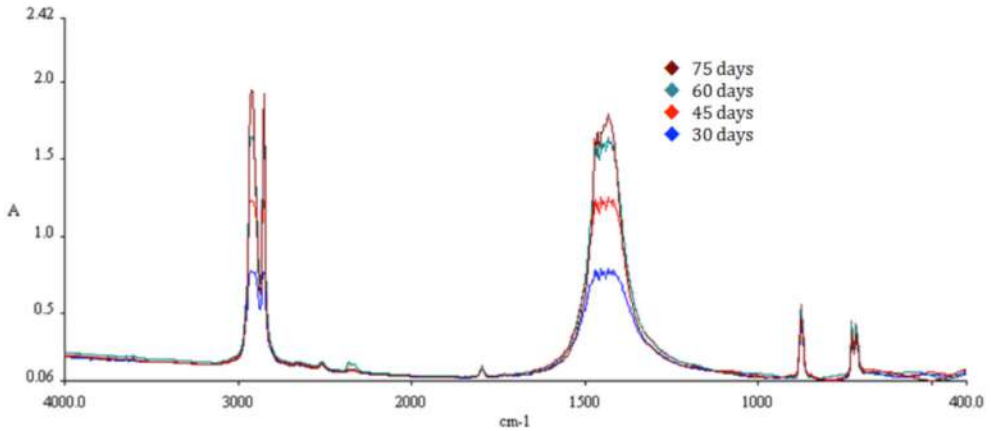

FIGURE 9 | Absorption spectrum for SMB-1 in Treatment D as a function of weathering time.

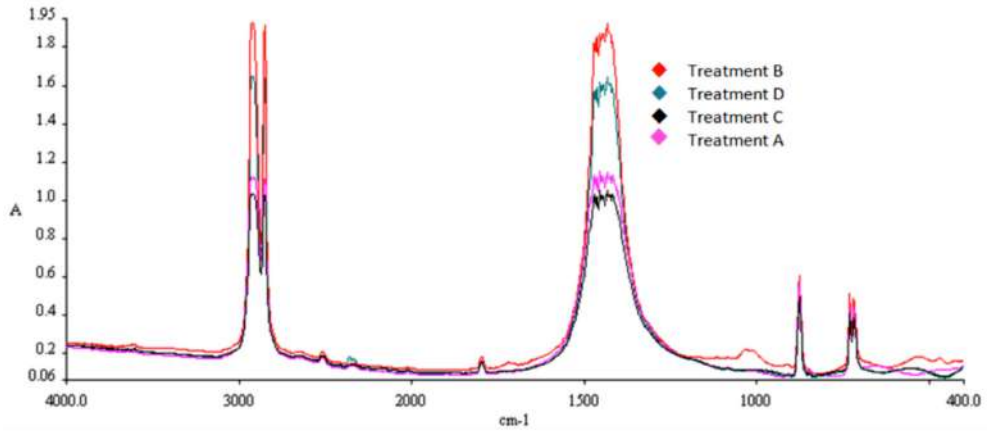

FIGURE 10 | Absorption spectrum for SMB-1 in Treatments A, B, C, and D after 80 days of weathering.

mL of sand, the collected plastic fragments are shown in **Figure 11A**, and after photographing (**Figure 11B**) and applying the MATLAB-based algorithm, the percentile decrease in area of each weathered strip was computed. The corresponding weight loss for SMB-1 and SMB-2 following the application of mild mechanical stress, are presented in **Table 2**. As seen, after 5 months of weathering on the sand beds outside (Treatment B), and after application of mild mechanical stress, SMB-1 and SMB-2 yielded a weigh loss of 13.9 and 13.7%, respectively. After 5.5 months, SMB-2 presented a 16.7% weight loss. The evolution of weathering for treatment B is shown in **Figure 12**. Samples from the seawater tanks (Treatment D) were also subjected to the application of mild mechanical stress, however, no weight loss was observed due to the insufficient weathering achieved.

Repetition of the mild mechanical stress procedure to supermarket carrier bag samples for residence times ranging from 4 to 24 h, illustrated that sufficient fragmentation of weathered samples was achieved after 12 h of rotation and there was no need to keep the procedure for 24 h.

Complete Fragmentation to Microplastics

For HDPE films of thickness 0.1 mm from supermarket bags without any additives to protect against UV exposure, the onset of fragmentation coincided with a cumulative luminance of 5.3 $\times$ 10^6 lux·d in the presence of atmospheric oxygen whereby the polymer films broke down partially to microplastics. As more UV irradiation is absorbed, the plastic pieces that broke off become smaller in size with the exertion of the slightest mechanical stress. When the UV exposure reached 7.2 $\times$ 10^6 lux·d the weathered plastic strips broke down fully to "invisible" microplastics with the application of a mild mechanical stress. The arrows in **Figure 13** indicate the two boundaries of the cumulative UV irradiation. Obviously, these boundaries are indicative, apply only to the specific composition and thickness of the plastic bags and for exposure to similar ambient temperatures over the weathering period.

Finally it should be noted that the weathering was accompanied by discoloration of the plastic strips, with the samples of Treatment B ending up almost white at the end of the 6-month experiment, while samples from Treatments A, C, and D were affected to a much less degree.

DISCUSSION

Exposure of polyethylene films to solar radiation induces weathering, altering the molecular weight and physicochemical properties of the polymer, through reactions with oxygen, cross-linking, and chain scission reactions (Abdelhafidi et al., 2015). Several studies on polymer weathering have used mechanical properties tests to measure the degree of weathering achieved. Recently, studies have focused on the potential for effective biodegradation of PE (Restrepo-Flórez et al., 2014; Kumar Sen and Raut, 2015).

Generally, tensile strength has been found to be inadequate in the determination of fragmentation (Andrady et al., 1993). Young's modulus (E) was used successfully by Carrasco et al. (2001); however, in our case it did not yield statistically significant changes when single measurements were considered. Furthermore, the ultimate elongation (ε_u) has been used many times as a measure of brittleness. Carrasco et al. (2001) reported a decrease of ultimate elongation from 231 to 7.4% in 120 days. Similarly, from our results the ultimate elongation appears to decrease in a statistically significant manner only when all measurements were considered together or at the very end of the weathering period when fragmentation has already begun. Essentially, at this degree of weathering no measurement is possible due to sample breakage (Andrady et al., 1993; Jabarin and Lofgren, 1994; Tidjani, 2000).

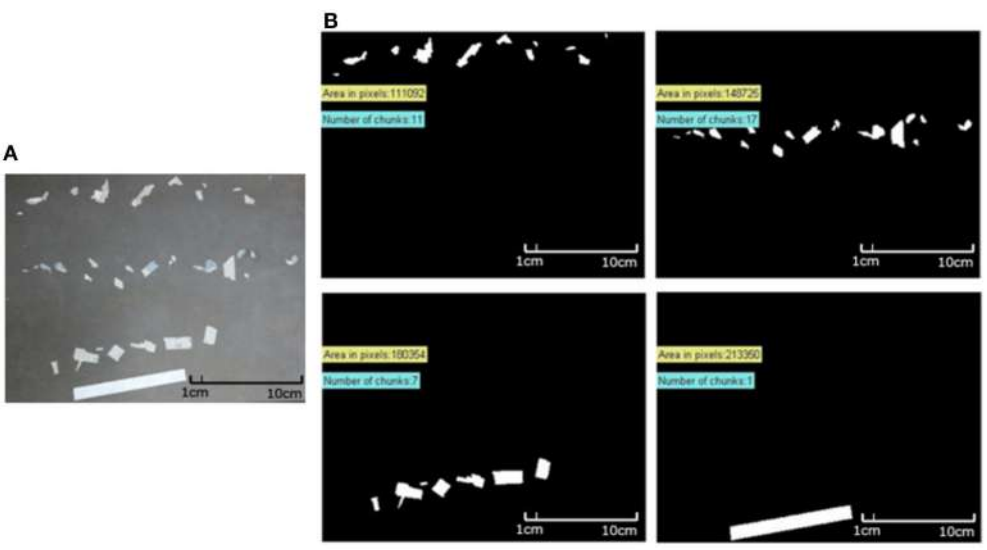

FIGURE 11 | (A) Collected fragments of three different strips from SMB-2 placed in parallel lanes on black paper. **(B)** Processed images of SMB-2 strips following fragmentation with mild mechanical stress; also shown the number of fragments with their total area in pixels and the area decrease (%) from initial sample.

TABLE 2 | Average weight loss after application of mild mechanical stress due to fragmentation to "invisible" microplastics (Treatment B).

Plastic type and weathering period	Lane/strip	Initial weight (mg)	Weight after mild stress (mg)	Weight loss as "invisible" plastics (mg)	Weight loss as "invisible" plastics (%)
SMB-1 (5 months)	Lane-3	18.986	18.258	0.728	3.8
SMB-1 (5 months)	Lane-2	14.688	13.251	1.437	9.8
SMB-1 (5 months)	Lane-1	15.217	10.957	4.260	28.0
Average loss for SMB-1				2.142	13.9
SMB-2 (5 months)	Lane-3	16.629	12.300	4.329	26.0
SMB-2 (5 months)	Lane-2	12.455	11.700	0.755	6.1
SMB-2 (5 months)	Lane-1	15.060	13.696	1.364	9.1
Average loss for SMB-2				2.149	13.7
SMB-2 (5.5 months)	Lane-3	11.294	8.963	2.331	20.6
SMB-2 (5.5 months)	Lane-2	15.329	14.270	1.059	6.9
SMB-2 (5.5 months)	Lane-1	14.444	11.179	3.265	22.60
Average loss for SMB-2				2.218	16.70
SMB-1 (6 months)	All lanes*	9.224	0**	9.224	100
SMB-2 (6 months)	All lanes*	5.269	0**	5.269	100
Average loss for SMB-1 and SMB-2					100

**Pieces collected from all three lanes were pooled together and placed in a rotating bottle with 50% sand.*

***After 24 h strips were very brittle and all pieces were readily fragmented into very small microplastics ("invisible" plastics) that could not be collected with forceps.*

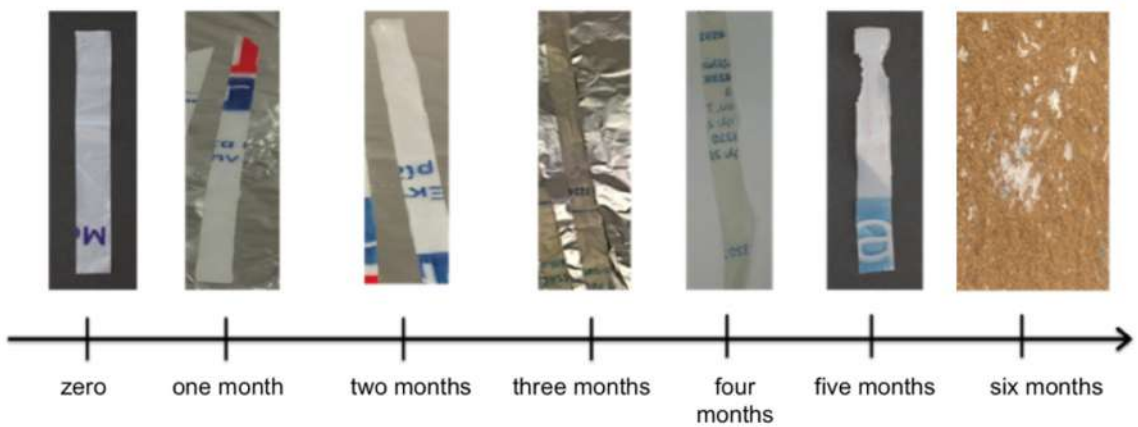

FIGURE 12 | Pictures of SMB-1 plastic strips weathered outdoors on sand bed (treatment B) with respect to time (last picture taken on sand).

FTIR has been frequently used to measure abiotic or biotic degradation of polymer pieces (Ioakeimidis et al., 2016) as well as to support mechanical properties test results and visual observations, for verifying changes in the chemical structure of the examined polymers. Higher peaks and slightly broader bands in the characteristic areas of the 2,923 and 1,471 cm^{-1} attest to the fact that the polymer has undergone oxidation and chemical alteration, dependent on the period of time the sample was exposed to UV radiation (**Figures 8–10**). However, the FTIR results can only be used qualitatively. Jabarin and Lofgren (1994), using FTIR to measure crystallinity were able to deduce that absorbance bands tended to be wider with higher peaks with exposure time, in a similar manner to Tidjani (2000). Increasing ratios of oxidized to non-oxidized carbon, associated with surface oxidation of polymers exposed to natural sunlight, can be related to polymer chain scission reactions, leading to polymer deterioration (Stark and Matuana, 2004). An increase in carbonyl index followed by a decrease was considered as an indication of biodegradation by Artham et al. (2009) which was verified by a weight loss of 1.6% for HDPE (1.9% for LDPE) after 12 months.

Changes in the molecular weight can also be linked to polymer deterioration. Jabarin and Lofgren (1994) reported that the molecular weight of HDPE decreased from 147,000 in the original sample to 34,100 after 6 months of exposure to artificial UV light. Both increase and decrease of molecular weight have been observed in PE biodegradation experiments. This is not surprising as abiotic fragmentation leads to a decrease in the average molecular weight whereas biodegradation

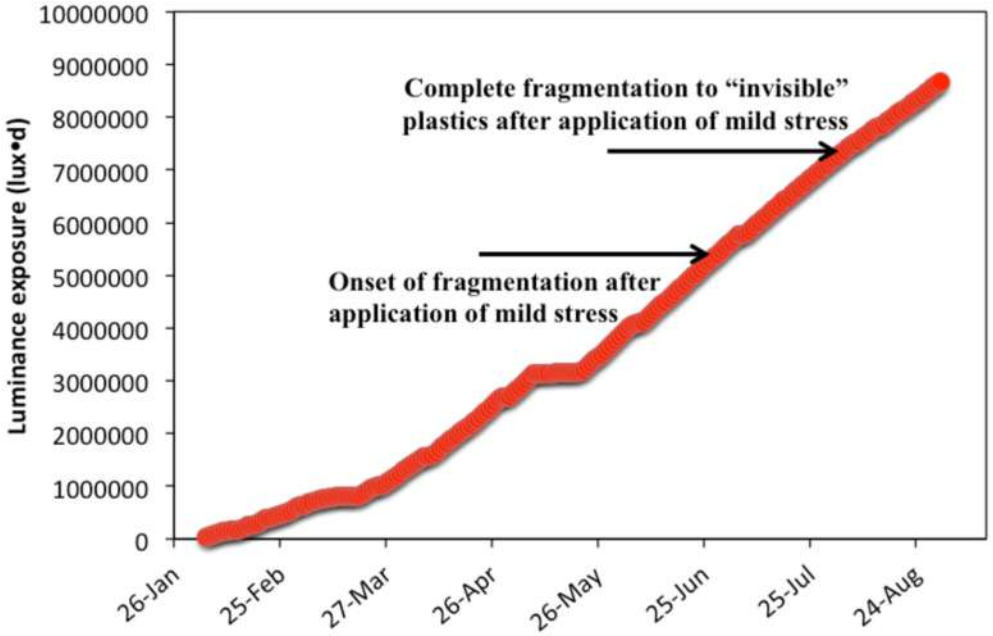

FIGURE 13 | Cumulative luminance exposure and onset of fragmentation for thin HDPE films of thickness 0.1 mm used in supermarket bags (Treatment B—outdoors on sand).

results in an increase or marginal changes in the average molecular weight, because microbes prefer to attack first the shorter polymeric chains. This behavior was also observed in our lab during the biodegradation of PE films. Other measurement methods, such as rheology and size exclusion chromatography have been proposed as alternatives to molecular weight measurements (Restrepo-Flórez et al., 2014). Although, early molecular weight measurements in this study were rather inconclusive in denoting the gradual weathering of the plastic strips, the fact that the molecular weight of SMB-1 decreased significantly (by 60%) only after 5 months of weathering, it suggests such measurements are of limited value as they can verify significant deterioration only fragmentation can also be visually conformed.

Polyethylene films degradation is faster and more effective in the presence of atmospheric oxygen than in the presence of seawater. Despite the fact that sorbed water molecules can accelerate degradation rates by increasing the accessibility to oxygen in the matrix and enabling the leaching of stabilizers, the amount of light available for light-induced oxidation is significantly lower in the water. Additionally, the temperatures on land are higher, allowing for further deterioration of the polymer possibly due to thermo-oxidation. The effect of fouling could also be decisive for the rate of degradation, since it implies the build-up of dark material on the surface of the polymer, thus making less amounts of light available for photo-oxidation. Likewise, fouling could cause a weight increase of the material, decreasing buoyancy and leading it deeper in the water, where it is harder for light to reach, despite the fact that biodegradation could occur, further deteriorating it (Andrady, 1990; Ho et al., 1999). Andrady (1990) reports that statistically significant changes in ultimate elongation of samples weathered on land vs. samples weathered in seawater where after twice as long (12 months) no fragmentation was observed. Similarly, our work showed only marginal weathering of SMB-1 and SMB-2 in both seawater treatments (C and D). Apart from the higher UV light exposure and temperatures shown in **Table 1**, these results may also be influenced by the difference in availability of oxygen in the two matrices. While ambient air contains 21% oxygen, the dissolved oxygen in water is usually 8–10 mg/L in the top layers, thus making the oxidation process less effective. Hydrolysis could be playing a role in the degradation of plastics in the marine environment, but it is a very slow process whereby the plasticizers are leached out first.

Mechanical stress exerted on weathered stranded plastics in the marine environment can accelerate the fragmentation process and this is particularly true for lost or abandoned fishing gear. However, the application of mild mechanical stress that has been used in this work to detect the onset of fragmentation is totally different. If the plastic sample being tested in not sufficiently weathered, no changes can be observed with the application of the mechanical forces excreted by the rotating sand. Further experiments performed after the 6-month experiment reported here, 12 h was found as sufficient period of time to have the maximum possible fragmentation for the current degree of weathering.

Brandon et al. (2016) examined FTIR spectra of long-term weathered plastics and found that chemical bonds exhibited some non-linear changes with environmental exposure and hence, they

can potentially approximate the weathering time of HDPE in particular. Combination of land conditions (temperature, UV, mechanical stress) can lead to relative rapid transformation of polyethylene films into microplastics, which are much harder to detect and collect from the seawater (da Costa et al., 2016). In general, secondary microplastics resulting from fragmentation, are harder, if not impossible, to collect (Andrady, 2011). They tend to accumulate over time and pose a threat to wildlife through ingestion (Gregory, 2009) or organic pollutant transfer (Teuten et al., 2009; Tanaka et al., 2013). Shopping bag samples exposed to sea turtle gastrointestinal fluids for 49 days showed no deterioration. Biodegradable bags exposed to the same conditions only lost 3–9% of their mass, as opposed to the 100% degradation suggested by the manufacturers (Müller et al., 2012).

Our results suggest that weathering of plastics in the marine environment is significantly higher onshore compared to plastics floating in seawater. Hence, it suggests that in the Mediterranean Sea where there is a plethora of small islands with many kilometers of beach zone, secondary microplastics are generated primarily after they are washed for a period of time on the shore. Particularly in the summer months, the degree of weathering plastics undergo in a couple of months under high temperatures could be sufficient to bring the plastic to the onset of fragmentation. Any further exposure will result in appreciable amount of microplastics being generated. Research should be encouraged on every aspect of plastic pollution, while legislation should rather sooner than later be implemented for its prevention and mitigation.

Finally, it is crucial to emphasize that this experiment is a springboard for further research, due to its simplicity in both setup and number of parameters investigated. The fragmentation of various polymer types should be examined, but most importantly *in situ* measurements with plastics floating in seawater should be performed. There are many challenges to be faced in the marine environment, but the prognosis is that floating plastic items become populated by microbes and suspended solids from the sea and as a result their density changes and start sinking well before they are weathered to the point of fragmentation. As a result, most plastic items, if they are not washed on a beach, they will most likely sink before they turn into microplastics due to weathering. A critical question that should also be answered is when do naturally weathered plastics like polyethylene films become biodegradable and in particular whether biodegradation rates are high enough prior to the onset of fragmentation. At the present time, we are systematically examining this question in our labs, yet we have recently obtained very encouraging results on the biodegradation of naturally weathered HDPE and LDPE plastics as they are readily degraded by consortia of special cultures with the indigenous bacteria or even with indigenous consortia only, well before the fragmentation to microplastics commences.

CONCLUDING REMARKS

In order to address the problem of quantification of macroplastics fragmentation to microplastics in the marine environment, a simple and easily reproducible test procedure was developed for polymer films based on weathering with sunlight and application of mild mechanical stress to pinpoint the onset of fragmentation. For polymer films, like supermarket plastic bags, it is the cumulative luminance exposure that appears to be the main indicator of the degree of weathering and it can be linked to the onset of fragmentation. A simple procedure to apply reliably and repeatedly mild mechanical stress to weathered strips has been proposed.

It is very important to have estimates of fragmentation rates of the plastics present in the marine environment if we wish to develop reliable models forecasting the environmental status of our oceans and seas.

Comparing the results from sunlight exposure on beach sand or in seawater near the surface, it is seen that fragmentation onshore is much faster. Hence, over a short period, beached plastic debris can be turned into microplastics and with the first event of high waves or strong winds, the generated microplastics are returned to the seawater where they are much more difficult to collect. Therefore, local authorities, NGOs and interested parties in general, should make every effort to regularly collect plastic debris from the beaches (especially at known debris accumulation areas) before they turn into microplastics and are returned to the sea.

AUTHOR CONTRIBUTIONS

KK helped in the analysis of the data and wrote the first draft of the manuscript, GK designed and conducted the experiments and the instrumental analysis and helped in the analysis of the data; ET conducted the experiments and the instrumental analysis and helped in the preparation of the manuscript; AG supervised the experimental measurements for the characterization of the polymer films; PP developed the image processing code in MATLAB and supervised the image analysis; FF critically reviewed the design of the whole project; NK supervised the whole project, helped in the data analysis and contributed in the write up of the manuscript.

ACKNOWLEDGMENTS

Funding by the European Union FP-7 project BIOCLEAN (grant agreement No. 312100) is highly appreciated.

SUPPLEMENTARY MATERIAL

The Supplementary Material for this article can be found online at: http://journal.frontiersin.org/article/10.3389/fmars.2017.00084/full#supplementary-material

REFERENCES

Abdelhafidi, A., Babaghayou, I. M., Chabira, S. F., and Sebaa, M. (2015). Impact of solar radiation effects on the physicochemical properties of polyethylene (PE) plastic film. *Procedia-Social Behav. Sci.* 195, 2922–2929. doi: 10.1016/j.sbspro.2015.09.002

Accinelli, C., Saccà, M. L., Mencarelli, M., and Vicari, A. (2012). Deterioration of bioplastic carrier bags in the environment and assessment of a new recycling alternative. *Chemosphere* 89, 136–143. doi: 10.1016/j.chemosphere.2012.05.028

Andrady, A. L. (1990). "Environmental degradation of plastics under land and marine exposure conditions," in *Second International Conference on Marine Debris (April 1989)* (Honolulu, HI), 848–869.

Andrady, A. L. (2011). Microplastics in the marine environment. *Mar. Pollut. Bull.* 62, 1596–1605. doi: 10.1016/j.marpolbul.2011.05.030

Andrady, A. L., Pegram, J. E., and Tropsha, Y. (1993). Changes in carbonyl index and average molecular weight on embrittlement of enhanced-photodegradable polyethylenes. *J. Environ. Polym. Degrad.* 1, 171–179. doi: 10.1007/BF01458025

Artham, T., Sudhakar, M., Venkatesan, R., Madhavan Nair, C., Murty, K. V. G. K., and Doble, M. (2009). Biofouling and stability of synthetic polymers in sea water. *Int. Biodeterior. Biodegradation* 63, 884–890. doi: 10.1016/j.ibiod.2009.03.003

Arthur, C., Baker, J., and Bamford, H. (2009). *Proceedings of the International Research Workshop on the Occurrence, Effects, and Fate of Microplastic Marine Debris*. Silver Spring, MD.

Barnes, D. K. A., Galgani, F., Thompson, R. C., and Barlaz, M. (2009). Accumulation and fragmentation of plastic debris in global environments. *Phil. Trans. R. Soc.* 364, 1985–1998. doi: 10.1098/rstb.2008.0205

Brandon, J., Goldstein, M., and Ohman, M. D. (2016). Long-term aging and degradation of microplastic particles: comparing *in situ* oceanic and experimental weathering patterns. *Mar. Pollut. Bull.* 110, 299–308. doi: 10.1016/j.marpolbul.2016.06.048

Brower, R. (2016). The social costs of beach litter along european coasts. *Ocean Coast. Manage.* 138, 38–49. doi: 10.1016/j.ocecoaman.2017.01.011

Carrasco, F., Pagès, P., Pascual, S., and Colom, X. (2001). Artificial aging of high-density polyethylene by ultraviolet irradiation. *Eur. Polym. J.* 37, 1457–1464. doi: 10.1016/S0014-3057(00)00251-2

Cheshire, A., Adler, E., Barbière, J., and Cohen, Y. (2009). *UNEP/IOC Guidelines on Survey and Monitoring of Marine Litter*. UNEP Regional Seas Reports and Studies, No. 186; IOC Technical Series. Available online at: http://www.unep.org/regionalseas/marinelitter/publications/docs/Marine_Litter_Survey_and_Monitoring_Guidelines.pdf

Cole, M., Lindeque, P., Halsband, C., and Galloway, T. S. (2011). Microplastics as contaminants in the marine environment: a review. *Mar. Pollut. Bull.* 62, 2588–2597. doi: 10.1016/j.marpolbul.2011.09.025

da Costa, J. P., Santos, P. S., Duarte, A. C., and Rocha-Santos, T. (2016). (Nano)plastics in the environment - Sources, fates and effects. *Sci. Tot. Environ.* 566–567, 15–26. doi: 10.1016/j.scitotenv.2016.05.041

Depledge, M. H., Galgani, F., Panti, C., Caliani, I., Casini, S., and Fossi, M. C. (2013). Plastic litter in the sea. *Mar. Environ. Res.* 92, 279–281. doi: 10.1016/j.marenvres.2013.10.002

Directive of the European Parliament and of the Council (2013). *Directive of the European Parliament and of the Council Amending Directive 94/62/EC on Packaging and Packaging Waste to Reduce the Consumption of Lightweight Plastic Carrier Bag*. Available online at: http://eur-lex.europa.eu/legal-content/EN/ALL/?uri=CELEX:52013SC0444

Gregory, M. R. (2009). Environmental implications of plastic debris in marine settings–entanglement, ingestion, smothering, hangers-on, hitch-hiking and alien invasions. *Philos. Trans. R. Soc. Lond. B Biol. Sci.* 364, 2013–2025. doi: 10.1098/rstb.2008.0265

Hidalgo-Ruz, V., and Thiel, M. (2013). Distribution and abundance of small plastic debris on beaches in the SE Pacific (Chile): a study supported by a citizen science project. *Mar. Environ. Res.* 87–88, 12–18. doi: 10.1016/j.marenvres.2013.02.015

Ho, K.-L. G., Pometto, A. L. III, and Hinz, P. N. (1999). Effects of temperature and relative humidity on polylactic acid plastic degradation. *J. Polym. Environ.* 7, 83–92. doi: 10.1023/A:1021808317416

Ioakeimidis, C., Fotopoulou, K. N., Karapanagioti, H. K., Geraga, M., Zeri, C., Papathanassiou, E., et al. (2016). The degradation potential of PET bottles in the marine environment: an ATR-FTIR based approach. *Sci. Rep.* 6:23501. doi: 10.1038/srep23501

Jabarin, S. A., and Lofgren, E. A. (1994). Photooxidative effects on properties and structure of high-density polyethylene. *J. Appl. Polym. Sci.* 53, 411–423. doi: 10.1002/app.1994.070530404

Kumar Sen, S., and Raut, S. (2015). Microbial degradation of low density polyethylene (LDPE): a review. *J. Environ. Chem. Eng.* 3, 462–473. doi: 10.1016/j.jece.2015.01.003

Martinho, G., Balaia, N., and Pires, A. (2017). The Portuguese plastic carrier bag tax: the effects on consumers' behavior. *Waste Manage.* 61, 3–12. doi: 10.1016/j.wasman.2017.01.023

Müller, C., Townsend, K., and Matschullat, J. (2012). Experimental degradation of polymer shopping bags (standard and degradable plastic, and biodegradable) in the gastrointestinal fluids of sea turtles. *Sci. Tot. Environ.* 416, 464–467. doi: 10.1016/j.scitotenv.2011.10.069

O'Brine, T., and Thompson, R. C. (2010). Degradation of plastic carrier bags in the marine environment. *Mar. Pollut. Bull.* 60, 2279–2283. doi: 10.1016/j.marpolbul.2010.08.005

Pham, C. K., Ramirez-Llodra, E., Alt, C. H., Amaro, T., Bergmann, M., Canals, M., et al. (2014). Marine litter distribution and density in European seas, from the shelves to deep basins. *PLoS ONE* 9:e95839. doi: 10.1371/journal.pone.0095839

PlasticsEurope (2015). *Plastics - the Facts 2014/2015: An Analysis of European Plastics Production, Demand and Waste Data*. Brussels: PlasticsEurope.

Restrepo-Flórez, J. M., Bassi, A., and Thompson, M. R. (2014). Microbial degradation and deterioration of polyethylene - a review. *Int. Biodeter. Biodegradation* 88, 83–90. doi: 10.1016/j.ibiod.2013.12.014

Ryan, P. G., Moore, C. J., van Franeker, J. A., and Moloney, C. L. (2009). Monitoring the abundance of plastic debris in the marine environment. *Philos. Trans. R. Soc. Lond. B Biol. Sci.* 364, 1999–2012. doi: 10.1098/rstb.2008.0207

Shah, A. A., Hasan, F., Hameed, A., and Ahmed, S. (2008). Biological degradation of plastics: a comprehensive review. *Biotechnol. Adv.* 26, 246–265. doi: 10.1016/j.biotechadv.2007.12.005

Stark, N. M., and Matuana, L. M. (2004). Surface chemistry changes of weathered HDPE/wood-flour composites studied by XPS and FTIR spectroscopy. *Polym. Degrad. Stabil.* 86, 1–9. doi: 10.1016/j.polymdegradstab.2003.11.002

Tanaka, K., Takada, H., Yamashita, R., Mizukawa, K., Fukuwaka, M. A., and Watanuki, Y. (2013). Accumulation of plastic-derived chemicals in tissues of seabirds ingesting marine plastics. *Mar. Pollut. Bull.* 69, 219–222. doi: 10.1016/j.marpolbul.2012.12.010

Teuten, E. L., Saquing, J. M., Knappe, D. R., Barlaz, M. A., Jonsson, S., Björn, A., et al. (2009). Transport and release of chemicals from plastics to the environment and to wildlife. *Philos. Trans. R. Soc. Lond. B Biol. Sci.* 364, 2027–2045. doi: 10.1098/rstb.2008.0284

Tidjani, A. (2000). Comparison of formation of oxidation products during photo-oxidation of linear low density polyethylene under different natural and accelerated weathering conditions. *Polym. Degrad. Stabil.* 68, 465–469. doi: 10.1016/S0141-3910(00)00039-2

United Nations Environment Programme (UNEP) (2014). *Plastic Debris in the Ocean. UNEP Year Book 2014 Emerging Issues Update* (Nairobi), 48–53.

United Nations Environment Programme (UNEP) (2015). *Plastic in Cosmetics* [Fact Sheet]. Nairobi. 1.24, 1–3.

Watson, R., Revenga, C., and Kura, Y. (2006). Fishing gear associated with global marine catches. I. Database development. *Fish. Res.* 79, 97–102. doi: 10.1016/j.fishres.2006.01.010

Conflict of Interest Statement: The authors declare that the research was conducted in the absence of any commercial or financial relationships that could be construed as a potential conflict of interest.

frontiers in Marine Science

REVIEW
published: 31 March 2017
doi: 10.3389/fmars.2017.00030

Using Numerical Model Simulations to Improve the Understanding of Micro-plastic Distribution and Pathways in the Marine Environment

Britta D. Hardesty[1], Joseph Harari[2], Atsuhiko Isobe[3], Laurent Lebreton[4,5], Nikolai Maximenko[6], Jim Potemra[6], Erik van Sebille[7], A. Dick Vethaak[8,9] and Chris Wilcox[1]*

[1] Commonwealth Scientific and Research Organization, Oceans and Atmosphere, Hobart, TAS, Australia, [2] Department of Physical, Chemical and Geological Oceanography, Oceanographic Institute, São Paulo University, São Paulo, Brazil, [3] Centre for Oceanic and Atmospheric Research, Research Institute for Applied Mechanics, Kyushu University, Fukuoka, Japan, [4] The Modelling House Ltd., Wellington, New Zealand, [5] The Ocean Cleanup Foundation, Delft, Netherlands, [6] International Pacific Research Center, School of Ocean and Earth Science and Technology, University of Hawaii, Honolulu, HI, USA, [7] Grantham Institute and Department of Physics, Imperial College London, London, UK, [8] Deltares, Marine and Coastal Systems, Delft, Netherlands, [9] Department of Chemistry and Biology, Institute for Environmental Studies, Vrije Universiteit Amsterdam, Amsterdam, Netherlands

OPEN ACCESS

Edited by:
Francois Galgani, French Research Institute for Exploitation of the Sea (Ifremer), France

Reviewed by:
Stefano Aliani, National Research Council, Italy
Olivia Gerigny, French Research Institute for Exploitation of the Sea (Ifremer), France

****Correspondence:***
Britta D. Hardesty
denise.hardesty@csiro.au

Specialty section:
This article was submitted to Marine Pollution, a section of the journal Frontiers in Marine Science

Received: *01 November 2016*
Accepted: *25 January 2017*
Published: *31 March 2017*

Citation:
Hardesty BD, Harari J, Isobe A, Lebreton L, Maximenko N, Potemra J, van Sebille E, Vethaak AD and Wilcox C (2017) Using Numerical Model Simulations to Improve the Understanding of Micro-plastic Distribution and Pathways in the Marine Environment. Front. Mar. Sci. 4:30. doi: 10.3389/fmars.2017.00030

Numerical modeling is one of the key tools with which we can gain insight into the distribution of marine litter, especially micro-plastics. Over the past decade, a series of numerical simulations have been constructed that specifically target floating marine litter, based on ocean models of various complexity. Some of these models include the effects of currents, waves, and wind as well as a series of processes that impact how particles interact with ocean currents, including fragmentation and degradation. Here, we give an overview of these models, including their spatial and temporal resolution, limitations, availability, and what we have learned from them. Then we focus on floating marine micro-plastics (<5 mm diameter) and we make recommendations for experimental research efforts that can improve the skill of the models by increasing our understanding of the processes that govern the dispersion of marine litter. In addition, we highlight the importance of knowing accurately the sources or entry points of marine plastic debris, including potential sources that have not been incorporated in previous studies (e.g., atmospheric contributions). Finally, we identify information gaps and priority work areas for research. We also highlight the need for appreciating and acknowledging the uncertainty that persists regarding the movement, transportation and accumulation of anthropogenic litter in the marine environment.

Keywords: accumulation modeling, fluxes, fragmentation, marine debris, microplastics, numerical modeling

INTRODUCTION

Pollution from marine plastic is a global issue of international concern. Marine litter comes from both land- and sea-based sources and can travel immense distances. Marine ecosystems worldwide are affected by human-made refuse, much of which is plastic (see Table 1 of Derraik, 2002). Resolving the biodiversity, environmental, economic, transport, navigation, and biological invasion hazards associated with anthropogenic litter in the marine environment requires a

substantial, sustained integrated effort from individuals, industry, governments, and international governmental organizations at local to regional and global scales. The increase in global plastic production and the recent estimate of ∼8 million metric tons of mismanaged plastic waste entering the ocean each year (Jambeck et al., 2015) points to the need to tackle the problem at a multitude of scales. There is no single solution, rather, a number of local and regional solutions will be required to effect change.

A necessary first step in addressing this problem is to get an estimate of the amount of plastic in the oceans, including knowledge about from where it originates, where it is accumulating, and the pathways by which it got there. This is a complex problem for a variety of reasons, including challenges in sampling both *in situ* (in the water column, sediments, etc.) and at the source (e.g., riverine input, coastal input, sea-surface input, etc.). Sampling micro-plastic is particularly and challenging since it is not easily observed due to its small size, its sources include not only direct inputs but it also results from the degradation of larger plastic pieces. Furthermore, organisms can alter the pathways in the marine environment by direct transport and/or altering the density of the particles.

For these reasons, a mass budget of micro-plastic debris will be challenging to construct based on empirical data alone. Instead, simulations using numerical models of ocean currents may be used to estimate the sources, sinks, and pathways of micro-plastic in the marine environment. This approach of integrating models predicting debris flows and distributions has been useful in extending the existing sparse observations to make estimates of budgets in some parts of the system, and flows of mass in a few cases (Cózar et al., 2014; van Sebille et al., 2015; others). Extending this approach of integrating simulation models and empirical observations can greatly improve our understanding of plastics, and particularly micro-plastics, in the marine environment at a systems level.

BACKGROUND

Marine debris or marine litter is defined as any persistent, manufactured, or processed solid material discarded, disposed of or abandoned in the marine and coastal environment (UN Environment Program, 2009). Some portion of plastic litter may reach microscopic sizes due to degradation (mechanical forces and/or photochemical processes) of macro-plastic debris (Gigault et al., 2016) or is already manufactured as microscopic particles. These are referred to here as micro-plastics. This aspect of marine litter is of special interest as its physical properties allow it to be transported over large distances and its small size makes it available for a wide range of marine biota (Ivar do Sul et al., 2014; GESAMP, 2016). Its small size, however, makes it difficult to observe remotely, thus limiting an accurate assessment of total amounts. Nevertheless, plastic debris can be observed in seas around the world, from concentrations exceeding 600,000 pieces per km^2 (Law et al., 2010) in the accumulation zones to more remote regions such as the waters of the Arctic (Bergmann et al., 2016) and the Antarctic (Barnes et al., 2010) where far fewer plastic pieces are observed. It has become clear that humanity's discarded litter is spreading throughout our seas and oceans (e.g., Pham et al., 2014; Jambeck et al., 2015; GESAMP, 2016).

Debris sampling and monitoring in the environment is most often carried out along the shoreline, but can also take place at sea or through sampling wildlife that have encountered debris. Most often, monitoring and surveys of litter take place in coastal regions, often as part of clean up activities or other community events. Using information from these activities as monitoring information raises a number of issues, as the activities can be idiosyncratic, may have uneven sampling, and frequently do not control sampling effort carefully. Designed surveys can provide much more robust data, however, these are much rarer globally [but see OSPAR (http://www.ospar.org/work-areas/eiha/marine-litter), CSIRO (http://www.csiro.au/en/Research/OandA/Areas/Marine-resources-and-industries/Marine-debris; Hardesty et al., 2016), and NOAA's (https://marinedebris.noaa.gov/) approaches].

Debris, especially plastics, can also be surveyed in the ocean, although coastal and high seas monitoring can be expensive and difficult to replicate. Typically, oceanic monitoring of marine litter takes place through surface trawl sampling, which is biased toward items within a particular size range—those that are small enough to fit in the mouth of the net, large enough to be stopped by the net mesh, are floating on or near the ocean's surface and can be and discerned by the human eye (see van Sebille et al., 2015; typically in the range between 0.25 and 0.0003 m). Surface sampling captures floating objects only and, given the vastness of the ocean, complex, and ever changing ocean circulation patterns and wind mixing, samples are often highly variable. At-sea sampling also requires large sample sizes to facilitate the statistical analysis required to detect potential changes in distribution and abundance, given the high spatial and temporal heterogeneity of marine litter, especially plastics in the ocean (Barnes et al., 2009).

Nearly all of the plastic (95% or more of the items or particles by count) recorded from surface trawl sampling efforts are smaller than 5 mm in diameter. Similarly, these smaller items make up the vast majority of debris found in coastal samples—at least for surveys that record smaller sizes of items (Hardesty et al., 2016). Because of technological challenges, however, field studies so far have only been able to analyse the large and middle-sized micro-plastics (>20 micrometer; Galgani et al., 2013). Hence, our discussion focuses on the distribution and movement of the fraction of floating micro-plastics in the ocean in this size range, from 5 to 0.02 mm in diameter.

How Much (Micro) Plastic Is in the Ocean?

There are a number of questions that remain unanswered regarding micro-plastic in the ocean. These questions are also valid for plastic in general, since it can be a major contributing source of micro-plastic. Perhaps the most straightforward, fundamental question is *how much plastic is in the ocean?* While recent work quantified plastic inputs from land into the ocean (Jambeck et al., 2015), the amount (whether by weight or volume) in the global ocean remains poorly understood, and estimates vary with orders of magnitude. Additional questions that fall

under this key knowledge gap involve understanding *what* are the sources, *where* micro-plastic occurs in the ocean, *what* its size spectra are, and *how much* there is in various locations around the globe. Identifying the contributing sources and sinks (where it comes from and where it ends up) as well as recognizing the proportion of micro-plastic that is from primary vs. secondary (e.g., breakdown) sources are key questions which inform our understanding of how much plastic is in the ocean. In essence, to address this fundamental question of the total load we need to better understand the sources, pathways and fate of (micro) plastic.

What Are the Main Contributing Sources of Plastic in the Ocean?

Approximately 80% of the plastic in the oceans is estimated to come from land-based sources or entry points (Sheavly and Register, 2007; Galgani et al., 2013) which includes beaches, rivers, stormwater runoff, aquaculture and fisheries, shipping transport, and atmospheric outfall (see GESAMP, 2016). Debris sampling, correspondingly, largely takes place via coastal activities and is likely biased by larger items that are easily discernible by the human eye. Primary microplastics, however, are often abrasives or similar purpose-produced small, regular sized particles and may be missed due to issues of visual detection.

We know relatively little about the proportion of micro-plastics entering the marine environment as primary versus secondary microplastics (resulting from the breakdown of larger items). However, it is reasonable to presume that the breakdown or transition of larger plastics to micro-plastics may be most common in the nearshore environment, due to the high energy of the coastal environment and the presence of other natural abrasives such as sand and rock. Further adding to the challenge of quantifying and identifying sources of microplastics is that many microplastics such as fibers are negatively buoyant and are therefore missed by most sampling methods. In sediment cores (and invertebrates) for example, fibers are common (Besseling et al., 2012; Woodall et al., 2014). However, most coastal and offshore microplastics sampling takes place in the upper surface of the ocean and hence samples positively buoyant items. As a result, our knowledge of sources of microplastics is affected by biased sampling, and most modeling to date is on the buoyant fraction of plastics in the ocean.

How Does Plastic Move in the Ocean?

The various factors that contribute to the pathways of micro-plastic in the ocean are an active area of research. Quantitative estimates of losses (and budgets) would fundamentally be improved with a more complete understanding of how micro-plastics move in the environment. Researchers are working on mesocosm or other small-scale experiments in the laboratory to look at wave action, fouling, and other aspects that affect movement (Gerritse et al., 2015; Fazey and Ryan, 2016a,b; ter Halle et al., 2016), but such exercises are relatively new and have yet to be applied at larger scales. There is a clear niche for experimental work in improving our understanding of plastic movement and the use of local, regional, and global models can significantly also significantly contribute to improving our understanding of the issue (see **Table 1** for some of the available ocean circulation models and oceanographic datasets used for marine debris modeling/tracking).

What is the Fate of Plastic in the Ocean?

Considering the fate of micro-plastic in the ocean requires improving our understanding of where plastic persists in reservoirs and what the rates of fragmentation are under various conditions (and for various material and sizes of primary plastic). Better estimates and data describing buoyancy, i.e., sinking and re-suspension or floating rates will also yield insights to the fate of plastics in the ocean. Furthermore, knowing the distribution of plastic and whether it ends up in locations where it can be removed or in places where it can break down to smaller pieces and/or re-enter the ocean will greatly inform the question of how much plastic is in the ocean.

CURRENT ASSESSMENT

Long term monitoring of micro-plastic abundance is costly, time consuming, and difficult to sustain. Importantly, however, though there are a number of long term monitoring efforts on coastlines, such as OSPAR's marine beach litter program in Europe (http://www.ospar.org), the International Coastal Cleanup (ICC) which is organized by the Ocean Conservancy (http://www.oceanconservancy.org) and NOAA's marine debris program which monitors coastal litter using multiple monitoring approaches (http://www.marinedebris.noaa.gov). These long term initiatives are important not only to detect long term trends and patterns in terms of coastal debris, but it can also allow one to evaluate the efficacy of legislation, to identify changes in sources, deposition, material types and potential impacts to wildlife. Furthermore, long term monitoring can help to identify opportunities for impact through local actions. Each of these initiatives, however, focuses on larger sized items (>5 mm) which means that they are useful in detecting likely sources of secondary micro-plastic quantities, types, and locations for point of entry to the marine environment, but such efforts fail to report on primary micro-plastic amounts, density, and changes through time.

Around the world, there are a number of different data collection strategies that have been developed and employed to monitor marine and coastal litter. While it is important to recognize that different questions require different monitoring approaches, the importance of standardization of approaches cannot be overstated (Barnes et al., 2009; e.g., does one report counts or weight or by surface area or volume?). To date, global harmonization of monitoring methods and data recording have remained unrealized, but working toward this remains an important goal (Cheshire et al., 2009; Galgani et al., 2013). Recently, the importance of global harmonization of monitoring methods are recognized by increasing number of scientists; see the Annex to Leaders' Declaration of Elmau G7 summit (http://www.mofa.go.jp/mofaj/files/000084023.pdf) and the Communique of G7 Toyama Environment Ministers' Meeting (http://www.env.go.jp/press/files/jp/102871.pdf).

TABLE 1 | Some available ocean circulation models and oceanographic datasets used for marine debris modeling/tracking.

Model/dataset	Description	References
BLUELink	CSIRO Ocean modeling and analysis tool used for accurately forecasting ocean conditions	Wilcox et al., 2013
Connie2	Australian Connectivity Interface, web-tool developed by CSIRO	Reisser et al., 2013
ECCO	Estimation of Circulation and Climate of the Ocean—Scripps Institution of Oceanography (SIO), the NASA Jet Propulsion Laboratory (JPL) and the Massachusetts Institute of Technology (MIT)	Potemra, 2012
ECMWF ORA-S3	Ocean analysis/reanalysis system of European Center for Medium-Range Weather Forecasts (ECMWF)	Potemra, 2012
Global drifter program	Satellite-tracked surface drifting buoy observations of currents, sea surface temperature, atmospheric pressure, winds, and salinity (NOAA)	Maximenko et al., 2012; van Sebille et al., 2012; Reisser et al., 2013
GNOME	General NOAA Operational Model Environment; interactive simulation system designed for modeling pollutant trajectories in marine environment	GNOME User's Manual, 2002
HYCOM	Hybrid Co-ordinate Model—forced by US Navy's Operational Global Atmospheric Prediction System (NOGAPS)	Lebreton et al., 2012; Potemra, 2012; Lebreton and Borrero, 2013
NCOM	1/8° global Navy Coastal Ocean Model (NAVOCEANO)—real time	Potemra, 2012
NEMO	Nucleus for European Modeling of the Ocean	Storkey et al., 2010
NLOM	1/32° global Navy Layered Ocean Model run daily by the Naval Oceanographic Office (NAVOCEANO)—real time	Potemra, 2012
OSCAR	Ocean Surface Current Analysis—Real time (NOAA)	Martinez et al., 2009
OSCURS	Ocean Current Simulator Model (NOAA Fisheries Service)	Ebbesmeyer and Ingraham, 1994; Ebbesmeyer et al., 2012
PELET-2D	Lagrangian particle tracking model (Helmholtz–Zentrum Geesthacht)	Neumann et al., 2014
plasticadrift.org	Web-tool developed by E. van Sebille based on trajectories of Global surface drifters	van Sebille, 2014
Pol3DD	Lagrangian 3-D numerical dispersal model	Lebreton et al., 2012; Lebreton and Borrero, 2013
SCUD	Surface Currents from Diagnostics—developed by International Pacific Research Centre	Maximenko and Hafner, 2010
SODA	Simple Ocean Data Assimilation model (by Cummings et al., 2005)	Potemra, 2012

Sustained monitoring is crucial to assess the efficacy of measures implemented to reduce the abundance of plastic debris, but it is complicated by large spatial and temporal heterogeneity in the amounts of plastic debris and by our limited understanding of the pathways followed by plastic debris and its long-term fate. Thus far, most monitoring has focused on beach surveys of stranded plastics and other litter, as mentioned above. Infrequent surveys of the standing stock of litter on beaches provide crude estimates of debris types and abundance, but are biased by differential removal of litter items by beachcombing, clean-ups and beach dynamics. However, there is increased sampling of and analyses of micro-plastics on the ocean's surface (Reisser et al., 2013; Cózar et al., 2014; Eriksen et al., 2014; Isobe et al., 2015; Ryan, 2015; van Sebille et al., 2015) with fewer studies reporting on sub-surface micro-plastics (but see Reisser et al., 2015; Kooi et al., 2016).

Reservoirs: Where Is Micro-plastic Found?

Plastic has been found throughout, the ocean from the surface, all the way through the water column to the deep ocean floor. It can reside in sediment, biota, and ice, and may be trapped along the coastline or in estuaries, waterways and lakes, and can even be suspended in the atmosphere (Dris et al., 2016; GESAMP, 2016). There is no reason to believe the presence of micro-plastic is any less wide-spread.

In this study, we divide locations into seven broad categories deemed most relevant for modeling movement of plastics in the ocean: surface, coastline/estuaries, ocean floor, sediments, ice, biota, and water column (**Figures 1**, **2**). While there are other reservoirs (e.g., the atmosphere, lakes, and waterways), we consider those to fall outside of the scope and focus of this paper. For our purposes they are considered as sources of micro-plastics entering the ocean.

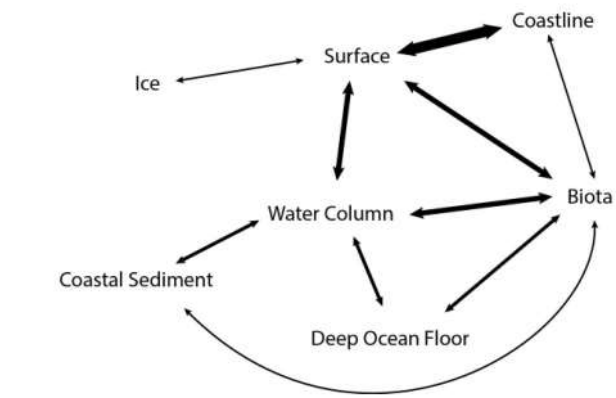

FIGURE 1 | Schematic representation of reservoirs and fluxes for marine plastics. The weight of the arrow indicates the magnitude of marine debris flux hypothesized to occur between compartments, and the fluxes or flows between them.

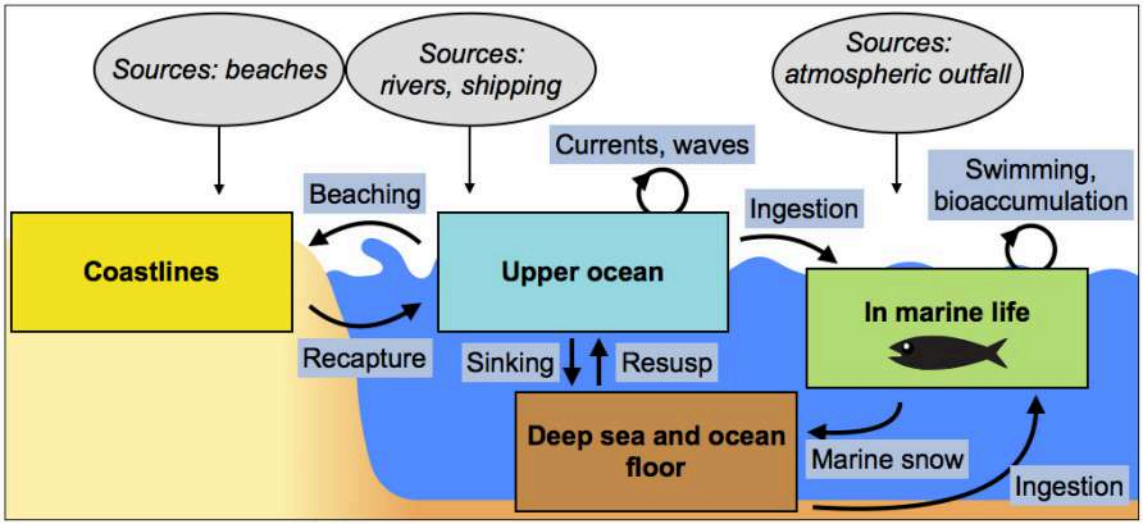

FIGURE 2 | The sources of anthropogenic debris entering the ocean (ovals), reservoirs, or oceanic compartments where debris occurs (boxes) and processes through which debris moves between compartments.

Evaluating budgets (sources and sinks into the environment) or leakage between these reservoirs or compartments requires understanding several key processes. Those deemed to be particularly important include rates of fragmentation, buoyancy/sinking/re-floating rates, as well as the rates and quantities of inputs of litter to the ocean and time trends for plastics in ocean.

When assessing the potential reservoirs of micro-plastic it is equally important to understand the uncertainty bounds. Identifying in which reservoirs there is the greatest uncertainty will facilitate a ranking of transitions on which efforts could be focused, taking into account the key question at hand (whether that relates to sources, losses between transition zones or impacts).

THE APPLICATION OF NUMERICAL MODELING

Overall, there are two ultimate goals to improve our modeling of plastic budgets and impacts of marine debris. Identifying where, how and why plastic enters (and leaves) the ocean is very different from understanding the biodiversity, economic, and environmental impact plastic is having in the marine environment. One difference is that the former (understanding the budget) requires modeling of the mass of plastic, while the latter (understanding the impacts) requires modeling the number of plastic particles. In this paper, we focus on understanding the budget.

Modeling Key Fluxes

There are three main fluxes that are considered here to be of highest priority (**Figure 1**). These include the fluxes that occur between the ocean and the coast; movements between the coast to ocean interface; and the fluxes between the ocean (whether surface, water column, or floor) and biota (and the other direction). The first two are considered most important since the near-shore environment is where most plastic must pass through to reach the open ocean. This is also a zone of high biodiversity and hence, where much of the biological impact is likely to occur.

This does not rule out the importance of movement between oceanic reservoirs or movement between the surface and water column. Rather it highlights the critical need for better understanding of movement between key reservoirs. Fluxes between ice and other reservoirs were considered to be of lesser importance, though there is agreement among oceanographers that modeling fluxes between ice and other reservoirs may not be particularly difficult.

Both for a mass balance modeling approach and to evaluate impacts, understanding of the accumulation of plastic in biota is needed. Importantly, this is a "sink" (and can act as a transport mechanism) where empirical data can be collected—whether through analysis of seabirds digestive tracts or fish guts or total body analysis of invertebrates, through excreta, or with non-invasive sampling techniques. There is a growth in the number of papers reporting on the interactions between plastics and marine fauna (see Gall and Thompson, 2015), with ingestion of debris, entanglement, and chemical contamination increasingly reported in the literature. It might now be reasonable to estimate micro-plastics residing in marine biota, but to date, an estimate of the overall mass of debris in wildlife (much less focusing on micro-plastics has yet to be carried out.

Needed Improvements

The marine debris problem can be viewed as a source, pathway and sink issue. Simulations using numerical models can be important tools in estimating or constraining any of these three when the other two are more well-known. Simulations can also be

used to test hypotheses addressing knowledge gaps within these three. Given the challenges of monitoring micro-plastic both before it arrives and once it is already in the marine environment, combining empirical data, and modeling approaches can be useful to help predict, or forecast, where micro-plastics occur in the marine environment.

Numerical modeling has been applied to track back or hindcast from where plastics in the ocean may have come (sensu; Kako et al., 2011), and these same approaches could be used for micro-plastic. Hindcasting is particularly useful for source identification, especially where accumulation regions have been identified. Ocean circulation models can further be used to identify where oceanic accumulation zones are most likely to occur. Coupling such tools and approaches with species distribution maps and other ecological information, we can combine disparate data types to predict or identify hotpots of risk to taxa or geographic regions of interest (Schuyler et al., 2013, 2015; Wilcox et al., 2015, 2016). We can also identify movement pathways or trajectories (Wilcox et al., 2013), identify hotspots, and develop scenario analysis tools to identify potential sources and sinks. We can further evaluate effectiveness of local actions and activities (see Hardesty et al., 2016), predict risk of invasion along pathways and evaluate costs of inaction and efficiency of action (Sherman and Van Sebille, 2016).

Modeling efforts have greatly improved in recent years, and as computing power increases, so too does our ability to incorporate additional parameters into simulating marine debris movement in the ocean. In addition to circulation models that provide estimates of ocean currents, there are other models that can be employed, including for example, risk models and bioaccumulation models (ecosystem scale modeling). Each has a relevant role to play in increasing our knowledge and understanding of marine litter transport, and the development and employment of different modeling approaches depends upon the questions asked, the region studied, and the overall aim of the research.

Currently, knowledge on plastic in the oceans is insufficient to accurately estimate the total plastic budget and we are unable to measure ocean (micro) plastic directly at scale. Modeling allows us to make estimates and predictions outside of where we have data and facilitates our ability to run process studies. With models we can focus on major drivers at a global scale and potentially can scale these down to consider local processes. There currently exist global data on wind, tides, waves, pressure, and other processes that are identified as critically important. The challenge is how to bring these typically coarse data sets down to the coastal or finer scales and thus apply them to improve our understanding of the factors that drive debris movement at regional and local scales. While there may be some loss in resolution through such scaling to consider smaller geographic regions, these approaches will nevertheless improve our ability to map risk—and impact—to marine biota, regions, and ecosystems.

There is a big gap between presently used ocean circulation models, commonly having 10-km horizontal and 10-m vertical resolution (see **Table 2**), and operational activities that would require 10-m details or even finer. Enhancement of numerical models to this fine grid would also require *O* (1 mm) vertical resolution and *O* (1 s) temporal resolution. With the exponentially growing computer power, high-resolution computation may become possible in some decades. However, it will require development of principally new models that include processes that are poorly understood today: e.g., momentum injection by breaking wind waves, diurnal cycle in the ocean and atmosphere boundary layers, etc. It is likely that such models will have to use the full-complexity "primitive" equations and will have to be coupled rather than forced models.

Forcing of the models will require a new generation of the global observing system [currently monitoring the ocean at *O* (100 km) resolution], designing satellite missions that can measure smaller debris (currently available at 30 cm resolution), measuring surface currents, as well as three-dimensional datasets incorporating bottom and land topography.

TABLE 2 | Transfers from reservoirs to reservoirs, with the approaches required to increase our understanding and improve models.

	Surface	Ocean floor	Sediment	Ice	Biota	Coastline	Water column
Surface	Lagrangian modeling, field tracking exper	Lab exper/modeling/ empirical	–	Modeling/Field measure	Field measure/ Spatial analysis	Lab and field exper	Lab exper/ modeling/empirical
Ocean floor	(Lab and Field exper)	Field exper	Lab/field exper	Field exper	Empirical sampling	–	Lab/field exper
Sediment	–	Field sampling of ocean floor sediments	–	Field exper	Lab exper	Monitoring/ sampling of sediment cores	Modeling/exper
Ice	Modeling	–	–	Modeling/Field obs	Field obs	Field obs	Modeling
Biota	Lab/field	Lab/field/Spatial analysis	Lab/field/Spatial analysis	Field obs	Field/lab/modeling	Lab/field/Spatial analysis	Lab/field/Spatial analysis
Coastline	Field, Modeling	–	Coastline Monitoring for sediments	–	Field/lab/modeling	Field/lab/modeling	Field/lab/modeling
Water column	Lab/modeling	Lab/modeling	Lab/modeling	Field obs	Field/lab/modeling	–	Lagrangian modeling, field tracking exper

*Dashes indicate a lack of direct interaction between compartments (e.g., movement takes place through an intervening reservoir; see **Figure 1**).*

Further, information about marine debris (sources, composition, fragmentation, fouling, sinks, etc.) will also be needed at the corresponding space-time resolution. High-resolution modeling can be done in selected regions but, because of the open boundary conditions and Lagrangian dynamics of the debris, these regions can't be small.

Nested modeling, cascading from relatively coarse resolution in the open ocean to fine resolution near critical locations may optimize the use of resources. While the greater the resolution is needed to include important dynamics, the importance of acknowledging the significant contributions to be made with coarser resolution (both vertically and horizontally) cannot be overstated.

Tracing plastics back to their sources is often highlighted by researchers and policy makers as critical. This can be difficult in part due to variability between and within regions, which is often greater than realized. Models can, however, be tuned to consider empirical data collected in various regions (e.g., incorporating country, region or basin specific inputs, waste mismanagement and other covariates). Even in the absence of complete data (e.g., information from all regions), including sparse or incomplete data can still prove valuable.

Overlapping spatial mapping of marine litter (i.e., from accumulation models) with species distributions, vulnerable species or environmental sensitivity maps facilitates our ability to quantify the risk of plastics to biodiversity and marine ecosystems (see Hardesty and Wilcox, 2017). Dynamically modeling the risk or impacts becomes critically important not only for individuals and populations, but also for marine species that are exposed to multiple threats to survival and persistence. Identifying key geographic regions and taxa at higher or lower threat from marine plastics (e.g., Schuyler et al., 2015; Wilcox et al., 2015) can provide a useful lever to drive policy.

Where possible, researchers should aim to validate models with independent data. Independent validation of models can be used to not only increase model utility and confidence in results, but also increases our understanding of uncertainty. Quantifying, and indeed, acknowledging uncertainty in model solutions can help identify research opportunities and key knowledge gaps. Validating models against empirical data may also yield greater insights to processes, highlight regions or taxa of greater (or less than) predicted risk, provide additional opportunities for policy impact, as well as improve model calibration.

KEY CHALLENGES AND OPPORTUNITIES

Presently, many current simulations conserve the total number of particles (e.g., there is no loss, as in the adrift framework; van Sebille, 2014). To improve on this, parameterizations of key processes such as sinking and fragmentation rates will be needed. Appropriate data will be required in order to develop these parameterizations. Furthermore, there are data gaps leading to limitations in simulations due to areas with no or poor drifter data. Additionally, many simulations employed include surface drifters only, thereby missing subsurface movement.

One of the first and most significant improvements would be to add a loss term to look at losses in the environment. One large uncertainty is in the rate of suspension/resuspension off/on shore. C*an we establish a reasonable loss term for coastal regions*? If so, what would be required? Adding a loss term would be an improvement and having data from standing stock surveys to look at the *Coast-Ocean-Coast* (C-O-C) suspension and resuspension would be critical.

To address the C-O-C knowledge gap, one way forward would be to have a transfer function from the coast to ocean and back again. Perhaps the best way to incorporate this into existing models is to find locations where there are long term data of coastline litter stocks. However, most coastal debris or clean up data focuses on macro rather than micro debris. Analysing such an empirical data set, coupled with relevant covariates (wind speed, direction, tides, etc.) would be useful. The ideal data set would be a long time series with frequent sampling intervals.

We further suggest that understanding marine micro-plastic movement would benefit from models that incorporate wind, waves, tides, data on rate, or frequency of active biofouling, and the rates of fragmentation and the processes leading to increased or decreased fragmentation (e.g., solar radiation; Isobe et al., 2014). To improve our knowledge modeling efforts would ideally be able to draw on a comprehensive list of datasets. These data sets would be geographically dispersed, long term, and with a high frequency of data collection.

CONCLUSIONS

Our understanding of litter sources, fate and movement is rapidly advancing. This is an exciting time in marine debris research as it is a growing speciality that can adapt, integrate and benefit from learning from other related research areas. While there remain a number of knowledge gaps with respect to marine litter modeling, there are significant advancements that can be, and are being, made in our understanding. Importantly, many of these advancements are being applied to underpin and inform policy and decision making at several scales, and we are seeing an increase in a collaborative approach to addressing the issue. While global plastic production continues unabated, the public's interest in and appetite for engagement through volunteering and citizen science can provide both broad and deep opportunities for data collection, high quality modeling, outreach, and behavioral change.

AUTHOR CONTRIBUTIONS

All authors listed, have made substantial, direct and intellectual contribution to the work, and approved it for publication.

ACKNOWLEDGMENTS

The ideas from this paper stemmed from the 2015 Modeling and Monitoring marine plastic workshops supported by the United Nations Environment Programme and CSIRO's Oceans and Atmosphere through the project 'Global Partnership on

Marine Litter; Out of sight, out of mind? Changing the state of marine litter globally.' We thank Heidi Savelli and Peter Kershaw for their thoughtful comments, insights and contributions. NM was partly supported by the NASA Ocean Surface Topography Science Team and the PICES ADRIFT Project Team; AI was supported by the Environmental Research and Technology Development Fund (4-1502) of the Ministry of the Environment, Japan.

REFERENCES

Barnes, D. K., Galgani, F., Thompson, R. C., and Barlaz, M. (2009). Accumulation and fragmentation of plastic debris in global environments. *Philos. Trans. R. Soc. Lond. B. Biol. Sci.* 364, 1985–1998. doi: 10.1098/rstb.2008.0205

Barnes, D. K., Walters, A., and Gonçalves, L. (2010). Macroplastics at sea around Antarctica. *Mar. Environ. Res.* 70, 250–252. doi: 10.1016/j.marenvres.2010.05.006

Bergmann, M., Sandhop, N., Schewe, I., and D'Hert, D. (2016). Observations of floating anthropogenic litter in the Barents Sea and Fram Strait, Arctic. *Polar Biol.* 39, 553–560. doi: 10.1007/s00300-015-1795-8

Besseling, E., Wegner, A., Foekema, E. M., van den Heuvel-Greve, M. J., and Koelmans, A. A. (2012). Effects of microplastic on fitness and PCB bioaccumulation by the lugworm *Arenicola marina* (L.). *Environ. Sci. Technol.* 47, 593–600. doi: 10.1021/es302763x

Cheshire, A., Adler, E., Barbière, J., Cohen, Y., Evans, S., Jarayabhand, S., et al. (2009). *UNEP/IOC Guidelines on Survey and Monitoring of Marine Litter*.

Cózar, A., Echevarría, F., González-Gordillo, J. I., Irigoien, X., Úbeda, B., Hernández-León, S., et al. (2014). Plastic debris in the open ocean. *Proc. Natl. Acad. Sci. U.S.A.* 111, 10239–10244. doi: 10.1073/pnas.1314705111

Cummings, J. A. (2005). Operational multivariate ocean data assimilation. *Q. J. R. Meteorol. Soc.* 131, 3583–3604.

Derraik, J. G. B. (2002). The pollution of the marine environment by plastic debris: a review. *Mar. Pollut. Bull.* 44, 842–852 doi: 10.1016/S0025-326X(02)00220-5

Dris, R., Gasperi, J., Saad, M., Mirande, C., and Tassin, B. (2016). Synthetic fibers in atmospheric fallout: a source of microplastics in the environment? *Mar. Pollut. Bull.* 104, 290–293. doi: 10.1016/j.marpolbul.2016.01.006

Ebbesmeyer, C. C., and Ingraham, W. J. (1994). Pacific toy spill fuels ocean current pathways research. *EOS* 75, 425–430. doi: 10.1029/94EO01056

Ebbesmeyer, C. C., Ingraham, W. J., Jones, J. A., and Donohue, M. J. (2012). Marine debris from the Oregon *Dungeness crab* fishery recovered in the Northwestern Hawaiian Islands: identification and oceanic drift paths. *Mar. Pollut. Bull.* 65, 69–75. doi: 10.1016/j.marpolbul.2011.09.037

Eriksen, M., Lebreton, L. C., Carson, H. S., Thiel, M., Moore, C. J., Borerro, J. C., et al. (2014). Plastic pollution in the world's oceans: more than 5 trillion plastic pieces weighing over 250,000 tons afloat at sea. *PLoS ONE* 9:e111913. doi: 10.1371/journal.pone.0111913

Fazey, F. M. C., and Ryan, P. G. (2016a). Debris size and buoyancy influence the dispersal distance of stranded litter. *Mar. Pollut. Bull.* 110, 371–377. doi: 10.1016/j.marpolbul.2016.06.039

Fazey, F. M. C., and Ryan, P. G. (2016b). Biofouling on buoyant marine plastics: an experimental study into the effect of size on surface longevity. *Environ. Pollut.* 210, 354–360. doi: 10.1016/j.envpol.2016.01.026

Galgani, F., Hanke, G., Werner, S., and De Vrees, L. (2013). Marine litter within the European marine strategy framework directive. *ICES J. Mar. Sci.* 70, 1055–1064. doi: 10.1093/icesjms/fst122

Gall, S. C., and Thompson, R. C. (2015). The impact of debris on marine life. *Mar. Pollut. Bull.* 92, 170–179. doi: 10.1016/j.marpolbul.2014.12.041

Gerritse, J., Leslie, H., and Vethaak, D. (2015). Fragmentation of plastic litter in the marine environment our plastic-littered seas and how they transition from 'extra chunky' soup to a plastic 'bouillon'. *Coastal and Marine. The CLEANSEA Project: An Interdisciplinary Study of Marine Litter in the EU. The Coastal and Marine Union (EUCC) Vol. 24,* 14. Available online at: http://www.cleansea-project.eu/drupal/sites/default/files/Coastalandmarine.pdf

GESAMP (2016). "Sources, fate and effects of microplastics n the marine environment: part two of a global assessment," in *IMO/FAO/UNESCO-IOC/UNIDO/WMO/IAEA/UN/UNEP/UNDP Joint Group of Experts on the Scientific Aspects of Marine Environmental Protection*, Report Studies GESAMP No 93, eds P. J. Kershaw and C. M. Rochman, 220.

Gigault, J., Pedrono, B., Maxit, B., and Ter Halle, A. (2016). Marine plastic litter: the unanalyzed nano-fraction. *Environ. Sci.* 3, 346–350. doi: 10.1039/c6en00008h

GNOME User's Manual (2002). Available online at: http://response.restoration.noaa.gov/sites/default/files/GNOME_Manual.pdf

Hardesty, B. D., Lawson, T. J., van der Velde, T., Lansdell, M., and Wilcox, C. (2016). Estimating quantities and sources of marine debris at a continental scale. *Front. Ecol. Environ.* 15, 18–25. doi: 10.1002/fee.1447

Hardesty, B. D., and Wilcox, C. (2017). A risk framework for tackling marine debris. *Anal. Methods* 9, 1429–1436. doi: 10.1039/C6AY02934E

Isobe, A., Kubo, K., Tamura, Y., Kako, S., Nakashima, E., and Fujii, N. (2014). Selective transport of microplastics and mesoplastics by drifting in coastal waters. *Mar. Pollut. Bull.* 89, 324–330. doi: 10.1016/j.marpolbul.2014.09.041

Isobe, A., Uchida, K., Tokai, T., and Iwasaki, S. (2015). East Asian seas: a hot spot of pelagic microplastics. *Mar. Pollut. Bull.* 101, 618–623. doi: 10.1016/j.marpolbul.2015.10.042

Ivar do Sul, J. A., Costa, M. F., Silva-Cavalcanti, J. S., and Araújo, M. C. (2014). Plastic debris retention and exportation by a mangrove forest patch. *Mar. Pollut. Bull.* 78, 252–257. doi: 10.1016/j.marpolbul.2013.11.011

Jambeck, J. R., Geyer, R., Wilcox, C., Siegler, T. R., Rerryman, M., Andrady, A., et al. (2015). Plastic waste inputs from land into the ocean. *Science* 347, 768–771. doi: 10.1126/science.1260352

Kako, S., Isobe, A., Magome, S., Hinata, H., Seino, S., and Kozima, A. (2011). Establishment of numerical beach litter hindcast/forecast models: an application to Goto Islands, Japan. *Mar. Pollut. Bull.* 62, 293–302. doi: 10.1016/j.marpolbul.2010.10.011

Kooi, M., Reisser, J., Slat, B., Ferrari, F. F., Schmid, M. S., Cunsolo, S., et al. (2016). The effect of particle properties on the depth profile of buoyant plastics in the ocean. *Sci. Rep.* 6:33882. doi: 10.1038/srep33882

Law, K. L., Morét-Ferguson, S., Maximenko, N. A., Proskurowski, G., Peacock, E. E., Hafner, J., et al. (2010). Plastic accumulation in the North Atlantic subtropical gyre. *Science* 329, 1185–1188. doi: 10.1126/science.1192321

Lebreton, L. C. M., and Borrero, J. C. (2013). Modeling the transport and accumulation floating debris generated by the 11 March 2011 Tohoku tsunami. *Mar. Pollut. Bull.* 66, 53–58. doi: 10.1016/j.marpolbul.2012.11.013

Lebreton, L. C.-M., Greer, S. D., and Borerro, J. C. (2012). Numerical modelling of floating debris in the world's oceans. *Mar. Pollut. Bull.* 64, 653–661. doi: 10.1016/j.marpolbul.2011.10.027

Martinez, E., Maamaatuaiahutapu, K., and Taillandier, V. (2009). Floating marine debris surface drift: convergence and accumulation toward the South Pacific subtropical gyre. *Mar. Pollut. Bull.* 58, 1347–1355. doi: 10.1016/j.marpolbul.2009.04.022

Maximenko, N. A., and Hafner, J. (2010). *SCUD: Surface Currents from Diagnostic Model.* IPRC Tech. Note 5, 17. Available online at: http://apdrc.soest.hawaii.edu/projects/SCUD/SCUD_manual_02_17.pdf

Maximenko, N. A., Hafner, J., and Niiler, P. P. (2012). Pathways of marine debris derived from trajectories of Lagrangian drifters. *Mar. Pollut. Bull.* 65, 51–62. doi: 10.1016/j.marpolbul.2011.04.016

Neumann, D., Callies, U., and Matthies, M. (2014). Marine litter ensemble transport simulations in the southern North Sea. *Mar. Pollut. Bull.* 86, 219–228. doi: 10.1016/j.marpolbul.2014.07.016

Pham, C. K., Ramirez-Llodra, E., Alt, C. H., Amaro, T., Bergmann, M., Canals, M., et al. (2014). Marine litter distribution and density in European seas, from the shelves to deep basins. *PLoS ONE* 9:e95839. doi: 10.1371/journal.pone.0095839

Potemra, J. T. (2012). Numerical modeling with application to tracking marine debris. *Mar. Pollut. Bull.* 65, 42–50. doi: 10.1016/j.marpolbul.2011.06.026

Reisser, J., Shaw, J., Wilcox, C., Hardesty, B. D., Proietti, M., Thums, M., et al. (2013). Marine plastic pollution in waters around Australia: characteristics, concentrations, and pathways. *PLoS ONE* 8:e80466. doi: 10.1371/journal.pone.0080466

Reisser, J., Slat, B., Noble, K., du Plessis, K., Epp, M., Proietti, M., et al. (2015). The vertical distribution of buoyant plastics at sea *Biogeosciences* 12, 1249–1256. doi: 10.5194/bg-12-1249-2015

Ryan, P. G. (2015). Does size and buoyancy affect the long-distance transport of floating debris? *Environ. Res. Lett.* 10:084018. doi: 10.1088/1748-9326/10/8/084019

Schuyler, Q. A., Wilcox, C., Townsend, K. A., Wedemeyer-Strombel, K. R., Balazs, G., van Sebille, E., et al. (2015). Risk analysis reveals global hotspots for marine debris ingestion by sea turtles. *Glob. Change Biol.* 22, 567–576. doi: 10.1111/gcb.13078

Schuyler, Q., Hardesty, B. D., Wilcox, C., and Townsend, K. (2013). A global analysis of anthropogenic debris ingestion by sea turtles. *Conserv. Biol.* 28, 129–139. doi: 10.1111/cobi.12126

Sheavly, S. B., and Register, K. M. (2007). Marine debris & plastics: environmental concerns, sources, impacts and solutions. *J. Polym. Environ.* 15, 301–305. doi: 10.1007/s10924-007-0074-3

Sherman, P., and Van Sebille, E. (2016). Modeling marine surface microplastic transport to assess optimal removal locations. *Environ. Res. Lett.* 11:014006. doi: 10.1088/1748-9326/11/1/014006

Storkey, D., Blockley, E. W., Furner, R., Guiavarc'h, C., Lea, D., Martin, M. J., et al. (2010). Forecasting the ocean state using NEMO: the new FOAM system. *J. Oper. Oceanogr.* 3, 3–15. doi: 10.1080/1755876X.2010.11020109

ter Halle, A., Ladirat, L., Gendre, X., Goudouneche, D., Pusineri, C., Routaboul, C., et al. (2016). Understanding the fragmentation pattern of marine plastic debris. *Environ. Sci. Technol.* 50, 5668–5675. doi: 10.1021/acs.est.6b00594

UN Environment Program (2009) *Marine Litter. A Global Challenge*. Nairobi: UNEP.

van Sebille, E. (2014). Adrift.org.au — a free, quick and easy tool to quantitatively study planktonic surface drift in the global ocean. *J. Exp. Mar. Biol. Ecol.* 461, 317–322. doi: 10.1016/j.jembe.2014.09.002

van Sebille, E., England, M. H., and Froyland, G. (2012). Origin, dynamics and evolution of ocean garbage patches from observed surface drifters. *Environ. Res. Lett.* 7:044040. doi: 10.1088/1748-9326/7/4/044040

van Sebille, E., Wilcox, C., Lebreton, L., Maximenko, N., Hardesty, B. D., Van Franeker, J. A., et al. (2015). A global inventory of small floating plastic debris. *Environ. Res. Lett.* 10:124006. doi: 10.1088/1748-9326/10/12/124006

Wilcox, C., Hardesty, B. D., Sharples, R., Griffin, D. A., Lawson, T. J., and Gunn, R. (2013). Ghostnet impacts on globally threatened turtles, a spatial risk analysis for northern Australia. *Conserv. Lett.* 6, 247–254. doi: 10.1111/conl.12001

Wilcox, C., Mallos, N. J., Leonard, G. H., Rodriguez, A., and Hardesty, B. D. (2016). Using expert elicitation to estimate the impacts of plastic pollution on marine wildlife. *Mar. Policy*, 65, 107–114. doi: 10.1016/j.marpol.2015.10.014

Wilcox, C., Van Sebille, E., and Hardesty, B. D. (2015). Threat of plastic pollution to seabirds is global, pervasive, and increasing. *Proc. Natl. Acad. Sci. U.S.A.* 112, 11899–11904. doi: 10.1073/pnas.1502108112

Woodall, L. C., Sanchez-Vidal, A., Canals, M., Paterson, G. L. J., Coppock, R., Sleight, V., et al. (2014). The deep sea is a major sink for microplastic debris. *R. Soc. Open Sci.* 1:140317. doi: 10.1098/rsos.140317

Conflict of Interest Statement: The authors declare that the research was conducted in the absence of any commercial or financial relationships that could be construed as a potential conflict of interest.

The reviewer OG and handling Editor declared their shared affiliation, and the handling Editor states that the process nevertheless met the standards of a fair and objective review.

frontiers in Environmental Science

ORIGINAL RESEARCH
published: 01 February 2017
doi: 10.3389/fenvs.2017.00005

Lagrangian Transport of Marine Litter in the Mediterranean Sea

Enrico Zambianchi[1,2]*, *Marilisa Trani*[1] and *Pierpaolo Falco*[1]

[1] Dipartimento di Scienze e Tecnologie, Università degli Studi di Napoli "Parthenope", CoNISMa, Naples, Italy, [2] Istituto di Scienze dell'Atmosfera e del Clima, CNR, UOS Roma, Rome, Italy

Concern about marine litter has been rising in the last decades, triggered by the discovery of the great mid-ocean garbage patches. The Mediterranean Sea is strongly affected by the presence of floating litter, as it has a very high amount of waste generated annually per person that eventually ends up in its waters, with plastic objects accounting for a large percentage of all manmade debris. In principle, the basin looks very vulnerable to possible accumulation of floating debris, since its dynamics is characterized by an inward surface flow of water from the Atlantic hampering surface floating items from being flushed out. Yet, no evidence of permanent litter accumulation areas has been reported so far in the Mediterranean. In this paper we utilized the largest available set of historical Lagrangian data gathered in the Mediterranean Sea to estimate the probability of debris particles to reach different subareas of the basin, with the main objective of singling out possible retention areas. Climatological reconstructions of the time evolution of litter distribution in the basin carried out on the basis of observed Lagrangian displacements suggest a general tendency of floating matter to collect in the southern portion of the basin, and in particular a long term accumulation in the southern and southeastern Levantine basin, areas not yet sampled by marine litter observation campaigns, whose targeted organization we strongly recommend at the end of this paper.

Keywords: near-surface drifters, plastics, marine pollution, Mediterranean, circulation, marine litter, floating debris, garbage patch

OPEN ACCESS

Edited by:
Francois Galgani, French Research Institute for Exploitation of the Sea, France

Reviewed by:
Erik Van Sebille, Imperial College London, UK
Laurent Lebreton, The Modelling House, New Zealand

***Correspondence:**
Enrico Zambianchi
enrico.zambianchi@uniparthenope.it

Specialty section:
This article was submitted to Marine Pollution, a section of the journal Frontiers in Environmental Science

Received: *28 October 2016*
Accepted: *16 January 2017*
Published: *01 February 2017*

Citation:
Zambianchi E, Trani M and Falco P (2017) Lagrangian Transport of Marine Litter in the Mediterranean Sea. Front. Environ. Sci. 5:5. doi: 10.3389/fenvs.2017.00005

INTRODUCTION

Marine litter in the Mediterranean Sea, which only recently became the object of extensive studies, is a very sensitive issue from several standpoints (ecological, social, and economic, see Galgani et al., 2014). Concern about marine litter has been rising in the last decades, triggered by the studies on the great mid-ocean garbage patches (Moore et al., 2001; Law et al., 2010; Lebreton et al., 2012; Maximenko et al., 2012; van Sebille et al., 2012; Eriksen et al., 2014; Cózar et al., 2015; van Sebille et al., 2015).

The current state of knowledge of this issue, with a particular focus on the Mediterranean Sea, was assessed in a dedicated workshop in June 2014 organized by the Mediterranean Science Commission (or CIESM, i.e., Commission Internationale pour l'Exploration Scientifique de la Méditerranée), resuming previous knowledge and encouraging new studies. The aspects treated in the workshop were sources, composition and abundance of litter and its degradation and transformation, particle transport by marine circulation, impacts on marine life and legal instruments (CIESM, 2014).

The Mediterranean region is one of the world areas characterized by the highest amount of man-generated solid waste (Galgani et al., 2014). In particular, the Mediterranean Sea is vulnerable to plastics (van Sebille et al., 2015): while they typically do not constitute a high percentage of discarded waste, they are the most important part of marine litter, constituting over 80% of floating items (Galgani, 2014; Suaria and Aliani, 2014). This particular pollutant is ubiquitous—due to its extensive worldwide use—and extremely persistent, degrading slowly into tiny pieces (Barnes et al., 2009). It can travel very far from its sources, because time scales of degradation and transformation of plastics are much longer than the scales of transport (Barnes et al., 2009; Andrady, 2011). It harms marine species and ecosystems: threating biodiversity, favoring the spreading of invasive alien species and entering the food chain—through which it is transferred to larger predators including humans (Deudero and Alomar, 2015). Attempts to quantify plastic debris in the Mediterranean date back to 1980, when a quantitative visual survey reported around 1300 plastic items per square kilometer in a central region of the basin (Morris, 1980).

The Mediterranean Sea (**Figure 1**) is not only surrounded by a massively waste-generating coastal zone and inland, subject to a heavy anthropic, urban, and industrial pressure; the structure of its circulation, as well as its being embedded in the global ocean conveyor belt, may promote retention of floating material inside the basin. The Mediterranean circulation (Malanotte-Rizzoli et al, 1999; Robinson et al., 2001) is characterized by an inward surface flow of waters from the Atlantic Ocean, with no significant outward flow anywhere along its coastline; the return flow into the Atlantic happens at the subsurface, thus hampering surface floating items from being expelled from the basin and destinating them to accumulating within it. At the global ocean level, the Mediterranean's possible sink role for floating particles of global origin was shown by Lebreton et al. (2012), who used a global numerical model simulating 30 years of input, transport, and accumulation of debris in the world ocean; their estimate is that the Mediterranean potentially retained between 6 and 8% of all particles introduced into the model, thus achieving one of the highest concentrations of marine litter in the world ocean. Yet, no evidence of permanent litter accumulation areas ("garbage patches") has been reported so far in the Mediterranean, as discussed by Cózar et al. (2015; see Section Conclusions on this point).

Zambianchi et al. (2014) provided a review of previous studies on transport and dispersion of debris due to marine circulation, the main methods used as well as findings at large and regional scales and in the Mediterranean Sea. Transport of particles in the ocean is generally investigated making use of Lagrangian particle models that describe the flow as formed by two components: a large scale adjective mean field and a smaller scale irregular field. Numerical models or velocity data from drifters draw the former component with high confidence, while the latter is much more complicated to investigate and quantify, and thus typically parameterized in various ways (e.g., Zambianchi and Griffa, 1994; Haza et al., 2012). Previous works employed numerical models to simulate both ocean circulation and the spread of particles

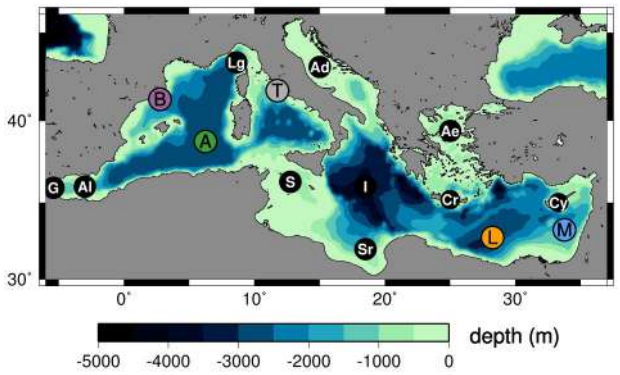

FIGURE 1 | Bathymetric map of the Mediterranean. Black circles correspond to key places (subbasins, straits, islands) explicitely mentioned in the paper (Ad, Adriatic Sea; Ae, Aegean Sea; Al, Alboran Sea; I, Ionian Sea; Lg, Ligurian Sea; Sr, Gulf of Sirte; G, Strait of Gibraltar; S, Sicily Strait; Cr, Crete Island; Cy, Cyprus Island). Colored circles indicate key places mentioned in the paper and specific locations sampled to build time evolution of local tracer concentration, as shown in **Figure 12** (A, Algerian Basin; B, Balearic Sea; L, Levantine Basin; M, Middle Eastern coast; T, Tyrrhenian Sea). Bathymetry is based on the ETOPO5 5-min gridded elevation data (Edwards, 1989) provided in the Generic Mapping Tools package (Wessel et al., 2013). For a map of the main features of the Mediterranean surface circulation we refer readers to Figure 12 of the paper by Poulain et al. (2012).

(Lebreton et al., 2012; Mansui et al., 2015), or statistical methods that use observed surface drifter trajectories as input to spread particles forward in time (Maximenko et al., 2012; van Sebille et al., 2012), which is the approach we also selected.

Regional studies on litter transport are very few compared to large scale ones; they are limited to the East Asian marginal seas and the ocean surrounding Hawaiian Islands (among the most recent, respectively, Carson et al., 2013; Kako et al., 2014). In the Mediterranean, several studies investigated the abundance of debris (see again CIESM, 2014, for comprehensive reviews), while studies on its transport are scarce. Aliani et al. (2003) and Ramirez-Llodra et al. (2013) gave hints about the possible transport mechanisms that could have led to the observed debris density, i.e., remote and local three dimensional oceanographic conditions. More recently, Mansui et al. (2015) used numerical models and simulations of particle spreading, identifying possible retention areas in the Mediterranean.

In the present paper, along the lines drawn by Maximenko et al. (2012) for the global ocean, we utilized the largest available set of historical Lagrangian data gathered in the Mediterranean Sea to estimate the probability of floating litter to reach different subareas of the basin, with the main objective of pointing out possible retention areas. As will be seen, our results suggest marine debris accumulation in the southern and southeastern Levantine basin. However, it should be noted that our study is fairly idealized, and that in reality the plastic distribution might be modulated by the basin inter- and intraseasonal variability which we do not resolve.

The method is illustrated in Section Lagrangian Data Analysis, while results are presented in Section Results and Discussion, along with their comparison with direct litter observations

in the basin. Conclusions and recommendations for future investigations follow in Section Conclusions.

LAGRANGIAN DATA ANALYSIS

Preliminary Data Treatment

The data utilized in this work come from the Mediterranean Drifter Data Base, which gathers virtually all near-surface drifters deployed in the Mediterranean in the last 30 years in the framework of the most diverse experiments (e.g., Poulain et al., 2012). We used drifter data spanning from 1987 to 2014 for a total of 1429 drifters. Drifters are of three types, listed here from the more to the less abundant: Surface Velocity Program (SVP), Coastal Ocean Dynamics Experiment (CODE), and Compact Meteorological and Oceanographic Drifters (CMOD).

SVP drifters are equipped with a holey-sock drogue centered at a 15 m depth (Lumpkin and Pazos, 2007). CODE and CODE-modified drifters are 70 cm to 1 m long plastic or aluminum cylinders with four perpendicular sails, whose vertical alignment is provided by four small floaters (Davis, 1985; for their water following characteristics see, e.g., Pisano et al., 2016 and references therein). CMOD drifters are 60 cm long aluminum tubes with a 35 cm-diameter buoyancy collar, drogued with a tether of variable length (4–100 m, the latter case being much more frequent, Selsor, 1993).

These three types of drifters have different water-following capabilities, the CMOD being more affected by windage as well as SVP drifters that happen to lose their drogue (Pazan, 1996). Such a variety of drifter designs could facilitate, in principle, the simulation of different kinds of debris dragged by winds and currents in various ways. However, the relative paucity of the available data did not allow us to distinguish among different kinds of behavior in a statistically reliable way, and for this reason we used all data together, as a bulk of undifferentiated items.

The Mediterranean drifter data are processed and archived by the Istituto Nazionale di Oceanografia e di Geofisica Sperimentale in Trieste, Italy, and are accessible through the MedSVP website (http://nettuno.ogs.trieste.it/sire/medsvp). They were filtered to remove high frequencies; positions and velocities are subsampled every 6 h (see Poulain et al., 2012, for further details about dataset and data treatment).

As to the temporal and spatial distributions of the data, drifter days were <500 before 1990, nearly 2000 from 1990 to 1995, and doubled on average thereafter (not considering the years 2000, 2001, and 2014 when they were again <500). **Figure 2A** shows the 6-hourly data density within the basin. The maximum concentration of drifters is in the Adriatic Sea and in the northern areas of the western basin. Other regions of high data density are the central Tyrrhenian Sea, the Sicily Strait, the Aegean Sea, and the sea area south of Cyprus. **Figure 2B** reports a histogram of the drifter lifetime in the Mediterranean; the average lifetime is 72 days. **Figure 2C** shows the time evolution of drifter lifetime averaged over five-year periods. Besides intrinsic failures, the main reasons why drifters "died" (Lumpkin et al., 2012) are stranding and being picked up by fishing boats; however, on the basis of the limited average lifetime shown by earlier drifters, after the turn of the millennium several investigators started to limit

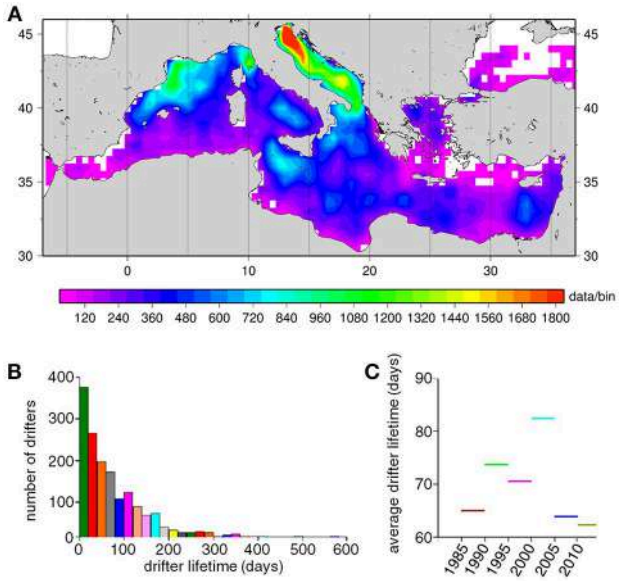

FIGURE 2 | Six hourly data density for the whole drifter dataset (A); histogram of drifter lifetime (B); drifter lifetime averaged over 5-year periods (C).

the programmed transmission time to around 90 days, in order to avoid wasteful expenditures in case of instruments being trapped on land.

Data are not sufficient to look at inter-annual variability, but they allow the study of seasonal variations. A first step to study seasonality has been to consider four seasons of the same duration: autumn (October–December), winter (January–March), spring (April–June), and summer (July–September). The total amount of data in each season is approximately the same; however, data density in the eastern basin is very low in summer, with <30 observations in ½° longitude by ½° latitude subregions for the most part of the area, while in the western basin it is lower during winter, especially in the Alboran, Algerian, and Tyrrhenian Sea. As a consequence, a winter and a summer season of 6 months each were considered a better choice to ensure statistical significance of the results. In previous studies of the Mediterranean Sea circulation using drifter data two extended seasons were also considered, choosing two opposite periods so as to maximize the differences between the resulting fields (Poulain and Zambianchi, 2007; Rinaldi et al., 2010; Poulain et al., 2012). In particular, the choice of the starting and ending times of the seasons was here optimized considering two different configurations: one with an extended summer starting in May and ending in October and another one starting in June and ending in November. In both cases differences between extended winter and summer spatial distributions of drifter density for each configuration are larger than between the two configurations of the same season (**Figures 3A–D**). This implies that the choice of the starting and ending time of the two seasons will likely not have a large impact on subsequent analysis in terms of statistical significance. The mean velocity

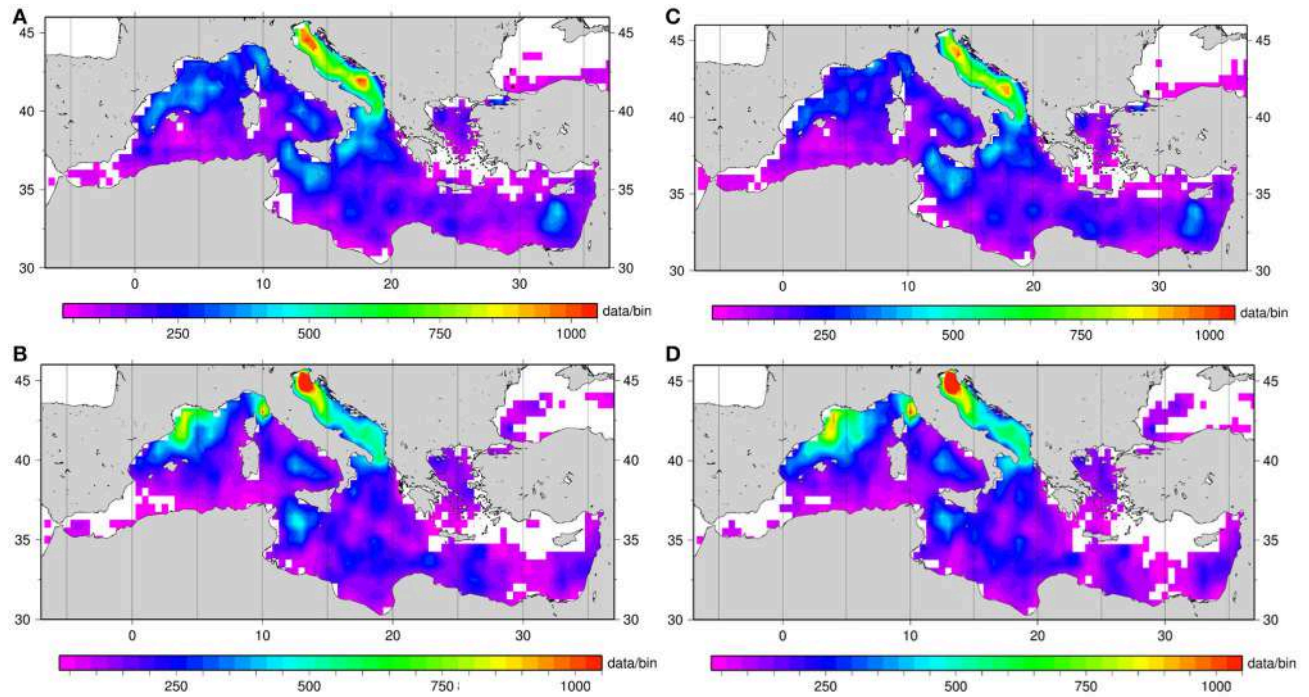

FIGURE 3 | Data density for extended winter (A) and summer (B) defined from October to March and from April to September; for extended winter (C) and summer (D) defined from November to April and from May to October.

field and the eddy kinetic energy (EKE) pattern obtained using the two configurations are also almost identical; however, the total amount of data per season is more evenly distributed using the second configuration and therefore only those obtained using the second configuration (i.e., with an extended summer between June and November and an extended winter between December and May) are presented in this paper.

The description of the near-surface circulation in the Mediterranean as derived from the drifter data was carried out using the so-called pseudoeulerian description (e.g., Falco and Zambianchi, 2011): the basin was sudivided into ½° longitude by ½° latitude subregions (bins) and the flow field was described in terms of velocity averages and residuals computed on all drifter passes within each individual bin (on more sophisticated ways to build such statistics see Lumpkin, 2003; Lumpkin and Garraffo, 2005; Peng et al., 2015; Lumpkin et al., 2017, and references therein). The bin size was chosen so as to be able to effectively separate the mean circulation from its variable portion while retaining a sufficient number of data points in each bin, thus ensuring a statistical significance of the results.

In particular, for each bin we estimated the mean flow, defined as the average velocity vector, the kinetic energy of the mean flow per unit mass (mean kinetic energy, or MKE), the mean kinetic energy of the velocity residuals per unit mass (eddy kinetic energy, or EKE). For a formal definition of these statistical quantities see Trani et al. (2014). They are displayed in **Figure 4** for the whole data set, and in **Figures 5**, **6** for the two extended seasons.

Methodology Used to Study Transport

In this study, we implemented a method proposed by Maximenko et al. (2012) to investigate litter transport on the basis of the Mediterranean drifter dataset. Starting from a prescribed initial distribution, this method reconstructs the evolution of the density of a passive tracer representing an adimensional proxy for floating litter (indicated as FLP, i.e., floating litter proxy, from now on), using a probability density function obtained from the drifter trajectories.

The process consists of two phases: first, the existing drifter data are utilized to estimate the probability for them to move between two bins in a fixed time; then the probability is used to estimate the evolution of litter over the basin in the same fixed time.

In particular, the number of times that a drifter moves from one bin to another within a determined time span (hereafter defined "travel time"), once normalized over all switches, is assumed to represent the probability for a drifter to move between the two bins. This allows to build a probability density function of particle displacement over different travel times.

For simplicity, the calculation of the probability for a drifter to move between two points in a fixed time assumes drifter spreading as a statistically stationary process, so that probability depends only on travel time and not on the start time.

In practical terms, we gridded the domain spanned by the 1429 drifter trajectories into ½° latitude by ½° longitude bins. Then we used all pairs of 6-hourly locations along the same

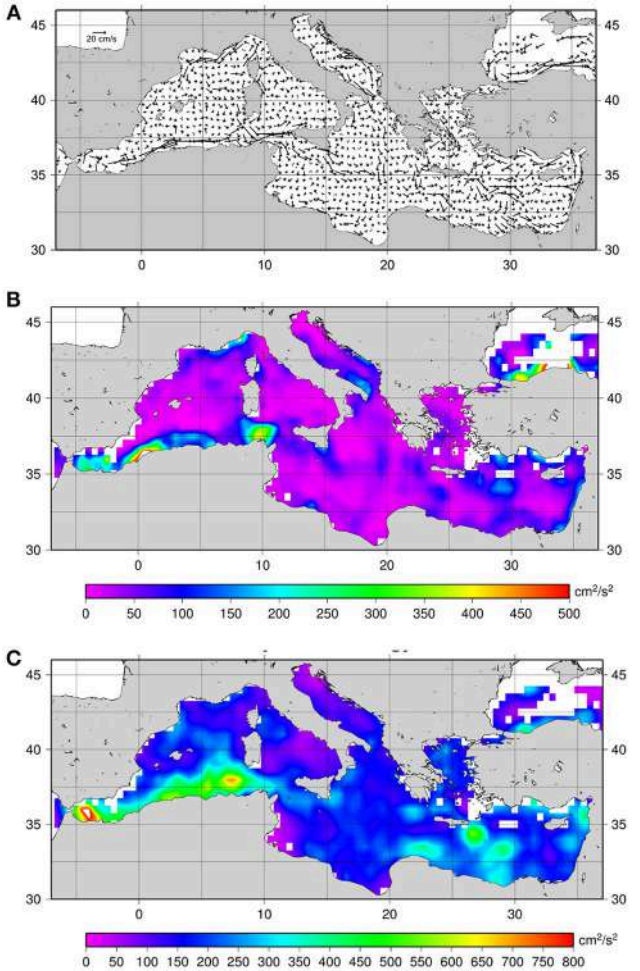

FIGURE 4 | Pseudoeulerian climatological fields of mean velocity (A), MKE (B), and EKE (C) obtained from the drifter data set.

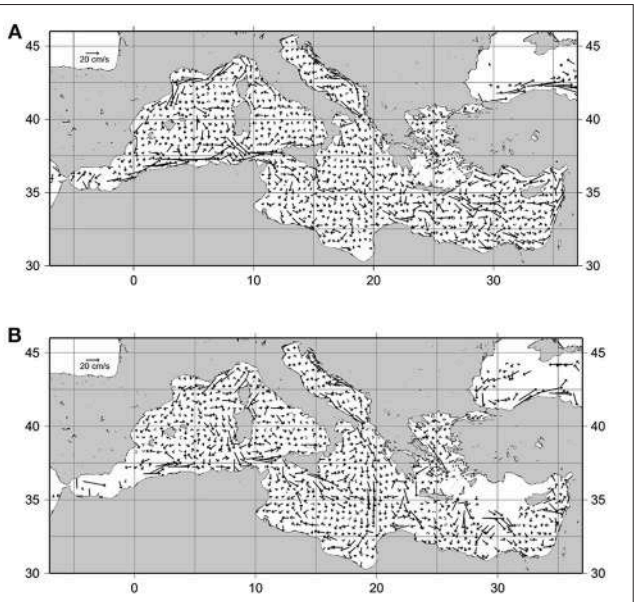

FIGURE 5 | Pseudoeulerian mean velocity fields for extended winter (A) and extended summer (B).

trajectory separated by the chosen travel time to compute the probability for a drifter to move between bin pairs. We tested five different travel times: 3 days, that is the typical Mediterranean Lagrangian time scale (Garcia-Olivares et al., 2007); 5 days, the time used by Maximenko et al. (2012); and 2, 4, and 6 days were also tested. Travel time has to be slightly higher than the Lagrangian time scale, but close to the time taken by a drifter to travel a distance close to the bin size (this is to limit cases of a "false" zero probability in bins that drifters cross without reaching them at exactly the travel time). The travel time values were tested counting the bins with a non-zero probability: results proved that 4 days was the best choice, with a number of non-zero bins very close to that obtained with 3 days where the maximum number is achieved.

It is worth underlining that, as explained by Maximenko et al. (2012, Appendix A), the qualitative outcome of our reconstruction in terms of FLP distribution in correspondence of its maxima is not crucially affected by the initial one, but is mainly due by the local flow regime at different scales.

The probability distribution obtained from the drifter trajectories was then used to initialize a procedure that iteratively computes a reconstructed evolution of FLP density in each bin over 4 days: it sums up in each arrival bin the densities of the starting bins at the previous time multiplied by the relative probabilities of reaching that bin in 4 days (see again Maximenko et al., 2012; Equation 2). Bins where at least one drifter ends and from which no drifters exit are considered as sinks. Thus we obtained an estimated FLP density in each bin every 4 days; these multiples of the 4-day travel times were chosen on basis of the characteristics of the Mediterranean Sea circulation and eddy structures (e.g., Rio et al., 2007; Poulain et al., 2013). Here we show the resulting distributions at different nominal target times, namely after a week, a month, 3 months, 1, 3, and 10 years (since target times have to be multiples of the 4-day travel time, the exact target times are 8, 28, 100, 364, 1096, 3648 days).

Two input scenarios have been considered, with two different initial distributions. Initial conditions were: a homogeneous distribution of FLP density = 1 per bin (the homogeneous initial distribution is indicated as HID from now on), and a distribution localized along the coasts based on the amount of coastal population (coastal initial distribution, or CID), the latter choice being motivated by the fact that main sources of litter in the basin are land-based (Galgani, 2014). Data of coastal population along the Mediterranean coasts have been extracted from the dataset provided by NCEAS Ocean Health Index project (Halpern et al., 2008). Raw data were provided in the Mollweide WGS84 symmetric projection therefore they were reprojected to longitude and latitude in the WGS84. Subsequently, all values in bins of size ½° latitude by ½° longitude were summed together and normalized to express each value in a bin as a fraction of the total.

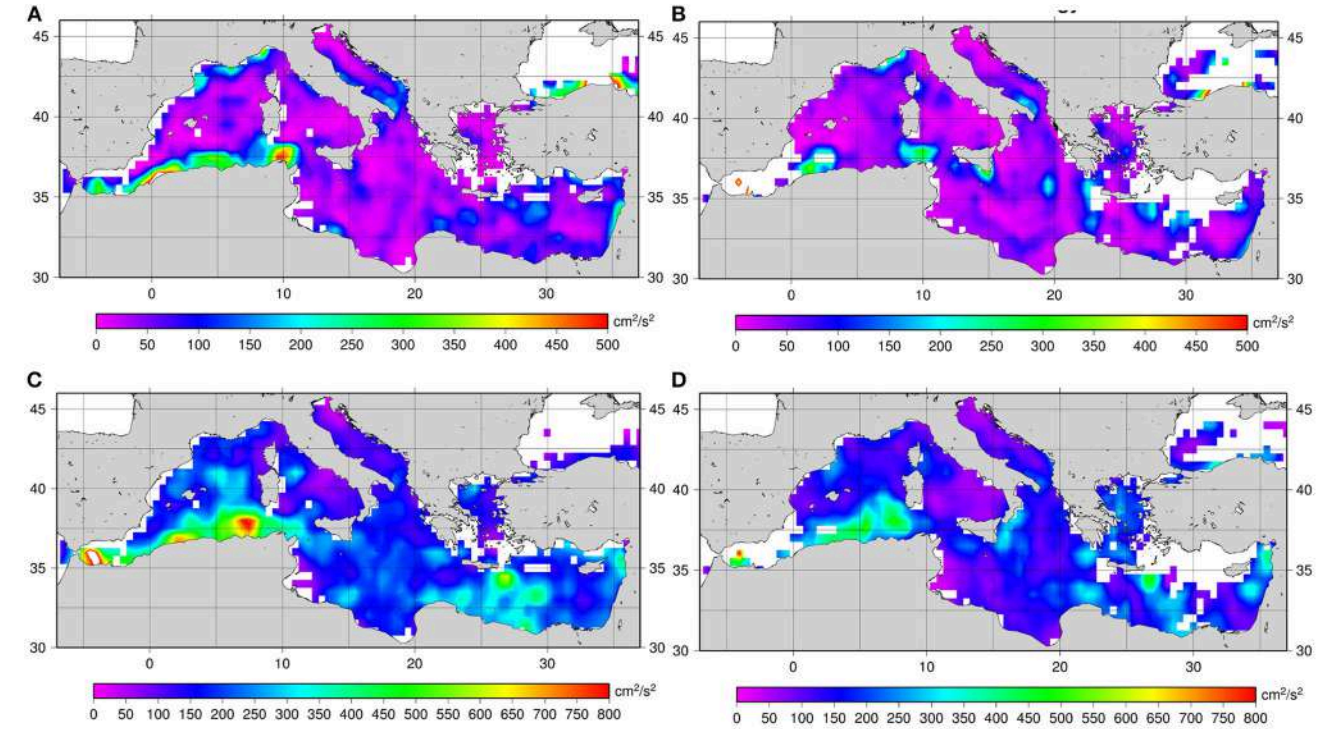

FIGURE 6 | Pseudoeulerian kinetic energies: extended winter MKE (A) and EKE (B); extended summer MKE (C) and EKE (D).

The total (non-dimensional) density of our FLP in the HID case was 1174, corresponding to the number of bins populated by the drifters utilized to build the probability matrix; in the CID case it was 1556, i.e., as close as the original drifter number as allowed by the constraint of following the coastal population. These values are given here for the sake of completeness, but we want to reiterate that our FLP density is an adimensional quantity, thus they do not have to be misinterpreted as the number of litter items floating in the basin, which is orders of magnitude larger (see references in the Introduction).

The probability distributions and the resulting FLP displacement reconstructions were obtained using the whole drifter dataset—hereafter called climatological pattern—and the seasonal, i.e., the extended summer and winter, data.

Our ultimate goal in this paper is to identify possible areas of litter accumulation. Different definitions of such a process are available in the literature, typically related with tracer particle Lagrangian displacement described as a stochastic process, and spanning through quite different dispersion scenarios: e.g., particle trapping in porous media (e.g., Koch and Brady, 1985), in convective cells (e.g., Guyon et al., 1987), in anomalous diffusion situations (Young, 1988). In oceanographic flows, particle retention has been assessed with tools derived from dynamical systems theory (e.g., Castiglione et al., 1999; Cencini et al., 1999); the attractive properties of Lagrangian coherent structures may play an important trapping role (Peacock and Haller, 2013; for a Mediterranean application see Rossi et al., 2014). Froyland et al. (2014) quantitatively assessed the location and effectiveness of particle attraction areas in the world ocean on the basis of synthetic Lagrangian trajectories interpreted in a Markovian approximation. Here we will limit ourselves to the most straightforward accumulation definition, i.e., a medium- and/or long-term local increase of FLP density (see also below, Section Lagrangian Transport Reconstruction).

RESULTS AND DISCUSSION

Traits of the Mediterranean Near-Surface Circulation Reconstructed by the Drifter Data

Figure 4A shows the pseudoeulerian mean velocity derived from the drifter data, averaged over the whole period (climatological). The binned current field displays the main, well-known currents, and semi-permanent eddy structures, consistently with the biased pseudoeulerian statistics by Poulain et al. (2012), who used a subset of the same drifter dataset, limited to 2010 data. Our analysis clearly shows the surface, eastward branch of the Mediterranean circulation (Malanotte-Rizzoli et al, 1999; Robinson et al., 2001), taking Modified Atlantic Water from the Strait of Gibraltar all the way to the Middle East Mediterranean coasts. The most evident feature is the swift current represented by the subsequence of the Algerian Current, of the Atlantic Ionian Stream, of the articulated and variable Mid-Ionian Jet and of the Mid-Mediterranean Jet, from which a number of side branches depart: the cyclonic circulations in

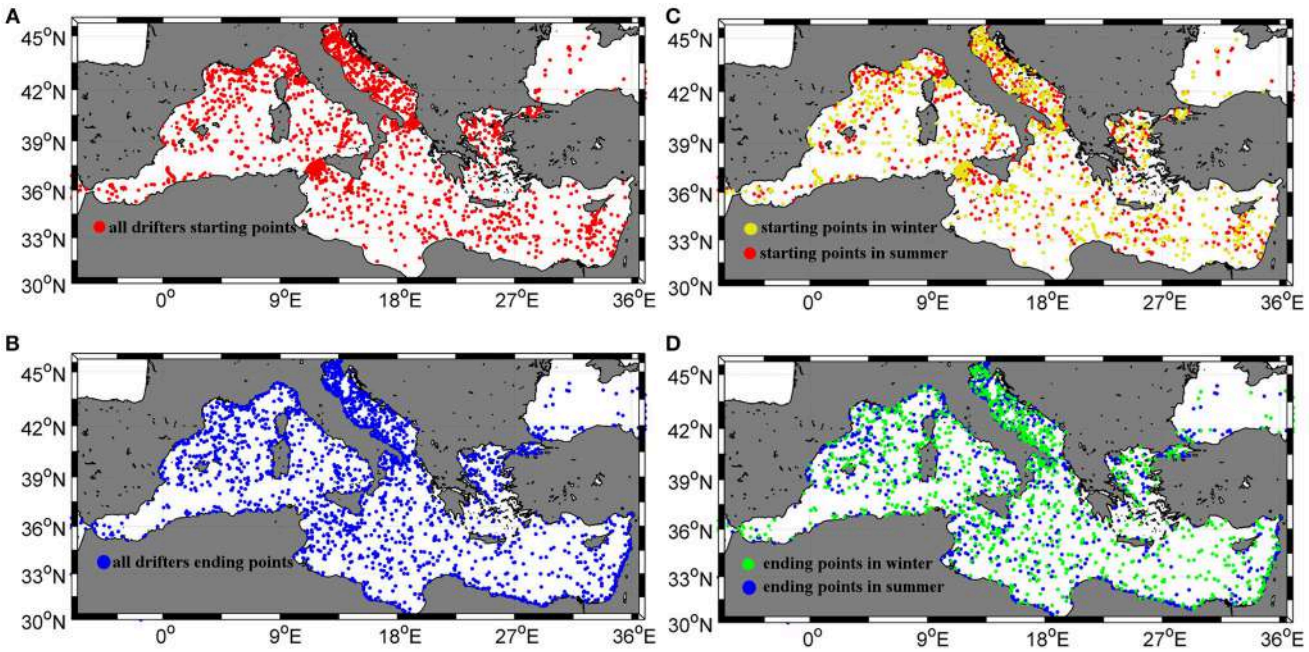

FIGURE 7 | Starting (A) and ending (B) points of all drifters; starting points of winter trajectories (light brown dots) and of summer trajectories (red dots, C); ending points of winter trajectories (green dots) and summer trajectories (blue dots, D).

the Algero-Provencal basin and in the Tyrrhenian Sea, which merge in the Northern Current, flowing in the Ligurian Sea and along the northern coasts of the Western Mediterranean; a series of alternating anticyclonic and cyclonic eddies from the south of the Peloponnese to the southeast of Crete and all the way to the middle eastern Mediterranean coasts; a system of strong coastal currents flowing cyclonically along the coasts of Egypt, Israel, Lebanon, Syria, and Turkey. The predominant mean flow is shown in the map of near-surface MKE drawn from the drifter data, where the inflow of Atlantic waters through the Alboran Sea and its first circulation branch along the Algerian coasts (Algerian Current) reaching the central Mediterranean is particularly evident, as its MKE-values are much higher than for the rest of the basin interior circulation (**Figure 4B**). The distribution of the EKE suggests that the Mediterranean circulation is strongly affected by variability, as EKE maxima faithfully retrace the main near-surface branch of the Mediterranean circulation, from the Strait of Gibraltar eastwards, clearly mirroring the Algerian Current, the Atlantic Ionian Stream, the Mid Ionian Jet, while in the Levantine basin the variability is strongly prevalent in correspondence of the major, persistent, well documented recirculations such as the Ierapetra, Rhodes, Mersa-Matruh gyres, and the Shikmona eddy (**Figure 4C**).

Winter and summer velocity fields and the relative MKE and EKE patterns showed differences in some areas that are worth considering (**Figures 5**, **6**). During winter, the eddy structures are more energetic than in summer, the two branches of the mid-Ionian current are weaker and the Algerian current is stronger. Poulain et al. (2012) noticed a scarce seasonal variability among the whole basin, with the exception of the Sicily Strait and the outflow toward the Levantine basin; however, it must be considered that they only refer to the geostrophic portion of the near-surface circulation. Poulain and Zambianchi (2007) also found a strong seasonal variability of the circulation in the Sicily Strait, furthermore stressing the crucial role of local wind forcing. Since the purpose of this work is to study transport of objects at the surface, the role of the wind-driven part of the currents and of its variability is extremely important, thus seasonality is expected to play some role, at least in the transient behavior.

Lagrangian Transport Reconstruction

Seasonal Transport Patterns

Before using drifter trajectories to study transport and dispersion properties of the mean and eddy current fields briefly described in the former section, maps of the starting and ending points of trajectories were produced, and are shown in **Figure 7**; they clearly suggested that the effect of the near-surface velocity field was stronger than that of the drifter initial deployment distribution, and moreover gave indications of a noticeable seasonal behavior. The majority of drifters were deployed in the northern sub-basins and in the Sicily Strait. The tendency of trajectories is to end along the coasts, but there is also a higher collection in the Ionian Sea and Balearic Sea with respect to the number of releases, while very few drifters end at the Cretan Passage and in the Levantine basin center despite the relatively high number of releases.

The comparison of the seasonal maps of starting and ending points confirmed the appropriateness of the choice of using

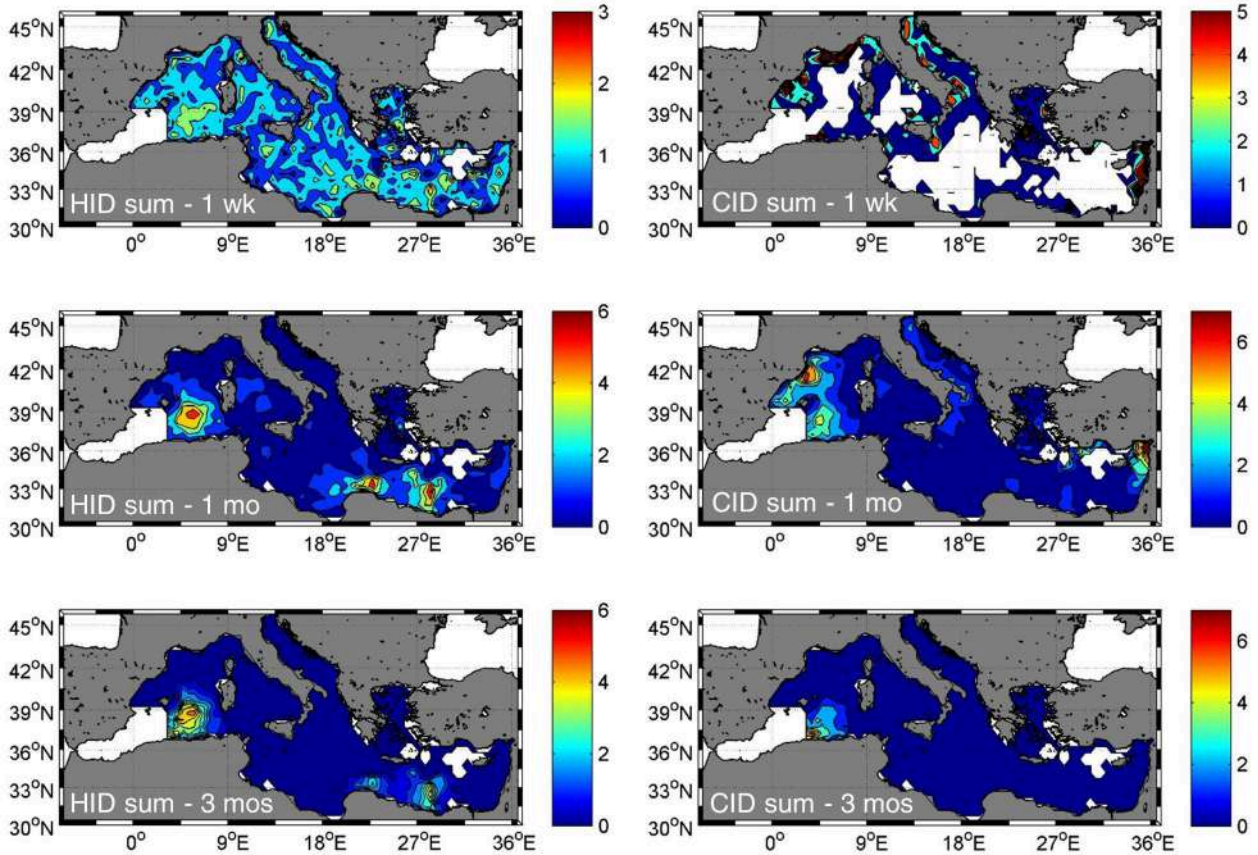

FIGURE 8 | FLP density distribution for the homogeneous initial distribution (HID, left panels) and the coastal population initial distribution (CID, right panels) at different target times in the extended summer season.

two seasons of 6 months rather than four. Maps obtained for the four seasons showed two, rather than four, different distributions of ending points despite the release locations were similar in all seasons (data not shown). Ending points were quite homogeneously distributed in all the Mediterranean in autumn and winter, while they crowded the coasts in spring and summer. No significant differences were observed between autumn and winter nor between spring and summer distributions.

Even though the deployment point distribution was similar in both extended seasons, the pattern of ending points resulted quite different. As can be seen, in the eastern Mediterranean, and in particular in the Levantine basin, the distribution of ending points during summer was markedly different from winter ones. Namely, a higher tendency of drifters to group toward the coast in summer was evident. In the western basin, such difference was less clear, though some regions showed a similar behavior, namely the Ligurian and the Balearic Sea. On the contrary, in winter the distribution of ending points was sensibly more homogeneous throughout the entire Mediterranean. Such an important seasonal character was also displayed by the transport reconstruction results.

This is confirmed by a first glance at the evolution of reconstructed FLP density after the three target times of 1 week, 1 month, and 3 months, shown in **Figures 8**, **9**. On both figures left panels refer to results obtained with the HID, right panels with the CID.

The subsequent FLP distributions for those target times resulted quite different from one another, showing a strong transient character of accumulation zones in the initial period. A combination of some of these characteristics was also found in the climatological reconstructions, as will be discussed in the next section.

In the summer reconstructions, maxima of FLP density were located in the Algerian basin and off the Libyan and Egyptian coasts for the HID case, while in the CID case they were confined very close to the coast, with a maximum transiting cyclonically in the Western Mediterranean and another maximum briefly appearing in the northeastern corner of the Levantine basin. The winter situation for the HID was similar to the summer one, while the CID case was characterized by an accumulation in the Gulf of Sirte, which also appears in the HID case at 3 months, and persists for both initial conditions at least up to 1 year (not shown: for the seasonal cases obviously one-year long reconstructions are not meaningful).

In these short-term seasonal reconstructions the initial condition is clearly bound to play an important role; this is why

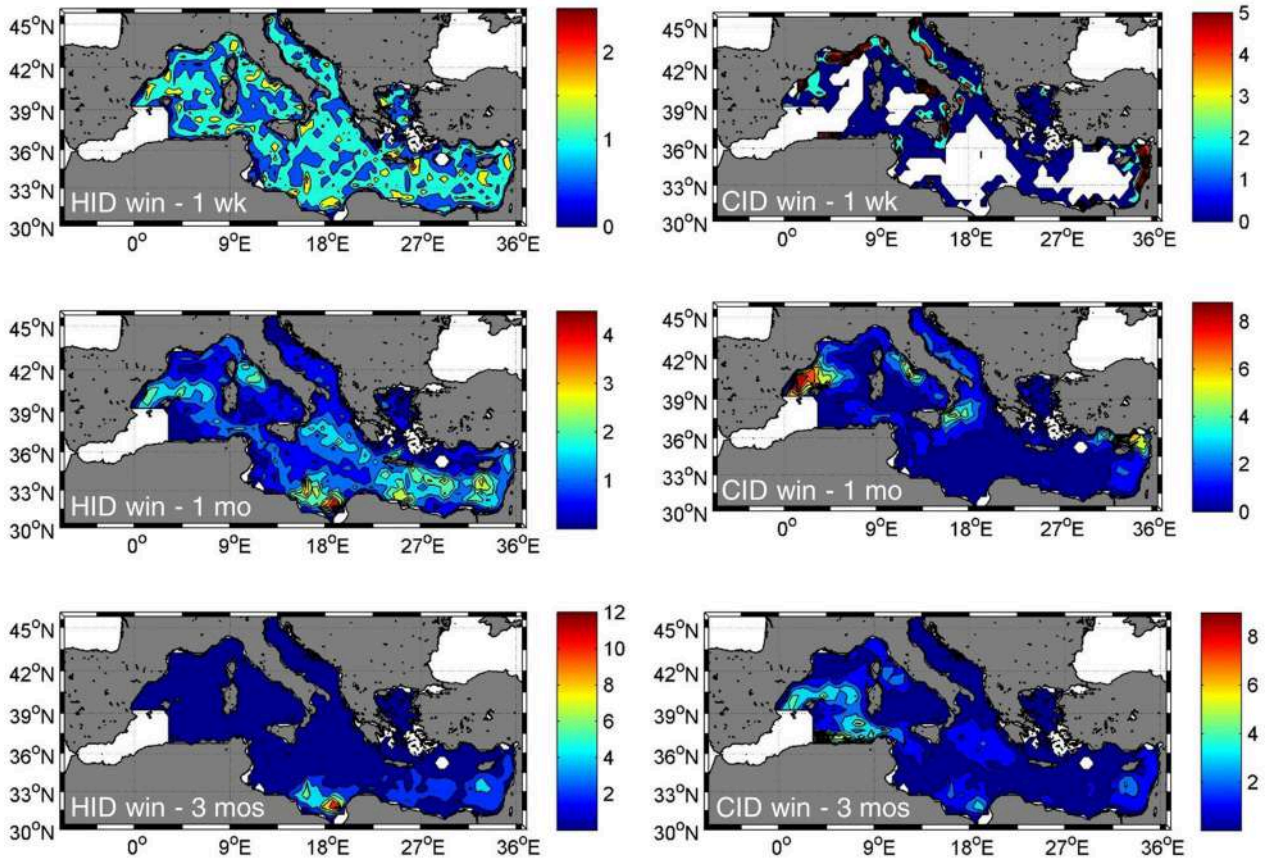

FIGURE 9 | Same as in Figure 8 for the extended winter season.

both CID reconstructions return similar results. On the other hand, the HID accumulation in the Gulf of Sirte in winter and off the Algerian coasts in summer can be interpreted looking at the mean current and EKE fields. In winter, strong currents and high EKE along the Algerian coast can contrast accumulation; in summer, currents are weak even though the EKE maintains a certain intensity. In the Gulf of Sirte, the surface current enters from the north in the summer and proceeds westward along the Libyan coast, preventing retention of FLP there; in winter the current from the north is weak, an eastward current along the Libyan coast enters the gulf and, in addition, the EKE is very low, causing retention of FLP.

Asymptotic Accumulation Patterns

Figures 10, **11** show results obtained with the climatological pattern for the two initial conditions: **Figure 10** displays the evolution from the HID and **Figure 11** the evolution from the CID at target times of a week, a month, 3 months, 1, 3, and 10 years. Just like in the seasonal case, the color scale indicates the FLP density. The same color range is used in all snapshots, stretched so as to cover the different intervals of FLP densities spanned at different target times. The changing maxima provide an indication of the increasing FLP density in the accumulation regions, further illustrated in **Figure 12**.

This allowed us to describe the transient initial displacement (up to 3 months) and the subsequent, asymptotic FLP behavior. The initial behavior is different in the two cases (as it was also in the seasonal cases, see above): while HID FLP by definition populated the interior of the Mediterranean right after deployment, the CID FLP distribution after 7 days still showed large gaps; after a month, the HID case showed a relatively widespread FLP aggregation pattern, with maxima in the Algerian basin, in the northern Tyrrhenian Sea and, more importantly, in the southern Ionian and Levantine basin. The two former relative maxima faded in the turn of another 2 months, showing a weak increase of the FLP density with respect to the background, while the maximum in the Levantine basin was at this point well defined, off the eastern Libyan and western Egyptian coasts. In the CID case, the FLP distribution after 1 month was still affected by specific source locations, combined with the current field: this was the case of the westernmost portion of the western Mediterranean subbasin and of the easternmost part of the Levantine basin; after 3 months a maximum in the Algerian basin was still present, while another, weak relative maximum off the Lybian/Egyptian coasts started to appear.

One year after deployments, both HID and CID FLP distributions showed a similar behavior, which proved to be

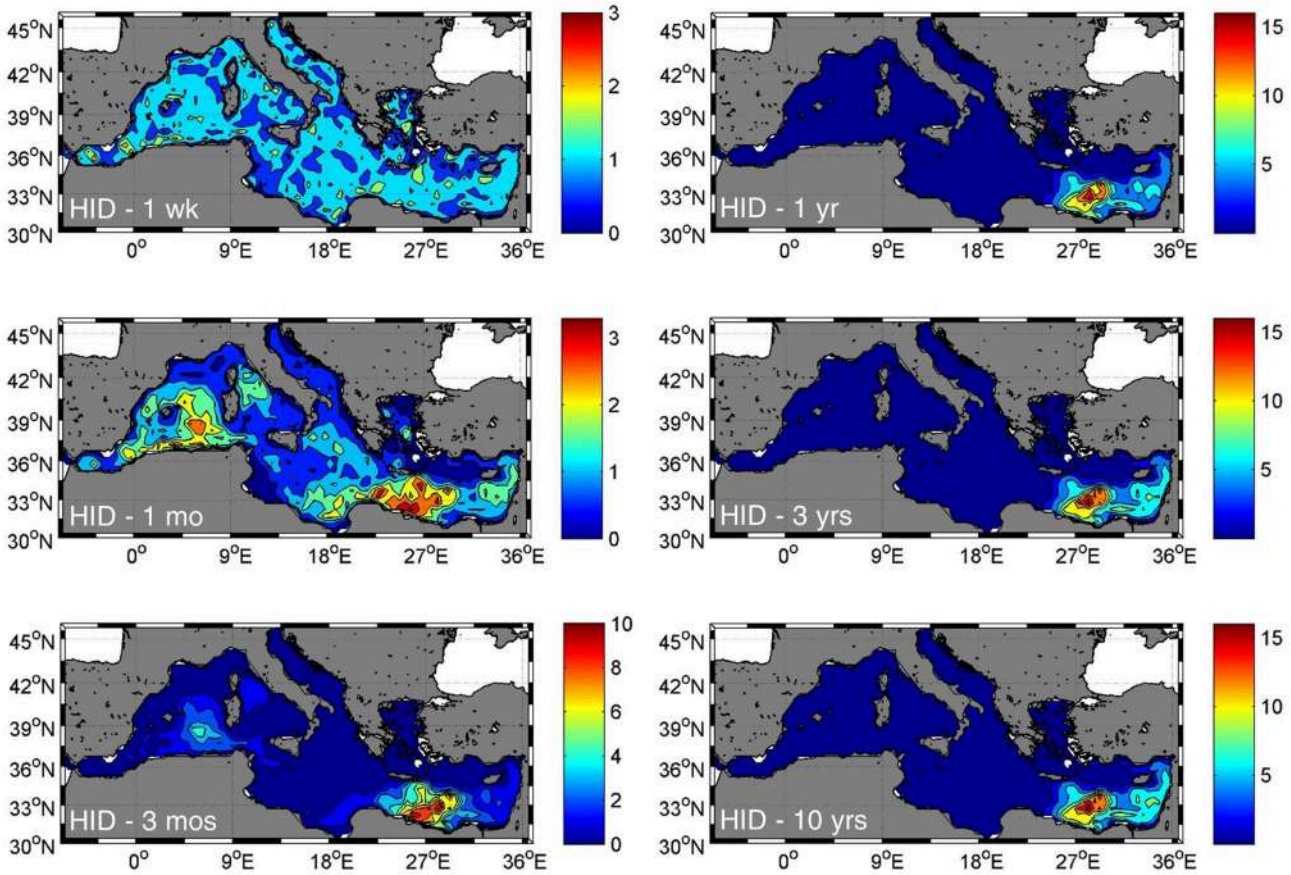

FIGURE 10 | FLP density distribution for the climatological pattern with the homogeneous initial distribution (HID) at different target times.

an asymptotic tendency to accumulate in the southern and southeastern Levantine basin, with an absolute maximum off the eastern Libyan and western Egyptian coasts and a further relative maximum widespread off the entire Middle Eastern coast. This is further illustrated by **Figure 12**, which shows the time evolution of the local FLP density in different locations of the Mediterranean: colored circles indicate key places mentioned in the paper and specific locations sampled to build the time evolution of local tracer concentration, as shown in **Figure 1** [A, Algerian Basin; B, Balearic Sea; L, Levantine Basin; M, Middle Eastern coast; T, Tyrrhenian Sea].

Upper panels refer to the HID initial conditions, lower panels to the CID one; left panels show the evolution over the first 2 years, right panels the evolution over 10 years, clearly displaying its asymptotic character. In particular, the southern/southeastern Levantine basin (L in the figure) shows a monotonic increase of FLP density which reaches its asymptotic values after five-six years.

Figure 12 displays different, typical FLP density trends revealed by our analysis: the southern and southeastern Levantine basin (L in the figure) is characterized by a monotonic increase followed by an asymptotic plateau reached after 5 to 6 years, with the absolute maximum FLP density in the whole Mediterranean; the FLP density off the Middle Eastern coast (M in the figure) steadily increases in the HID case, while in the CID case it reaches its absolute maximum after the very first few weeks, as may be expected since it is a coastal location, then decreases and later increases again, reaching after 6 years its asymptotic value, of the order of one half of the absolute maximum attained in L. The presence of a transient maximum at different initial times is also noticeable for the Algerian basin (A in the figure) where, however, the FLP density vanishes at asymptotic times. In addition to locations L, M and A, presented for both the HID and CID cases, **Figure 12** shows the time evolution of the FLP density in the Tyrrhenian Sea for the former initial condition, and in the Balearic Sea for the latter (T and B in the figure). With the HID, the Tyrrhenian behavior is quite similar to the Algerian one, even though the FLP density range is more confined; with the CID, the FLP density in the Balearic attains two subsequent initial relative maxima, as a consequence of its coastal location in a reconstruction dominated at short time scales by coastal population effects, and then vanishes at asymptotic times.

The maxima of the color scale of **Figures 10**, **11** and the time history of FLP densities of **Figure 12** show that the southern/southeastern Levantine basin is indeed a place of

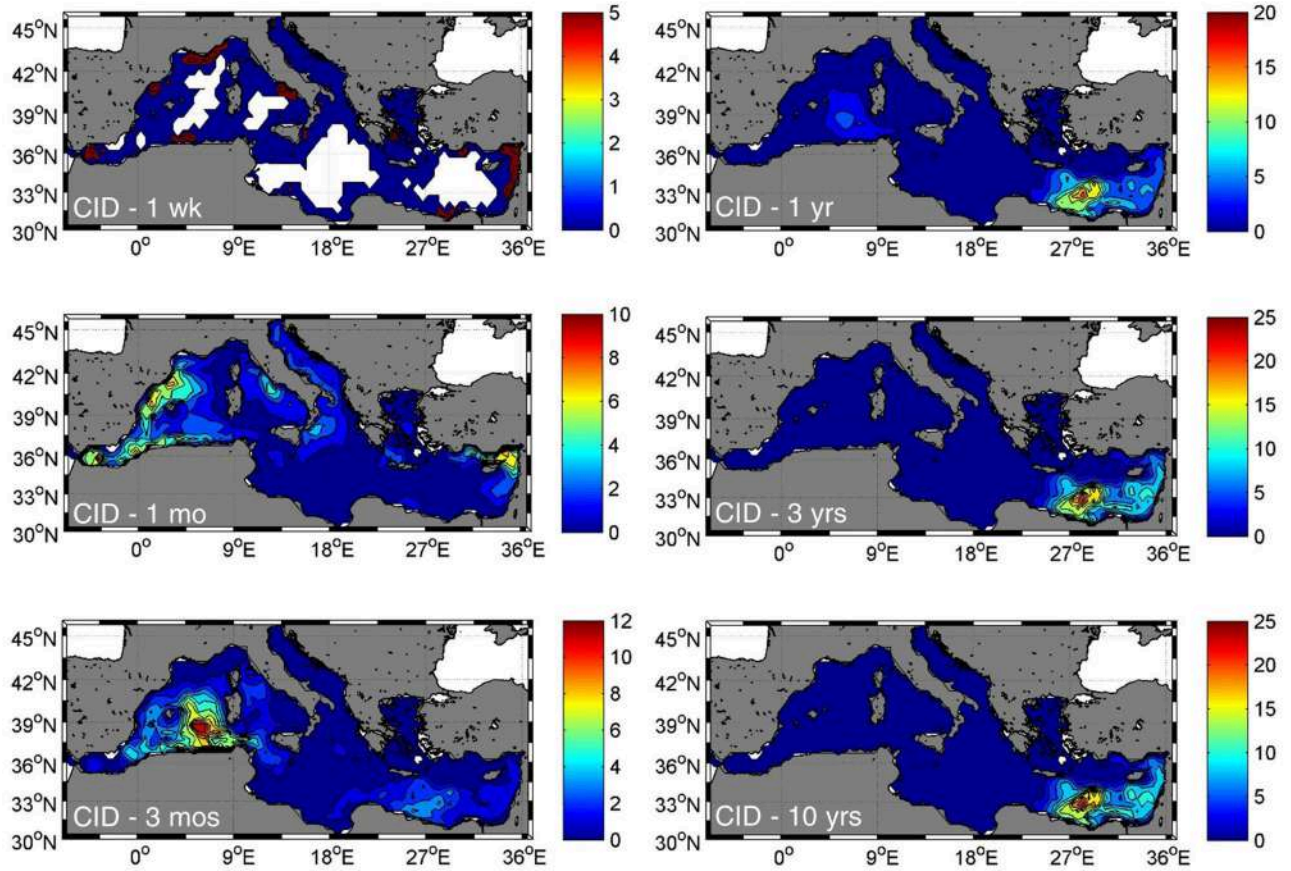

FIGURE 11 | Same as in Figure 10 with the coastal population initial distribution (CID).

sustained enhanced local increase of FLP. Maxima, however, do not exceed a 25-fold increase of the initial value over 10 years. Such a figure is of the same order found by Maximenko et al. (2012) for the northern Atlantic and the southern Indian ocean, but far from the values attained in the Pacific. Whether these high FLP density areas may be considered as potential "garbage patches" depends on patch definition, really. Since the FLP initial density was set to 1, values attained by its distribution at different target times roughly correspond to the Tracer Amplification Factor (TAF) introduced by van Sebille et al. (2012); however, their threshold value TAF >2 to define patches would most likely not be appropriate for the Mediterranean, as at least in the short-term transient we see strong positive and negative variations of features with a FLP density larger than 5 or 10. This leads us to consider the latter, i.e., a 10-fold increase of FLP density for the long-term reconstruction, as a valid threshold value for the Mediterranean.

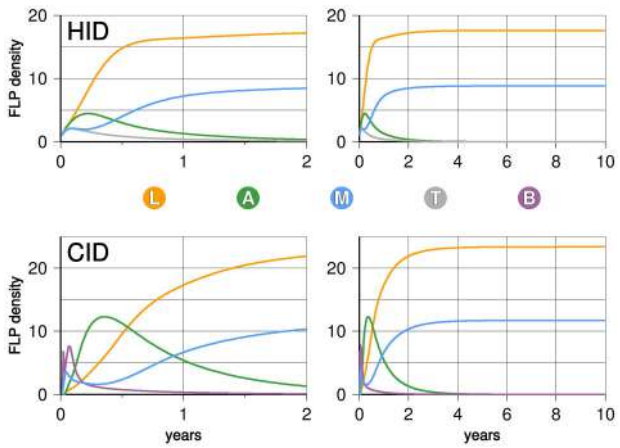

FIGURE 12 | Time history of reconstructed FLP density in different key areas defined in Figure 1.

Comparison with *In Situ* Litter Observations

The comparison of our outcomes with the results of *in situ* litter observations is far from straightforward; this is mainly due to the sporadic character of observations, strongly constrained by research vessel time and routes, and inevitably not synoptic (see, e.g., the review of observations provided by Deudero and Alomar (2015), which displays the presence of large gaps in the coverage of the Mediterranean). A proper validation would

call for systematic in space and repeated in time measurement campaigns that are currently not even planned (we will return to this point in the conclusions).

In particular, our results suggest the presence of asymptotic accumulation in the southeastern portion of the Levantine basin. Unfortunately, gathering detailed *in situ* data along the southern coasts of the Mediterranean is very difficult for a number of reasons, particularly in specific areas. This causes observations in those regions to be episodic and with coarse resolution; however, a strong presence of floating debris off the southern Mediterranean coasts is suggested by the most overarching recent observational work in the Mediterranean, by Cózar et al. (2015), which shows high concentrations south-east off Crete, in a position roughly corresponding to our HID and CID climatological long-term reconstruction maxima.

Eriksen et al. (2014) report results from 24 expeditions (2007–2013) across the world ocean, including coastal Australia, the Bay of Bengal and the Mediterranean Sea, and use those data to calibrate a Lagrangian debris dispersion model in the same areas. Their perspective is global and much coarser than ours, but a clear zonation of debris in the Mediterranean Sea is visible, and their results agree with the outcomes of our analysis, showing relative maxima in the southern portion of the basin, both in the western and in the eastern Mediterranean. Their long-term predictions nicely mirror, in an integrated manner, our asymptotic distributions, as well as our intermediate (1-month) ones.

Again at a coarser resolution, van Sebille et al. (2015) use three different, pre-existing global ocean circulation models to spatially interpolate a global dataset of plastic marine debris observations, after a careful preprocessing. Their outcomes, in particular the microplastic distributions based on the Lebreton et al. (2012) and the (van Sebille et al., 2012; van Sebille, 2014) models, appear clearly compatible with our results in terms of an asymptotic increased density of FLP in the southeastern Levantine basin.

Finally, but in terms of model-only results, it is worth underlining that the southern coastal strip of the eastern Mediterranean was identified by Mansui et al. (2015), if not as an accumulation area, as a preferential beaching destination.

As far as the other regions, characterized by transient accumulation according to our reconstruction, for the already mentioned logistic reasons we cannot find any observational confirmation of the high debris concentration expected in the Gulf of Sirte, clearly shown to be a likely retention area in the drifter data by Poulain and Zambianchi (2007), contained in the dataset utilized in this work, and representing one of three major retention areas resulting from the modeling study by Mansui et al. (2015).

Floating debris have been observed in the Algero Provencal basin by all recent samplings: see the above mentioned study by Cózar et al. (2015), in the Sardinia Channel and south of the Balearic Island, with further high concentration areas in the north, associated with the Northern Current or with the northward propagation of Algerian eddies (Millot, 1999; Salas et al., 2001, 2002; Salas, 2003; Isern-Fontanet et al., 2004; for a very recent census of eddies in the Mediterranean see Le Vu et al., 2016).

Other findings in the Sardinia Channel, along with observations in the southern portion of the Algerian basin, are reported by Suaria and Aliani (2014) and discussed by Zambianchi et al. (2014), and resemble very closely our results obtained for the case of litter sources located in correspondence of the most populated coastal areas, in particular the 1-month distribution for both extended seasons and for the climatological reconstructions.

A short-term FLP-populated area appears in our results in the northern Tyrrhenian Sea, but does not represent an accumulation area, as its signal is present only up to 1 month and disappears in the longer reconstructions. Observations in the Tyrrhenian rather suggest more abundance in the southern portion of the basin, characterized by very slow, basically stagnating dynamics (Rinaldi et al., 2010; for a discussion see Zambianchi et al., 2014; this is also in agreement with the modeling results by Mansui et al., 2015) and in the Corsica Channel (Suaria and Aliani, 2014; Cózar et al., 2015). The former is not to be seen in our reconstruction, while the latter is compatible with the 1-month results for the CID FLP distribution (**Figure 10**). It has to be underlined that the Corsica Channel represents the chokepoint for waters passing from the Tyrrhenian to the Ligurian Sea, thus possibly inducing an enhanced concentration of floating material transiting through, but not accumulating in, the strait.

Further indications can be provided by observations of the bottom distribution of debris. However, also in this case possible comparisons are constrained by the strongly uneven sampling, as shown by the maps displayed in the papers by Ramirez-Llodra et al. (2013, see their Figure 4), Pham et al. (2014, see their Figure 1), Tubau et al. (2015, see their Figure 12 and the studies summarized in it).

The results of the comparison are quite interesting: obviously, the observed distribution at the sea bottom is largely influenced by the vertical detail of the Mediterranean circulation, that in our study based on near-surface drifters cannot be accounted for, at least in terms of asymptotic zonation. However, on one hand observations confirm a relatively stronger long-term presence of litter in the southern Algerian basin and southeast off Crete. At the same time, our short-term distribution agrees, e.g., with observations in areas characterized by bottom litter abundance corresponding to the presence of canyons and other areas influenced by strong sinking patterns, such as the Gulf of Lyons. This is shown by **Figure 10** for the CID case at 1 week and 1 month for the northern Ligurian Sea and Algero Provencal basin, in which we clearly observe the signature of the Northern Current which might be at least partly at the origin of the coincident bottom abundance. In other words, in such an area the asymptotic distribution is the result of horizontal advection and sinking, and the final destiny of debris is at the sea bottom.

CONCLUSIONS

The largest available near-surface drifter dataset for the area has been utilized to study transport of marine litter in the Mediterranean Sea. The drifter data have been first processed to provide Lagrangian displacement probabilities; from these

probabilities we have then drawn estimates of the evolution throughout the basin of the density of a passive tracer, considered as a proxy of floating litter. Two kinds of sources have been considered, an initial homogeneous distribution and a more realistic one, simulating land-based coastal sources of pollution. The distribution of our floating litter proxy has been reconstructed for different travel times, in the climatological case and for two opposite extended seasons, a 6-month summer and a 6-month winter.

Decadal reconstructions of Lagrangian trajectories for the climatological case showed a quite clear asymptotic pattern of accumulation of our litter proxy (in terms of a local increase of density) in the southern and southeastern Levantine basin. This was true for both initial distributions (homogeneous over the basin vs. based on coastal population), the asymptotic behavior being achieved from 5 to 6 years on.

As is well known, no evidence of localized permanent debris accumulation ("garbage patch") has been reported so far in the Mediterranean. However, as pointed out by Cózar et al. (2015) and van Sebille (2015), the term "garbage patch" itself might be misleading, as it suggests accumulation visible by the naked eye, which is not the case even in the most plastic-crowded regions of the global ocean. Moreover, no targeted litter observation campaigns have been yet carried out in the areas that our reconstructions identified as subject to asymptotic density enhancement of our litter proxy, that anyway found some agreement with the very few available data.

It is worth adding that our seasonal recontructions showed transient accumulation in locations varying over time and different from one season to another. This suggests that the surface flow temporal variability might play a role in shaping litter accumulation pattern; the structure of our experiment does not allow to assess such effects in the long term. The latter argument calls for some caution in considering the outcomes of an investigation like ours, carried out on a climatological, i.e., long-term averaged, data set. However, we want to underline that our shorter-term results, both seasonal and climatological, were found in good agreement with existing sightings of marine litter at the surface as well as at depth in selected locations.

Our results clearly indicate the need for a systematic floating litter observation activity, that may shed light on the likely accumulation in the southern and southeastern Levantine basin; the outcomes of our study lead us to strongly recommend the organization of regular, synoptic campaigns enabling the assessment of marine litter distribution over the whole Mediterranean Sea.

As a general remark, it has to be pointed out that the lack of solid observations, so far, of localized accumulation shall not anyway suggest a lack of an environmental problem, and should not decrease our concern: among the marginal basins of the world ocean the Mediterranean is one of the most affected by marine litter and plastics, and a strong and continuous effort is required to contain the deployment of garbage into its waters.

AUTHOR CONTRIBUTIONS

EZ: Contribution to the main structure and contents of all sections, experiment design, result analysis, drafting, review, and final approval of the submitted version. MT: Contribution to the main structure and contents of all sections, experiment design and execution, result analysis, drafting, review, and final approval of the submitted version. PF: Contribution to the main structure and contents of all sections, result analysis, drafting, review, and final approval of the submitted version.

ACKNOWLEDGMENTS

The authors are indebted to Erik van Sebille and Laurent Lebreton for very useful and constructive criticisms on this paper. We thank Marco Uttieri for useful comments on the manuscript. This work was partly funded by the Flagship Project RItMare (The Italian Research for the Sea), by the EU 7th Framework Programme project COCONET (Grant agreement No. 287844, http://www.coconet-fp7.eu/), by the Parthenope University Individual Research fund (DR 727/2015 and 954/2016) and by the Italian Ministry of the Environment in the framework of the implementation of the Marine Strategy Framework Directive.

REFERENCES

Aliani, S., Griffa, A., and Molcard, A. (2003). Floating debris in the Ligurian Sea, northwestern Mediterranean. *Mar. Pollut. Bull.* 46, 1142–1149. doi: 10.1016/S0025-326X(03)00192-9

Andrady, A. L. (2011). Microplastic in the marine environment. *Mar. Pollut. Bull.* 62, 1596–1605. doi: 10.1016/j.marpolbul.2011.05.030

Barnes, D. K., Galgani, F., Thompson, R. C., and Barlaz, M. (2009). Accumulation and fragmentation of plastic debris in global environments. *Philos. Trans. R. Soc. B* 364, 1985–1998. doi: 10.1098/rstb.2008.0205

Carson, H. S., Lamson, M. R., Nakashima, D., Toloumu, D., Hafner, J., Maximenko, N., et al. (2013). Tracking the sources and sinks of local marine debris in Hawaii. *Mar. Environ. Res.* 84, 76–83. doi: 10.1016/j.marenvres.2012.12.002

Castiglione, P., Cencini, M., Vulpiani, A., and Zambianchi, E. (1999). Transport in finite size systems: an exit time approach. *Chaos* 9, 871–879. doi: 10.1063/1.166459

Cencini, M., Lacorata, G., Vulpiani, A., and Zambianchi, E. (1999). Mixing in a Meandering Jet: a markovian approximation. *J. Phys. Oceanogr.* 29, 2578–2594. doi: 10.1175/1520-0485(1999)029<2578:MIAMJA>2.0.CO;2

CIESM (2014). *CIESM Workshop Monograph n° 46*. Monaco: CIESM Publisher.

Cózar, A., Sanz-Martín, M., Martí, E., González-Gordillo, J., Ubeda, B., Gálvez, J., et al. (2015). Plastic accumulation in the Mediterranean Sea. *PLoS ONE* 10:e0121762. doi: 10.1371/journal.pone.0121762

Davis, R. E. (1985). Drifter observations of coastal currents during CODE: the method and descriptive view. *J. Geophys. Res.* 90, 4741–4755. doi: 10.1029/jc090ic03p04741

Deudero, S., and Alomar, C. (2015). Mediterranean marine biodiversity under threat: reviewing influence of marine litter on species. *Mar. Pollut. Bull.* 98, 58–68. doi: 10.1016/j.marpolbul.2015.07.012

Edwards, M. O. (1989). *Global Gridded Elevation and Bathymetry on 5-minute Geographic Grid (ETOPO5)*. Boulder, CO: NOAA, National Geophysical Data Center.

Eriksen, M., Lebreton, L. C. M., Carson, H. S., Thiel, M., Moore, C. J., Borrero, J. C., et al. (2014). Plastic pollution in the world's oceans: more than 5 trillion plastic pieces weighing over 250,000 Tons Afloat at Sea. *PLoS ONE* 9:e111913. doi: 10.1371/journal.pone.0111913

Falco, P., and Zambianchi, E. (2011). Near-surface structure of the Antarctic Circumpolar Current derived from World Ocean Circulation Experiment drifter data. *J. Geophys. Res.* 116:C05003. doi: 10.1029/2010jc006349

Froyland, G., Stuart, R. M., and van Sebille, E. (2014). How well-connected is the surface of the global ocean? *Chaos* 24:033126. doi: 10.1063/1.4892530

Galgani, F. (2014). "Distribution, composition and abundance of marine litter in the Mediterranean and Black Seas," in *CIESM Workshop Monograph 46: Marine Litter in the Mediterranean and Black Seas*, ed F. Briand (Monaco, CIESM Publisher), 23–30.

Galgani, F., Barnes, D. K. A., Deudero, S., Fossi, M. C., Ghiglione, J. F., Hema, T., et al. (2014). "Executive Summary," in *CIESM Workshop Monograph 46: Marine Litter in the Mediterranean and Black Seas*, ed F. Briand (Monaco, CIESM Publisher), 7–20.

Garcia-Olivares, A., Isern-Fontanet, J., and García-Ladona, E. (2007). Dispersion of passive tracers and finite-scale Lyapunov exponents in the Western Mediterranean Sea. *Deep Sea Res. I* 54, 253–268. doi: 10.1016/j.dsr.2006.10.009

Guyon, E., Pomeau, Y., Hulin, J. P., and Baudet, C. (1987). Dispersion in the presence of recirculation zones. *Nucl. Phys. B-Proc.* 2, 271–280. doi: 10.1016/0920-5632(87)90023-5

Halpern, B. S., Walbridge, S., Selkoe, K. A., Kappel, C. V., Micheli, F., D'Agrosa, C., et al. (2008). A global map of human impact on marine ecosystems. *Science* 319, 948–952. doi: 10.1126/science.1149345

Haza, A. C., Özgökmen, T. M., Griffa, A., Garraffo, Z. D., and Piterbarg, L. (2012). Parameterization of particle transport at submesoscales in the Gulf Stream region using Lagrangian subgridscale models. *Ocean Modell.* 42, 31–49. doi: 10.1016/j.ocemod.2011.11.005

Isern-Fontanet, J., Font, J., García-Ladona, E., Emelianova, M., Millot, C., and Taupier-Letage, I. (2004). Spatial structure of anticyclonic eddies in the Algerian basin (Mediterranean Sea) analyzed using the Okubo–Weiss parameter. *Deep Sea Res. II* 51, 3009–3028. doi: 10.1016/j.dsr2.2004.09.013

Kako, S. I., Isobe, A., Kataoka, T., and Hinata, H. (2014). A decadal prediction of the quantity of plastic marine debris littered on beaches of the East Asian marginal seas. *Mar. Pollut. Bull.* 81, 174–184. doi: 10.1016/j.marpolbul.2014.01.057

Koch, D. L., and Brady, J. F. (1985). Dispersion in fixed beds. *J. Fluid Mech.* 154, 399–427. doi: 10.1017/S0022112085001598

Law, K. L., Morét-Ferguson, S., Maximenko, N. A., Proskurowski, G., Peacock, E. E., Hafner, J., et al. (2010). Plastic accumulation in the North Atlantic subtropical gyre. *Science* 329, 1185–1188. doi: 10.1126/science.1192321

Lebreton, L. C. M., Greer, S. D., and Borrero, J. C. (2012). Numerical modeling of floating debris in the world's oceans. *Mar. Pollut. Bull.* 64, 653–661. doi: 10.1016/j.marpolbul.2011.10.027

Le Vu, B., Stegner, A., and, T., Arsouze (2016). Atlas of eddies in Mediterranean sea from satellite imagery. *Rapp. Comm. Int. Mer. Médit.* 41:73.

Lumpkin, R. (2003). Decomposition of surface drifter observations in the Atlantic Ocean. *Geophys. Res. Lett.* 30:1753. doi: 10.1029/2003GL017519

Lumpkin, R., and Garraffo, Z. (2005). Evaluating the decomposition of tropical Atlantic drifter observations. *J. Atmos. Oceanic Technol.* 22, 1403–1415. doi: 10.1175/JTECH1793.1

Lumpkin, R., Maximenko, N., and Pazos, M. (2012). Evaluating where and why drifters die. *J. Atmos. Oceanic Technol.* 29, 300–308. doi: 10.1175/JTECH-D-11-00100.1

Lumpkin, R., and Pazos, M. (2007). "Measuring surface currents with Surface Velocity Program drifters: the instrument, its data, and some recent results," in *Lagrangian Analysis and Prediction of Coastal and Ocean Dynamics*, eds A. Griffa, A. D. Kirwan A. J. Jr., Mariano, T. Özgökmen, and H. T. Rossby (Cambridge, UK: Cambridge University Press), 39–67.

Lumpkin, R., Özgökmen, T., and Centurioni, L. (2017). Advances in the applications of surface drifters. *Ann. Rev. Mar. Sci.* 9, 59–81. doi: 10.1146/annurev-marine-010816-060641

Malanotte-Rizzoli, P., Manca, B., Ribera d'Alcalà, M., Theocharis, A., Brenner, S., Budillon, G., et al. (1999). The eastern Mediterranean in the 80s and in the 90s: the big transition in the intermediate and deep circulations. *Dyn. Atmos. Oceans* 29, 365–395. doi: 10.1016/s0377-0265(99)00011-1

Mansui, J., Molcard, A., and Ourmieres, Y. (2015). Modelling the transport and accumulation of floating marine debris in the Mediterranean basin. *Mar. Pollut. Bull.* 91, 249–257. doi: 10.1016/j.marpolbul.2014.11.037

Maximenko, N., Hafner, J., and Niiler, P. (2012). Pathways of marine debris derived from trajectories of Lagrangian drifters. *Mar. Pollut. Bull.* 65, 51–62. doi: 10.1016/j.marpolbul.2011.04.016

Millot, C. (1999). Circulation in the Western Mediterranean Sea. *J. Mar. Syst.* 20, 423–442.

Moore, C. J., Moore, S. L., Leecaster, M. K., and Weisberg, S. B. (2001). A comparison of plastic and plankton in the North Pacific Central Gyre. *Mar. Pollut. Bull.* 42, 1297–1300. doi: 10.1016/S0025-326X(01)00114-X

Morris, R. J. (1980). Floating plastic debris in the Mediterranean. *Mar. Pollut. Bull.* 11:125. doi: 10.1016/0025-326x(80)90073-9

Pazan, S. E. (1996). "Intercomparison of drogued and undrogued drift buoys," in *OCEANS'96. MTS/IEEE. Prospects for the 21st Century*, Vol. 2, eds C. P. Brancart and A. M. Clark (Fort Lauderdale, FL), 864–872. doi: 10.1109/OCEANS.1996.568343

Peacock, T., and Haller, G. (2013). Lagrangian coherent structures: the hidden skeleton of fluid flows. *Physics Today* 66:41. doi: 10.1063/PT.3.1886

Peng, S., Qian, Y. K., Lumpkin, R., Li, P., Wang, D., and Du, Y. (2015). Characteristics of the near-surface currents in the Indian Ocean as deduced from satellite-tracked surface drifters. *Part II: Lagrangian Statistics. J. Phys. Oceanogr.* 45, 459–477. doi: 10.1175/JPO-D-14-0049.1

Pham, C. K., Ramirez-Llodra, E., Alt, C. H. S., Amaro, T., Bergmann, M., Canals, M., et al. (2014). Marine litter distribution and density in European seas, from the shelves to deep basins. *PLoS ONE* 9:e95839. doi: 10.1371/journal.pone.0095839

Pisano, A., De Dominicis, M., Biamino, W., Bignami, F., Gherardi, S., Colao, et al. (2016). An oceanographic survey for oil spill monitoring and model forecasting validation using remote sensing and *in situ* data in the Mediterranean Sea. *Deep-Sea Res. Part II.* 133, 132–145. doi: 10.1016/j.dsr2.2016.02.013

Poulain, P. M., Bussani, A., Gerin, R., Jungwirth, R., Mauri, E., Menna, M., et al. (2013). Mediterranean surface currents measured with drifters. *Oceanography* 26, 38–47. doi: 10.5670/oceanog.2013.03

Poulain, P. M., Menna, M., and Mauri, E. (2012). Surface geostrophic circulation of the Mediterranean Sea derived from drifter and satellite altimeter data. *J. Phys. Oceanogr.* 42, 973–990. doi: 10.1175/JPO-D-11-0159.1

Poulain, P. M., and Zambianchi, E. (2007). Surface circulation in the central Mediterranean Sea as deduced from Lagrangian drifters in the 1990s. *Cont. Shelf Res.* 27, 981–1001. doi: 10.1016/j.csr.2007.01.005

Ramirez-Llodra, E., De Mol, B., Company, J. B., Coll, M., and Sarda, F. (2013). Effects of natural and anthropogenic processes in the distribution of marine litter in the deep Mediterranean Sea. *Prog. Oceanogr.* 118, 273–287. doi: 10.1016/j.pocean.2013.07.027

Rinaldi, E., Buongiorno Nardelli, B., Zambianchi, E., Santoleri, R., and Poulain, P.-M. (2010). Lagrangian and Eulerian observations of the surface circulation in the Tyrrhenian Sea. *J. Geophys. Res. Oceans* 115:C4024. doi: 10.1029/2009JC005535

Rio, M. H., Poulain, P. M., Pascual, A., Mauri, E., Larnicol, G., and Santoleri, R. (2007). A mean dynamic topography of the Mediterranean Sea computed from altimetric data, *in-situ* measurements and a general circulation model. *J. Mar. Syst.* 65, 484–508. doi: 10.1016/j.jmarsys.2005.02.006

Robinson, A. R., Leslie, W. G., Theocharis, A., and Lascaratos, A. (2001). "Mediterranean Sea circulation," in *Encyclopedia of Ocean Sciences*, eds J. H. Steele, K. K. Turekian, and S. A. Thorpe (London: Academic Press), 1689–1706.

Rossi, V., Ser-Giacomi, E., López, C., and Hernández-García, E. (2014). Hydrodynamic provinces and oceanic connectivity from a transport network help designing marine reserves. *Geophys. Res. Lett.* 41, 2883–2891. doi: 10.1002/2014GL059540

Salas, J. (2003). Evolution of the open-sea eddy ALGERS '98 in the Algerian basin with Lagrangian trajectories and remote sensing observations. *J. Mar. Syst.* 43, 105–131. doi: 10.1016/j.jmarsys.2003.08.001

Salas, J., Garcıa-Ladona, E., and Font, J. (2001). Statistical analysis of the surface circulation in the Algerian Current using Lagrangian buoys. *J. Mar. Syst.* 29, 69–85. doi: 10.1016/S0924-7963(01)00010-0

Salas, J., Millot, C., Font, J., and Garcıa-Ladona, E. (2002). Analysis of mesoscale phenomena in the Algerian basin from drifting buoys and infrared images. *Deep Sea Res. I* 49, 245–266. doi: 10.1016/S0967-0637(01)00052-8

Selsor, H. D. (1993). Data from the sea: navy drift buoy program. *Sea Technol.* 34, 53–58.

Suaria, G., and Aliani, S. (2014). Floating debris in the Mediterranean Sea. *Mar. Pollut. Bull.* 86, 494–504. doi: 10.1016/j.marpolbul.2014.06.025

Trani, M., Falco, P., Zambianchi, E., and Sallée, J. B. (2014). Aspects of the Antarctic circumpolar current dynamics investigated with drifter data. *Progr. Oceanogr.* 125, 1–15. doi: 10.1016/j.pocean.2014.05.001

Tubau, X., Canals, M., Lastras, G., Rayo, X., Rivera, J., and Amblas, D. (2015). Marine litter on the floor of deep submarine canyons of the Northwestern Mediterranean Sea: the role of hydrodynamic processes. *Progr. Oceanogr.* 134, 379–403. doi: 10.1016/j.pocean.2015.03.013

van Sebille, E. (2014). Adrift.org.au — a free, quick and easy tool to quantitatively study planktonic surface drift in the global ocean. *J. Exp. Mar. Biol. Ecol.* 461, 317–322. doi: 10.1016/j.jembe.2014.09.002

van Sebille, E. (2015). The oceans' accumulating plastic garbage. *Phys. Today* 68, 60–61. doi: 10.1063/PT.3.2697

van Sebille, E., England, M. H., and Froyland, G. (2012). Origin, dynamics and evolution of ocean garbage patches from observed surface drifters. *Environ. Res. Lett.* 7:044040. doi: 10.1088/1748-9326/7/4/044040

van Sebille, E., Wilcox, C., Lebreton, L., Maximenko, N., Hardesty, B. D., Van Franeker, J. A., et al. (2015). A global inventory of small floating plastic debris. *Environ. Res. Lett.* 10:124006. doi: 10.1088/1748-9326/10/12/124006

Wessel, P., Smith, W. H. F., Scharroo, R., Luis, J. F., and, F., Wobbe (2013). Generic mapping tools: improved version released. *EOS Trans. AGU* 94, 409–410. doi: 10.1002/2013EO450001

Young, W. R. (1988). Arrested shear dispersion and other models of anomalous diffusion. *J. Fluid Mech.* 193, 129–149. doi: 10.1017/S0022112088002083

Zambianchi, E., and Griffa, A. (1994). Effects of finite scales of turbulence on dispersion estimates. *J. Mar. Res.* 52, 129–148. doi: 10.1357/0022240943076731

Zambianchi, E., Iermano, I., Suaria, G., and Aliani, S. (2014). "Marine litter in the Mediterranean Sea: an oceanographic perspective," in *CIESM Workshop Monograph 46: Marine litter in the Mediterranean and Black Seas,* ed F. Briand (Monaco, CIESM Publisher), 31–41.

Conflict of Interest Statement: The authors declare that the research was conducted in the absence of any commercial or financial relationships that could be construed as a potential conflict of interest.

frontiers in Marine Science

ORIGINAL RESEARCH
published: 04 April 2017
doi: 10.3389/fmars.2017.00078

Combining Litter Observations with a Regional Ocean Model to Identify Sources and Sinks of Floating Debris in a Semi-enclosed Basin: The Adriatic Sea

Daniel F. Carlson[1,2], Giuseppe Suaria[3,4], Stefano Aliani[3]*, Erick Fredj[5], Tomaso Fortibuoni[6,7], Annalisa Griffa[3], Aniello Russo[8†] and Valentina Melli[9]*

[1] Department of Earth, Ocean, and Atmospheric Sciences, Florida State University, Tallahassee, FL, USA, [2] Arctic Research Centre, Aarhus University, Aarhus, Denmark, [3] Consiglio Nazionale delle Ricerche, Istituto di Scienze Marine, La Spezia, Italy, [4] Centro Oceanográfico de Baleares, Instituto Español de Oceanografía, Palma de Mallorca, Spain, [5] Department of Computer Science, Jerusalem College of Technology, Jerusalem, Israel, [6] National Institute of Oceanography and Experimental Geophysics, Trieste, Italy, [7] Italian National Institute for Environmental Protection and Research, Chioggia, Italy, [8] DiSVA, Università Politecnica delle Marche, Ancona, Italy, [9] National Institute of Aquatic Resources, Technical University of Denmark Aqua, Hirtshals, Denmark

Visual ship transect surveys provide crucial information about the density, and spatial distribution of floating anthropogenic litter in a basin. However, such observations provide a 'snapshot' of local conditions at a given time and cannot be used to deduce the provenance of the litter or to predict its fate, crucial information for management and mitigation policies. Particle tracking techniques have seen extensive use in these roles, however, most previous studies have used simplistic initial conditions based on bulk average inputs of debris to the system. Here, observations of floating anthropogenic macro debris in the Adriatic Sea are used to define initial conditions (number of particles, location, and time) in a Lagrangian particle tracking model. Particles are advected backward and forward in time for 60 days (120 days total) using surface velocities from an operational regional ocean model. Sources and sinks for debris observed in the central and southern Adriatic in May 2013 and March 2015 included the Italian coastline from Pescara to Brindisi, the Croatian island of Mljet, and the coastline from Dubrovnik through Montenegro to Albania. Debris observed in the northern Adriatic originated from the Istrian peninsula to the Italian city of Termoli, as well as the Croatian island of Cres and the Kornati archipelago. Particles spent a total of roughly 47 days afloat. Coastal currents, notably the eastern and western Adriatic currents, resulted in large alongshore displacements. Our results indicate that anthropogenic macro debris originates largely from coastal sources near population centers and is advected by the cyclonic surface circulation until it strands on the southwest (Italian) coast, exits the Adriatic, or recirculates in the southern gyre.

Keywords: marine litter, floating debris, Adriatic Sea, lagrangian particle tracking, ROMS

OPEN ACCESS

Edited by:
Francois Galgani, French Research Institute for Exploitation of the Sea, France

Reviewed by:
Gotzon Basterretxea, Consejo Superior de Investigaciones Científicas, Spain
Svitlana Liubartseva, Fondazione CMCC - Centro Euro-Mediterraneo sui Cambiamenti Climatici, Italy
Carlo Brandini, Consiglio Nazionale delle Ricerche (CNR), Italy

****Correspondence:***
Daniel F. Carlson
danfcarlson@gmail.com
Stefano Aliani
stefano.aliani@ismar.cnr.it

†Present Address:
Aniello Russo, Science and Technology Organisation - Centre for Maritime Research and Experimentation (STO CMRE), NATO, La Spezia, Italy

Specialty section:
This article was submitted to Marine Pollution, a section of the journal Frontiers in Marine Science

Received: *01 November 2016*
Accepted: *07 March 2017*
Published: *04 April 2017*

Citation:
Carlson DF, Suaria G, Aliani S, Fredj E, Fortibuoni T, Griffa A, Russo A and Melli V (2017) Combining Litter Observations with a Regional Ocean Model to Identify Sources and Sinks of Floating Debris in a Semi-enclosed Basin: The Adriatic Sea. Front. Mar. Sci. 4:78. doi: 10.3389/fmars.2017.00078

1. INTRODUCTION

Advancing the study and management of anthropogenic marine debris (AMD) requires accurate identification of source regions (Critchell and Lambrechts, 2016) and quantification of temporal variability of injection rates. Identifying sources and sinks of AMD can assist resource managers maximize the effectiveness of prevention and response efforts by providing scientific support to the implementation of public policies. While progress has been made, most relevant studies either relied on observations of beached AMD (Yoon et al., 2010; Kako et al., 2011, 2014; Neumann et al., 2014), made assumptions about the amount of AMD as well as its temporal and/or spatial distributions (Lebreton et al., 2012; Critchell et al., 2015; Mansui et al., 2015; Liubartseva et al., 2016), or used coarse resolution velocity data and/or idealized surface currents (Aliani and Molcard, 2003; Maximenko et al., 2012; van Sebille et al., 2012; Reisser et al., 2013; Isobe et al., 2014). Such studies have identified the physical processes relevant to the transport and accumulation of debris, however, the efficacy of models in aiding management efforts depends strongly on the assumptions applied in the particle tracking scheme (Critchell and Lambrechts, 2016) as well as the resolution and accuracy of the underlying velocity field (Putman and He, 2013). Beaching, for example, is a complex process that is not properly represented in most particle tracking models (Lebreton et al., 2012) as ocean model domains typically extend to some minimum depth and, therefore, do not resolve the shoreline. Furthermore, even relatively high-resolution regional models, like the one employed here, cannot resolve complex shoreline topography. Additionally, a resource manager coordinating cleanup efforts is not faced with the mean state, which is most commonly reported by modeling studies, but instead must respond to debris loads that can vary in space and time (Kako et al., 2010, 2011) in response to numerous environmental (Critchell and Lambrechts, 2016) and human factors (Slavin et al., 2012; Munari et al., 2016).

Here, observed position, time, and abundance of floating macro AMD are used to specify initial conditions in a Lagrangian particle tracking model, thereby removing assumptions about debris injection rates and locations. Backward-in-time and forward-in-time particle trajectory computations identify potential coastal sources and sinks, respectively, for the observed AMD. Furthermore, only AMD observations within the model domain and at least 4 km from a boundary were used to initialize the particle tracking model. The particle tracking model brings the "snapshot" AMD surveys to life while, at the same time, realistic initial conditions based on the AMD surveys can arguably lead to identification of debris "hot spots" (Galgani, 2015). In the remainder of the manuscript we describe the methodology, apply it to the Adriatic Sea, discuss strengths and weaknesses of the proposed methodology, and suggest improvements to both our method, and AMD modeling in general.

Abbreviations: AMD, anthropogenic marine debris.

2. METHODS

2.1. Study Area

Twenty five years of surface drifter studies have effectively characterized the basin-scale and mesoscale surface currents of the Adriatic Sea, as well as their variability (Poulain, 1999, 2001; Ursella et al., 2006; Carlson et al., 2016). The surface Lagrangian pathways relevant to the transport of AMD at synoptic to seasonal time scales are the cyclonic coastal currents and the northern, central, and southern cyclonic sub-gyres (Poulain, 2001). The east Adriatic current (EAC) flows northwestward along the eastern shore and the west Adriatic current (WAC) flows southeastward along the western (Italian) shore (Poulain, 2001). At the timescales considered here, the surface currents vary in response to river runoff, heat fluxes, and exchange through the Strait of Otranto (Artegiani et al., 1997) . In general, westward surface transport dominates the surface circulation and the WAC acts as an effective transport pathway to export drifters, and presumably surface waters and AMD, out of the basin (Carlson et al., 2016). Relatively short drifter (Poulain, 2001) and particle (Liubartseva et al., 2016) half-lives of 40–45 days suggest little accumulation of floating AMD in the Adriatic basin at longer timescales. For a detailed review of surface Lagrangian transport in the Adriatic see Carlson et al. (2016) and references therein.

As elsewhere in the world, anthropogenic waste has been found in all compartments of the Adriatic marine environment. Plastic litter has been reported from northern Adriatic beaches (Laglbauer et al., 2014; Munari et al., 2016), coastal sediments (Vianello et al., 2013; Blašković et al., 2017), surface waters (Suaria and Aliani, 2014; Gajšt et al., 2016; Suaria et al., 2016) and in very large amounts on the seafloor (Galgani et al., 2000; Strafella et al., 2015; Pasquini et al., 2016), where litter densities are among the highest of the entire Mediterranean basin. Ingestion of plastic by Adriatic fauna has been reported for marine turtles (Lazar and Gračan, 2011; Poppi et al., 2012), sperm whales (Mazzariol et al., 2011) and dolphins (Pribanic et al., 1999) as well as from commercial fish (Avio et al., 2015) and crustacean species (Wieczorek et al., 1999).

Liubartseva et al. (2016) modeled the transport of AMD using a high-resolution ocean model and a Markov chain to simulate passive particle trajectories, based on transition probability computed from ensemble model trajectories. Liubartseva et al. (2016) assumed a constant annual input of AMD, which was split into terrestrial and marine sources and terrestrial inputs were further split according to population. The methodology presented here differs from Liubartseva et al. (2016) in that we use observed debris as input to the particle tracking model. Furthermore, Liubartseva et al. (2016) used a statistical approach while we consider specific events that takes variability into account. Finally Liubartseva et al. (2016) parameterized sub-grid-scale turbulence and windage, which are not considered in our methodology (see Section 2.4).

2.2. Debris Surveys

Time, date, position, abundance, and typology of floating macro debris were recorded during three visual ship surveys

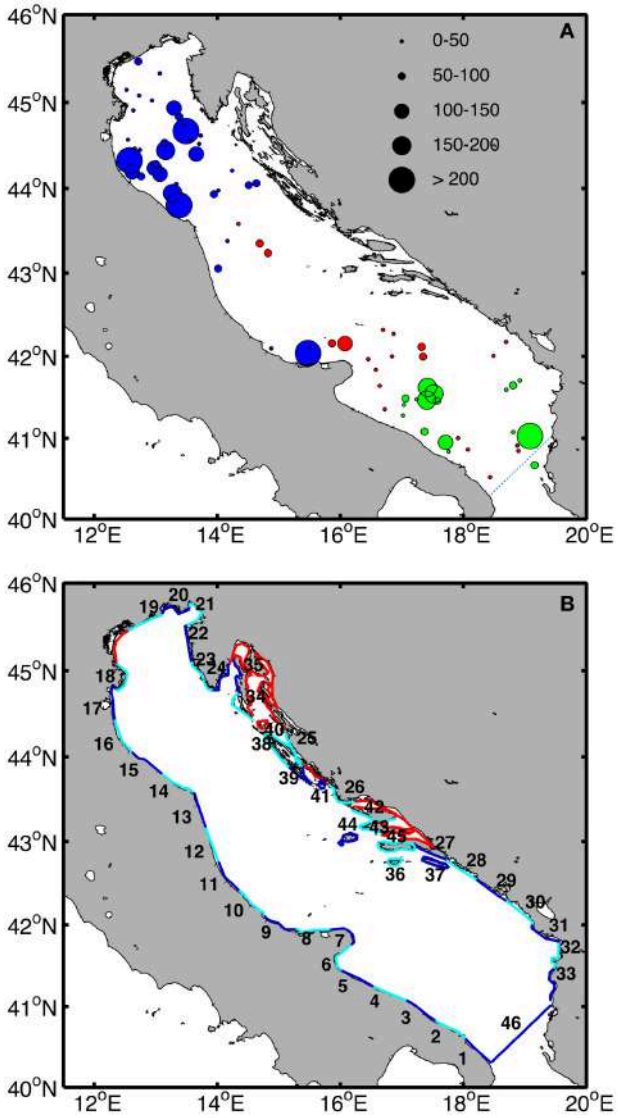

FIGURE 1 | (A) Abundances of anthropogenic marine debris (items km^{-2}) observed in the Adriatic Sea during ship-based visual surveys in May 2013 (red), March 2015 (green), and November–December 2015 (blue). **(B)** Coastline segments used to identify potential sources and sinks of debris are numbered for reference in **Figures 4**–**10** and are highlighted in alternating dark and light blue. Red segments lack numbers as they were not identified as a source or a sink of debris.

performed in the Adriatic Sea in May 2013 and in March and November-December 2015 (**Figure 1A**). The May 2013 observations are summarized in Suaria and Aliani (2014) and the March 2015 observations were made by the same observer following the same monitoring protocol.

The November-December 2015 observations were made during the SoleMon trawl-survey (Grati et al., 2013) following a 10 m fixed-width monitoring protocol as recommended by EU MSFD guidelines (Galgani et al., 2013). In all three surveys, all litter items larger than 2.5 cm were recorded along short transects of ∼30 min (mean length 7.7 ± 2.6 km) during daytime

TABLE 1 | Summary of visual transect surveys of floating macro anthropogenic debris in the Adriatic Sea.

Month	N_t	N_o	T_w	A_{avg}	A_{sd}	N_p
May 2013	32	282	31.0	31.52	30.97	1597
Mar. 2015	33	859	23.6	114.75	172.55	4079
Nov. 2015	55	223	10.0	74.78	74.27	3722

The number of transects (N_t), total number of objects sighted (N_o), transect width (T_w; meters), average debris abundance (A_{avg}; items km^{-2}), and standard deviation (A_{sd}; items km^{-2}) are reported for each survey. The total number of virtual particles, N_p, released in each experiment is also reported. N_p is obtained using the observed abundances in Equation 2.

navigation and under good visibility conditions (i.e., wind speed < 20 kts). AMD abundances (expressed as items km^{-2}) were then computed for all transects and plotted in **Figure 1A**. Overall results are summarized in **Table 1**.

2.3. Regional Ocean Model

Surface velocities from the AdriaROMS 4.0 ocean model (Russo et al., 2013a,b) are used to model the Lagrangian transport of the observed AMD. AdriaROMS 4.0 is the operational implementation of the Regional Ocean Modeling System (ROMS; Shchepetkin and McWilliams, 2005; Haidvogel et al., 2008) for the Adriatic Sea (see Russo et al., 2013b for details). The AdriaROMS model domain extends to the 5 m isobath, which varies in distance from the actual coastline due to differences in bottom slope across the Adriatic, and the open boundary in the southern Adriatic is shown in **Figure 1**. AdriaROMS has spatial and temporal resolutions of $\frac{1}{45}^\circ$ (approximately 2 km) and 1 h, respectively, with 22 terrain-following sigma levels. Fluxes are derived from the Consortium for Small-Scale Modeling (COSMO-I7) atmospheric model and river runoff includes daily Po River discharge and climatological discharges for other Adriatic rivers (Russo et al., 2009; Benetazzo et al., 2013).

Carlson et al. (2016) showed how synoptic wind events can alter surface Lagrangian pathways in the Adriatic and, as such, COSMO winds at 10 m height are use to qualitatively examine the role of winds in the transport of floating AMD, following Carlson et al. (2016). Basin-averaged wind is used as previous studies found high correlations in both magnitude and direction of surface winds over the Adriatic (Magaldi et al., 2010; Carlson et al., 2016).

2.4. Lagrangian Particle Tracking Model

Floating AMD are treated as buoyant, passive particles and are advected by modeled ocean currents using the Particle Tracking and Analysis TOolbox (PaTATO) for Matlab (Fredj et al., 2016). Particle positions are computed at hourly intervals by interpolating velocities to particle positions and integrating:

$$\mathbf{v}(\mathbf{x}, t) = \frac{d\mathbf{x}}{dt} \tag{1}$$

where $\mathbf{v}, \mathbf{x}$, and t correspond to the spatially and temporally varying velocity obtained from AdriaROMS, position, and time, respectively (Fredj et al., 2016). Velocities on the Arakawa C grid are interpolated to the center of each grid cell. The particle

TABLE 2 | Summary of particle tracking experiments.

Month	Backwards					Forward						
	%Bch	%Flt	%Opn	T_{avg}	T_{ci}	%Bch	%Flt	%Opn	T_{avg}	T_{ci}	T_{res}	T_{ci}
May '13	62	25	13	22.8	[21.7 23.9]	41	13	46	38.7	[37.5 39.7]	61.1	[58.9 63.2]
Mar. '15	41	17	42	24.9	[24.1 25.7]	35	40	25	31.4	[30.5 32.3]	45.1	[42.8 47.4]
Nov. '15	88	12	0	23.3	[22.9 23.8]	82	17.9	0.1	21.5	[21.1 21.9]	45.3	[44.5 45.9]
Total	63	16	21	22.9	[22.4 23.3]	55	27	18	24.3	[23.9 24.7]	47.2	[46.5 47.8]

The percentage of particles beached (%Bch), afloat (%Flt), and on the open boundary (%Opn) are summarized separately for backward and forward trajectories. The bootstrap estimates of the average time from source to sighting location and sighting location to sink (T_{avg}) and the 95% confidence intervals (T_{ci}) are also reported. The average residence time (T_{res}) indicates the average time required to travel from a coastal sink to a coastal source.

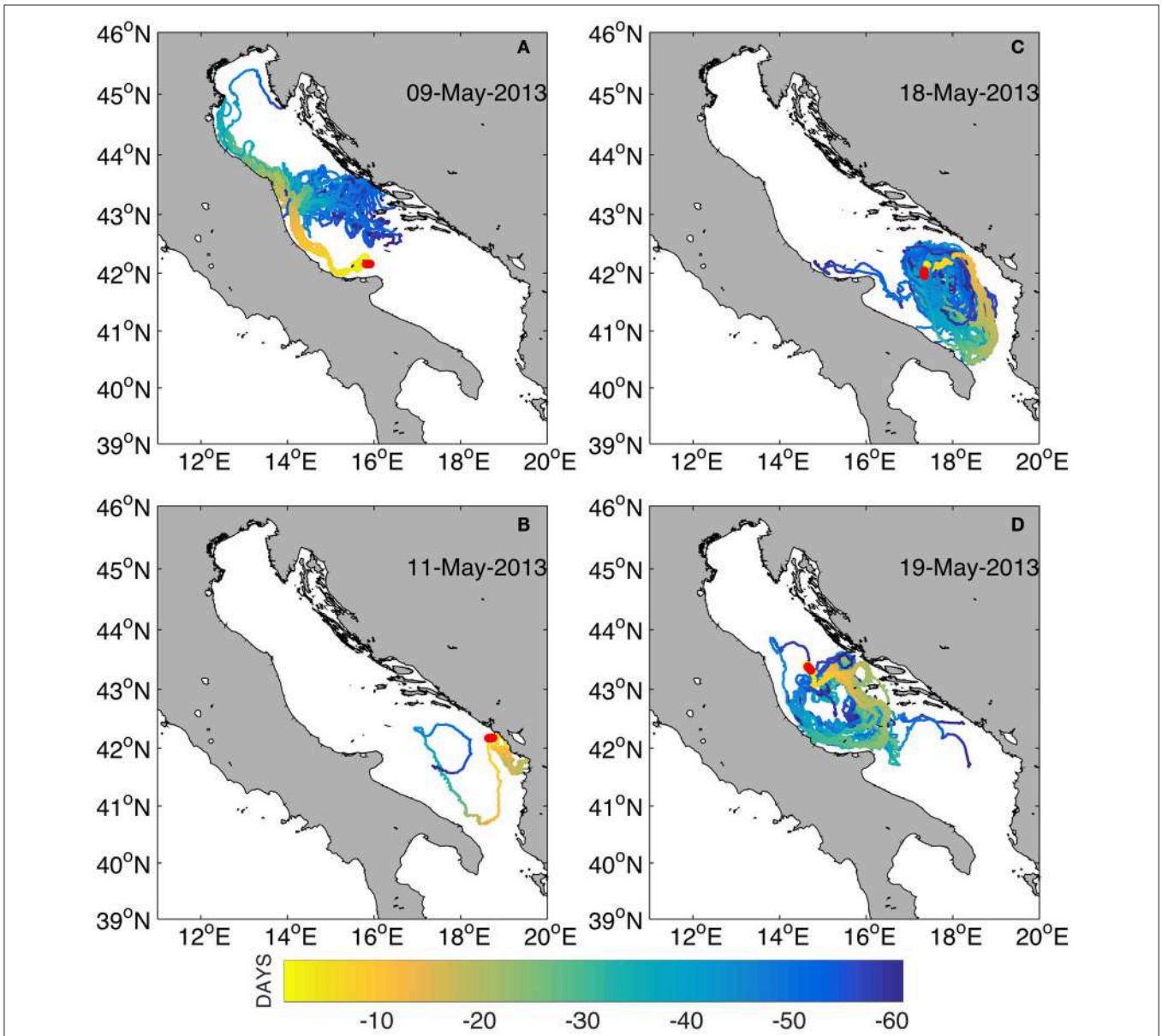

FIGURE 2 | Selected backward particle trajectories based on observations of floating anthropogenic marine debris on 9 May 2013 (A), 11 May 2013 **(B)**, 18 May 2013 **(C)**, and 19 May 2013 **(D)**. The release locations are indicated by red circles and the color scale corresponds to time in days since initial release.

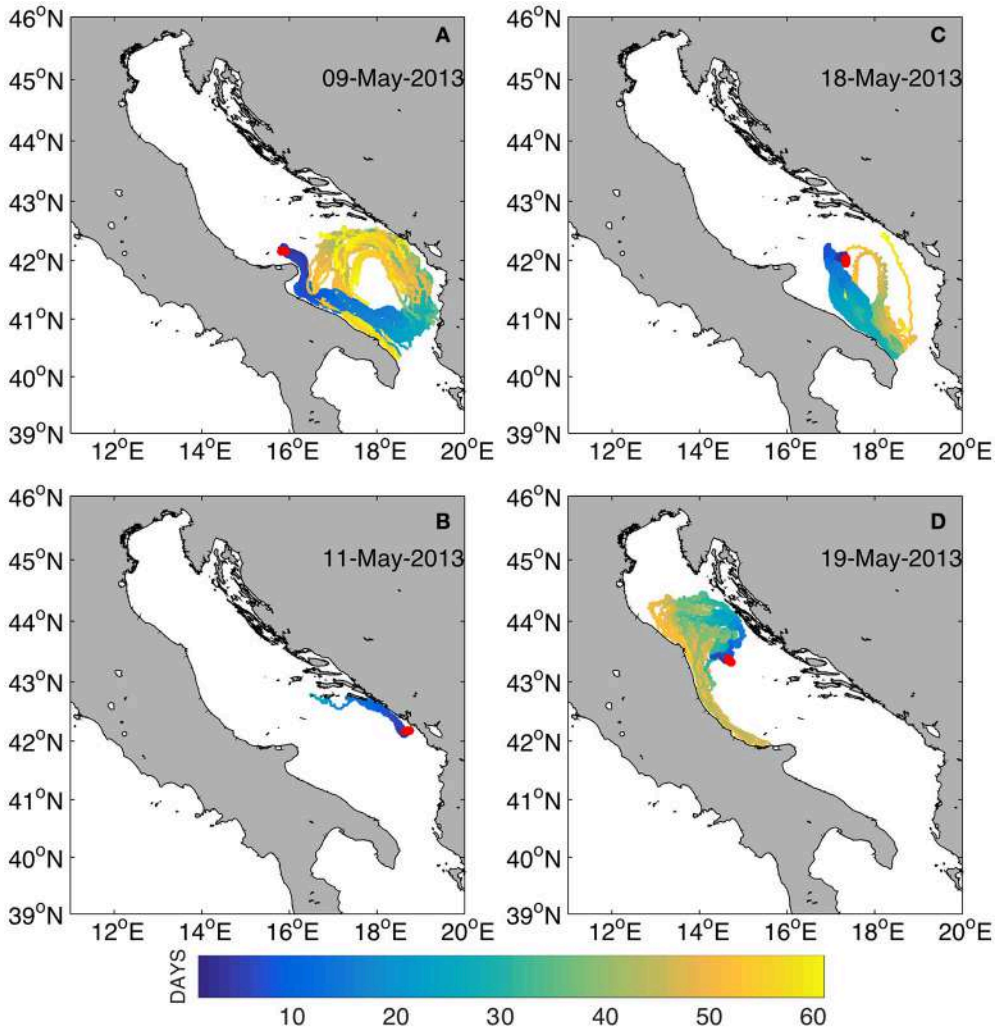

FIGURE 3 | Selected forward particle trajectories based on observations of floating anthropogenic marine debris on 9 May 2013 (A), 11 May 2013 **(B)**, 18 May 2013 **(C)**, and 19 May 2013 **(D)**. The release locations are indicated by red circles and the color scale corresponds to time in days since initial release.

tracking scheme was validated by Carlson et al. (2016) by comparing virtual particle trajectories to observed surface drifter trajectories. Thus, the strengths and weaknesses of the model, in a Lagrangian sense, were known *a priori* in this case. The main weaknesses of the model are the drifter-particle separation rate and the difficulty in reproducing observed Lagrangian transport around the many small islands found in the eastern Adriatic Sea. Furthermore, considering that flows become non-linear close to shore, the dynamics of debris in these boundary areas are not included in this modeling. Particles are not re-floated or reflected at the boundaries and no attempts are made to model sub-grid-scale processes, windage, or degradation of AMD. Stagnation at a solid boundary signifies beaching (Lebreton et al., 2012; Mansui et al., 2015) and particles that encountered the open boundary are marked as having left the basin and are excluded from subsequent analyses. While these processes are undoubtedly important, the uncertainty associated with each parameter remains quite large (Critchell and Lambrechts, 2016). Furthermore, we did not use subgrid processes parametrization under 2 km because the parameters of subgrid processes are basically unknown at those scales and we would have added further uncertainty in the results (Griffa, 1996; Haza et al., 2012; Carlson et al., 2016).

Observed AMD positions, times and abundances are used to specify initial positions of virtual particles, which are tracked for 60 days forward and backward in time (120 days total). Transects within 4 km (2 grid points) of the AdriaROMS boundaries were discarded. Of the 120 transects conducted, 75 were located within the model domain and recorded non-zero AMD abundances. The number of particles, N_p, to be released along each transect is defined as:

$$N_p = D \times L \times W \tag{2}$$

where D, L, and W correspond to the observed AMD abundance for a given transect (items km^{-2}), transect length (km), and transect width, respectively. Here, we set $W = 0.2$ km, as

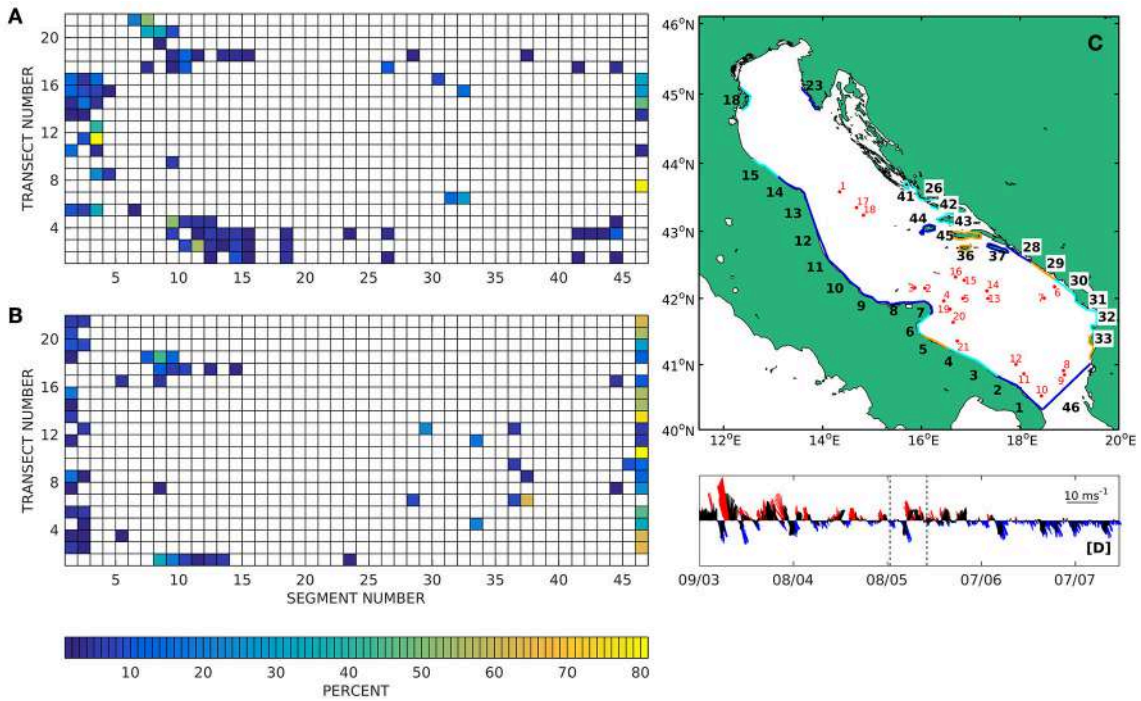

FIGURE 4 | Percentages of particles from a given transect (rows) that reach a given coastal segment (columns) for backwards (A) and forwards **(B)** trajectories computed from the May 2013 debris observations. **(C)** Coastline segments that served as both sources and sinks are plotted in dark blue. Light blue segments acted as sources only and orange segments acted as sinks. Transect locations and numbers are shown in red. **(D)** Stick plot of winds during the particle tracking experiment. Red (blue) indicates Sirocco (Mistral) winds and the vertical dashed lines denote the time period of the AMD observations.

the majority of debris sighted in Suaria and Aliani (2014) were within 100 m of the observer. In other words, while most of the AMD was observed along either a 10 m or 30 m strip width, the abundance estimates are assumed to be representative of a 100 m strip on either side of the vessel. Particles are distributed randomly in each polygon and released at the mid-point of the transect. A sensitivity test (not shown) using particles distributed uniformly along the transect line showed no differences. In total, 9,398 particles were released, with the number of particles per transect varying from 20 to 1693.

2.5. Analysis Methods

Potential near-shore sources and sinks are identified by dividing the Adriatic coastline into 50 km segments (**Figure 1B**). The model domain extends to the 5 m isobath, thereby preventing identification of actual terrestrial sources and sinks. Islands large enough to be resolved by AdriaROMS model are also included, resulting in 64 coastal segments. Small islands with short coastlines, like Tremiti and Palagruza, are not included in the analysis. The open boundary at the Otranto Strait is treated as a single segment, for a total of 65 segments. For clarity, only segments that served potential sources or sinks are shown. Percentages of particles beached, afloat, and that encounter the open boundary in backward and forward time are reported. The connection percentage, or percentage of particles reaching a coastline segment from a given transect, provides indications of coastal areas that could serve as sources and sinks.

The residence time is defined as the total duration of a particle in the Adriatic marine environment and is the sum of the time afloat in backwards and forwards time. Particles that remained afloat at the end of the $\pm$ 60 day integration period were not included in estimates of the residence time. Bootstrap estimates of the averages (Efron and Tibshirani, 1986) are used as the distributions of residence times are non-normal.

3. RESULTS

3.1. Floating Debris Survey

While this paper focuses on using observed AMD abundances to initialize a particle tracking model, we briefly summarize the visual survey observations. Overall, 120 visual transect surveys were performed during the three cruises, covering a total length of 922.2 km. A total of 1,364 macro AMD objects were observed floating on the Adriatic. On average, the highest AMD abundances were observed in March 2015 in the southern gyre (**Figure 1A**, **Table 1**). In May 2013 litter abundances were significantly lower than in both March ($p = 0.0016$; Mann-Whitney U test with Bonferroni correction) and November–December 2015 ($p = 0.008$). On the other hand, no significant difference was found between the two surveys carried out in 2015 ($p = 0.926$). The available data cannot easily explain the differences in abundances observed in the three surveys as different regions of the Adriatic Sea were sampled in different seasons over two separate years.

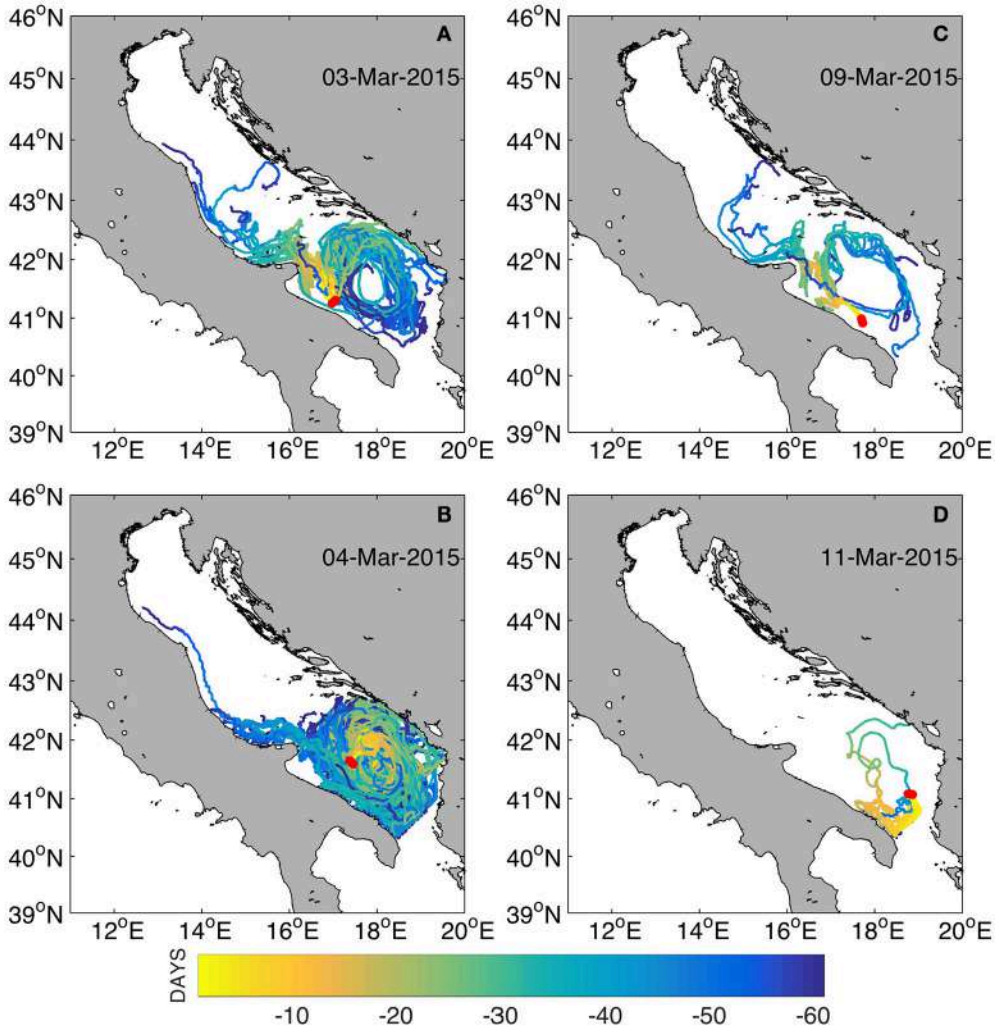

FIGURE 5 | Selected backwards particle trajectories based on observations of floating anthropogenic marine debris on 3 March 2015 (A), 4 March 2015 **(B)**, 9 March 2015 **(C)**, and 11 March 2015 **(D)**. The release locations are indicated by red circles and the color scale corresponds to time in days since initial release.

3.2. Debris Tracking

3.2.1. May 2013: Central and Southern Adriatic Sea

Sixty two, twenty five, and thirteen percent of backward particle beached, remained afloat, or encountered the open boundary, respectively (**Table 2**). The average time from source to sighting location was 22.8 days. The forward trajectories suggest significant export, with 46% of particles encountering the open boundary. 41% of particles beached and 13% were still afloat after 60 days. The average time from sighting location to a coastal sink was approximately 39 days.

Example backward trajectories reveal spatial and temporal variability in surface transport pathways. AMD observed 9 May 2013 at approximately 42° N, 16° E (**Figure 2A**) were transported by the EAC, the central cyclonic sub-gyre, and the WAC while debris observed 9 days later and about 100 km to the east (42° N, 17° E) originated almost exclusively from the southern cyclonic sub-gyre (**Figure 2C**). AMD observed near the east coast originated from the nearby coastline and were transported by the EAC, with a small subset from the southern sub-gyre (**Figure 2B**). Backwards trajectories suggest that AMD observed 19 May at approximately 15° N, 43.5° E originated from the east and west coasts and were transported in the cyclonic central sub-gyre.

Example forward trajectories show the influence of the same large-scale features, namely the EAC, WAC, and the southern gyre (**Figures 3A–C**). However, AMD observed 19 May at approximately 15° N, 43.5° E traveled north toward the Croatian coastline before looping west until they were entrained in the WAC and transported alongshore toward the Gargano Peninsula (**Figure 3D**).

The backwards and forwards connection percentages show that a continuous 400 km stretch of the central Italian coast (segments 7–14) acted as both sources and sinks (**Figure 4**). Segment 4, near Bari, provided more than 80% of the AMD sighted on transect 11. Much of the Croatian shoreline acted as

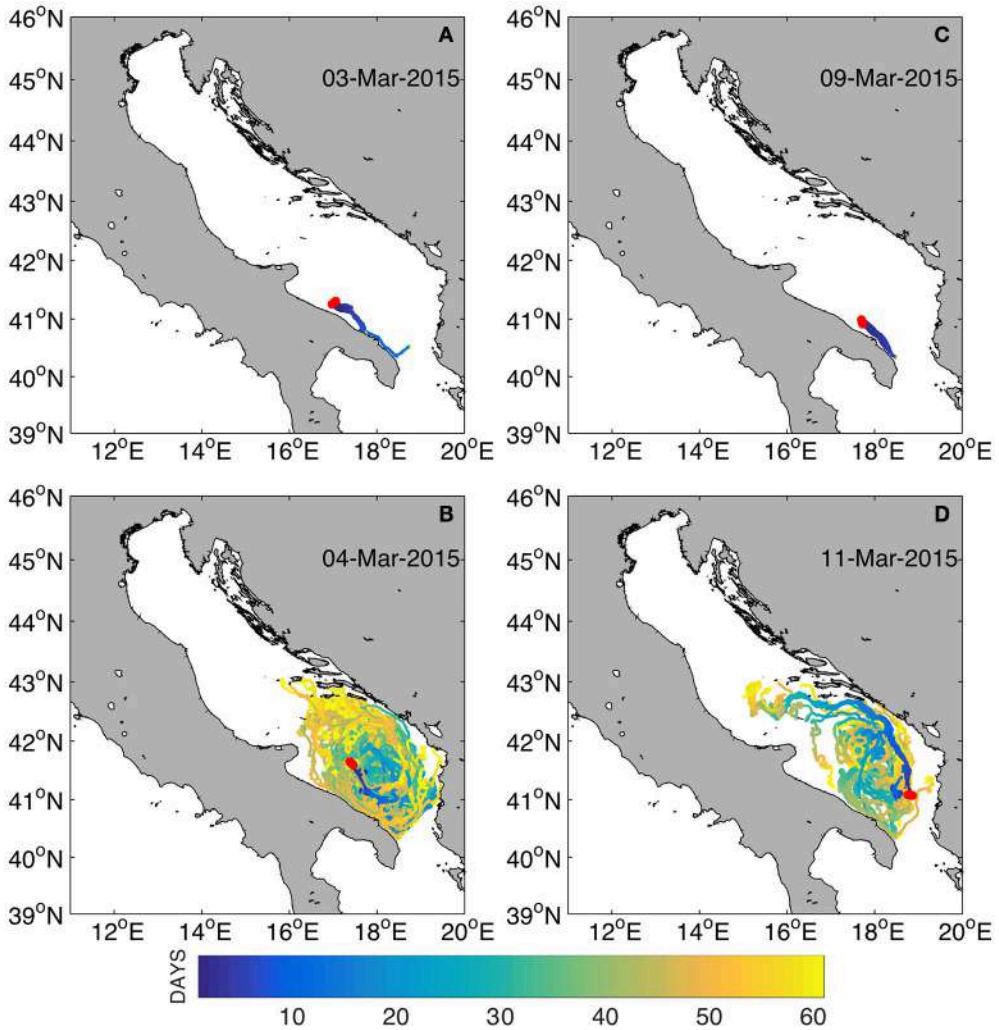

FIGURE 6 | Selected forward particle trajectories based on observations of floating anthropogenic marine debris on 3 March 2015 (A), 4 March 2015 **(B)**, 9 March 2015 **(C)**, and 11 March 2015 **(D)**. The release locations are indicated by red circles and the color scale corresponds to time in days since initial release.

both source and sink as well. Import and export of observed AMD across the open boundary is also likely, with large connection percentages observed along the open boundary segment for both backward and forward particle trajectories.

Winds during the backwards trajectories (9 March–9 May) were highly variable with several strong, sustained Sirocco events interspersed with weaker Mistral winds (**Figure 4D**). Winds remained variable, with a weaker Sirocco event, during visual debris sightings before transitioning to weaker, but more persistent Mistral winds from June to August 2013 (**Figure 4D**). Particles afloat after −60 days were distributed between the central and southern cyclonic sub-gyres while the 13% of particles afloat after +60 days were concentrated largely in the southern gyre (**Figures 11A,B**).

3.2.2. March 2015: Southern Adriatic Sea

Forty one, seventeen, and forty two percent of backwards particles beached, remained afloat, and originated from the open boundary, respectively, within −60 days of observation (**Table 2**). The average time from source to sighting location was 25 days. Thirty five, forty, and twenty five percent of forward particles beached, remained afloat, and reached the open boundary, respectively, within +60 days of observation. The average time from sighting location to coastal sink was 31.4 days. Example backwards trajectories reveal the influence of the southern cyclonic gyre and, to a lesser extent, the WAC and EAC (**Figure 5**). Forward trajectories suggest export via the WAC (**Figures 6A,C**) and recirculation in the southern gyre accompanied by limited exchange with the central Adriatic via the EAC (**Figures 6B,D**).

Connection percentages (**Figure 7**) show that a 200 km stretch of the Italian coastline from the Otranto Strait to south of the Gargano Peninsula (segments 1–5) acted as both sources and sinks for the observed debris. The central Italian coastline, from the Gargano Peninsula to Conero (segments 7–13) acted as sources. Much of the central, eastern coast, from 42°N to 44°N

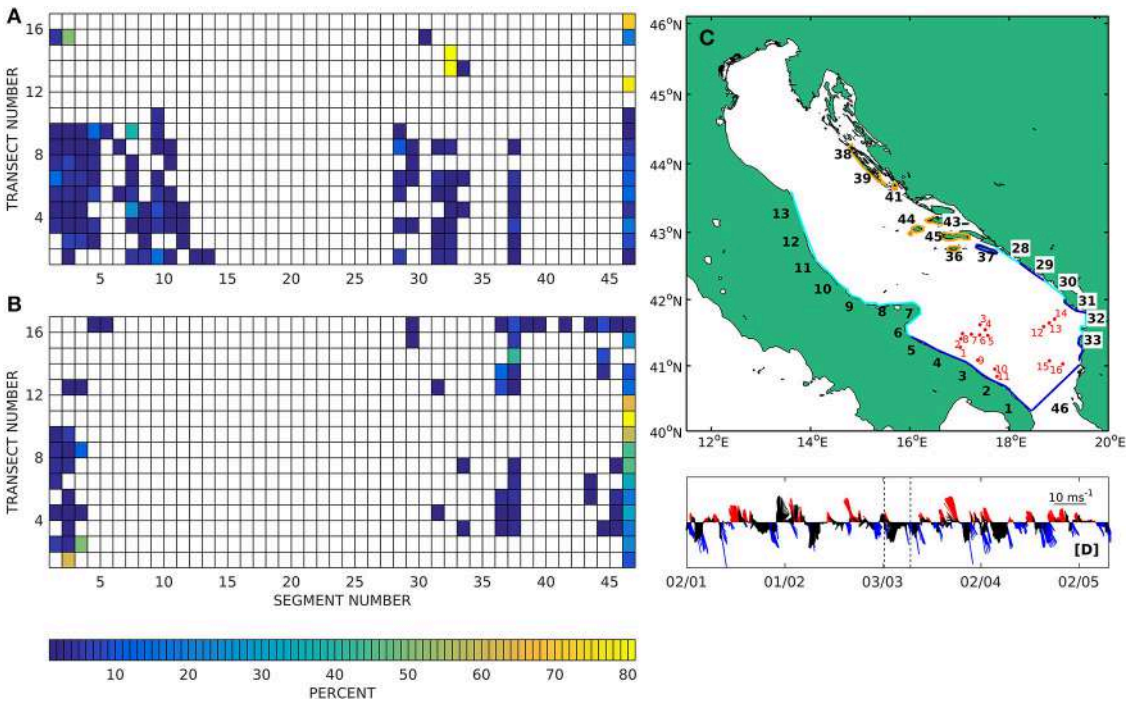

FIGURE 7 | Percentages of particles from a given transect (rows) that reach a given coastal segment (columns) for backward (A) and forward **(B)** trajectories computed from the March 2015 debris. **(C)** Coastline segments that served as both sources and sinks are plotted in dark blue. Light blue segments acted as sources only and orange segments acted as sinks. Transect locations and numbers are shown in red. **(D)** Stick plot of winds during the particle tracking experiment. Red (blue) indicates Sirocco (Mistral) winds and the vertical dashed lines denote the time period of the AMD observations.

acted as sinks. The southeastern coast acted as sources and sinks, with segment 33 on the Albanian coast providing over 80% of debris sighted on transects 13 and 14. Winds throughout the entire period were highly variable, with alternating Mistral and Sirocco events (**Figure 7D**).

3.2.3. November 2015: Northern Adriatic Sea

Backwards particle trajectories suggest that sighted debris originated within the Adriatic, as none of the particles came from the open boundary (**Table 2**, **Figures 8**, **10A**). Eighty eight and twelve percent of backwards particles were beached and still afloat, respectively, within −60 days of sighting (**Table 2**). The average time from source to sighting location was approximately 23 days. Example backward trajectories illustrate the complex, unpredictable nature of Lagrangian transport (**Figure 8**). Particles were transported by the EAC and the northern arm of the central cyclonic gyre, as well as the southern gyre (**Figure 8**). Backwards connection percentages confirm that most of the sighted debris originated from the central and northern Adriatic (**Figure 10A**). On the central Italian coastline, the most active source regions were segments 10 and 14 (**Figure 10A**). In the northern Adriatic, the Istrian Peninsula was also an active source (segments 21–24). Segment 38 was the most active source on the east coast, corresponding to the Croatian Island of Dugi otok.

Forward trajectories also remained largely in the Adriatic region, with 82% beached and 17.9% afloat within +60 days of sighting (**Table 2**). A very small subset (0.1%) of forward particles reached the open boundary. The average time from coastal sink to sighting location was 21.5 days. Example forward trajectories show unexpected northward transport (**Figure 9A**) and recirculation (**Figure 9B**), as well as more typical alongshore transport in the WAC (**Figures 9C,D**). Connection percentages show that the central and southern Italian coastline acted as sinks, with the Po River delta (segment 18) and the northern Gargano Peninsula (segments 7–8) receiving much of the sighted debris (**Figure 10B**). Strong Sirocco wind events were likely responsible for deviations from mean circulation patterns. For example, the reversal of particles observed in forward particles (**Figure 9A**) was likely driven by upwelling-favorable Sirocco winds (**Figure 10D**).

3.3. General Summary

Overall, the observed AMD originated largely from coastal segments near population centers and major rivers and was transported by the cyclonic surface circulation until either stranding, exiting the Adriatic, or recirculating in the southern gyre (**Figures 2–9**). Overall, 63, 16, and 21% of backwards particles beached, remained afloat, or originated from the open boundary, respectively (**Table 2**). In forward time, 55, 27, and 18% of particles beached, remained afloat, or were transported to the open boundary. The average residence time was 47.2 days and was slightly longer in forward time (24.3 days) when compared to backward time (22.9 days).

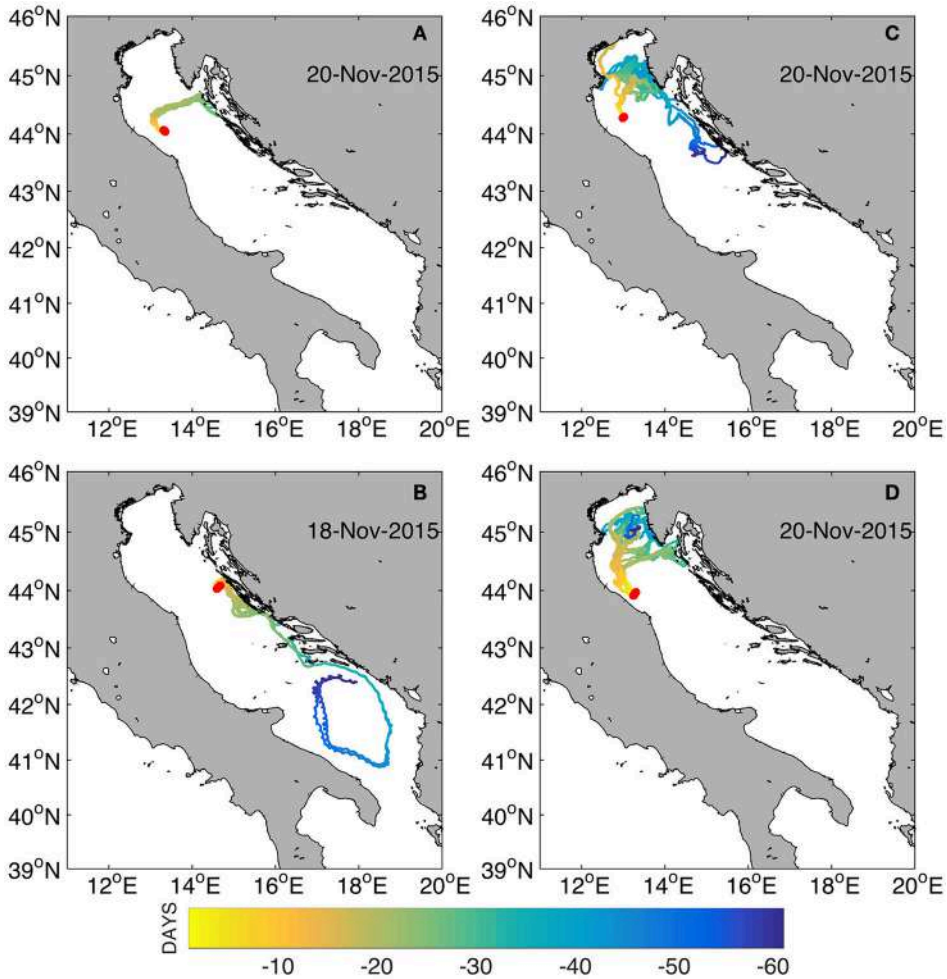

FIGURE 8 | Selected backwards particle trajectories based on observations of floating anthropogenic marine debris on 20 November 2015 (A), 18 November 2015 **(B)**, 20 November 2015 **(C)**, and 20 November 2015 **(D)**. The release locations are indicated by red circles and the color scale corresponds to time in days since initial release.

Of the 64 coastal segments used to identify possible sources and sinks of floating AMD in the Adriatic Sea, 41 segments acted as sources and 32 acted as sinks (**Figure 1**). The Venice lagoon segment did not serve as a source or sink for the observed floating AMD in any of the three experiments. The remaining unaffected coastal segments were concentrated in the northeastern Adriatic on the inshore, eastern sides of islands and peninsulas (**Figure 1**).

The results suggest that the central and southern gyres could have supplied AMD in May 2013 and March 2015 (**Figure 11**). Similarly, particles remained in the southern gyre in all three experiments after +60 days, suggesting that these regions can act as retention zones. However, the finite and relatively short integration period does not accurately reflect the lifetimes of AMD, especially plastics, and this restriction is addressed in Section 4.2.

4. DISCUSSION

The results suggest that the proposed methodology can advance the study and mitigation of marine debris by removing an often unrealistic and limiting assumption about abundances and source locations of macro debris. Here we discuss Adriatic-specific results and general aspects of the proposed methodology separately, and then propose improvements.

4.1. The Adriatic Sea

Potential coastal sources and sinks of floating AMD in the Adriatic Sea were identified using a two-way Lagrangian particle tracking model that was initialized by observed locations and times of debris abundances. Particle trajectories were computed using Equation 1 largely for simplicity but also because the Lagrangian validation presented in Carlson et al. (2016) suggests that an advective scheme is sufficient. Inclusion of a stochastic term complicates backwards particle tracking (see Section 4.2) and near-shore stochastic motion could cause a particle to erroneously "jump" onto, or off of, land (Carlson et al., 2010). Windage and degradation are not considered as the effects of both variables on the transport of AMD are still poorly understood (Yoon et al., 2010; Critchell and Lambrechts, 2016). As such, the results presented here are most applicable to buoyant AMD with

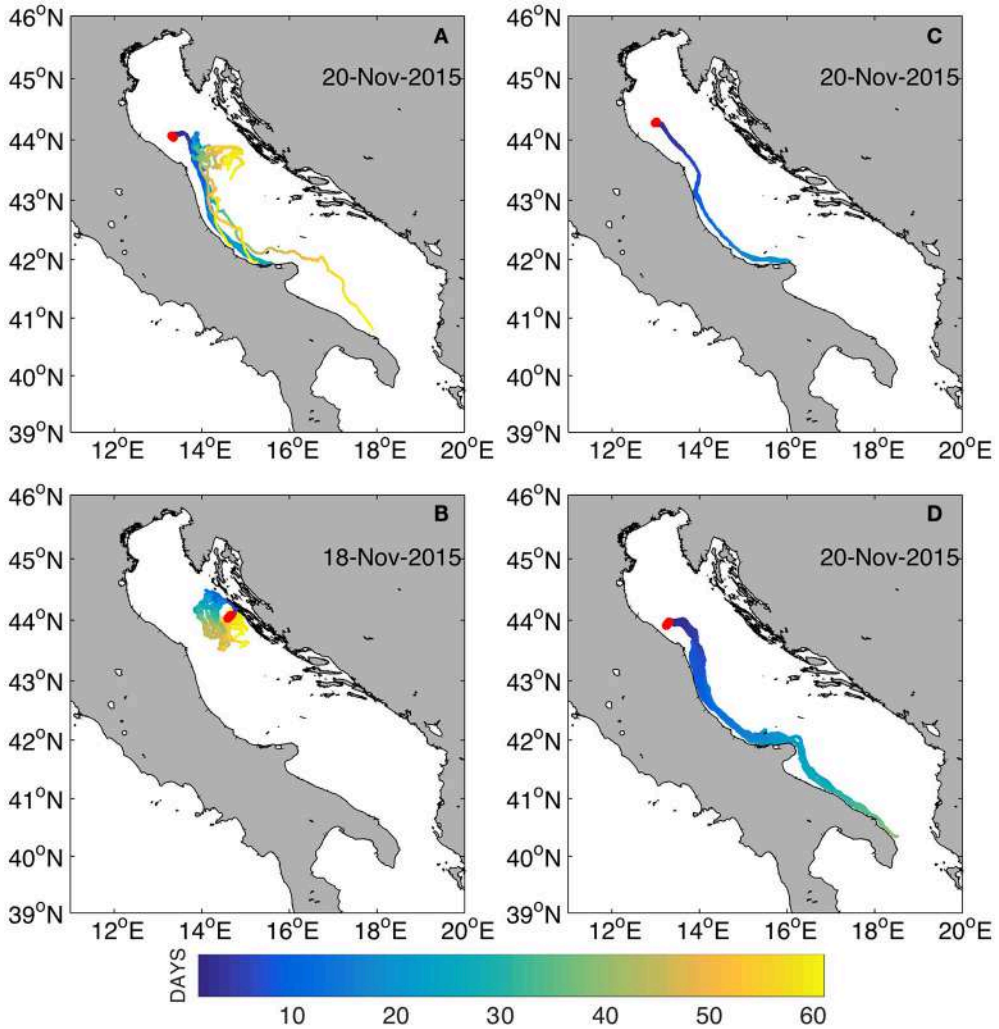

FIGURE 9 | Selected forward particle trajectories based on observations of floating anthropogenic marine debris on 20 November 2015 (A), 18 November 2015 **(B)**, 20 November 2015 **(C)**, and 20 November 2015 **(D)**. The release locations are indicated by red circles and the color scale corresponds to time in days since initial release.

minimal above-water surface area, such as fragments made of polyethylene and polypropylene, which indeed represent the two most abundant polymers found in surface waters worldwide, as well as in the Mediterranean Sea (Suaria et al., 2016).

The 60 day integration time scale was chosen based on the average half-life of drifters and particles, drifter-particle separation rates (Carlson et al., 2016), and transit times reported in the literature. A ∼45 day half-life of both drifters (Poulain, 2001) and virtual particles (Liubartseva et al., 2016) supports the 60 day integration time, allowing sufficient time for a particle to transit the Adriatic Sea while still maintaining a somewhat realistic trajectory.

The 5 m minimum depth of the AdriaROMS domain necessitates the use of a commonly-used, but physically unrealistic, assumption about beaching. Specifically, particles that stagnate on the boundary are treated as beached. Additionally, the model domain does not extend to the northern Ionian Sea and particles stagnate on the open boundary and cannot technically leave, nor re-enter the Adriatic Sea. As a result, the origin/fate of approximately 20% of particles from both backward and forward trajectories cannot be determined. Similarly, particles that remained afloat after ±60 days provide no definitive information about sources or sinks of the sighted debris. Additionally, the model domain does not extend to the shoreline and, therefore, result in additional uncertainty in the source and sink estimates.

The transport pathways, residence times, and probable sources and sinks identified agree well with previous studies of the surface circulation (Poulain, 1999, 2001; Ursella et al., 2006; Poulain and Hariri, 2013; Carlson et al., 2016) and marine debris (Liubartseva et al., 2016) in the Adriatic Sea. Carlson et al. (2016) also reported average transit times of 20–60 days from a

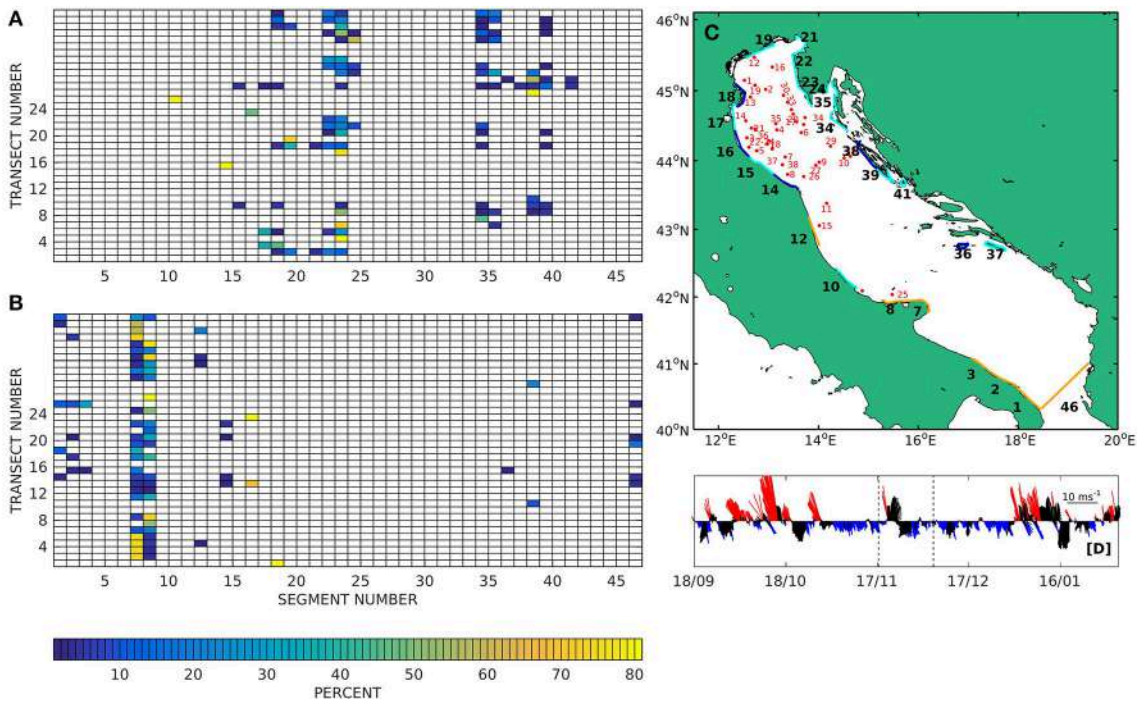

FIGURE 10 | Percentages of particles from a given transect (rows) that reach a given coastal segment (columns) for backward (A) and forward **(B)** trajectories computed from the November 2015 debris. **(C)** Coastline segments that served as both sources and sinks are plotted in dark blue. Light blue segments acted as sources only and orange segments acted as sinks. Transect locations and numbers are shown in red. **(D)** Stick plot of winds during the particle tracking experiment. Red (blue) indicates Sirocco (Mistral) winds and the vertical dashed lines denote the time period of the AMD observations.

coastal region in the northwest Adriatic to a coastal region in the southwest. Liubartseva et al. (2016) attempted to identify sources and sinks, as well as AMD concentrations in marine areas (see Section 2.1). The results presented here are derived from a simple advective Lagrangian particle tracking scheme and are consistent with the findings of Liubartseva et al. (2016), which were based on relatively complex Markov chain and ensemble techniques. Liubartseva et al. (2016) found high concentrations along the northwest coast as well as enhanced concentrations in the gyres during winter and higher concentration near the southeastern coast in fall. Their results also show qualitative agreement with the debris observation in **Figure 1A**, upon which our study is based. The main difference is the lack of debris originating from and traveling to the Venice coastal segment, which may simply be due to the timing and location of the debris surveys, pointing to the need for additional measurements to support the modeling component.

Finally, the application of the methodology to the Adriatic represents opportunistic synergy of marine litter surveys and Lagrangian particle tracking. The debris surveys were not designed with a modeling component in mind nor was the model designed to include beaching or stranding of debris, or export from the basin. Using observed abundances also limits the total number of particles available for analysis thereby impacting the statistical significance of the results. Improvements to the Adriatic implementation include higher resolution observations and velocity fields, validation of particle tracking results using observations of stranded debris, and resolution of near-shore dynamics. While the debris survey data used here represent the most comprehensive observations of floating macro debris in the Adriatic Sea, gaps exist in both space and time (**Figure 1A**). These biases are evident in complex, semi-enclosed basins like the Adriatic Sea where the mesoscale dominates the variability in the surface transport (Carlson et al., 2016).

4.2. General Assessment

While global and country-specific production, consumption, and disposal rates of plastic are available (Lebreton et al., 2012; Hardesty et al., 2015; Jambeck et al., 2015; Liubartseva et al., 2016), reliable estimates of the spatial and temporal distributions of plastic sources are lacking (Reisser et al., 2013). As a result, modeling studies often assume population-dependent, time-invariant AMD input (Lebreton et al., 2012; Liubartseva et al., 2016) or use spatially uniform initial positions (Yoon et al., 2010; Mansui et al., 2015). The consequences of such deployment schemes cannot be assessed until more reliable estimates of source locations and injection rates become available.

The proposed methodology merits continued development given the satisfactory agreement with previous studies in terms of identifying potential coastal source and sink regions as well as residence times (Poulain, 1999, 2001; Poulain and Hariri, 2013; Carlson et al., 2016; Liubartseva et al., 2016). The main deficiencies identified in Section 4.1 are not unique to the Adriatic Sea and should be addressed to maximize

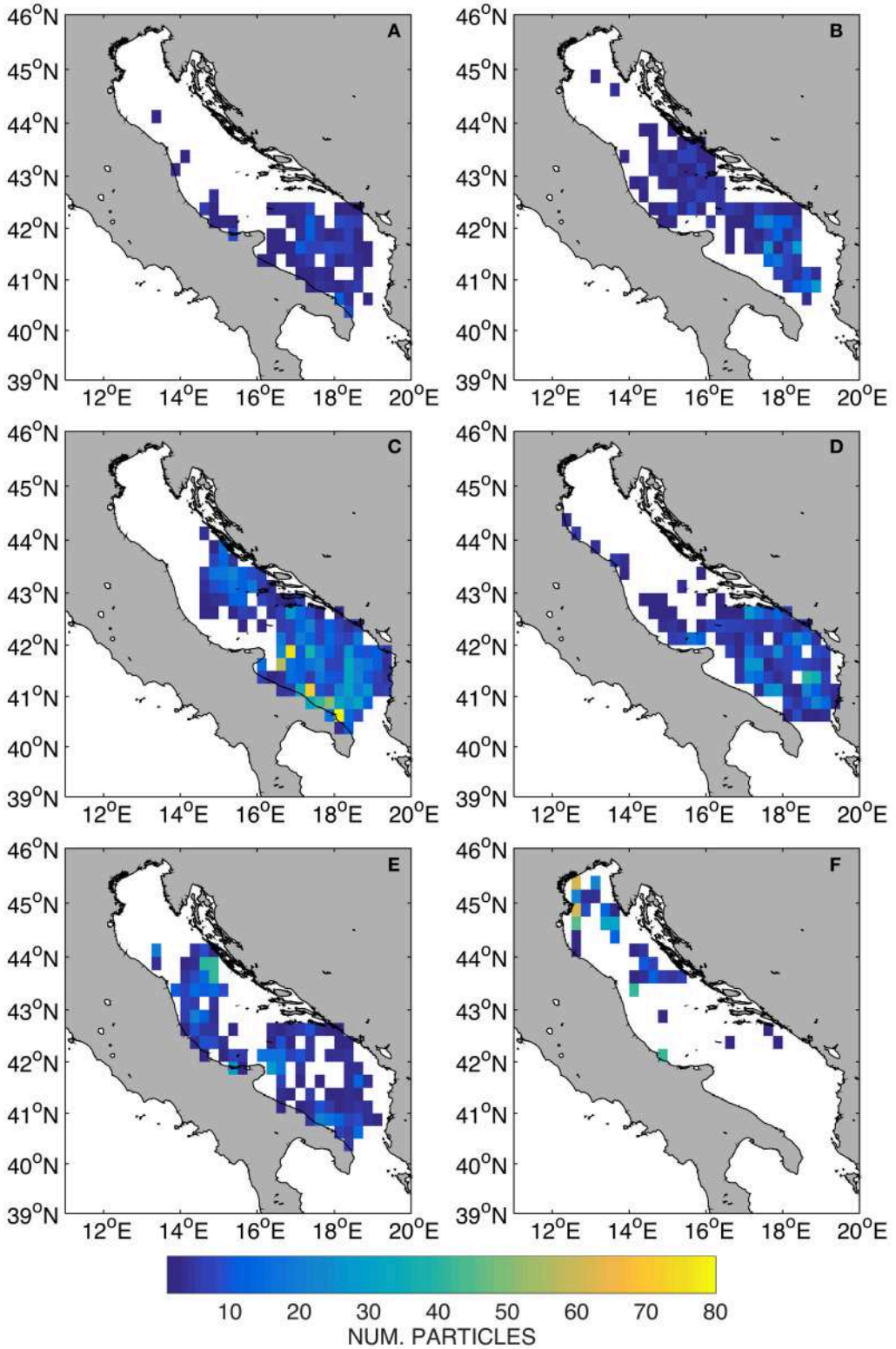

FIGURE 11 | The number of particles per $\frac{1}{4}^{\circ}$ bin reveals the spatial distribution particles still afloat after 60 days in forward (left column) and backward (right column) time for debris observed in May 2013 (A,B), March 2015 **(C,D)**, and November 2015 **(E,F)**.

the potential of this method. Successful implementation of the methods demonstrated here will require observations of actual AMD abundances (Hardesty et al., 2015), high-resolution ocean models, observations of beaching and re-floating of debris over a wider range of coastline types (sandy beaches, rocky shores, marshes, etc.), and improved parameterizations of AMD lifetimes, degradation rates, windage, etc.

Boundary conditions in current Lagrangian particle tracking models poorly represent interactions of real AMD with actual shorelines. This, combined with the limited ability of most models to resolve nearshore dynamics, results in unrealistic numerical representations of beaching/stranding and re-floating of AMD. Beaching is a complex process that depends on a combination of coastline type, bathymetry, waves, winds, and tides, and other factors. Furthermore, cross-shore velocities outside the surf zone tend to be small (Largier, 2003) and "sticky waters" have been observed to retain tracers some distance offshore (Restrepo et al., 2014).

The temporal and spatial resolutions of the velocities employed in the particle tracking model must also adequately resolve the most energetic circulation features. However, even high-resolution models cannot resolve motion at the scales relevant to actual debris (mm to m). As a result, sub-grid-scale motions are often represented by adding a stochastic term to the particle velocities (Carlson et al., 2010; Fredj et al., 2016). Such an approach assumes that the flow can be decomposed into either a mean or "large-scale" component and a perturbation (Falco et al., 2000; Carlson et al., 2010). However, no clear separation has been observed in the wave number-frequency spectrum calling into question such an assumption (Carlson et al., 2010). Furthermore, the most common implementation of stochastic Lagrangian models assumes constant, isotropic eddy diffusivity, which may not be appropriate, especially near shore. The type of stochastic model, i.e., random walk or random flight, also depends on the statistics of the perturbation term (Carlson et al., 2010), a fact that is often glossed over in applied settings. Finally, a stochastic term complicates backwards particle tracking as the integration is no longer a reversible process. Thus, Lagrangian modeling of AMD, while a potentially powerful management tool, can be complicated by a number of factors, including assumptions about the amount of AMD and source regions, debris behavior parameters, and the proper sub-grid-scale turbulence parameterization.

Lagrangian evaluations of ocean model performance are also lacking (Zambianchi et al., 2017). As the transport of marine debris is inherently a Lagrangian problem, both ocean models and debris transport models should be evaluated more extensively using Lagrangian observations (Hardesty et al., 2017). Lagrangian assessments typically compare surface or drogued drifter trajectories to virtual particle trajectories (Liu and Weisberg, 2011; Carlson et al., 2016), yet quantitative comparisons between drifter and AMD trajectories over large distances in oceanic environments have not yet been reported. Parameterizations of AMD behavior (i.e., windage, degradation, and settling) also require validation (Critchell and Lambrechts, 2016). The proposed methodology can be implemented in any region where both AMD surveys are conducted and a high-resolution numerical model solution is in place.

AUTHOR CONTRIBUTIONS

Visual surveys of floating debris were performed by GS, TF, and VM. EF developed the particle tracking scheme and analysis methods. AR ran the ocean and atmospheric models. DC performed the particle tracking and analysis. DC and GS prepared the bulk of the manuscript. DC, GS, SA, AG, EF, AR, and TF contributed to the experimental design and editing of the manuscript for publication.

FUNDING

Funding for ship-time was provided through EU FP-7 project COCONET (Grant Agreement No. 287844), the SOLEMON survey was supported by the FAOADRIAMED regional project. VM was supported by the DeFishGear (Derelict Fishing Gear Management System in the Adriatic Region) IPA Adriatic strategic project 1 str/00010 implemented with co-funding by the European Union, Instrument for Pre-Accession Assistance (IPA).

ACKNOWLEDGMENTS

The authors are thankful to crews and officers of RV Urania, RV Minerva Uno, and RV G. Dallaporta.

REFERENCES

Aliani, S., and Molcard, A. (2003). Hitch-hiking on floating marine debris: macrobenthic species in the western Mediterranean Sea. *Hydrobiologia* 503, 59–67. doi: 10.1023/B:HYDR.0000008480.95045.26

Artegiani, A., Bregant, D., Paschini, E., Pinardi, N., Raicich, F., and Russo, A. (1997). Applications of stochastic particle models to oceanographic problems. *J. Phys. Oceanogr.* 27, 1515–1532.

Avio, C. G., Gorbi, S., and Regoli, F. (2015). Experimental development of a new protocol for extraction and characterization of microplastics in fish tissues: first observations in commercial species from Adriatic Sea. *Mar. Environ. Res.* 111, 18–26. doi: 10.1016/j.marenvres.2015.06.014

Benetazzo, A., Carniel, S., Sclavo, M., and Bergamasco, A. (2013). Wave-current interaction: effect on the wave field in a semi-enclosed basin. *Ocean Model.* 70, 152–165. doi: 10.1016/j.ocemod.2012.12.009

Blašković, A., Fastelli, P., Čižmek, H., Guerranti, C., and Renzi, M. (2017). Plastic litter in sediments from the Croatian marine protected area of the natural park of Telaščica bay (Adriatic Sea). *Mar. Pollut. Bull.* 114, 583–586. doi: 10.1016/j.marpolbul.2016.09.018

Carlson, D., Griffa, A., Zambianchi, E., Suaria, G., Corgnati, L., Magaldi, M., et al. (2016). Observed and modeled surface Lagrangian transport between coastal regions in the Adriatic Sea with implications for marine protected areas. *Cont. Shelf Res.* 118, 23–48. doi: 10.1016/j.csr.2016.02.012

Carlson, D. F., Fredj, E., Gildor, H., and Rom-Kedar, V. (2010). Deducing an upper bound to the horizontal eddy diffusivity using a stochastic

Lagrangian model. *Environ. Fluid Mech.* 10, 499–520. doi: 10.1007/s10652-010-9181-0

Critchell, K., Grech, A., Schlaefer, J., Andutta, F., Lambrechts, J., Wolanski, E., et al. (2015). Modelling the fate of marine debris along a complex shoreline: lessons from the Great Barrier Reef. *Estuar. Coast. Shelf Sci.* 167, 414–426. doi: 10.1016/j.ecss.2015.10.018

Critchell, K., and Lambrechts, J. (2016). Modelling accumulation of marine plastics in the coastal zone; what are the dominant physical processes? *Estuar. Coast. Shelf Sci.* 171, 111–122. doi: 10.1016/j.ecss.2016.01.036

Efron, B., and Tibshirani, R. (1986). Bootstrap methods for standard errors, confidence intervals, and other measures of statistical accuracy. *Stat. Sci.* 1, 54–77. doi: 10.1214/ss/1177013815

Falco, P., Griffa, A., Poulain, P.-M., and Zambianchi, E. (2000). Transport properties in the Adriatic Sea as deduced from drifter data. *J. Phys. Oceanogr.* 30, 2055–2071. doi: 10.1175/1520-0485(2000)030<2055:TPITAS>2.0.CO;2

Fredj, E., Carlson, D. F., Amitai, Y., Gozolchiani, A., and Gildor, H. (2016). The particle tracking and analysis toolbox (PaTATO) for Matlab. *Limnol. Oceanogr. Methods* 14, 586–599. doi: 10.1002/lom3.10114

Gajšt, Tamarat, T., Bizjak, T., Palatinus, A., Liubartseva, S., and Kržan, A. (2016). Sea surface microplastics in slovenian part of the northern adriatic. *Mar. Pollut. Bullet.* 113, 392–399. doi: 10.1016/j.marpolbul.2016.10.031

Galgani, F. (2015). Marine litter, future prospects for research. *Front. Mar. Sci.* 2:87. doi: 10.3389/fmars.2015.00087

Galgani, F., Hanke, G., Werner, S., Oosterbaan, L., Nilsson, P., Fleet, D., et al. (2013). *Monitoring Guidance for Marine Litter in European Seas.* JRC Scientific and Policy Reports, EUR 26113 EN, 120.

Galgani, F., Leaute, J., Moguedet, P., Souplet, A., Verin, Y., Carpentier, A., et al. (2000). Litter on the sea floor along European coasts. *Mar. Pollut. Bullet.* 40, 516–527. doi: 10.1016/S0025-326X(99)00234-9

Grati, F., Scarcella, G., Polidori, P., Domenichetti, F., Bolognini, L., Gramolini, R., et al. (2013). Multi-annual investigation of the spatial distributions of juvenile and adult sole (*Solea solea* L.) in the Adriatic Sea (northern Mediterranean). *J. Sea Res.* 84, 122–132. doi: 10.1016/j.seares.2013.05.001

Griffa, A. (1996). "Stochastic modeling in physical oceanography," in *Applications of Stochastic Particle Models to Oceanographic Problems*, Vol. 39, eds R. Adler, P. Müller, and B. L. V. Rozovskii (Boston, MA: Springer Science & Business Media), 114–140.

Haidvogel, D., Arango, H., Budgell, W., Cornuelle, B., Curchitser, E., Lorenzo, E. D., et al. (2008). Ocean forecasting in terrain-following coordinates: formulation and skill assessment of the regional ocean modeling system. *J. Comput. Phys.* 227, 3595–3624. doi: 10.1016/j.jcp.2007.06.016

Hardesty, B., Good, T., and Wilcox, C. (2015). Novel methods, new results and science-based solutions to tackle marine debris impacts on wildlife. *Ocean Coast. Manage.* 115, 4–9. doi: 10.1016/j.ocecoaman.2015.04.004

Hardesty, B., Harari, J., Isobe, A., Lebreton, L., Maximenko, N., Potemra, J., et al. (2017). Using numerical model simulations to improve the understanding of micro-plastic distribution and pathways in the marine environment. *Front. Mar. Sci.* 4:30. doi: 10.3389/fmars.2017.00030

Haza, A. C., Özgökmen, T. M., Griffa, A., Garraffo, Z. D., and Piterbarg, L. (2012). Parameterization of particle transport at submesoscales in the Gulf Stream region using Lagrangian subgridscale models. *Ocean Modell.* 42, 31–49. doi: 10.1016/j.ocemod.2011.11.005

Isobe, A., Kubo, K., Tamura, Y., Kako, S., Nakashima, E., and Fujii, N. (2014). Selective transport of microplastics and mesoplastics by drifting in coastal waters. *Mar. Pollut. Bullet.* 89, 324–330. doi: 10.1016/j.marpolbul.2014.09.041

Jambeck, J. R., Geyer, R., Wilcox, C., Siegler, T. R., Perryman, M., Andrady, A., et al. (2015). Plastic waste inputs from land into the ocean. *Science* 347, 768–771. doi: 10.1126/science.1260352

Kako, S., Isobe, A., Kataoka, T., and Hinata, H. (2014). A decadal prediction of the quantity of plastic marine debris littered on beaches of the East Asian marginal seas. *Mar. Pollut. Bullet.* 81, 174–184. doi: 10.1016/j.marpolbul.2014.01.057

Kako, S., Isobe, A., and Magome, S. (2010). Sequential monitoring of beach litter using webcams. *Mar. Pollut. Bullet.* 60, 775–779. doi: 10.1016/j.marpolbul.2010.03.009

Kako, S., Isobe, A., Magnome, S., Hinata, H., Seino, S., and Kojima, A. (2011). Establishment of numerical beach-litter hindcast/forecast models: an application to Goto Islands, Japan. *Mar. Pollut. Bullet.* 62, 293–302. doi: 10.1016/j.marpolbul.2010.10.011

Laglbauer, B. J., Franco-Santos, R. M., Andreu-Cazenave, M., Brunelli, L., Papadatou, M., Palatinus, A., et al. (2014). Macrodebris and microplastics from beaches in Slovenia. *Mar. Pollut. Bullet.* 89, 356–366. doi: 10.1016/j.marpolbul.2014.09.036

Largier, J. (2003). Considerations in estimating larval dispersal distances from oceanographic data. *Ecol. Appl.* 13, S71–S89. doi: 10.1890/1051-0761(2003)013[0071:CIELDD]2.0.CO;2

Lazar, B., and Gračan, R. (2011). Ingestion of marine debris by loggerhead sea turtles, *Caretta caretta*, in the Adriatic Sea. *Mar. Pollut. Bullet.* 62, 43–47. doi: 10.1016/j.marpolbul.2010.09.013

Lebreton, L., Greer, S., and Borrero, J. (2012). Numerical modelling of floating debris in the world's oceans. *Mar. Pollut. Bullet.* 64, 653–661. doi: 10.1016/j.marpolbul.2011.10.027

Liu, Y., and Weisberg, R. H. (2011). Evaluation of trajectory modeling in different dynamic regions using normalized cumulative Lagrangian separation. *J. Geophys. Res. Oceans* 116, C09013. doi: 10.1029/2010jc006837

Liubartseva, S., Coppini, G., Lecci, R., and Creti, S. (2016). Regional approach to modeling the transport of floating plastic debris in the Adriatic Sea. *Mar. Pollut. Bullet.* 103, 115–127. doi: 10.1016/j.marpolbul.2015.12.031

Magaldi, M., Özgökmen, T., Griffa, A., and Rixen, M. (2010). On the response of a turbulent coastal buoyant current to wind events: the case of the western Adriatic current. *Ocean Dyn.* 60, 93–122. doi: 10.1007/s10236-009-0247-9

Mansui, J., Molcard, A., and Ourmières, Y. (2015). Modelling the transport and accumulation of floating marine debris in the Mediterranean basin. *Mar. Pollut. Bullet.* 91, 249–257. doi: 10.1016/j.marpolbul.2014.11.037

Maximenko, N., Hafner, J., and Niiler, P. (2012). Pathways of marine debris derived from trajectories of Lagrangian drifters. *Mar. Pollut. Bullet.* 65, 51–62. doi: 10.1016/j.marpolbul.2011.04.016

Mazzariol, S., Di Guardo, G., Petrella, A., Marsili, L., Fossi, C. M., Leonzio, C., et al. (2011). Sometimes sperm whales (*Physeter macrocephalus*) cannot find their way back to the high seas: a multidisciplinary study on a mass stranding. *PLoS ONE* 6:e19417. doi: 10.1371/journal.pone.0019417

Munari, C., Corbau, C., Simeoni, U., and Mistri, M. (2016). Marine litter on Mediterranean shores: analysis of composition, spatial distribution and sources in north-western Adriatic beaches. *Waste Manage.* 49, 483–490. doi: 10.1016/j.wasman.2015.12.010

Neumann, D., Callies, U., and Matthies, M. (2014). Marine litter ensemble transport simulations in the North Sea. *Mar. Pollut. Bullet.* 86, 219–228. doi: 10.1016/j.marpolbul.2014.07.016

Pasquini, G., Ronchi, F., Strafella, P., Scarcella, G., and Fortibuoni, T. (2016). Seabed litter composition, distribution and sources in the Northern and Central Adriatic Sea (Mediterranean). *Waste Manage.* 58, 41–51. doi: 10.1016/j.wasman.2016.08.038

Poppi, L., Zaccaroni, A., Pasotto, D., Dotto, G., Marcer, F., Scaravelli, D., et al. (2012). Post-mortem investigations on a leatherback turtle *Dermochelys coriacea* stranded along the northern Adriatic coastline. *Dis. Aquat. Org.* 100, 71–76. doi: 10.3354/dao02479

Poulain, P.-M. (1999). Drifter observations of surface circulation in the Adriatic Sea between December 1994 and March 1996. *J. Mar. Syst.* 20, 231–253. doi: 10.1016/S0924-7963(98)00084-0

Poulain, P.-M. (2001). Adriatic Sea surface circulation as derived from drifter data between 1990 and 1999. *J. Mar. Syst.* 29, 3–32. doi: 10.1016/S0924-7963(01)00007-0

Poulain, P.-M., and Hariri, S. (2013). Transit and residence times in the Adriatic Sea surface as derived from drifter data and Lagrangian numerical simulations. *Ocean Sci.* 9, 713–720. doi: 10.5194/os-9-713-2013

Pribanic, S., Holcer, D., and Miokovic, D. (1999). First report of plastic ingestion by striped dolphin (*Stenella coeruleoalba*) in the Croatian part of the Adriatic Sea. *Eur. Res. Cetaceans* 13, 443–446.

Putman, N. F., and He, R. (2013). Tracking the long-distance dispersal of marine organisms: sensitivity to ocean model resolution. *J. R. Soc. Interface* 10:20120979. doi: 10.1098/rsif.2012.0979

Reisser, J., Shaw, J., Wilcox, C., Hardesty, B., Proietti, M., Thums, M., et al. (2013). Marine plastic pollution in waters around Australia: Characteristics, concentrations, and pathways. *PLoS ONE* 8:e80466. doi: 10.1371/journal.pone.0080466

Restrepo, J., Venkataramani, S., and Dawson, C. (2014). Nearshore sticky waters. *Ocean Model.* 80, 49–58. doi: 10.1016/j.ocemod.2014.06.003

Russo, A., Carniel, S., and Benetazzo, A. (2013a). Support for ICZM and MSP in the Adriatic Sea region. *Sea Technol.* 54, 27–35.

Russo, A., Coluccelli, A., Carniel, S., Benetazzo, A., Valentini, A., Paccagnella, T., et al. (2013b). "Operational models hierarchy for short term marine predictions: the Adriatic Sea example," in *OCEANS, Bergen, 2013 MTS/IEEE*, 1–6. doi: 10.1109/OCEANS-Bergen.2013.6608139

Russo, A., Coluccelli, A., Iermano, I., Falcieri, F., Ravaioli, M., Bortoluzzi, G., et al., M. R. (2009). An operational system for forecasting hypoxic events in the northern Adriatic Sea. *Geofizika* 26, 191–213.

Shchepetkin, A., and McWilliams, J. (2005). The regional ocean modeling system (ROMS): a split-explicit, free-surface, topography-following-coordinate oceanic model. *Ocean Model.* 9, 347–404. doi: 10.1016/j.ocemod.2004.08.002

Slavin, C., Grage, A., and Campbell, M. (2012). Linking social drivers of marine debris with actual marine debris on beaches. *Mar. Pollut. Bullet.* 64, 1580–1588. doi: 10.1016/j.marpolbul.2012.05.018

Strafella, P., Fabi, G., Spagnolo, A., Grati, F., Polidori, P., Punzo, E., et al. (2015). Spatial pattern and weight of seabed marine litter in the northern and central Adriatic Sea. *Mar. Pollut. Bullet.* 91, 120–127. doi: 10.1016/j.marpolbul.2014.12.018

Suaria, G., and Aliani, S. (2014). Floating debris in the Mediterranean Sea. *Mar. Pollut. Bullet.* 86, 494–504. doi: 10.1016/j.marpolbul.2014.06.025

Suaria, G., Avio, C. G., Mineo, A., Lattin, G. L., Magaldi, M. G., Belmonte, G., et al. (2016). The Mediterranean Plastic Soup: synthetic polymers in Mediterranean surface waters. *Sci. Rep.* 6:37551. doi: 10.1038/srep37551

Ursella, L., Poulain, P.-M., and Signell, R. P. (2006). Surface drifter derived circulation in the northern and middle Adriatic Sea: response to wind regime and season. *J. Geophys. Res. Oceans* 111, C03S04. doi: 10.1029/2005JC003177

van Sebille, E., England, M. H., and Froyland, G. (2012). Origin, dynamics, and evolution of ocean garbage patches from observed surface drifters. *Environ. Res. Lett.* 7:044040. doi: 10.1088/1748-9326/7/4/044040

Vianello, A., Boldrin, A., Guerriero, P., Moschino, V., Rella, R., Sturaro, A., et al. (2013). Microplastic particles in sediments of Lagoon of Venice, Italy: first observations on occurrence, spatial patterns and identification. *Estuar. Coast. Shelf Sci.* 130, 54–61. doi: 10.1016/j.ecss.2013.03.022

Wieczorek, S., Campagnuolo, S., Moore, P., Froglia, C., Atkinson, R., Gramitto, E., et al. (1999). The composition and fate of discards from *Nephrops* trawling in Scottish and Italian waters. *EC Study Project Rep.* 96:092.

Yoon, J.-H., Kawano, S., and Igawa, S. (2010). Modeling of marine litter drift and beaching in the Japan Sea. *Mar. Pollut. Bullet.* 60, 448–463. doi: 10.1016/j.marpolbul.2009.09.033

Zambianchi, E., Trani, M., and Falco, P. (2017). Lagrangian transport of marine litter in the Mediterranean Sea. *Front. Environ. Sci.* 5:5. doi: 10.3389/fenvs.2017.00005

Conflict of Interest Statement: The authors declare that the research was conducted in the absence of any commercial or financial relationships that could be construed as a potential conflict of interest.

The reviewer CB declared a shared affiliation, though no recent collaboration, with two of the authors AG and SA to the handling Editor, who ensured that the process nevertheless met the standards of a fair and objective review.

frontiers in Marine Science

ORIGINAL RESEARCH
published: 20 June 2017
doi: 10.3389/fmars.2017.00191

Modeling the Fate and Distribution of Floating Litter Particles in the Aegean Sea (E. Mediterranean)

Dimitrios V. Politikos[1,2], *Christos Ioakeimidis*[1,3]*, *George Papatheodorou*[3] and *Kostas Tsiaras*[1]

[1] Hellenic Centre for Marine Research, Institute of Oceanography, Anavyssos, Greece, [2] Department of Environmental Sciences, Institute of Marine and Coastal Sciences, Rutgers University, New Brunswick, NJ, United States, [3] Laboratory of Marine Geology and Physical Oceanography, Department of Geology, University of Patras, Patras, Greece

A circulation model is coupled to a Lagrangian particle-tracking model to simulate the transport floating litter particles in the Aegean Sea, Greece (Eastern Mediterranean). Considering different source regions and release dates, simulations were carried out to explore the fate and distribution of floating litter over 1990–2009, taking into account the seasonal and interannual variability of surface circulation. Model results depicted recurrently high concentrations of floating litter particles in the North Aegean plateau, the Saronikos Gulf, and along Evia and Crete islands. Modeled transport pathways of floating litter demonstrated that source regions are interconnected, with Saronikos Gulf being a main receptor of litter from other sources. Notably higher percent of litter exit (∼35%) than enter the model domain (∼7%) signified that Aegean Sea seems to act as a source rather than receptor of floating litter pollution in the Eastern Mediterranean Sea. Beached litter was found around 10%, mostly located in the western part of the Aegean Sea. This is the first modeling study to explore the transport of floating marine litter in Greek waters.

Keywords: floating marine litter, particle-tracking model, Aegean Sea, fate, distribution, pathways

OPEN ACCESS

Edited by:
Christopher Kim Pham, University of the Azores, Portugal

Reviewed by:
Stefano Aliani, Consiglio Nazionale Delle Ricerche, Italy
Giovanni Coppini, Fondazione Centro Euro-Mediterraneo sui Cambiamenti Climatici, Italy
Joseph Harari, Instituto Oceanográfico da USP, Brazil

***Correspondence:**
Christos Ioakeimidis
cioakeim@hcmr.gr

Specialty section:
This article was submitted to Marine Pollution, a section of the journal Frontiers in Marine Science

Received: *29 November 2016*
Accepted: *01 June 2017*
Published: *20 June 2017*

Citation:
Politikos DV, Ioakeimidis C, Papatheodorou G and Tsiaras K (2017) Modeling the Fate and Distribution of Floating Litter Particles in the Aegean Sea (E. Mediterranean). Front. Mar. Sci. 4:191. doi: 10.3389/fmars.2017.00191

INTRODUCTION

Marine litter is a documented threat for marine and human life, being present in vast quantities in the marine and coastal environments (Barnes et al., 2009). Recent studies have estimated ∼5 trillion particles to be present into the world's oceans (Eriksen et al., 2014). Plastics typically enter the ocean from land- and marine-based sources, are carried via oceanic currents and dragged by winds, and finally accumulate in open sea and coastal regions (Galgani, 2015; Sebille et al., 2015; UNEP/MAP, 2016), after covering long and complex pathways (Maximenko et al., 2012; Ryan, 2015). Once deposited into the oceans, plastics are gradually fragmented into smaller particles (< 5 mm), due to the synergistic effect of environmental variables and the inherent material instability, and this forms floating marine debris (Thompson et al., 2004; Pastorelli et al., 2014). Floating litter items are found in oceans around the world, such as in the Pacific ocean (Martinez et al., 2009; Law et al., 2014), the southeast Atlantic gyre (Ryan, 2014), the North Atlantic sub-tropical gyre (Reisser et al., 2015), and the Mediterranean Sea (Suaria and Aliani, 2014; Cózar et al., 2015).

General circulation models linked to particle-tracking models are widely used to track the transport of different kinds of passive drifters in the marine environment, such as oil spill pollutants, fish eggs and larvae, marine debris, and buoys (Pollani et al., 2001; Lynch et al., 2014; Mansui et al., 2015). Marine litter modeling is a growing field aiming

at understanding of litter sources, fate, transport and accumulation in oceans (NOAA, 2016). Neumann et al. (2014) performed transport simulations, forward and backward in time, to identify accumulation and potential source regions of marine litter in the southern North Sea. Similarly, the drift and beaching of floating marine litter was examined numerically in the Sea of Japan (Yoon et al., 2010). Considering input of marine litter into the North Pacific Ocean by the 2011 Tohoku tsunami, Lebreton and Borrero (2013) suggested that tsunami debris would eventually accumulate to the North Pacific Ocean subtropical gyre. Finally, the study of Kubota (1994) simulated the trajectories of 50 virtual marine debris in the northern Hawaiian Islands and provided potential mechanisms of their accumulation, related to winds, geostrophic currents and Ekman drift.

Available Greek field data indicate that litter come from the Ionian Sea, Patraikos Gulf (Stefatos et al., 1999; Koutsodendris et al., 2008) and the Aegean Sea (Katsanevakis and Katsarou, 2004; Ioakeimidis et al., 2014, 2015; Papadopoulou et al., 2015). These studies have focused on detecting big marine litter items on the seafloor. In contrast, available data on floating litter distribution are scarce, and the ecological problem of floating litter transport and accumulation is largely unknown. Recently, Mansui et al. (2015) proposed specific gyres and regions that could retain and export floating items in the Mediterranean Sea. However, their model set up did not allow to properly resolve the litter dynamics in the Aegean Sea due to its complex coastline which includes hundreds of islands.

Extensive field studies have documented high concentrations of floating plastic pollution in the Mediterranean Sea (Cózar et al., 2015; Pedrotti et al., 2016). Concurrently, modeling studies have identified potential sites of floating litter accumulation in open sea and coastal areas in the Mediterranean Sea (Lebreton et al., 2012; Mansui et al., 2015; Liubartseva et al., 2016). In this study, we link a circulation model with a particle-tracking model to simulate the transport of floating litter particles in the Aegean Sea, Greece (Eastern Mediterranean). Source regions of litter were related to big cities, rivers, the inflow of Black Sea Waters through the Dardanelles strait, and open sea. Different release dates, on monthly and annual scales, were considered to explore the seasonal and interannual variability of floating litter drift over 1990–2009. The main objectives of the study are to: (1) investigate the fate and distribution of floating litter particles after being released from source regions, (2) explore whether and to what extent the Aegean Sea may act as a source or receptor of floating litter pollution in the Mediterranean Sea, and (3) depict the litter distribution in shoreline areas. This is the first modeling study discussing the transport of floating litter particles in the Greek waters.

MATERIALS AND METHODS

Study Area: The Aegean Sea

The Aegean Sea is located northwest of the Eastern Mediterranean basin, providing a strong hydrodynamic connection between the Eastern Mediterranean and the Black Sea through the Dardanelles Strait (**Figure 1**). The Aegean Sea exhibits a complicated physiography in terms of seafloor morphology and island configuration. It has an irregular and extended coastline and hundreds of islands scattered all over the region (Theocharis et al., 1993). The Aegean Sea can be divided in three broad areas: (a) the North Aegean Sea which consists of North Aegean trough, the Skyros basin and three main shelf areas: Thermaikos, Samothraki and Limnos; (b) the Central Aegean Sea which is characterized by the Chios basin; and (c) South Aegean Sea which shows a complex physiography consisting of the Myrtoan and Cretan basins, and the Cyclades plateau (**Figure 1**).

The general surface circulation of the Aegean Sea is characterized by complex patterns consisting of basin scale cyclonic flows, sub-basin scale recurrent gyres, transient eddies, and other mesoscale features. The inflow of low-salinity waters from the Black Sea (BSW), through the Dardanelles straits, is considered to be the most significant buoyant input into the Aegean Sea. The BSW subsequently flow westwards with bifurcations to the north toward the north Aegean plateau and to the southwest reaching the south Aegean Sea (Nittis and Perivoliotis, 2002). The northern part of the Aegean Sea is characterized by an overall cyclonic circulation with a semi-permanent large anticyclone, being present in the northeastern part which is significantly influenced by the inflow of low-salinity BSW (Olson et al., 2007). Other important mesoscale features are the cyclonic eddies in the Chios basin, the boundary current along the eastern coast of the Evia island, the Myrtoan Cyclone and the East Cretan Cyclone. The southern Aegean Sea circulation is characterized by two cyclonic gyres, two anticyclonic eddies and other smaller scale structures, interconnected by currents and jets, which are variable in space and time (Theocharis et al., 1999). **Figure 1** provides a schematic representation of the main features of the general surface circulation in the Aegean Sea.

Models

Circulation Model

A three-dimensional hydrodynamic model, based on the Princeton Ocean Model (POM, Blumberg and Mellor, 1983), was used to obtain the surface water circulation in the Aegean Sea. POM is a widely used community model (http://www.ccpo.odu.edu/POMWEB/) with numerous applications both for ocean and regional modeling studies. POM has been implemented in the Mediterranean Sea at basin/sub-basin scale (Zavatarelli and Mellor, 1995; Horton et al., 1997; Korres and Lascaratos, 2003, among others) and also on regional studies, including the Aegean Sea (Korres et al., 2010; Androulidakis et al., 2012; among others). It is a primitive equation, sigma coordinate and free surface elevation model that employes a 2.5 turbulence closure scheme (Mellor and Yamada, 1982) for vertical mixing.

The hydrodynamic model domain extends from the East (19.5°–30°) to the North (30°–41°), with a horizontal resolution of 1/15° (∼7.5 Km), 25 sigma layers in the vertical, a logarithmic distribution near the surface and bottom, and a time step of 12 min for the external and internal modes. The hydrodynamic properties along the model's open boundaries (eastern/western) are obtained from a basin scale Mediterranean hydrodynamic

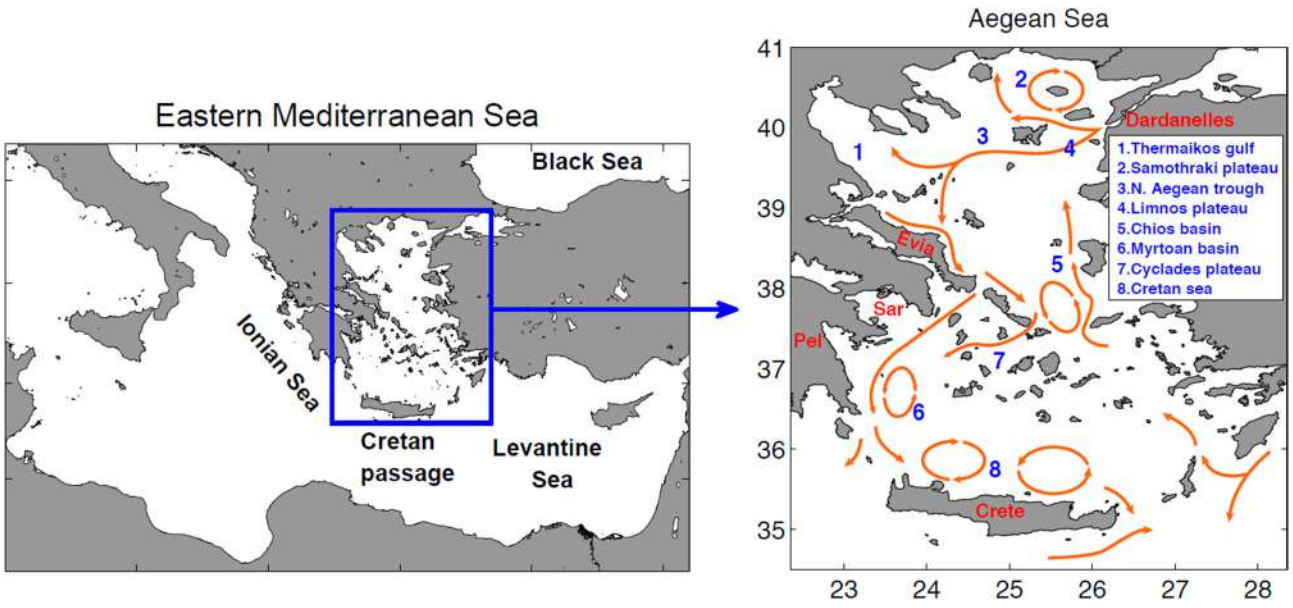

FIGURE 1 | Map of the Aegean Sea. Numbers 1 to 8 denote major basins, gulfs and plateaus, and abbreviations denote place names: Peloponnese (Pel), Saronikos Gulf (Sar), Evia island, Dardanelles strait and Crete island. Schematic representation of the general Aegean Sea upper circulation is also shown (**Map modified after** Nittis and Perivoliotis, 2002; Nittis et al., 2003; Olson et al., 2007).

model (Korres et al., 2007) simulation over the same period. The Dardanelles water exchange (surface inflow of BSW, subsurface outflow of Aegean water) is parameterized through a two-layer open boundary condition (Nittis et al., 2003), with prescribed water inflow/outflow and salinity adopting seasonal climatological data (Tugrul et al., 2002). The atmospheric forcing was obtained from HIRHAM5 climate model hindcast simulation over a 20-year (1990–2009) period (Christensen et al., 2006), downscaling ERA-interim dataset to 1/10° resolution. The heat and freshwater fluxes, at the air-sea interface, are calculated using hourly fields of wind velocity (10 m), relative humidity (2 m), air temperature (2 m), precipitation, net incoming short wave radiation and incoming long wave radiation, using properly tuned bulk formulae set (Korres and Lascaratos, 2003). The circulation model implemented in this study has been validated through various applications with finer (e.g., Kourafalou et al., 2006; Korres et al., 2010) or coarser horizontal resolution (Korres et al., 2007; Tsiaras et al., 2014). The same model is currently operational with a slightly higher resolution (1/30°) as part of the POSEIDON forecasting system (www.poseidon.hcmr.gr).

Particle-Tracking Model

Simulations were conducted using the Lagrangian model described in Pollani et al. (2001). In this study, floating litter particles were treated as passive drifters, exclusively driven by surface circulation and diffusion. We did not include other particle properties (e.g., oil evaporation, vertical dispersion and emulsification, wave drift) used in Pollani et al. (2001) for oil spill prediction. Thus, the horizontal advection of a particle is defined by the surface current velocities provided by the POM. The position of a particle is updated in two dimensions, as follows:

$$x(t+dt) = x(t) + u(x,y,t) * dt + R_x * \sqrt{6 * K_h * dt}$$
$$y(t+dt) = y(t) + v(x,y,t) * dt + R_y * \sqrt{6 * K_h * dt},$$

where (x, y) define the two-dimension position of the particle, dt is the time step, (u, v) are the surface current velocities in x, y dimensions, K_h is the horizontal diffusion coefficients, which is dynamically computed in the hydrodynamic model, and (R_x, R_y) are random numbers distributed between -1 and $+1$.

Simulations

Marine litter usually enters the ocean from land-based (e.g., riverine inputs, large cities, ports) and sea-based sources (e.g., straits, shipping, fisheries) (Yoon et al., 2010; Lebreton et al., 2012; Galgani, 2015; Liubartseva et al., 2016; UNEP/MAP, 2016). In this study, five regions in the Aegean Sea (**Table 1**, letters: A, B, C, D, E; **Figure 2**) have been selected as the major sources to initiate the simulations around which particles were uniformly distributed. Two additional marine litter sources outside the Aegean Sea (**Figure 2** and **Table 1**, letters: F and G) were also considered to study the hypothesis if Eastern Mediterranean Sea could act as a source of floating litter for the Aegean Sea.

To investigate the fate and distribution of floating litter particles, we conducted three experiments (**Table 1**). All experiments were run for 1 year. We then repeated the annual simulations for multiple years (from 1990 to 2009) to take into account the inter-annual variability of surface circulation in our analysis. The particle-tracking model was on-line coupled with

TABLE 1 | Model setup describing source regions and experiments.

Setups	Description
Source regions	Release points A, B, C, D, E, F and G are shown in **Figure 2**.
A	Axios River, City of Thessaloniki, Thessaloniki Port, Major Commercial Fishing Ground.
B	Strymonas and Nestos Rivers, City of Kavala, Port of Kavala, Major Commercial Fishing Ground.
C	Evros River, Major Commercial Fishing Ground.
D	Black Sea Water inflow through Dardannelles Strait.
E	Saronikos Gulf, City of Athens, Piraeus Port.
F	Southwest of the Aegean Sea.
G	Southeast of the Aegean Sea.
Experiments	All the runs repeated annually from 1990 to 2009.
Experiment A	
Case A1	Particles initiated on January-1 from sources A,B,C,D,E and tracked for1 year.
Case A2	Particles initiated on April-1 from sources A,B,C,D,E and tracked for 1 year.
Case A3	Particles initiated on July-1 from sources A,B,C,D,E and tracked for 1 year.
Case A4	Particles initiated on October-1 from sources A,B,C,D,E and tracked for 1 year.
Experiment B	Particles initiated first of each month (January to December) from sources A to E; simulation period is 1 year.
Experiment C	Particles initiated first of each month (January to December) from sources F to G; simulation period is 1 year.

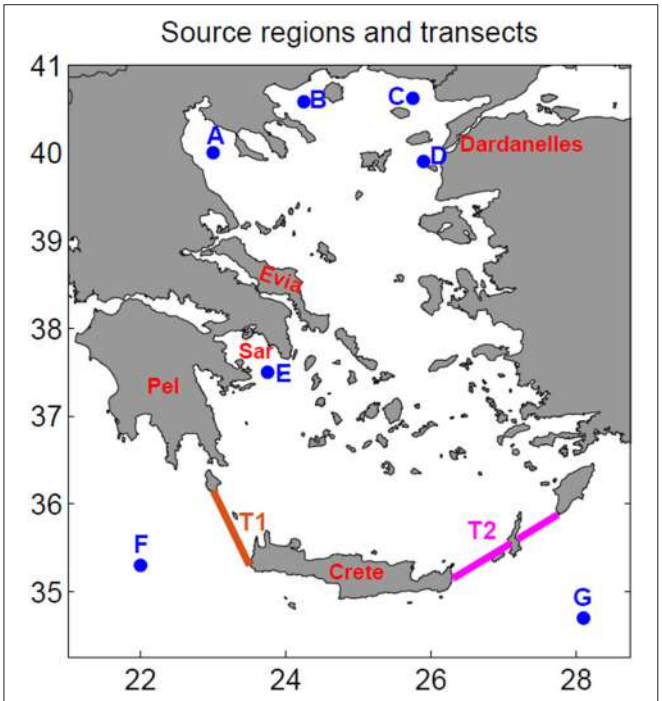

FIGURE 2 | Letters A,B,C,D,E,F, and G denote considered source regions of floating litter. Two transects, marked as T1 (orange) and T2 (magenta) lines, are used to compute the floating litter exchange between the Aegean Sea and the Eastern Mediterranean Sea.

the circulation model and resolved with a 12 min time step; outputs were saved and plotted daily, and a total number of 9,000 particles was considered sufficient to obtain a statistically valid representation of the results, while maintaining a reasonable computational cost. The setup of the three experiments is as follows:

Experiment A

Particles are released from the sources A, B, C, D, and E (**Figure 2**), assuming four different release dates; i.e., January 1st (Case A1), April 1st (Case A2), July 1st (Case A3), and October 1st (Case A4) (**Table 1**). The goal is to track the fate and distribution of floating litter particles, after being released from the source regions. Different release dates aimed to explore the role of the surface circulation seasonal variability on particle drift. The main interest of this experiment is to explore the contribution of source regions to the final concentration of particles in specific areas.

Experiment B

Particles are released from sources A, B, C, D, and E (**Figure 2**), on the first of every month and tracked for 1 year. The objective is to identify areas in which particles tend to concentrate, considering a more realistic scenario of periodic inputs of litter in the model domain.

Experiment C

Particles are released from sources F and G (**Figure 2**) on the first of every month along and tracked for 1 year. The objective is to test to what extent the Aegean Sea may act as a receptor of floating litter particles originated outside the Aegean Sea.

Stranding of particles is not included in our simulations, so when particles were found on land cells due to random movement, they were bounced back to the sea, still considered to be part of the computational process. A particle is marked as "beached" if it drifted in cells adjacent to land, following Lebreton et al. (2012). However, beached particles may still drift at any point of the simulation process, during which offshore surface currents occur. The number of beached litter particles was calculated to assess the distribution of floating litter along shoreline areas.

Outputs

Average and standard deviation maps of particle distribution were produced over 1990–2009 period, on a grid of 30 × 90 cells. Then, these maps were combined to classify the distribution of particles into three categories: recurrent, occasional and rare. To accomplish this, each cell was assigned to a category following the classification approach presented in Saraux et al. (2014). This classification has been previously applied on multi-annual fish egg distribution data to characterize favorable spawning habitats (Bellier et al., 2007; Giannoulaki et al., 2013; Saraux et al., 2014). The approach assumes that cells with high mean and low standard deviation are considered as recurrent, signifying high concentration of litter particles for most of the years. Cells with high standard deviation are considered as occasional, implying that litter particles are not necessarily found every year. Cells with low mean and medium standard deviation are defined as rare, implying that litter particles are rarely found in these areas.

The limiting thresholds, which define low and high values for the average and standard deviation maps, were calculated using K-means clustering algorithm (Jain, 2010). K-means provides partitions of a given data set into a number of clusters, and provides cluster indices for each data point. K-means is applied on the average and standard deviation maps, assuming three clusters. This results in cut-off points which define intervals of low, medium and high values, based on the number of particles found in the cells for the average map, and the values of standard deviation for the standard deviation map. The calculations were performed with k-means clustering function provided from Matlab R2012 (www.Mathworks.com). The code is available upon request. The threshold values that define the classification areas are listed in **Table A.1** (Appendix A).

Two transects, marked as T1 (orange) and T2 (green) lines (**Figure 2**), were used to calculate the percentage of particles daily exiting the Aegean Sea from the western and eastern part, respectively; these particles were considered as "escaped." The variability in percentage of escaped particles from repeated annual simulation over 1990–2009 was represented with boxplots. In addition, particles found below 33°N, western of 19°E, or eastern of 30°E were considered as "lost"; the movement of these particles was detained during the analysis of the results.

RESULTS

Simulated Circulation in the Aegean Sea

Seasonal averages of the simulated near surface circulation, were calculated over the 1990–2009 period (**Figure 3**). As a validation exercise, simulated drifter tracks with the present model were compared (**Figure 4**) against available observed drifters in the North Aegean during 2002 (Olson et al., 2007), adequately reproducing known circulation features, discussed below. The overall cyclonic circulation simulated in the Aegean Sea is in agreement with previous observations (Theocharis and Georgopoulos, 1993; Olson et al., 2007). This is related to the northward flow of more saline water from the Levantine sea, carried out by a branch of the Asia Minor current along the eastern side of the Aegean and particularly to the pathway of low-salinity BSW (**Figures 3B–D**). Simulated current fields depict that BSW, initially spreads westwards branching around Limnos Island and then either follows a pathway to the west toward Evia island and Thermaikos Gulf (**Figures 3B–D**, **4C,D**) or to the North East, forming the semi-permanent Samothraki anticyclone from July to October (**Figures 3C,D**, **4B**). This pathway agrees with observations obtained by Olson et al. (2007) and Zervakis and Georgopoulos (2002). In autumn, and particularly during the summer period, the BSW moves mostly south of Limnos Island in accordance with Zervakis and Georgopoulos (2002), due to strong northerly Etesian winds creating a larger anticyclone covering the entire North East area. The westward BSW branch flows either toward the Thermaikos Gulf or directly to the west, in both cases resulting in the formation of a southward coastal current along Evia (**Figures 3A,B,D**, **4A**) consistent with Olson et al. (2007). In January and October (**Figures 3A,D**), this Evia jet appears stronger in the model simulation, passing toward the Southern Aegean Sea mainly through the strait south of Evia Island, while in spring and summer (**Figures 3B,C**), there is a more diffuse flow from Cyclades plateau, contributed also by redirected Levantine water from the Eastern Aegean.

Other known circulation features reproduced by the model are the permanent cyclonic gyre in Chios basin (Nittis and Perivoliotis, 2002; Olson et al., 2007), the Skyros cyclonic eddy (Olson et al., 2007) and the cyclonic circulation in Sporades basin (Kontoyiannis et al., 2003). The later has been found to be occasionally anticyclonic (Olson et al., 2007), as simulated during July (**Figure 3C**). The Myrtoan cyclone (Nittis and Perivoliotis, 2002) is mainly reproduced during winter, while it has been occasionally observed to turn into anticyclonic during spring and autumn (Olson et al., 2007; Sayin et al., 2011). The known cyclonic circulation in the Cretan Sea (Nittis and Perivoliotis, 2002) is also partly reproduced, along the dominant eastward current on the coast of Crete island (**Figure 3**).

Distribution of Floating Litter Particles

The combination of average and standard deviation maps of particle distributions over 1990–2009, resulted in classification maps associated with recurrent, occasional and rare presence of floating litter particles (**Figure 5**). For Cases A1-A4, high concentration of litter particles was found in areas closely related to the southward pathway of waters from the North Aegean Sea, where the most important sources of floating litter particles were located. These areas include the North Eastern Aegean Sea, receiving inputs from Evros/Strymonikos Rivers and the Dardanelles strait, with the semi-permanent anticyclonic circulation in Samothraki and Limnos plateau resulting in the relatively higher residence time of litter particles. Other areas where litter were found to accumulate are the Sporades basin and the eastern coast of Evia, being in the pathway of waters coming from North Eastern Aegean Sea, including BSW, and also receiving inputs from the Thermaikos Gulf. Further south, increased litter particle accumulation was found in the Saronikos Gulf and the Myrtoan basin, and occasionally in the Cyclades plateau and the Cretan Sea.

The release of particles on monthly basis, assumed in Experiment B, resulted in high concentration of floating litter particles in the North Aegean plateau, the Myrtoan basin

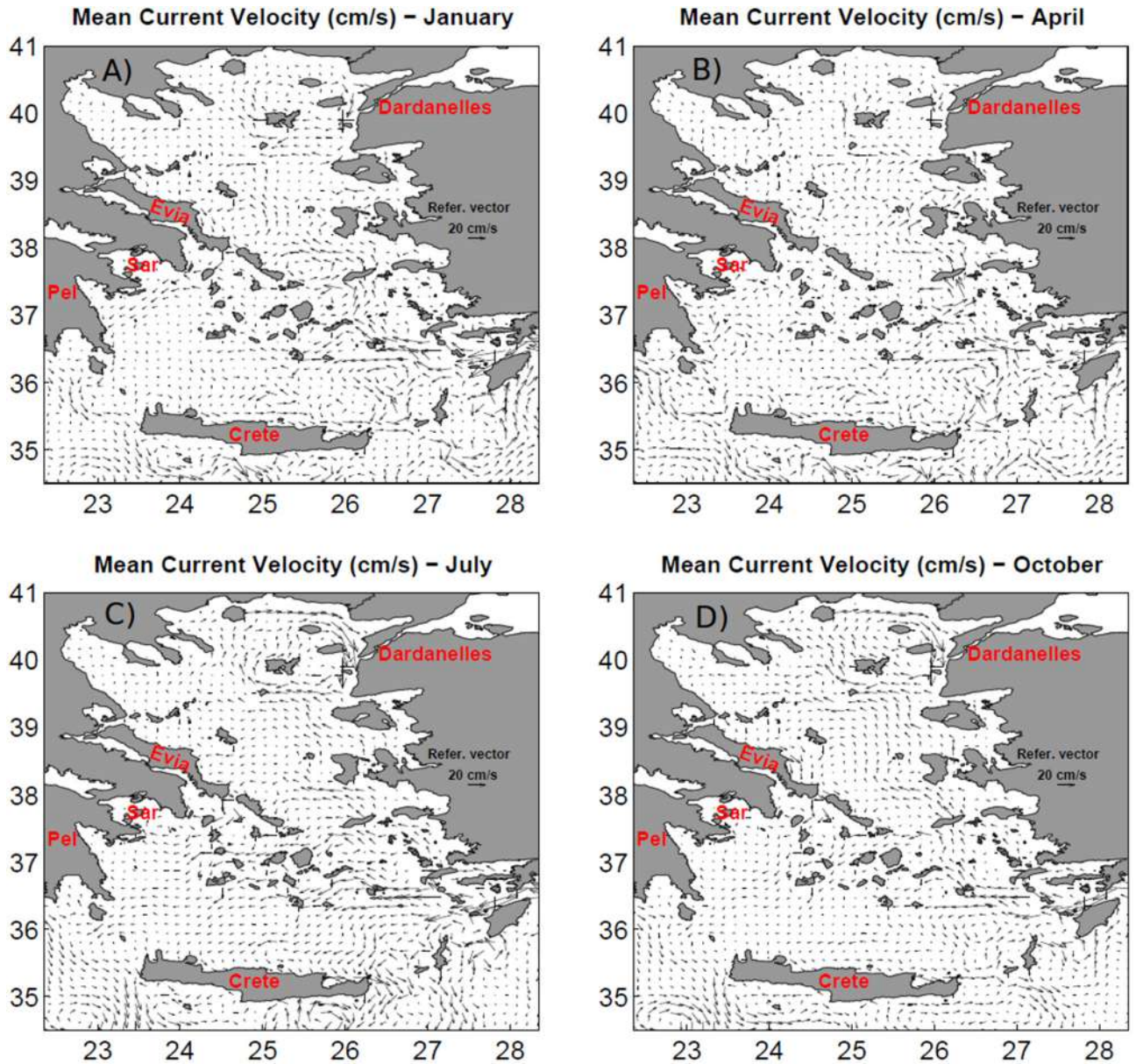

FIGURE 3 | Mean current field every fourth grid point averaged from 1990 to 2009 over **(A)** January, **(B)** April, **(C)** July, and **(D)** October.

and the areas outside the Saronikos and Thermaikos Gulf (**Figure 5O**). High values in standard deviation map of litter distribution (**Figure 5N**) implied occasional presence of floating litter particles mainly in the central Aegean, Cretan Sea and the region between Peloponnese and Crete island. The formulation of these concentration areas is driven by similar effects of surface circulation, as in Experiment A. Nevertheless, Experiment B tended to formulate recurrently high concentration of litter particles close to source regions and with larger geographic range, compare to Experiment A. These patterns were associated with the periodic inputs of litter in the model domain (once a month), which reduced gradually the advection time of particles; for instance, particles released in January tracked for 12 months, whereas particles released in December tracked for 1 month.

Differences in the distribution patterns of floating litter particles were noticed among Cases A1-A4. In Case A1, particles released on January and recurrently concentrated along Evia Island, in the Myrtoan basin, and the coastal waters of Crete island (**Figure 5C**). During January, the strong Evia coastal current turns southwest following a direct pathway along the Peloponnese coast (**Figure 3A**) resulting in the occasional retention of floating litter particles south of Peloponnese. Particles were occasionally found also in the central part of the Aegean Sea and in the Cretan Sea. Particles released on

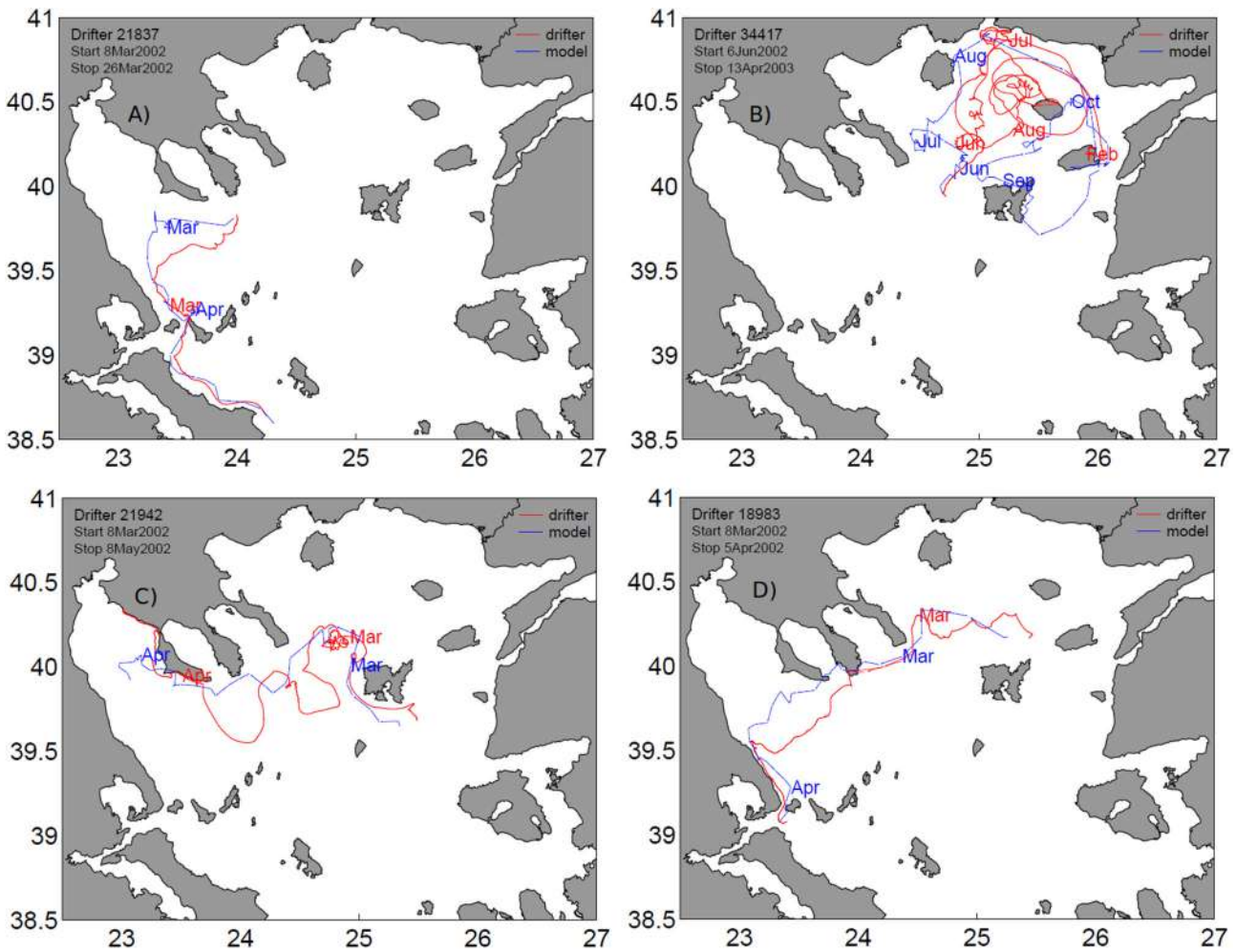

FIGURE 4 | Simulated drifter tracks (blue line) against observed drifter tracks (red line) in 2002 (Olson et al., 2007). Fifty model drifters are released on the same time period and within a small radius from the actual release location to remove sensitivity from initial release. The best model drifters in reproducing the observed patterns are shown: **(A)** drifter 21837, **(B)** drifter 34417, **(C)** drifter 21942, and **(D)** drifter 18983. The month is indicated on its 15th day along the simulated (blue color) and observed (red color) drifter tracks.

April (**Figure 5F**) were mostly aggregated in the Samothraki plateau, along the Evia coastline and the coast of Crete. In April, an inflow of modified Atlantic water is simulated through the straight between Crete and Peloponnese, also observed by Theocharis et al. (1993) spreading over the Myrtoan and Cretan Sea and thus resulting in relatively low concentration of litter. A similar inflow of Atlantic water was also observed by Theocharis et al. (1993). Meanwhile the southwest current from Evia to Peloponnese, simulated in January is diminished, resulting in a higher accumulation of floating litter particles along Evia coast and further south over the Cyclades plateau.

Simulations initiated in July (Case A3) and October (Case A4) resulted in relatively higher concentration of floating litter particles in the open waters of the Thermaikos Gulf (**Figures 5I,L**), which was absent in the other experiments. This was related to the anticyclonic circulation in Sporades basin in July, apparently blocking the strong southward Evia jet and thus preventing the fast advection of particles from Thermaikos Gulf. In October (Case A4) this was related to the relatively stronger westward current of BSW. The accumulation of floating litter particles in Saronikos Gulf, simulated in Case A3, can be attributed to the anticyclonic pathway of water coming from Evia Island and Central Aegean Sea and being directed into the gulf. The anticyclonic circulation in Saronikos and Myrtoan basin during October appears also to be responsible for the increase of floating litter particles in the broader area, and resulting to a very low abundance of floating particles in the Cretan Sea.

Classification areas, showing the concentration of floating particles originated separately from each source A, B, C,D, and E, were also depicted in **Figures 6–9**. Particles released from Source A (Thermaikos Gulf) ended up mostly in Saronikos Gulf and Myrtoan basin. This was particularly observed in Case A1 (January) and Case A4 (October) (**Figures 6A,D**), in which a strong current from Thermaikos Gulf was simulated

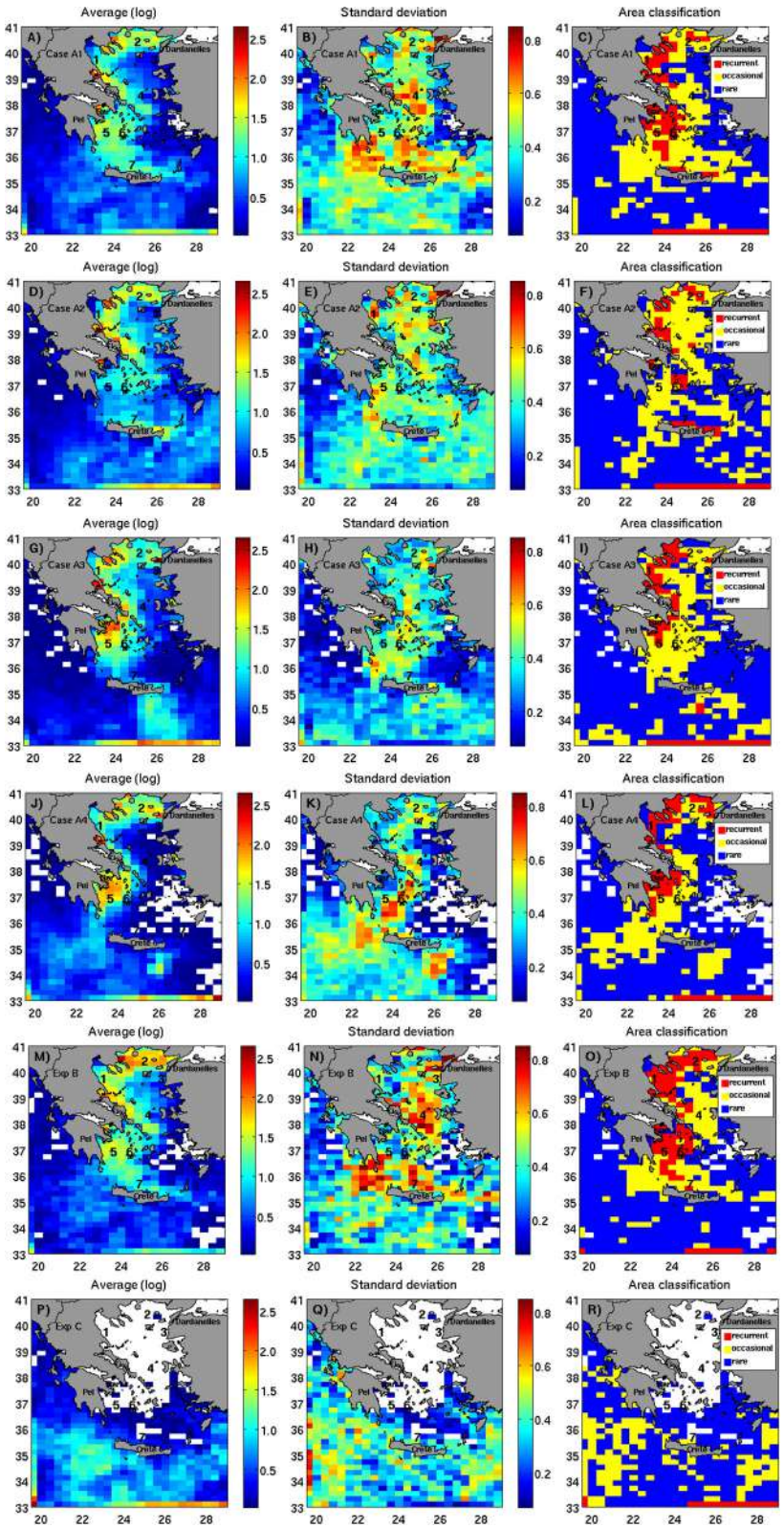

FIGURE 5 | Average, standard deviation and classification maps of floating litter distributions for Cases A1 **(A–C)**, A2 **(D–F)**, A3 **(G–I)**, and A4 **(J–L)**, Experiment B **(M–O)**, and Experiment C **(P–R)**. First row refers to Case A1, second row to Case A2, third row to Case A3, fourth row to Case A4, fifth row to Experiment B and sixth row to Experiment C.

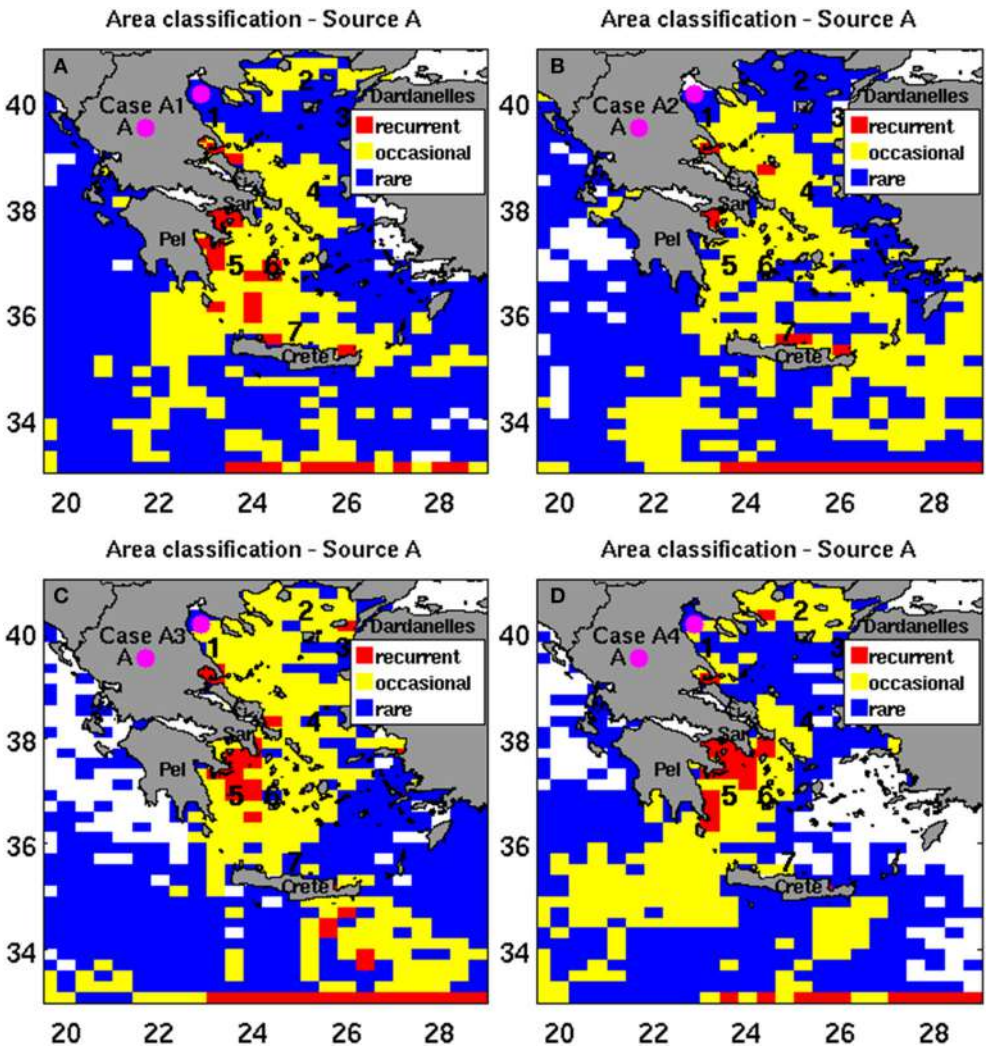

FIGURE 6 | Area classification maps of floating litter particles originated from Source region A (Thermaikos Gulf) in Cases **(A)** A1, **(B)** A2, **(C)** A3, and **(D)** A4. Magenta dot point indicates the source region A.

along Evia coast and then was directed southwest (**Figure 3**). A more diffuse distribution of floating litter particles from source A can be observed in Case A2 (April) and Case A3 (July) (**Figures 6B,C**), associated with the much slower advection of floating particles from Thermaikos Gulf. For the sources B and C, high concentrations of floating particles were found in their corresponding source regions (North East Aegean). In the same extent, significant floating particle distribution was observed along their pathway in all different experiments, mainly along the Evia coast (**Figures 7A,B,C**), Thermaikos gulf (**Figure 7D**) and Saronikos Gulf (**Figures 7A,C**). Occasionally, the eastern part of the Cyclades plateau retained a significant number of floating particles. A somehow similar fate (with sources B, C) was found for particles originating from source D (Dardanelles strait), following a similar southward pathway from North East Aegean (**Figure 8**). Finally, the fate of floating particle distribution was observed in the Cretan Sea and particularly outside the model domain with no specific pattern (**Figure 9**).

Finally, classification areas of floating particle distribution, derived from Experiment C, showed that litter particles were largely dispersed, leading to many cells with high standard deviation (**Figure 5Q**), and consequently to occasional areas without notable recurrent patterns of floating particle distribution (**Figure 5R**). Most particles were advected southern of the model domain; <7% particles, finally ended in the Aegean Sea.

Floating Litter Particles Escaping the Aegean Sea

The percentage of floating litter particles, escaping toward the western and eastern side of the Aegean Sea across the two transects T1 and T2, varied among the different source regions and experiments (**Figure 10**). Particles from all source regions escaped on average by 19.5% from transect T1 and by 14.5% from transect T2. With respect to source regions, particles originated from Source E (Saronikos Gulf) displayed

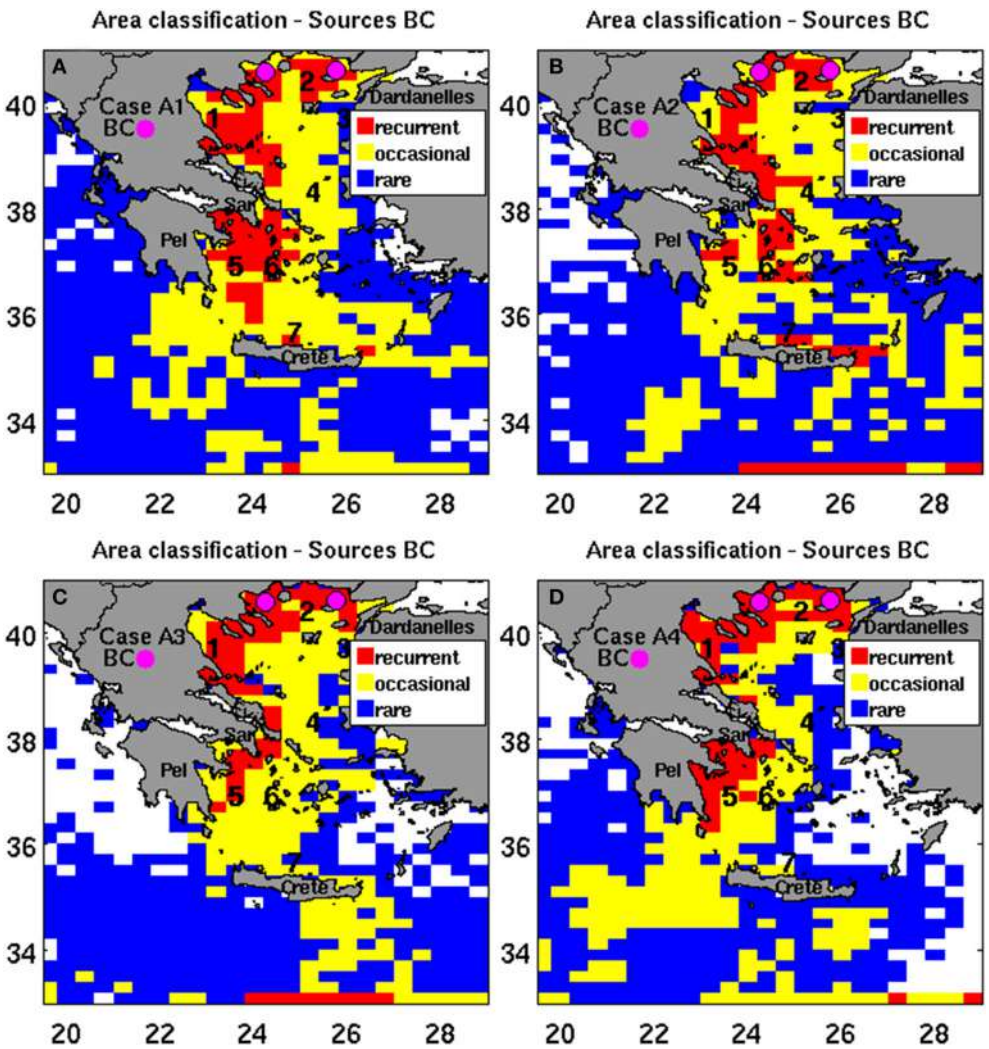

FIGURE 7 | Area classification maps of floating litter particles originated from Source regions B, C (North Aegean) in Cases **(A)** A1, **(B)** A2, **(C)** A3, and **(D)** A4. Magenta dot points indicate the source regions B,C.

the highest percent of escape: 47% from T1 and 42% from T2 (**Figures 10A,B**). In contrast, particles originated from Sources B and C escaped to a small extent: by 10.3% from T1 and by 5.8% from T2. In addition, Source A displayed higher percent of escaped litter (26.6% from T1, 20% from T2) compared to source D (18% from T1, 12.6% from T2) (**Figures 10A,B**). In Experiment B, particles showed low percentage of escape: by 11% from T1 and by 4% from T2 (**Figure 10C**).

Figure 11 shows the daily percent of escaped litter from transects T1, T2, averaged from annual simulations over 1990–2009. Particles started to escape from T1 after day-50 in Cases A2, A3 and day-20 in Cases A1 and A4 (**Figure 11A**). For all Cases A1-A4, particles escaped from transect T2 after day-80 (**Figure 11B**). Different release dates induced notable differences in the seasonal variations of escaped particles from transect T2; their final percent ranged from 4% (**Figure 11B:** Experiment B, green line) to 20% (**Figure 11B:** Case A4, yellow line). Experiment B illustrated that litter particles escaped mostly after day-20 from T1 and after day-80 from T2 (**Figure 11**, green lines).

Beaching of Floating Litter Particles

The distribution of floating litter particles, ending up in shoreline cells (define here as "beached"), was also depicted. Beached litter particles were mainly found along the coastline of Saronikos Gulf (Sar), eastern Peloponnese (Pel) and Pagasitikos Gulf (Pagas) (**Figure 12**). The topography of Aegean Sea, including hundreds of islands, favored also the beaching of some particles in several islands in Cyclades plateau, and specific gulfs in Crete island (**Figures 12C,D**), whereas few particles found all along the eastern part of Aegean Sea. Different release dates of particles did not change markedly the beaching patterns. The percent of beached particles changed slightly among the experiments: Case A1: 13.8%; Case A2: 11.4%; Case A3: 9.1%; Case A4: 9.9%; and Experiment B: 5.6%.

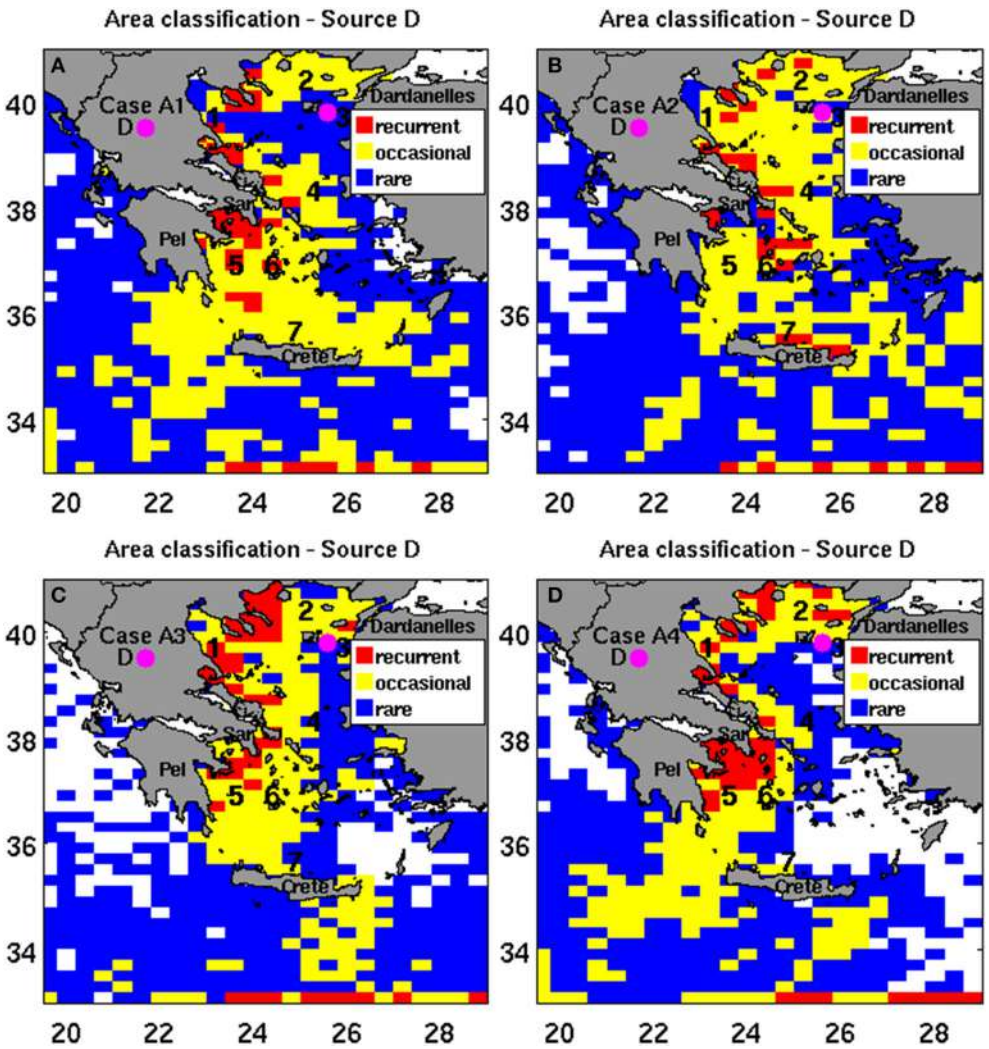

FIGURE 8 | Area classification maps of floating litter particles originated from region D (Dardanelles strait) in Cases **(A)** A1, **(B)** A2, **(C)** A3, and **(D)** A4. Magenta dot point indicates the source region D.

DISCUSSION

Fate and Concentration of Floating Litter Particles

Our simulations investigated possible scenarios regarding the fate and distribution of floating litter particles originated from specific source regions in the Aegean Sea. High concentration of floating litter was recurrently found in the North Aegean Sea (Cases A1-A4, Experiment B), alongside the northeastern side of Evia island and in the wider area of Saronikos Gulf (Cases A1, A3, A4; Experiment B), and alongside Crete island (Cases A1, A2) (**Figure 5**). Despite differences in the occasional presence of litter items among the experiments, floating litter particles were exhibited occasional presence in most Cases in the Myrtoan basin (southwestern Aegean Sea) and the area between Crete and Peloponnese. In contrast, the eastern Aegean Sea, was identified as a region with relatively rare presence of floating litter particles (**Figure 5**). This area is found on the pathway of Levantine inflowing water, which has been assumed to be more or less free of floating litter in the simulations.

The transfer of floating litter particles between the different sea areas is another challenging task that the present study attempted to undertake, particularly related with the corresponding exchanges of floating litter particles with the eastern Mediterranean Sea. Simulation results demonstrated that particles escaped on average by 35% for experiment A and by 15% for experiment B from the Aegean Sea toward the Eastern Mediterranean Sea (**Figure 10**). In contrast, only 7% of the floating litter particles was found to end up in the Aegean Sea, after being released outside the model domain (**Figure 5**, Experiment C). These findings suggest that Aegean Sea might act mostly as a source rather than a receptor of floating litter pollution in the Eastern Mediterranean. Another factor that was investigated was the floating litter particles ending up on

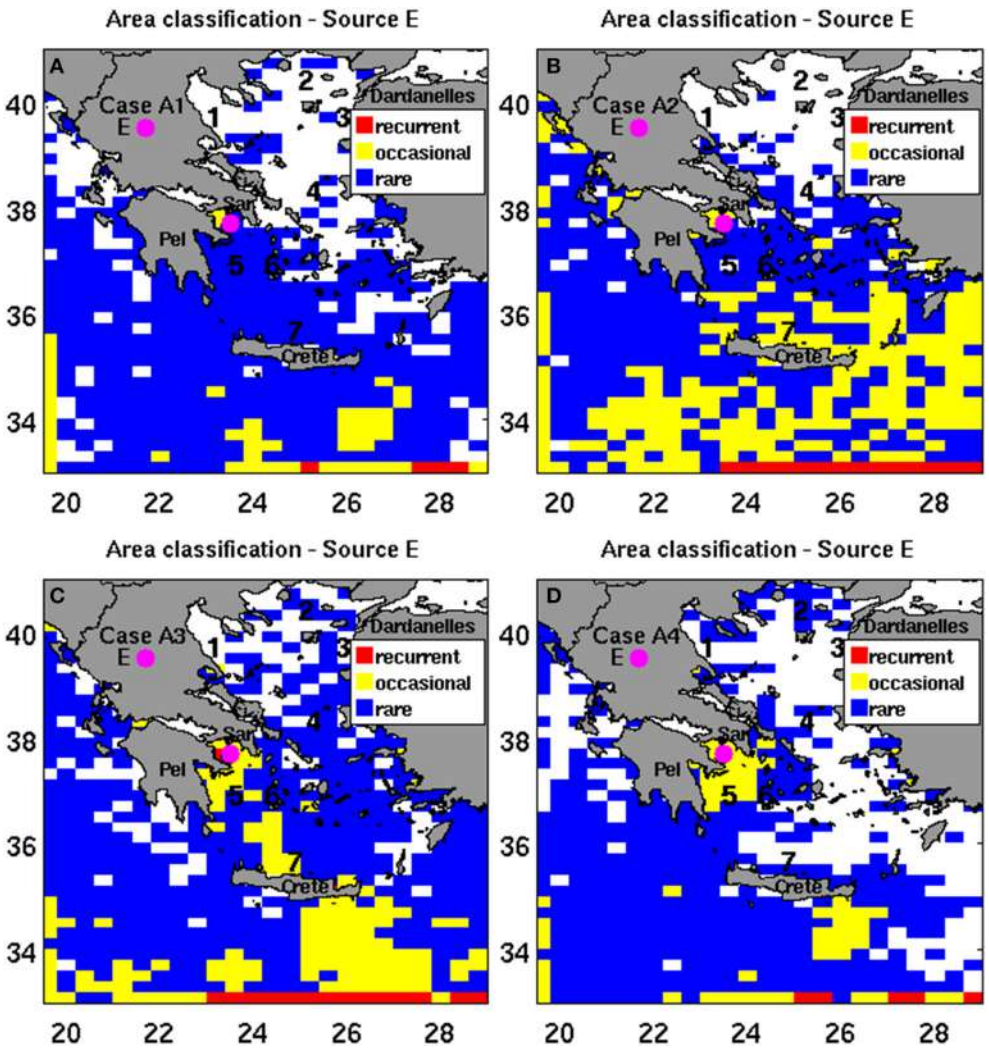

FIGURE 9 | Area classification maps of floating litter particles originated from Source region E (Saronikos Gulf) in Cases **(A)** A1, **(B)** A2, **(C)** A3, and **(D)** A4. Magenta dot point indicates the source region E.

beaches (i.e., beaching). In the present study, on average 10% of floating litter particles were found in coastline cells. Most of them were found in the western Aegean Sea (**Figure 12**), which is in accordance with the areas where floating litter particles were found.

Transport Pathways

The major transport pathways of floating litter particles illustrated that source regions are interconnected (**Figure 13**). A characteristic example is the case of the Saronikos Gulf (Source Region E), from which 92% of particles escaped through transects T1 and T2 to eastern Mediterranean Sea, whereas it received particles from sources A, B, C, and D. In the same extent, source A (Thermaikos Gulf) received floating litter particles originating from the North Aegean Sea (sources B, C), while floating litter particles released from source D tended to occasionally be directed toward sources B and C. In addition, the northeastern area alongside the Evia island received particles that were released from sources B, C and D. Cretan Myrtoan Similar to other model studies (Yoon et al., 2010; Neumann et al., 2014; Mansui et al., 2015; Liubartseva et al., 2016), our results identified source-receptor transport pathways among the different sub-regions, demonstrating the transboundary character of the problem, with particles traveling far from their initial source points and finally concentrating into new regions.

Model Accuracy

One of the most critical point of the marine litter modeling studies is the validation of the results with data from surveys. Data on the distribution of floating litter are sparse in the Aegean Sea to validate rigorously the simulations and it is a problem that most of the relevant studies are facing. In this study, we evaluated the accuracy of the model by comparing qualitatively

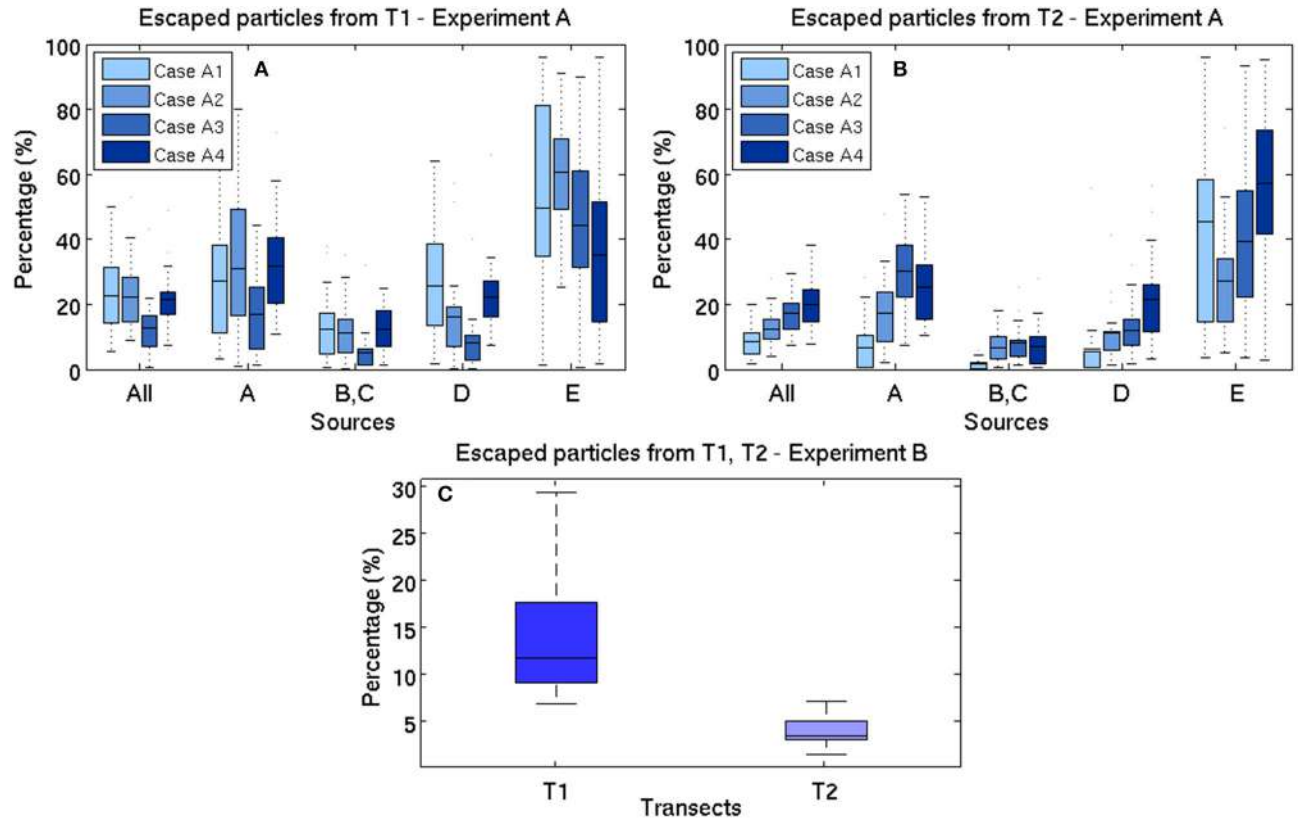

FIGURE 10 | Box plots depicting the percentages of escaped particles across: **(A)** transect T1 in Experiment A; **(B)** transect T2 in Experiment A, and **(C)** transects T1, T2 in Experiment B.

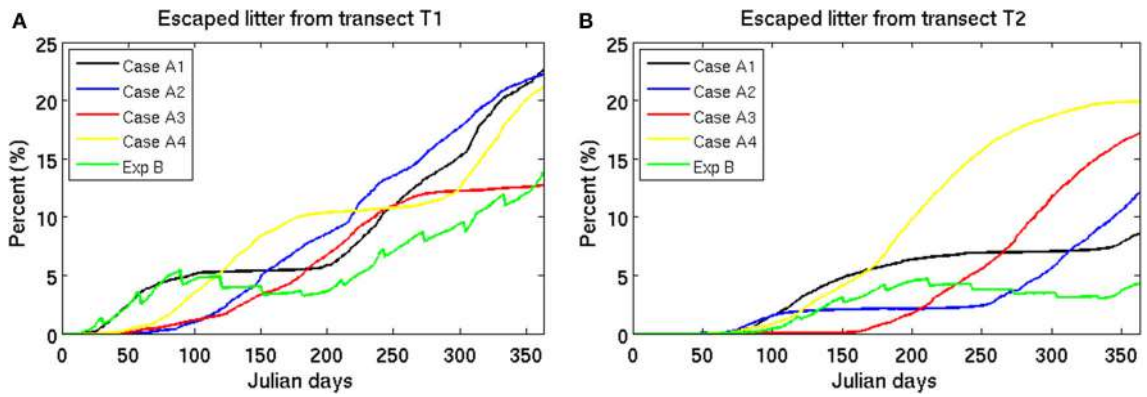

FIGURE 11 | Daily percent of escaped particles across transects **(A)** T1 and **(B)** T2 in Cases A1-A4 and Experiment B.

the simulated distribution of floating litter particles with available data compiled from different sub-regions and studies, marked as R1 to R6 in **Figure 14**. Observed floating litter abundance and the corresponding references are listed in **Table 2**. Although there is no direct way to distinguish if the measurements are the result of litter transport or source of litter, the model was adequate to predict high concentration of litter in the Saronikos Gulf (sub-region R1) and Crete island (sub-region R4). Similar to data, model predicted low litter concentration and beached particles in the eastern coastline of Aegean Sea (sub-region R3). Results for sub-region R3 (Topcu et al., 2010) refer to bigger floating litter particles. However, they have been included in the verification of the model knowing that different sized items have different buoyancy properties, but also knowing that the transportation mechanisms still remain the same. The model did not predict high floating litter particles distribution in the northern part of

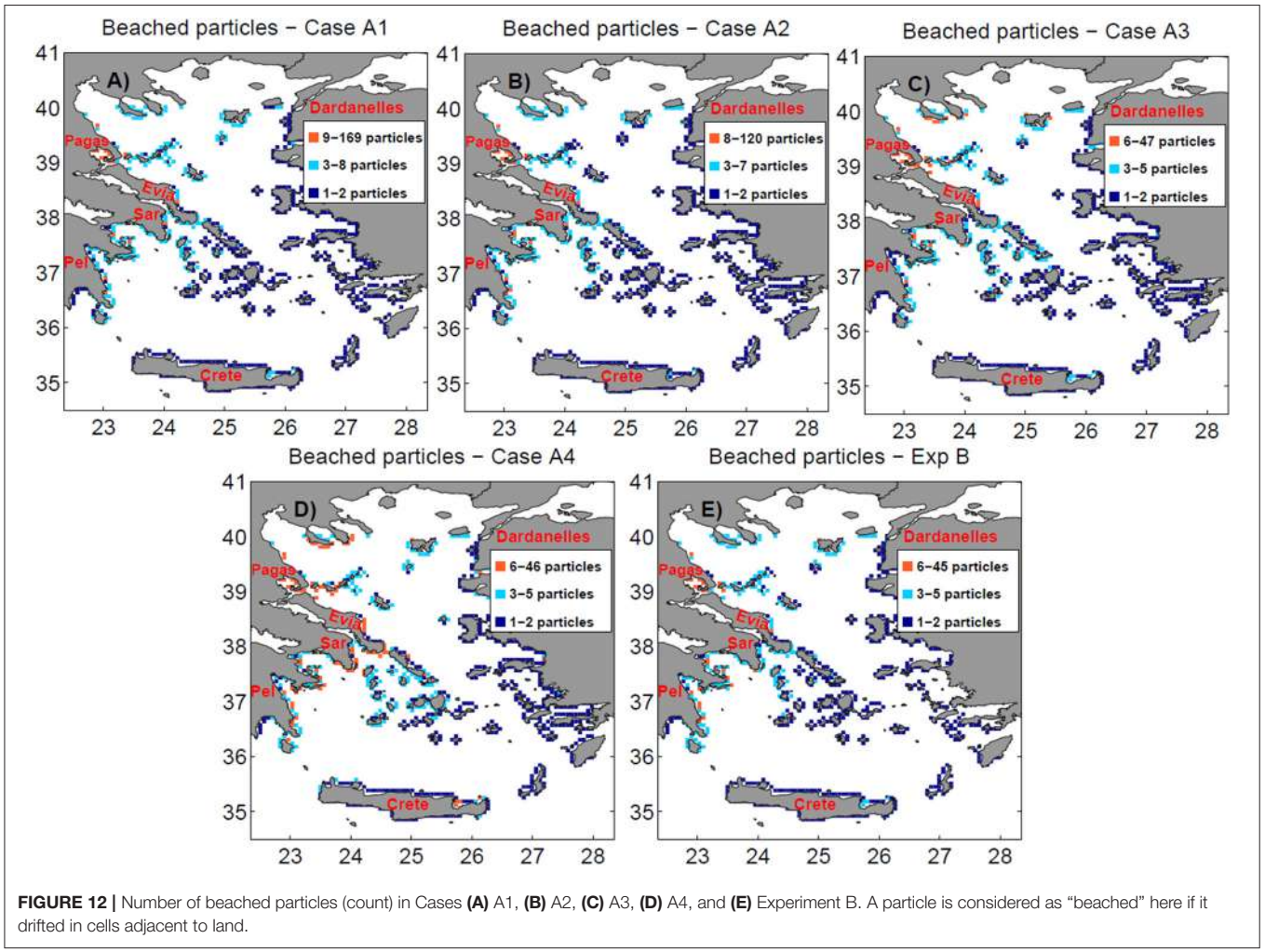

FIGURE 12 | Number of beached particles (count) in Cases **(A)** A1, **(B)** A2, **(C)** A3, **(D)** A4, and **(E)** Experiment B. A particle is considered as "beached" here if it drifted in cells adjacent to land.

Thermaikos Gulf (sub-region R2); however it was considered correctly as a source of litter through source region A. Finally, occasional presence of litter predicted by the model in the area between Crete island and Peloponnese agrees with observed floating litter in sub-regions R5 and R6. This signifies that this area may be indeed a passage of escaped litter, since it does not appear as an evident source of litter pollution.

Model Results and Hypotheses

Model results are subject to assumptions taken into consideration during the model setup. First, different source regions were considered as the starting point of the floating litter particles, based on big coastal cities, major rivers, ports, maritime and fisheries activity and coastal activity (e.g., tourism). However, including other unspecified sources (e.g., maritime and shipping, small-scale fisheries, or potential sources in eastern coastline of the Aegean Sea) might partially modify the obtained information regarding the distribution of floating litter particles in the Aegean Sea. Second, beaching of litter particles is another factor which significantly contributes to the congregation of litter particles on the coastlines (Yoon et al., 2010; Lebreton et al., 2012; Mansui et al., 2015). Herein, particles did not strand when found on land cells, following Neumann et al. (2014) who treated coasts as reflective boundaries. This assumption was essential, since the complex topography of the Aegean Sea, with hundred of islands, caused the vast majority of particles to be stuck on them due to random part of the particle-tracking model. In addition, our study refers to floating particles and not to bigger litter for which wash up on shore is common. Exploring how beaching of particles affect the model performance is, however, a worthy issue for future consideration. Third, assuming simulations with integration time of 1 year, we included the effect of seasonal surface circulation variability. This integration time was also proper for studying the drift of litter particles on regional scale, as proposed by Mansui et al. (2015). Identification of long-term trends and possible permanent accumulation areas would require simulations with multi-annual integration time (Lebreton et al., 2012). Fourth, floating litter particles have been considered here as passive drifters advected exclusively by surface currents. So, we did not include other particle properties related to buoyancy (Yoon et al., 2010; Carlson et al., 2017), windage (Neumann et al., 2014), subsurface movement, and sinking (Hardesty et al., 2017). All these properties need to be better understood and taken into account in further modeling.

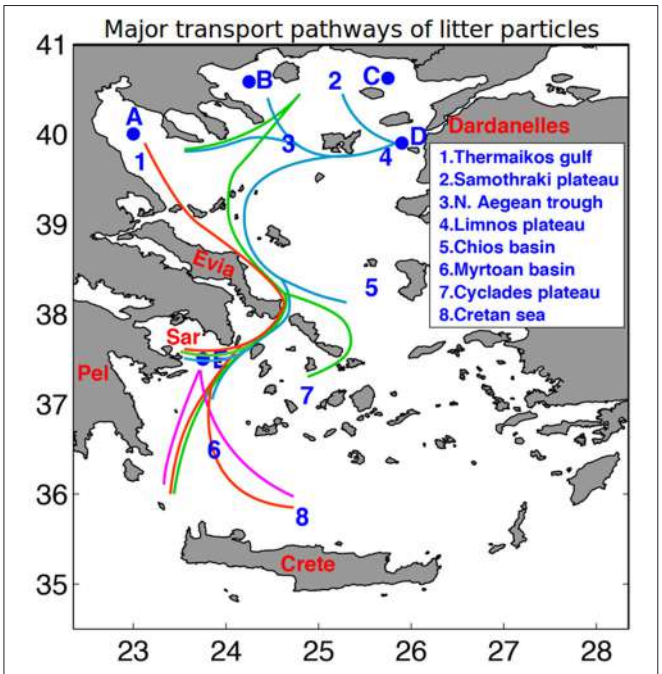

FIGURE 13 | Schematic representation of major pathways of floating litter transport among the source regions. Different colors represent pathways originated from source regions A,B,C,D, and E.

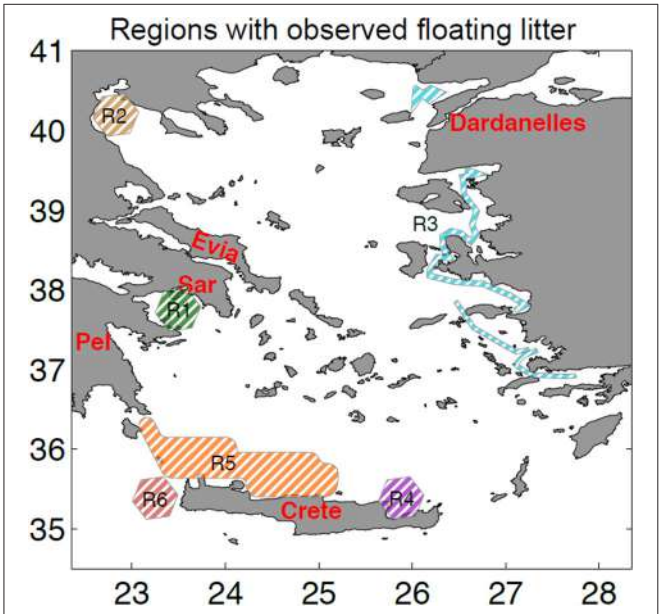

FIGURE 14 | Subregions of sampled floating litter in the Aegean Sea; R1: Saronikos Gulf (Valavanidis and Vlachogianni, 2012; MERMAID Report, 2016), R2: Thermaikos Gulf (Valavanidis and Vlachogianni, 2012), R3: Eastern Aegean Sea (Topcu et al., 2010), R4: Crete island (Cózar et al., 2015), R5: Southwest Aegean Sea (Kornilios et al., 1998), and R6: Crete island (Cózar et al., 2015).

Summary and Conclusion

The Mediterranean Sea has been described as one of the areas most affected by marine litter in the world (UNEP/MAP, 2016).

TABLE 2 | Measurements of floating litter abundance from different subregions (R1 to R6) in the Aegean Sea.

Subregions	Abundance	References
R1	11,510–304,805 items km^{-2} (1–5 mm) 1.47–3.46 m^3/day	Valavanidis and Vlachogianni, 2012; MERMAID Report, 2016
R2	400 items m^{-3}	Valavanidis and Vlachogianni, 2012
R3	0–0.18 items km^{-2} (offshore), 1.75–3.52 items km^{-2} (inshore),	Topcu et al., 2010
R4	200–500 g km^{-2}	Cózar et al., 2015
R5	1–1,160 g km^{-2} (1–5 mm)	Kornilios et al., 1998
R6	50–200 g km^{-2}	Cózar et al., 2015

The coverage of the subregions is marked in ***Figure 14****.*

The Aegean Sea is an archipelagos with extended coastline and numerous islands and no information on the exact pathways of floating litter transport and distribution exists. The use of coupled ocean circulation and particle-tracking models is important to better understand these processes and guide scientists on surveying and monitoring floating litter particles (Yoon et al., 2010; Neumann et al., 2014; Liubartseva et al., 2016).

In this study, we conducted a series of transport simulations to describe the fate and distribution of floating litter particles, after being released from specific source regions in the Aegean Sea. Model analysis pictured that floating litter particles tend to concentrate mostly over in the north Aegean Sea, in the Saronikos Gulf and Evia and Crete islands, while the eastern part of the Aegean archipelagos was the least affected. Beached washed up litter items were mainly found along the coastline of Saronikos Gulf, eastern Peloponnese and Pagasitikos Gulf while the Aegean Sea physiography favored the beaching of litter items in Cyclades island and in specific gulfs of Crete island. The beaches and offshore areas of high floating litter concentration may be considered under priority for future surveys; this will help importantly to assess the status of floating litter pollution in the Aegean Sea, improve the credibility of future model studies in our study area, and after all guide science and policy judgment.

AUTHOR CONTRIBUTIONS

DP: Conceptualized and guided the study, analyzed the results and wrote parts of the paper; CI: Analyzed the results and wrote parts of the paper; GP: Contributed to the discussion of the results; KT: Performed the simulations, analyzed the results and wrote parts of the paper. All authors read and edited the paper.

ACKNOWLEDGMENTS

Support for this research came from the LIFE DEBAG project (LIFE14 GIE/GR/001127). The drifter data were obtained from a study funded by the U.S. Office of Naval Research (ONR grants N000140110134 and N000140310439), in collaboration with Villy Kourafalou, Don Olson and Bill Johns of the University of Miami. The manuscript was greatly improved by the three reviewers.

REFERENCES

Androulidakis, Y. S., Krestenitis, Y. N., and Kourafalou, V. H. (2012). Connectivity of North Aegean circulation to the Black Sea water budget. *Cont. Shelf Res.* 48, 8–26. doi: 10.1016/j.csr.2012.08.019

Barnes, D. K. A., Galgani, F., Thompson, R. C., and Barlaz, M. A. (2009). Accumulation and fragmentation of plastic debris in global environments. *Phil. Trans. R. Soc. B* 364, 1985–1998. doi: 10.1098/rstb.2008.0205

Bellier, E., Planque, B., and Petitgas, P. (2007). Historical fluctuations in spawning location of anchovy (*Engraulis encrasicolus*) and sardine (*Sardina pilchardus*) in the Bay of Biscay during 1967-73 and 2000-2004. *Fish. Oceanogr.* 16, 1–15. doi: 10.1111/j.1365-2419.2006.00410.x

Blumberg, A. F., and Mellor, G. L. (1983). Diagnostic and prognostic numerical circulation studies of the South Atlantic Bight. *J. Geophys. Res.* 88 , 4579–4592. doi: 10.1029/JC088iC08p04579

Carlson, D. F., Suaria, G., Aliani, S., Fredj, E., Fortibuoni, T., Griffa, A., et al. (2017). Combing litter observations with a regional ocean model to identify sources and sinks of floating debris in a semi-enclosed basin: the adriatic sea. *Front. Mar. Sci.* 4:78. doi: 10.3389/fmars.2017.00078

Christensen, O. B., Drews, M., Christensen, J. H., Dethloff, K., Ketelsen, K., Hebestadt, I., et al. (2006). *The HIRHAM Regional Climate Model, Version 5 (β).* Techical Report. Available online at: www.dmi.dk/dmi/tr06-17.

Cózar, A., Sanz-Martín, M., Martí, E., González-Gordillo, J. I., Ubeda, B., Gálvez, J. Á., et al. (2015). Plastic accumulation in the Mediterranean Sea. *PLoS ONE* 10:e0121762. doi: 10.1371/journal.pone.0121762

Eriksen, M., Lebreton, L. C. M., Carson, H. S., Thiel, M., Moore, C. J., Borerro, J. C., et al. (2014). Plastic pollution in the world's oceans: more than 5 trillion plastic pieces weighing over 250,000 Tons Afloat at Sea. *PLoS ONE* 9:e111913. doi: 10.1371/journal.pone.0111913

Galgani, F. (2015). Marine litter, future prospects for research. *Front. Mar. Sci.* 2:87. doi: 10.3389/fmars.2015.00087

Giannoulaki, M., Iglesias, M., Tugores, M. P., Bonanno, A., Patti, B., De Felice, A., et al. (2013). Characterizing the potential habitat of European anchovy *Engraulis encrasicolus* in the Mediterranean Sea, at different life stages. *Fish. Oceanogr.* 22, 69–89. doi: 10.1111/fog.12005

Hardesty, B. D., Harari, J., Isobe, A., Lebreton, L., Maximenko, N., Potemra, J., et al. (2017). Using numerical model simulations to improve the understanding of micro-plastic distribution and pathways in the marine environment. *Front. Mar. Sci.* 4:30. doi: 10.3389/fmars.2017.00030

Horton, C., Clifford, M., Schmitz, J., and Kantha, L. H. (1997). A real time oceanographic nowcast/forecast system for the Mediterranean Sea. *J. Geophys. Res.* 102, 25123–25156. doi: 10.1029/97JC00533

Ioakeimidis, C., Papatheodorou, G., Fermeli, G., Streftaris, N., and Papathanassiou, E. (2015). Use of ROV for assessing marine litter on the seafloor of Saronikos Gulf (Greece): a way to fill data gaps and deliver environmental education. *Springerplus* 4:463. doi: 10.1186/s40064-015-1248-4

Ioakeimidis, C., Zeri, C., Kaberi, H., Galatchi, M., Antoniadis, K., Streftaris, N., et al. (2014). A comparative study of marine litter on the seafloor of coastal areas in the Eastern Mediterranean and Black Seas. *Mar. Pollut. Bull.* 89, 296–304. doi: 10.1016/j.marpolbul.2014.09.044

Jain, A. K. (2010). Data clustering: 50 years beyond K-means. *Pattern Recogn. Lett.* 31, 651–666. doi: 10.1016/j.patrec.2009.09.011

Katsanevakis, S., and Katsarou, A. (2004). Influences on the distribution of marine debris on the seafloor of shallow coastal areas in Greece (Eastern Mediterranean). *Water Air Soil Pollut.* 158, 325–337. doi: 10.1023/B:WATE.0000049183.17150.df

Kontoyiannis, H., Kourafalou, V. H., and Papadopoulos, V. (2003). The seasonal characteristics of the hydrology and circulation in the Northwest Aegean Sea (Eastern Mediterranean): observations and modeling. *J. Geophys. Res.* 108:3302. doi: 10.1029/2001JC001132

Kornilios, S., Drakopoulos, P. G., and Dounas, C. (1998). Pelagic tar, dissolved/dispersed petroleum hydrocarbons and plastic distribution in the Cretan Sea, Greece. *Mar. Pollut. Bull.* 36, 989–993. doi: 10.1016/S0025-326X(98)00102-7

Korres, G., Hoteit, I., and Triantafyllou, G. (2007). Data assimilation into a Princeton Ocean Model of the Mediterranean Sea using advanced Kalman filters. *J. Mar. Syst.* 65, 84–104. doi: 10.1016/j.jmarsys.2006.09.005

Korres, G., and Lascaratos, A. (2003). A one-way nested, eddy resolving model of the Aegean and Levantine basins: implementation and climatological runs. *Ann. Geophys.* 21, 205–220. doi: 10.5194/angeo-21-205-2003

Korres, G., Nittis, K., Perivoliotis, L., Tsiaras, K., Papadopoulos, A., Triantafyllou, G., et al. (2010). Forecasting the Aegean Sea hydrodynamics within the POSEIDON-II operational system. *J. Oper. Oceanogr.* 3, 37–49. doi: 10.1080/1755876X.2010.11020112

Kourafalou, V., Tsiaras, K., Olson, D., Johns, B., Papadopoulos, A., Kontoyiannis, H., et al. (2006). "North Aegean circulation: results from a drifter array and model simulations," in *Proceedings of 8th Panhellenic Symposium on Oceanography and Fisheries* (Thessaloniki), 515–518.

Koutsodendris, A., Papatheodorou, A., Kougiourouki, O., and Georgiadis, M. (2008). Benthic marine litter in four Gulfs in Greece, Eastern Mediterranean; abundance, composition and source identification. *Estuarine Coast. Shelf Sci.* 77, 501–512. doi: 10.1016/j.ecss.2007.10.011

Kubota, M. (1994). A mechanism for the accumulation of floating marine debris north of Hawaii. *J. Phys. Ocean.* 24, 1059–1604. doi: 10.1175/1520-0485(1994)024<1059:AMFTAO>2.0.CO;2

Law, K. L., Morét-Ferguson, S. E., Goodwin, D. S., Zettler, E. R., DeForce, E., Kukulka, T., et al. (2014). Distribution of surface plastic in the eastern Pacific Ocean from an 11-year data set. *Environ. Sci. Technol.* 48, 4732–4738. doi: 10.1021/es4053076

Lebreton, L. C. M., and Borrero, J. C. (2013). Modeling the transport and accumulation floating debris generated by the 11 March 2011 Tohoku tsunami. *Mar. Pollut. Bull.* 66, 53–58. doi: 10.1016/j.marpolbul.2012.11.013

Lebreton, L. C. M., Greer, S. D., and Borrero, J. C. (2012). Numerical modeling of floating debris in the worlds oceans. *Mar. Pollut. Bull.* 64, 653–661. doi: 10.1016/j.marpolbul.2011.10.027

Liubartseva, S., Coppini, G., Lecci, R., and Creti, S. (2016). Regional approach to modeling the transport of floating plastic litter in the Adriatic Sea. *Mar. Pollut. Bull.* 103, 115–127. doi: 10.1016/j.marpolbul.2015.12.031

Lynch, D. R., Greenberg, D. A., Bilgili, A., McGillicuddy, D. J., Manning, J. P., and Aretxabaleta, A. L. (2014). *Particles in the Coastal Ocean: Theory and Applications*. Cambridge University Press, 560.

Mansui, J., Molcard, A., and Ourmières, Y. (2015). Modeling the transport and accumulation of floating marine debris in the Mediterranean basin. *Mar. Pollut. Bull.* 91, 249–257. doi: 10.1016/j.marpolbul.2014.11.037

Martinez, E., Maamaatuaiahutapu, K., and Taillandier, V. (2009). Floating marine debris surface drift: convergence and accumulation toward the South Pacific subtropical gyre. *Mar. Pollut. Bull.* 58, 1347–1355. doi: 10.1016/j.marpolbul.2009.04.022

Maximenko, N., Hafner, J., and Niiler, P. (2012). Pathways of marine litter derived from trajectories of Langarian drifters. *Mar. Pollut. Bull.* 65, 51–62. doi: 10.1016/j.marpolbul.2011.04.016

Mellor, G. L., and Yamada, T. (1982). Development of a turbulence closure model for geophysical fluid problems. *Rev. Geophys.* 20, 851–875, doi: 10.1029/RG020i004p00851

MERMAID Report (2016). "Test the designed monitoring programs applied in the study areas (Deliverable 3.3)," in *Marine Environmental Targets Linked to Regional Management Schemes Based on Indicators Developed for the Mediterranean (MERMAID)*, eds O. Guven (IMS-METU), B. Salihoğlu (IMS-METU), F. Witkowski (IFREMER), R. Verney (IFREMER), S. Bonhommeau (IFREMER), B. Andral (IFREMER), M. Pantazi (HCMR), H. Kaberi (HCMR), C. Zeri (HCMR), C. Tsangaris (HCMR), E. Prifti (HCMR), C. Ioakeimidis (HCMR).Ioakeimidis C., Zeri C., Tsangkari K. et al. (Athens: Assessment of Microplastic Abundance in the Saronikos Gulf).

Neumann, D., Callies, U., and Matthies, M. (2014). Marine litter ensemble transport simulations in the southern North Sea. *Mar. Pollut. Bull.* 86, 219–228. doi: 10.1016/j.marpolbul.2014.07.016

Nittis, K., Lascaratos, A., and Theocharis, A. (2003). Dense water formation in the Aegean Sea: numerical simulations during the Eastern Mediterranean Transient. *J. Geophys. Res.* 108:8120. doi: 10.1029/2002JC001352

Nittis, K., and Perivoliotis, L. (2002). Circulation and hydrological characteristics of the North Aegean Sea: a contribution from real-time buoy measurements. *Med. Mar. Sci.* 3, 21–32. doi: 10.12681/mms.255

NOAA (2016). *National Oceanic and Atmospheric Administration Marine Debris Program*. Report on Modeling Oceanic Transport of Floating Marine Litter. Silver Spring, MD. 21.

Olson, D. B., Kourafalou, V. H., Johns, W. E., Samuels, G., and Veneziani, M. (2007). Aegean Surface Circulation from a Satellite-Tracked Drifter Array. *J. Phys. Ocean.* 37, 1898–1917. doi: 10.1175/JPO3028.1

Papadopoulou, K.-N., Anastasopoulou, A., Mytilineou, C. H., Smith, C. J., and Stamouli, C. (2015). "Seabed marine litter, comparison of 4 Aegean trawling grounds," in *Proceedings of 11th Panhellenic Symposium of Oceanography and Fisheries* (Lesvos), 381–385.

Pastorelli, G., Cucci, C., Garcia, O., Piantanida, G., Elnaggar, A., Cassar, M., et al. (2014). Environmentally induced colour change during natural degradation of selected polymers. *Polym. Degrad. Stab.* 107, 198–209. doi: 10.1016/j.polymdegradstab.2013.11.007

Pedrotti, M. L., Petit, S., Elineau, A., Bruzaud, S., Crebassa, J.-C., Dumontet, B., et al. (2016). Changes in the floating plastic pollution of the Mediterranean Sea in relation to the distance to land. *PLoS ONE* 11:e0161581. doi: 10.1371/journal.pone.0161581

Pollani, A., Triantafyllou, G., Petihakis, G., Konstantinos, N., Dounias, K., and Koutitas, C. (2001). The Poseidon operational tool for the prediction of floating pollutant transport. *Mar. Pollut. Bull.* 43, 270–278. doi: 10.1016/S0025-326X(01)00080-7

Reisser, J., Slat, B., Noble, K., du Plessis, K., Epp, M., Proietti, M., et al. (2015). The vertical distribution of buoyant plastics at sea: an observational study in the North Atlantic Gyre. *Biogeosciences* 12, 1249–1256. doi: 10.5194/bg-12-1249-2015

Ryan, P. G. (2014). Litter survey detects the South Atlantic "garbage patch." *Mar. Pollut. Bull.* 79, 220–224. doi: 10.1016/j.marpolbul.2013.12.010

Ryan, P. G. (2015). Does size and buoyancy affect the long-distance transport of floating litter? *Environ. Res. Lett.* 10:084019. doi: 10.1088/1748-9326/10/8/084019

Saraux, C., Fromentin, J.-M., Bigot, J.-L., Bourdeix, J.-H., Morfin, M., Roos, D., et al. (2014). Spatial Structure and Distribution of Small Pelagic Fish in the Northwestern Mediterranean Sea. *PLoS ONE* 9:e111211. doi: 10.1371/journal.pone.0111211

Sayin, E., Eronat, C., Uçkaç S., and BeÅ§iktepe, Åd. T. (2011). Hydrography of the eastern part of the Aegean Sea during the East Mediterranean Transient (EMT). *J. Mar. Syst.* 88, 502–515. doi: 10.1016/j.jmarsys.2011.06.005

Sebille, E., Wilcox, C., Lebreton, L., Maximenko, N., Hardesty, B. D., Franeker, J. A., et al. (2015). A global inventory of small floating plastic debris. *Environ. Res. Lett.* 10:124006. doi: 10.1088/1748-9326/10/12/124006

Stefatos, A., Charalampakis, M., Papatheodorou, G., and Ferentinos, G. (1999). Marine debris on the seafloor of the Mediterranean Sea: examples from two enclosed gulfs in Western Greece. *Mar. Pollut. Bull.* 36, 389–393. doi: 10.1016/S0025-326X(98)00141-6

Suaria, G., and Aliani, S. (2014). Floating debris in the Mediterranean Sea. *Mar. Pollut. Bull.* 86, 494–504. doi: 10.1016/j.marpolbul.2014.06.025

Theocharis, A., Balopoulos, E., Kioroglou, S., Kontoyiannis, H., and Iona, A. (1999). A synthesis of the circulation and hydrography of the south Aegean Sea and the Straits of the Cretan Arc (March 1994-January 1995). *Progr. in Ocean.* 44, 469–509. doi: 10.1016/S0079-6611(99)00041-5

Theocharis, A., and Georgopoulos, D. (1993). Dense water formation over the Samothraki and Limnos plateaux in the North Aegean Sea (Eastern Mediterranean Sea). *Cont. Shelf Res.* 13, 919–939. doi: 10.1016/0278-4343(93)90017-R

Theocharis, A., Georgopoulos, D., Lascaratos, A., and Nittis, K. (1993). Water masses and circulation in the central region of the eastern Mediterranean: eastern Ionian, south Aegean and northwest Levantine, 1986-1987. *Deep-Sea Res. Pt II* 40, 1121–1142. doi: 10.1016/0967-0645(93)90064-T

Thompson, R. C., Olsen, Y., Mitchell, R. P., Davis, A., Rowland, S. J., John, A. W. G., et al. (2004). Lost at sea: where is all the plastic? *Science* 304, 838. doi: 10.1126/science.1094559

Topcu, E. D., Tonay, A. M., and Öztürk, B. (2010). Preliminary study on marine litter in the Aegean Sea. *Rapp. Comm. int. Mer Médit.* 39:804.

Tsiaras, K. P., Petihakis, G., Kourafalou, V. H., and Triantafyllou, G. (2014). Impact of the river nutrient load variability on the North Aegean ecosystem functioning over the last decades. *J. Sea Res.* 86, 97–109. doi: 10.1016/j.seares.2013.11.007

Tugrul, S., Besiktepe, S., and Salihoglu, I. (2002). Nutrient exchange fluxes between the Aegean and Black Seas through the Marmara Sea. *Mediterr. Mar. Sci.* 3, 33–42. doi: 10.12681/mms.256

UNEP/MAP (2016). *Marine litter assessment in the Mediterranean 2015. United Nations Environment Programme Mediterranean Action Plan (UNEP/MAP)*, 86. Available online at: http://hdl.handle.net/20.500.11822/7098

Valavanidis, A., and Vlachogianni, T. (2012). *MARINE LITTER: Man-made Solid Waste Pollution in the Mediterranean Sea and Coastline. Abundance, Composition and Sources Identification. Science Advances on Environmental Chemistry, Toxicology and Ecotoxicology.*

Yoon, J. H., Kawanob, S., and Igawa, S. (2010). Modeling of marine litter drift and beaching in the Japan Sea. *Mar. Pollut. Bull.* 60, 448–463. doi: 10.1016/j.marpolbul.2009.09.033

Zavatarelli, M., and Mellor, G. L. (1995). A numerical study of the Mediterranean Sea circulation. *J. Phys. Oceanogr.* 25, 1384–1414. doi: 10.1175/1520-0485(1995)025<1384:ANSOTM>2.0.CO;2

Zervakis, V., and Georgopoulos, D. (2002). Hydrology and circulation in the north Aegean (eastern Mediterranean) throughout 1997-1998. *Mediterr. Mar. Sci.* 3, 7–21. doi: 10.12681/mms.254

Conflict of Interest Statement: The authors declare that the research was conducted in the absence of any commercial or financial relationships that could be construed as a potential conflict of interest.

APPENDIX

List of Threshold Values That Define Classification Areas of Floating Litter Distribution

The limiting thresholds that defined the low, medium and high values of average and standard deviation maps of floating litter distribution were calculated using the K-means clustering algorithm (Jain, 2010). The limiting values are listed in **Table A1** and used to classify the distribution of particles into three categories: recurrent, occasional, and rare, following the approach of Saraux et al. (2014). The classification criteria are also presented in **Table A1**.

TABLE A1 | Intervals defining the low, medium and high ranges of average and standard deviation maps for experiments A, B and C.

Experiment	Average maps, intervals	Standard deviation maps, intervals	Classification criteria
Experiment A; Case A1	low = (0.02, 0.40) medium = (0.40, 0.96) high = (0.97, 2.68)	low = (0.07, 0.29) medium = (0.29, 0.48) high = (0.48, 0.88)	Recurrent: high mean and low or medium standard deviation Occasional: high standard deviation Rare: low or medium mean and low or medium standard deviation
Experiment A; Case A2	low = (0.02, 0.47) medium = (0.47, 1.10) high = (1.11, 2.56)	low = (0.07, 0.27) medium = (0.28, 0.43) high = (0.44, 0.88)	
Experiment A; Case A3	low = (0.02, 0.51) medium = (0.52, 1.22) high = (1.22, 2.63)	low = (0.07, 0.22) medium = (0.23, 0.38) high = (0.38, 0.66)	
Experiment A; Case A4	low = (0.02,0.40) medium = (0.40, 1.10) high = (1.12,2.67)	low = (0.07, 0.24) medium = (0.25, 0.44) high = (0.45, 0.74)	
Experiment B	low = (0.04, 0.43) medium = (0.45, 1.04) high = (1.05, 2.42)	low = (0.11, 0.31) medium = (0.32, 0.53) high = (0.53, 1.11)	
Experiment C	low = (0.04, 0.52) medium = (0.53, 1.37) high = (1.55, 3.43)	low = (0.09, 0.26) medium = (0.26, 0.43) high = (0.43, 0.78)	

The threshold values were calculated applying the k-means algorithm and the criteria to define classification areas followed the approach of Saraux et al. (2014).

frontiers in Environmental Science

ORIGINAL RESEARCH
published: 19 July 2017
doi: 10.3389/fenvs.2017.00045

Distribution and Modeled Transport of Plastic Pollution in the Great Lakes, the World's Largest Freshwater Resource

*Rachel N. Cable[1], Dmitry Beletsky[2], Raisa Beletsky[2], Krista Wigginton[3], Brendan W. Locke[1] and Melissa B. Duhaime[1]**

[1] Department of Ecology and Evolutionary Biology, University of Michigan, Ann Arbor, MI, United States, [2] School of Natural Resources and the Environment, Cooperative Institute for Great Lakes Research, University of Michigan, Ann Arbor, MI, United States, [3] Department of Civil and Environmental Engineering, University of Michigan, Ann Arbor, MI, United States

Most plastic pollution originates on land. As such, freshwater bodies serve as conduits for the transport of plastic litter to the ocean. Understanding the concentrations and fluxes of plastic litter in freshwater ecosystems is critical to our understanding of the global plastic litter budget and underpins the success of future management strategies. We conducted a replicated field survey of surface plastic concentrations in four lakes in the North American Great Lakes system, the largest contiguous freshwater system on the planet. We then modeled plastic transport to resolve spatial and temporal variability of plastic distribution in one of the Great Lakes, Lake Erie. Triplicate surface samples were collected at 38 stations in mid-summer of 2014. Plastic particles >106 μm in size were quantified. Concentrations were highest near populated urban areas and their water infrastructure. In the highest concentration trawl, nearly 2 million fragments km^{-2} were found in the Detroit River—dwarfing previous reports of Great Lakes plastic abundances by over 4-fold. Yet, the accuracy of single trawl counts was challenged: within-station plastic abundances varied 0- to 3-fold between replicate trawls. In the smallest size class (106–1,000 μm), false positive rates of 12–24% were determined analytically for plastic vs. non-plastic, while false negative rates averaged ∼18%. Though predicted to form in summer by the existing Lake Erie circulation model, our transport model did not predict a permanent surface "Lake Erie Garbage Patch" in its central basin—a trend supported by field survey data. Rather, general eastward transport with recirculation in the major basins was predicted. Further, modeled plastic residence times were drastically influenced by plastic buoyancy. Neutrally buoyant plastics—those with the same density as the ambient water—were flushed several times slower than plastics floating at the water's surface and exceeded the hydraulic residence time of the lake. It is likely that the ecosystem impacts of plastic litter persist in the Great Lakes longer than assumed based on lake flushing rates. This study furthers our understanding of plastic pollution in the Great Lakes, a model freshwater system to study the movement of plastic from anthropogenic sources to environmental sinks.

Keywords: plastic debris, Great Lakes, freshwater pollution, transport model

OPEN ACCESS

Edited by:
Julia Reisser, The Ocean Cleanup, Netherlands

Reviewed by:
Mario Barletta, Federal University of Pernambuco, Brazil
Francisco José A. Cysneiros, Federal University of Pernambuco, Brazil
Dick Vethaak, Deltares, Netherlands

****Correspondence:***
Melissa B. Duhaime
duhaimem@umich.edu

Specialty section:
This article was submitted to Marine Pollution, a section of the journal Frontiers in Environmental Science

Received: *05 December 2016*
Accepted: *03 July 2017*
Published: *19 July 2017*

Citation:
Cable RN, Beletsky D, Beletsky R, Wigginton K, Locke BW and Duhaime MB (2017) Distribution and Modeled Transport of Plastic Pollution in the Great Lakes, the World's Largest Freshwater Resource. Front. Environ. Sci. 5:45. doi: 10.3389/fenvs.2017.00045

INTRODUCTION

In recent years, anthropogenic litter in the form of plastic debris has been documented in widespread and diverse marine (Law et al., 2010, 2014; Cózar et al., 2014; Fischer et al., 2015; van Sebille et al., 2015; Law, 2016), freshwater (Eriksen et al., 2013; Free et al., 2014; Mani et al., 2015; Baldwin et al., 2016; Mason et al., 2016), and even aeolian (Dris et al., 2015) biomes. It is estimated that 4.8–12.7 million tons of plastic enters the ocean in a single year (Jambeck et al., 2015), with a quarter of a million tons currently floating in the world's oceans (Eriksen et al., 2014). It is estimated that 70–80% of marine litter (most of which is plastic) originates from inland sources via rivers (GESAMP, 2010). In the absence of mechanisms to incentivize improved waste management and behavior change, this number will continue to rise, reflecting the exponentially increasing global production of plastic goods (PlasticsEurope: Association of Plastics Manufacturers, 2015). Studies have shown that aquatic organisms ingest plastic pollutants (Boerger et al., 2010; Foekema et al., 2013). Consumption results in energetic and fitness costs (Besseling et al., 2012; Wright et al., 2013) and other morbid impacts (Rochman et al., 2013). There is a high likelihood that humans are consuming plastic derived from fish and shellfish (Van Cauwenberghe and Janssen, 2014; Rochman et al., 2015b), with as of yet unknown health consequences. In the wake of these discoveries, the United Nations has declared plastic pollution among the most critical emerging environmental issues of our time (UNEP, 2016). The scientific consensus is that plastic pollution must be reduced to avoid the risk of irreversible ecosystem harm (Rochman et al., 2016). Yet, an incomplete understanding of the global plastic litter budget hinders the strategic development of mitigation and prevention policy. To effectively target major sources and pathways, the question remains: what drives the concentration and flux of plastic debris across environmental reservoirs?

Plastic pollution first was reported in the ocean over 40 years ago (Carpenter and Smith, 1972; Colton et al., 1974; Wong et al., 1974) and has continued to be a focus of extensive research efforts (Moore et al., 2001; Thompson et al., 2004; Law et al., 2010, 2014; Cózar et al., 2014). Recently, there has been a call to bring similar focus to freshwater (Wagner et al., 2014; Dris et al., 2015; Eerkes-Medrano et al., 2015). Concentrations of microplastics—plastics <5 mm in the largest dimension—in lakes and rivers have been reported as high, or higher, than in central oceans gyres (Eriksen et al., 2013; Castañeda et al., 2014; Free et al., 2014; Lechner et al., 2014; Yonkos et al., 2014; Corcoran et al., 2015; Mani et al., 2015; Baldwin et al., 2016; Mason et al., 2016). Freshwater ecosystems play a critical role in the global water cycle and human health. They connect the inland watersheds that provide drinking water for most of the global population. It is essential to understand the nature and impacts of emergent contaminants, such as, plastic litter, their associated persistent organic toxins (Koelmans et al., 2016; O'Connor et al., 2016), and properties of plastic-toxin interactions (Hankett et al., 2016) to effectively preserve this resource.

The North American Great Lakes system contains one-fifth of the world's freshwater and is arguably one of the continent's most valuable natural resources. Field surveys have confirmed the presence of microplastics in Great Lakes surface water (Eriksen et al., 2013; Mason et al., 2016), sediment (Corcoran et al., 2015; Ballent et al., 2016), and beaches (Zbyszewski and Corcoran, 2011; Hoellein et al., 2014; Zbyszewski et al., 2014; Driedger et al., 2015), as well as the rivers (Baldwin et al., 2016) and wastewater treatment plant (WWTP) effluents (Michielssen et al., 2016) that directly feed into the Great Lakes. Yet, these data are sparse. There is currently insufficient knowledge of spatial and temporal resolution of plastic debris in the Great Lakes to efficiently focus strategic mitigation and management.

The study of plastic in the environment is a rapidly growing field of research. Studies from many sectors have employed diverse analytical methods for the isolation, identification, and quantification of plastic particles in environmental samples. While studies continue to resolve the limits of the myriad new methods used, it remains difficult to obtain, with meaningful throughput and accuracy, a seemingly simple data type: plastic counts. For instance, in the absence of replicate sampling, we do not know how representative single samples are of the environments from which they are collected. Further, most studies rely on visual inspection of samples to identify and count plastic particles. Yet, visual identification can incur error rates from 20 (Eriksen et al., 2013) to 70% (Hidalgo Ruz et al., 2012), with nearly 99% misidentification for sediment samples (Löder and Gerdts, 2015). These challenges hinder future research efforts, as well as our ability to leverage existing data describing environmental plastic.

In this study, we addressed five objectives and sought to answer: (i) What is the spatial distribution of plastic litter across three of the Great Lakes (Lakes Superior, Huron, and Erie) and one connecting lake (Lake St. Clair) down to the smallest particle size yet explored (106 μm)? We hypothesized that plastic concentrations would correlate with proximity to urban areas and that the concentrations observed would dwarf those reported using a larger size cut-off (333 μm; Eriksen et al., 2013). (ii) How is the distribution and the residence time of plastic litter influenced by physical properties of the plastic particles (e.g., buoyancy)? We hypothesized that neutrally buoyant particles, which move three dimensionally through the water column, would have a longer residence time than floating particles that experience surface drift only. (iii) Do permanent features of high plastic pollution exist (e.g., a "Lake Erie Garbage Patch") where mitigation could be focused? Based on existing hydrodynamic models of Lake Erie that predict summer convergence (Beletsky et al., 2013), we hypothesized that permanent features of high plastic pollution would exist in surface drift models and field survey data in anticyclonic anomalies. To inform method development and data interpretation in this study and across the field, we sought to answer (iv) how variable are plastic concentrations among triplicate trawls sampled consecutively at the same location? We hypothesized that within-station variability in count data would not be even across sites, but rather could depend on weather and sampling conditions. Finally, we asked (v) what is the false-positive rate for discerning plastic from non-plastic particles based on visual inspection? As dozens of previous studies have relied on visual inspection alone, we hypothesized that false-positive rates would be <50%, implying

that this method was not prohibitively error-prone. Collectively, these efforts lead to a better understanding of the drivers of freshwater plastic pollution in the Great Lakes and around the globe.

MATERIALS AND METHODS

Lake Sampling

To assess the spatial distribution of plastics across three Great Lakes and Lake St. Clair (objective i) surface water samples were collected at 38 stations (**Figure 1**) throughout the summer (May–August) of 2014 using a rectangular manta trawl 16 cm high by 61 cm wide towing a 100 μm Nitex mesh net 3 m long (Wildco) with a 100 μm Nitex mesh cod-end 28 cm long by 15.5 cm in diameter and a flowmeter (General Oceanics Model 2030R Mechanical Standard Rotor). The net was towed outside the wake of the boat at ∼2 knots for 20 min. For precision comparison at each station (objective iv), consecutive triplicate trawls were performed over the same transect. The difference in flow meter readings was multiplied by the manufacturer rotor constant and the width of the net mouth to calculate the area of water sampled. In order to standardize and compare plastics concentrations with previous studies (Eriksen et al., 2013; Mason et al., 2016), counts were divided by respective trawl area to achieve concentrations of plastics km^{-2}.

Stations were categorized as basin (>12 km from coast, $n = 7$), non-urban (<12 km from coast with <5,000 inhabitants km^{-2}, $n = 15$), urban (<12 km from coast with >5,000 inhabitants km^{-2}, $n = 6$), river plume ($n = 5$), and WWTP (sampled from environment near where final effluent is released, $n = 5$; **Figure 1**). Environmental data describing conditions at the start of each trawl, including wind speed, cloud cover, water temperature, air temperature, wave height, eastward surface water velocity, northward surface water velocity, wave direction, and wave period, were collected from the Great Lakes Observing System Point Query Tool of the Great Lakes Coastal Forecasting System[1]. Hourly data (or 3-h data, in the case of water temperature) for before and after the start time of each trawl were pulled, and the average was weighted by the number of minutes between data points. Descriptors of all trawls are available (Supplementary Data Sheet 1) where data interpolation was possible (e.g., no data existed for stations in Lake St. Clair or rivers).

Samples were recovered by rinsing the contents of the cod-end into a series of brass-framed sieves (Humboldt Mfg. Co.; Elgin, IL, USA) with stainless steel mesh sizes 4.75 mm, 212 μm, and 45 μm (**Figure 2A**; Humboldt Mfg. Co.). Each fraction was rinsed into a plastic bottle (HDPE bottle, PP screw top, Fisher Scientific 03-313-6C, 03-313-6B) with 70% ethanol for

[1]http://data.glos.us/glcfs/

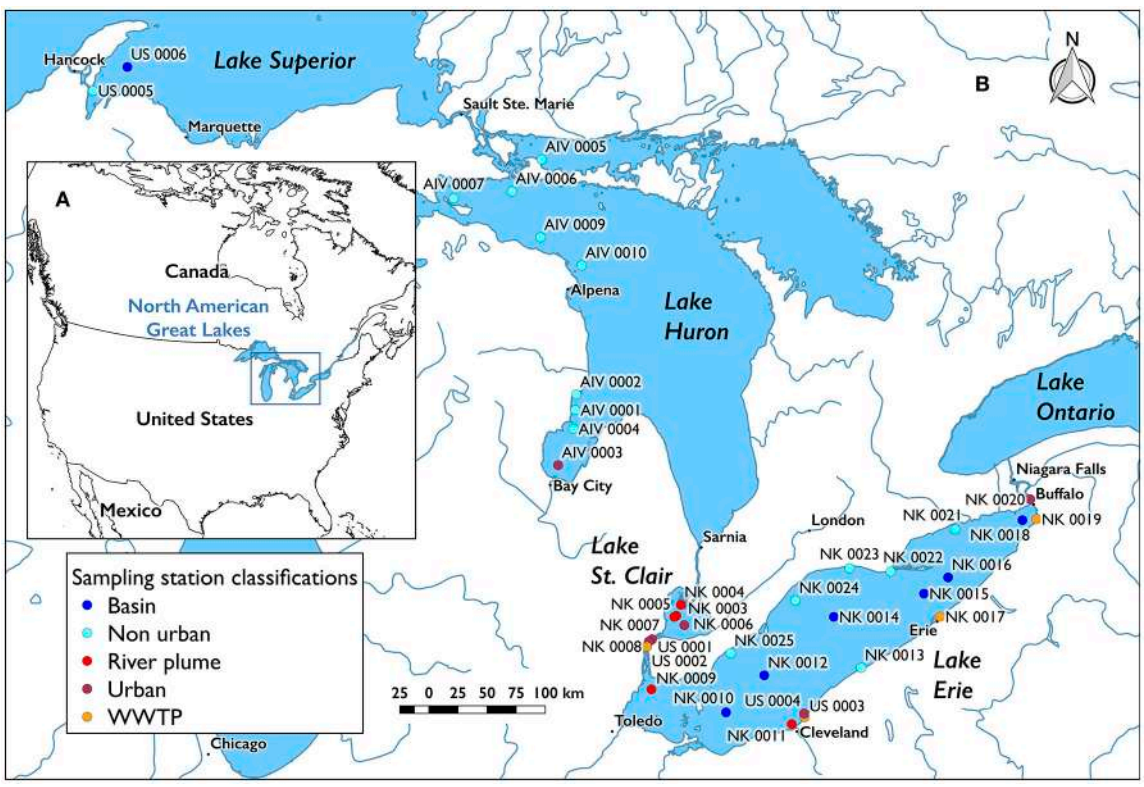

FIGURE 1 | Maps of all stations sampled. Each station contained replicate trawls. **(A)** Overview and location of the North American Great Lakes on the North American continent. **(B)** Station locations and classifications in Lake Superior, Lake Huron, Lake St. Clair, and Lake Erie.

FIGURE 2 | Photographs of samples at various stages of processing, as well as examples of different shape classes. Arrows indicate plastic amidst co-sampled nonplastic organic matter; blue: fragment, dark red: line, yellow: nurdles, cyan: sphere/bead, brown: fiber. **(A)** Bulk sample directly upon retrieval from Manta on a stack of a series of sieves. This sample contained an abundance of algal biomass. **(B)** Bulk sample drying on a 53 μm mesh net. **(C)** Sample after enzymatic processing, which included an incubation in hydrogen peroxide that bleached much of the non-plastic organic matter. This bleaching aided in differentiating plastic (tended to retain color) from non-plastic (prone to bleaching) particles. **(D)** Examples of plastic of sphere class; zoomed in subset of sample in **(B)**. **(E)** Smallest size fraction (106–1,000 μm) after WPO. Note colored plastic fibers (brown arrows) enmeshed in mass of natural fibers bleached white from hydrogen peroxide treatment. **(F–H)** Examples of plastic of fragment, film and line shape classes, respectively; ruler markings are in cm units. **(J,I)** Examples of plastic of paint chip and fiber shape classes, respectively; grid squares are in 5 mm units.

preservation. Sampled items that were too large to fit in a bottle were stored in Ziploc XL bags for later examination. All liquids used directly on the samples were filtered through 100 or 20 μm Nitex mesh in the field.

Sample Processing and Counting

Field-collected samples were spread over 53 μm Nitex mesh (**Figure 2B**), weighed for wet mass, dried at 60°C, and subsequently weighed for dry mass. Large pieces of organic material (e.g., sticks, leaves, etc.) were removed manually. The sample was mixed at a 1:1 ratio with 10% sodium dodecyl sulfate (Acros Organics 226140025) and incubated at 50°C, rotating at 80 rpm for least 24 h. Samples were then size-fractionated through a series of brass and stainless steel sieves (Humboldt Mfg. Co.; Elgin, IL, USA) with mesh sizes 4.75 mm, 1,000 μm, and 106 μm.

The 106–1,000 μm fraction of each sample was digested to remove non-plastic labile organic matter. The first digestion method used consecutive incubations with proteinase, cellulase, and chitinase, followed by incubation in 30% H_2O_2 for 24 h [*sensu* (Lorenz, 2014); **Figure 2C**: sample images]. Following the release of a NOAA Marine Debris Technical Memorandum providing guidelines on the analysis of microplastics in the marine environment (Masura et al., 2015), all previously processed samples were re-processed, and all subsequent samples were processed using only the wet peroxide oxidation (WPO) protocol recommended therein (2015). After oxidation, the remaining material was filtered over 104 μm stainless steel filters (TWP Inc., 150 Mesh T304 Stainless 0.0026; Berkeley, CA), and transferred to a glass petri-dish with 70% ethanol and dried.

Plastic pieces were manually pulled from the <4.75 mm fraction. The raw 1.00–4.75 mm and digested 106–1,000 μm fractions were visually sorted with the aid of a stereo dissecting microscope (10–80x; Zeiss SteREO Discovery.V8; Oberkochen, Germany). Each plastic piece in the two larger size classes was categorized by shape (**Figures 2E–I**): fragment (secondary plastic broken down from larger debris), film (e.g., thin plastic from bags and wrappers), fiber (e.g., individual filaments of textile threads, very thin and frequently curled), line (e.g., fishing line, straighter, and thicker than fiber), nurdle (preproduction plastic pellet), sphere, foam, or paint (consistent with multiple studies that consider paint a plastic or confirm it is composed of, e.g., alkyds and (poly)acrylate/styrene; Lima et al., 2014; Kang et al., 2015; Neves et al., 2015; Song et al., 2015; Imhof et al., 2016; Nizzetto et al., 2016). Such detailed categorization was not possible for the smallest size class (106–1,000 μm), so the smallest particles were classified as either fragment or fiber.

Substantial effort was invested in gaining experience and establishing confidence in visually and tactilely distinguishing plastic from non-plastic particles, especially in the smallest (106–1,000 μm) size class. A collection of characteristics was established to distinguish plastic from non-plastic and to categorize plastics into morphological types. Physical features (color, hardness, fragility, shape) were considered. Features that frequently indicated plastic fragments included: malleability (not brittle), defined jagged shape, shiny surface, and presence of artificial dyes. Dye-free plastic particles were identified by their opaque and white nature. Features that often indicated an inorganic particle included: brittleness or unresponsiveness to force applied by tweezers, audible scratching noise when scraped, transparency, and well-defined crystalline structures and right-angle fractures.

Precaution was taken to minimize risk of sample contamination from handling and the laboratory environment. All liquid that came in contact with the samples (water for sieving, ethanol for storing) was filtered to remove particles >10 μm, glassware for storage was blasted with high-pressure air before use. Thin Teflon sheets (0.005 "Natural Virgin PTFE Roll Stock 12" Wide, Ridout Plastics Co. Inc.) were inserted between storage glassware and their plastic screw tops, as Teflon is rare among environmental plastics and its diagnostic fluoride ion could be detected analytically downstream if contamination did occur. Samples were processed in a laminar-flow or fume hood and remained covered otherwise. Cotton laboratory coats were worn by all individuals. Blank samples consisting of one 1,500 ml and two 500 ml aliquots of 10 μm-filtered MilliQ were processed and counted alongside field samples to account for environmental plastics incorporated during the sampling process that would lead to false positive plastic counts.

All data treatment and statistics were performed using the R statistical environment (version R-3.3.1; Team, 2014). All R code generated to create figures and perform calculations is freely available[2][3] Maps of trawl locations and counts were generated with Quantum GIS (v. 2.18; QGIS Development Team, 2016).

Scanning Electron Microscopy Energy-Dispersive X-Ray Spectroscopy (SEM-EDS)

To assess human error and determine our false positive vs. false negative rates in the assignment of the smallest particles as plastic (objective v), a subset of particles from the smallest size class were randomly chosen from each of the suspected plastic ($n = 10$) and suspected non-plastic particle ($n = 10$) pools across 10 trawls. These particles were characterized analytically (described below). In addition, we prepared a library of 35 known standards to inform our ability to differentiate plastic, mineral, and non-synthetic organic matter and identify potential contamination of our samples from plastic in the processing environment. Standard items included virgin polymers, plasticware, and instruments used for sample collection, processing, and storage, paint from a sampling vessel (R/V *Nancy K*), fibers from lab coats, hair from sample processors, phytoplankton carcasses, and mineral particles.

SEM-EDS was performed to acquire an atomic signature for the 260 particles and standards assessed. Particles were mounted on an SEM peg (0.5 in. diameter; Electron Microscopy Sciences, Cat. 75160; PA, USA) with a piece of double-sided carbon tape (Electron Microscopy Sciences, Cat. 77816; PA, USA). A thin layer (∼40 nm) of gold was applied to the sample using a gold sputter coating machine (120 s, Denton Vacuum Inc., Desk II, Cherry Hill, N.J.). Each particle was imaged using a JEOL JSM-7800F SEM at an accelerating voltage of 15 keV and an acquisition time of 20 s. A rectangular well-focused central area on each particle was excited via EDS. The resulting spectra were analyzed with Oxford AZtec 3.1 EDS software. The auto-ID function using default parameters verified the presence of elements on the surface of each particle. Following data acquisition, particles were assigned to each of three classes based on peak elements and surface texture: inorganic/mineral (IO), non-plastic (NP) organic matter, and plastic (P). Some gradation was allowed between discrete classes resulting in 5 different categories: P, P-NP, NP, NP-IO, IO.

Lake Erie Plastic Transport Model

It is not feasible to perform the high-resolution spatial and temporal sampling required to understand the lake-wide distribution and movements of plastic pieces. Thus, a Lagrangian particle transport model previously used in Lake Erie (Michalak

[2]https://github.com/DuhaimeLab/Frontiers_2017_GreatLakesPlasticDistrib
[3]http://www-personal.umich.edu/~duhaimem/Rpubs_code/GreatLakes_Plastic_Pollution_Study_Cable_etal_2017.html

et al., 2013; Fraker et al., 2015; Beletsky et al., 2017) was applied to simulate transport of microplastics over a variety of timescales and plastic properties (e.g., its buoyancy; objectives ii and iii). In this model, particle trajectories were calculated with the hydrodynamic model velocity recorded at regular time intervals (e.g., hourly). For each particle, the gridded velocities were interpolated to its location and the particle was moved to a new location based on the interpolated velocity and the time step of the particle transport model (Lynch et al., 2014). The three-dimensional particle trajectory code is based on the second order accurate horizontal trajectory code, as described in Bennett and Clites (1987), with the addition of vertical position tracking. Plastic "particles" in the model are neutrally buoyant (i.e., have the same density as the ambient water), passive (i.e., they follow local three-dimensional currents), and biochemically inert. If collision with model boundaries occurs, particles remain in the nearshore zone. The model includes horizontal and vertical diffusion, as introduced by Smagorinsky (i.e., with a non-dimensional coefficient of 0.005 in the horizontal diffusion parameterization; Smagorinsky, 1963) and random-walk approaches, respectively. Vertical diffusion was set at 5×10^{-4} m^2 s^{-1}. Because the size of most particles in this study is <1 mm, they are considered fully submerged and therefore windage is zero. In experiments that examine the effect of plastic buoyancy on residence time and transport, floating particles were driven by surface currents only, which were obtained from the top layer of the 3D hydrodynamic model.

Advection fields used by the particle model were produced by the three-dimensional finite-difference hydrodynamic model based on the Princeton Ocean Model (Blumberg and Mellor, 1987), driven by the wind, heat flux, and tributary flow from 22 major rivers and two outflows (listed in Schwab et al., 2009). The hydrodynamic model used a uniform 2 km horizontal grid with 21 vertical levels. Six years of hourly current data (2004–2005, 2007, and 2009–2011) obtained from previous applications (Beletsky et al., 2013) were used to model microplastic transport in summer months (including the month of June, the month of Lake Erie field sampling). In addition, year-long simulations were conducted when particles were continuously released throughout each year. To calculate residence times, the sequence of years was looped because longer time periods were required to flush the vast majority of particles from the lake.

In each model simulation, virtual particles were released daily to Lake Erie surface water at 29 tributaries (Supplementary Table 2) and two WWTPs in the Cleveland area. Particles left the lake through Niagara River and Welland Canal (easternmost edge of Lake Erie). For residence time calculations, particles were released during the first year (2004) and then tracked until the percentage of particles remaining in the lake dropped to 1% (eight years for neutrally buoyant particles).

RESULTS AND DISCUSSION

This dataset represents the largest single-season effort of plastic quantification in the Great Lakes to date. Plastic was counted in 108 surface trawl samples, which spanned 38 stations across Lakes Superior, Huron, St. Clair, and Erie. Plastic was found at every station sampled (**Figure 3**). The trawl with the highest total concentration of plastic contained 4-fold higher plastic than yet reported in the surface of the Great Lakes (Eriksen et al., 2013; Mason et al., 2016). The vast majority of plastic counted was <1 mm in size (**Figure 4A**).

Concentrations and Distributions of Great Lakes Plastic

Plastic Concentrations Were Highest at Urban Centers

Total plastic abundances per surface trawl spanned an order of magnitude. They ranged from 1,910,562 particles km^{-2} in the Detroit River plume (NK0008-3) to 126,933 particles km^{-2} in the Straits of Mackinac in Lake Huron (NK 0007-1; **Figure 3D**; Supplementary Data Sheet 1). Notably, these total concentrations and all that follow do not include counts of fibers, as during sample processing it became evident that fibers could not be quantified with equally high confidence across size fractions, an issue which is discussed at length below. Fiber concentrations were analyzed separately to explore patterns in the data.

The highest concentrations of plastic were found in samples collected within 12 km of the coast of populated urban cities, in river plumes, or directly at the effluent of WWTPs (**Figures 3**, **4B**). All of the most concentrated samples but one were collected in Lake Erie or the urban river and estuary-like lake directly feeding it (Detroit River and Lake St Clair; **Figure 2**). Our empirical data support recent model predictions that the loads of Lake Erie plastic inputs are 4- and 80-fold higher than Lakes Huron and Superior, respectively (Hoffman and Hittinger, 2017). Notably, the plastic input loads for this model were scaled to census-derived population density of the coastlines (Hoffman and Hittinger, 2017)—an underlying presumed correlation our field data support. The lowest counts were collected at non-urban coastal stations and offshore basin stations, with the exception of the deepest point of the Eastern Basin of Lake Erie (**Figures 3**, **4B**). These findings support previous reports of a correlation between plastic concentrations and proximity to urban centers in the Great Lakes (Baldwin et al., 2016), as well as other enclosed and semi-enclosed aquatic environments across the world, such as, tributaries to the Chesapeake Bay, USA (Yonkos et al., 2014), the Bay of Brest in France (Frère et al., 2017), the Xiangzi Bay upstream of the three Gorges Dam (Zhang et al., 2017), inland lakes around Wuhan, China (Wang et al., 2017), and estuaries in and around Durban, South Africa (Naidoo et al., 2015). Attributes that are likely to contribute to elevated plastic concentrations in urban vs. non-urban locales include higher population densities (Jambeck et al., 2015), increased particulate aeolian inputs (including plastic; Dris et al., 2015), and increased areas of impervious substrate. The percent of a watershed comprised of impervious substrate is positively correlated with higher plastic concentrations in the Great Lakes watershed (Baldwin et al., 2016), likely due to greater volume and higher velocity runoff during storm and snow melt events. The higher concentrations in river plumes

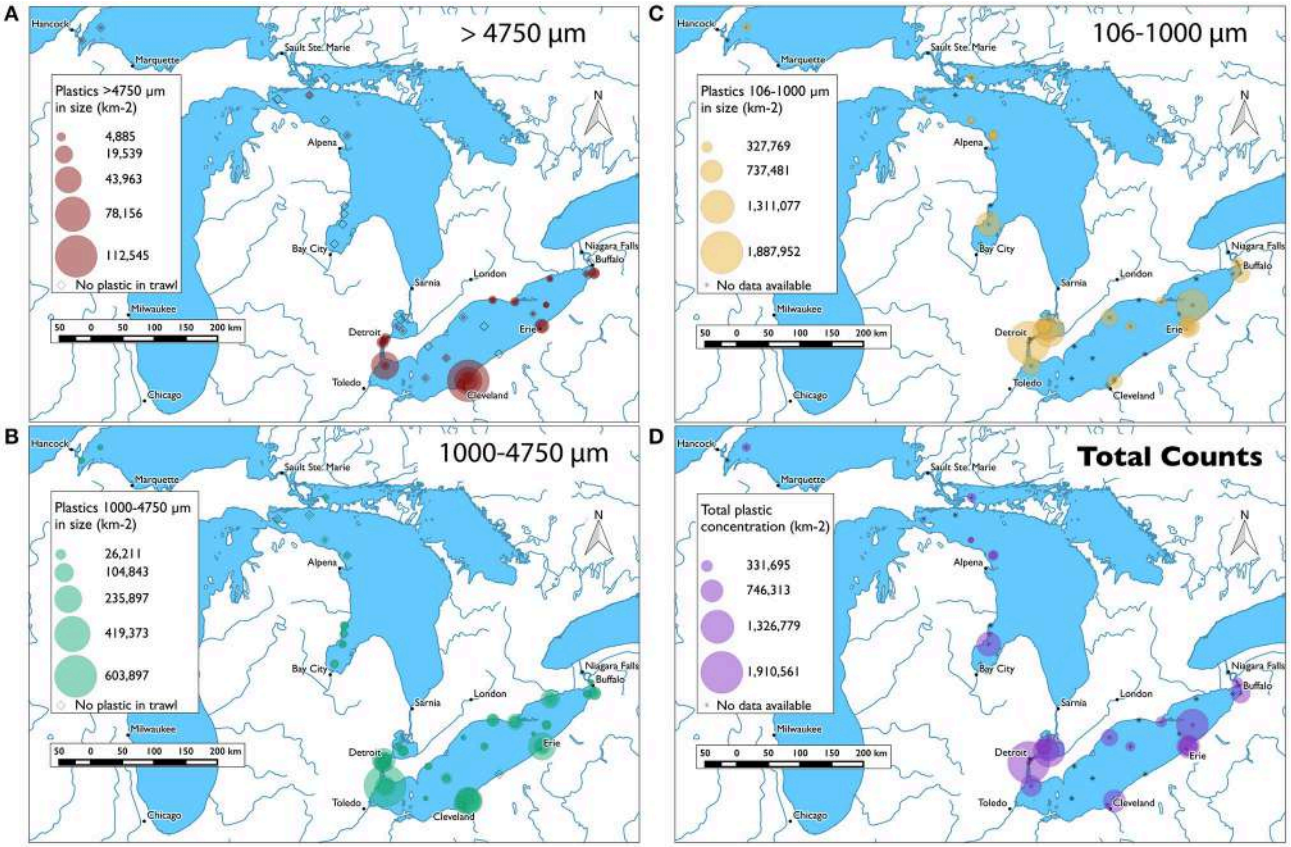

FIGURE 3 | Maps of plastic concentrations across the lakes sampled, where magnitude of concentration is depicted by size of circle around trawl location. Note, fiber counts are not included in these figures, as discussed below. **(A)** Mapped counts of plastic litter >4,750 µm. **(B)** Mapped counts of plastic litter 1,000–4,750 µm. **(C)** Mapped counts of plastic litter 106–1,000 µm. **(D)** Total mapped counts for the stations where all three size classes were quantified.

and near WWTP effluents than in coastal areas (**Figure 4B**) suggest these inputs to be sources (McCormick et al., 2014) and that plastic debris enters this system from inland waterways and human activity. Increasing the degree of pervious substrate in watersheds, such as, the implementation of green infrastructure catchments, should be explored as an effective measure to capture plastic debris in runoff and reduce loads ultimately reaching waterways. As the number of storm events is expected to increase with a changing climate (IPCC, 2012), such innovations are timely to preventatively buffer our freshwater systems from being inundated with stormwater-delivered debris.

Single Trawls Are Imprecise: Within-Station Variability Can Vary 3-Fold

This is the first survey of freshwater plastic litter to address variability in counts by conducting replicate trawls at each of 38 stations. The distributions of all trawl concentrations, total concentrations, and station concentrations deviated significantly from normal distribution (Shapiro Wilks test, $p << 0.01$) with high skewness (1.9–6.62) and kurtosis (3.5–49.25; Supplementary Figure 1). As a result, non-parametric tests were used (e.g., Spearman's rank correlation) and metrics that do not represent strongly skewed data (e.g., standard deviation) were not used to describe and interpret the results. Rather, to assess factors that influence within-station variability, we calculated a metric we termed the mean-normalized range (MNR) by dividing the count range (max–min) of each station by the mean of the station.

The vast majority of trawl concentrations from the same station varied more than 100%, as depicted by a mean normalized range (MNR) >1 (**Figure 5**; Supplementary Data Sheet 3). In other words, the accuracy of a single trawl at one station is quite low and repeated trawls at the same location can vary in precision by up to 3-fold. We suspect that the magnitude of MNR at certain stations is due to undersampling. Precision increases as the plastic concentration sampled increases, as MNR is significantly negatively correlated with total trawl concentration (Spearman's $rho = -0.629$, $p = 0.000$; **Figure 5**). MNR is <1 for all counts in the smallest size class, which have the largest concentrations ($M = 0.09$) and most frequently >1 in the largest size class ($M = 1.94$; **Figure 5**, Supplementary Figure 2), which have relatively lower concentrations. While dependent on plastic concentration, the MNR was not significantly influenced by air velocity ($rho = -0.093$, $p = 0.245$), east-west surface current velocity ($rho = -0.072$, $p = 0.364$), wave period ($rho = -0.078$, $p = 0.330$), or wave height ($rho = -0.093$, $p = 0.242$)—all local conditions that could influence the distribution of plastics at the water surface

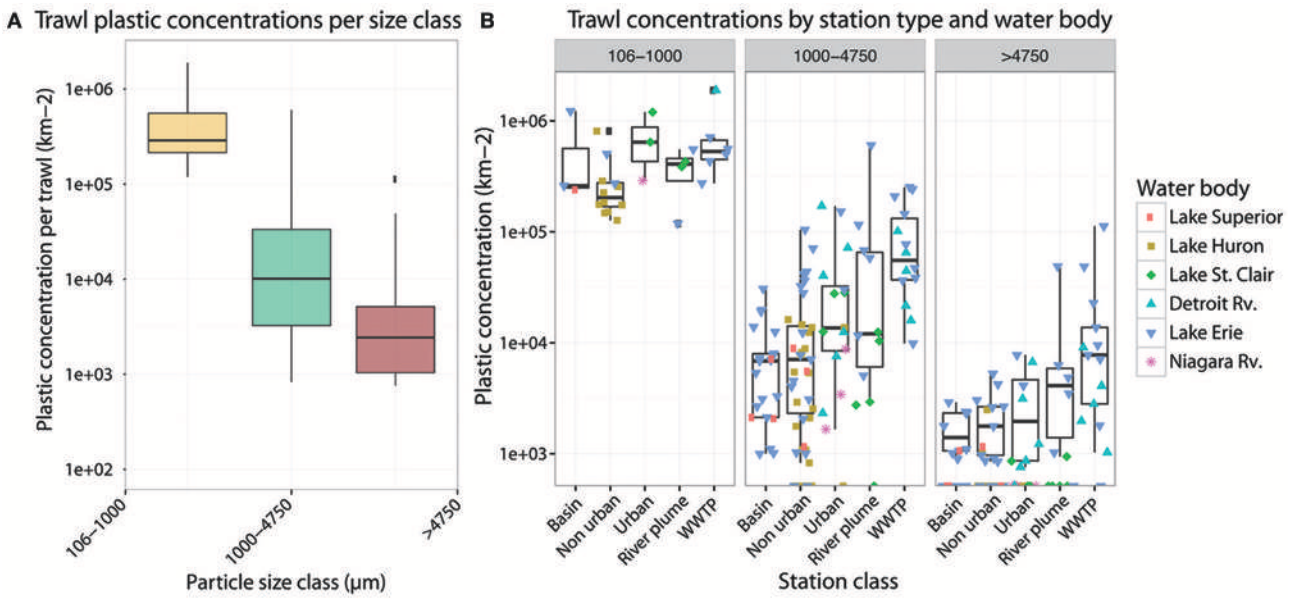

FIGURE 4 | (A) Boxplots depicting the means and spreads of all individual trawl counts by particle size fraction. **(B)** Boxplots depicting the means and spreads of individual trawl counts by size class, station type, and water body: Lake Superior (pink square), Lake Huron (brown square), Lake St. Clair (green diamond), the Detroit Rv. (blue upright triangle), Lake Erie (dark blue upside-down triangle), and the Niagara Rv. (purple star).

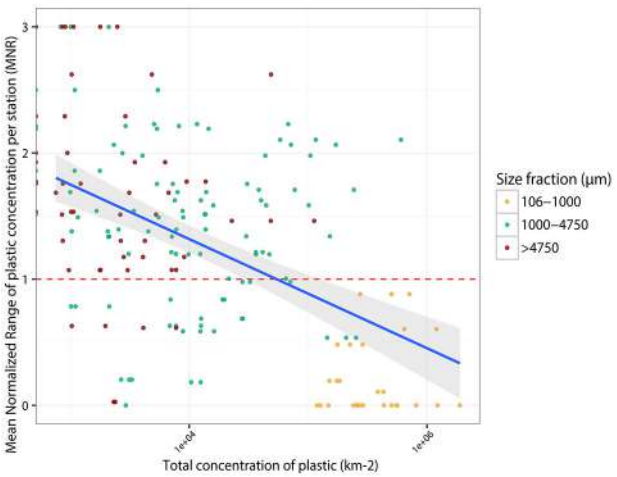

FIGURE 5 | Plot of trawl mean normalized ranges (MNR) across stations vs. the log of plastic concentration in each individual trawl. Regression line of the linear model used to predict MNR from plastic concentration is shown (R^2 = 0.442, slope = −0.357, intercept = 2.737, p < 2.2e-16). The gray band depicts the 95% confidence level interval for predictions from the linear model.

between trawls. However, longitudinal surface current velocity positively varied with MNR ($rho = 0.166$, $p = 0.037$); an increase in north-south current velocity was correlated with a decrease in precision between trawls. As currents in the lake are mostly wind-driven and winds on Lake Erie predominantly blow west to east, increases in north-south current velocity may indicate a local weather anomaly, such as, a squall or storm. These features are known to build up and die down quickly; it was not uncommon to experience a short burst in weather change over the course of the 1–2 h spent sampling at a single station. Such dynamic local conditions could increase the variability between trawl counts within a single station and decrease the accuracy of a trawl. To maximize reliability of surface plastic counts, we suggest samples not be taken around wind-related weather anomalies.

A similar survey of marine plastic debris assessed variability with replicate sample quantification in the North Pacific Gyre (Goldstein et al., 2013). This study found a mean within-station coefficient of variation (CoV; calculated as the station standard deviation divided by the station mean) of 51.4% for net-collected samples. CoV depends on the station standard deviation, which we deemed an inappropriate representation of data as heavily positively skewed as ours (Supplementary Figure 1). Yet, for purposes of comparison, we determined the CoV across the stations in this study and found they ranged from 1.5 to 173% (Supplementary Figure 3). The CoV of the smallest size class was less than that of the North Pacific study, whereas the CoV of larger size classes was greater (Supplementary Data Sheet 3). In the power analysis performed by Goldstein et al. (2013), statistical power increased when number of samples increased. In the case of our data, within-station variability appeared more influenced by the plastic count in each sample than the number of samples counted (as $n = 28$ for the smallest size class, and $n = 108$ for the two larger size classes). In order to reduce the within-station variability of the larger two size classes at stations with low overall plastic concentrations, greater counts are needed per trawl, thus sampling should occur over a larger area. We suggest a minimum MNR of <1 and ideally lower. As field survey data is time consuming and costly, recognition of this count-dependent variability and the importance of replication is critical

TABLE 1 | Mean and standard deviations of plastic type concentrations (km^{-2}) across all trawls and size classes quantified.

Size (μm)	Fragment	Film	Line	Nurdle	Sphere	Foam	Paint	Total Plastic	*n*
106–1,000	465,606 ± 403,378	NA	NA	NA	NA	NA	NA	465,606 ± 403,378	28
1,000–4,750	19,237 ± 42,995	1,607 ± 3,195	1,109 ± 2,040	3,742 ± 19,500	966 ± 3,343	4,443 ± 12,953	1,115 ± 2,475	32,219 ± 73,576	108
>4,750	2,009 ± 8,500	880 ± 2,883	168 ± 460	19 ± 138	0 ± 0	427 ± 1,865	0 ± 0	3,503 ± 12,766	108

for maximizing the value of such datasets, especially as future field survey studies are designed and implemented.

Plastic Less than 1 mm Dominated the Dataset

The mean concentration of plastic in the smallest size class (106–1,000 μm) was 15-fold higher than the middle size class (1,000–4,750 μm) and 130-fold higher than the largest size class (>4,750 μm; **Figure 4A**, **Table 1**). A similar pattern was maintained in all trawls, regardless of water body or types of stations sampled (**Figure 4B**). These findings are consistent with surveys of other lakes, such as, lakes near Wuhan, China where more than 80% of the plastics found were 2 mm and smaller (Wang et al., 2017). However, plastics 1–5 mm in size were most abundant in sections of the Xiangxi River, perhaps due to a shorter residence time and less weathering while in the river (Zhang et al., 2017). Previous surveys of Great Lakes plastic have found a 40- and 6-fold difference between the smallest and largest size classes (Eriksen et al., 2013; Mason et al., 2016). It is likely that the order of magnitude increase in the relative abundance of the smallest size class between previous Great Lakes surveys and the overall maximum abundance in our study can be attributed to our use of a 106 μm size mesh collection net, as opposed to the 333 μm mesh used previously in the Great Lakes and their tributaries (Eriksen et al., 2013; Baldwin et al., 2016; Mason et al., 2016) and in most aquatic plastic debris surveys to date (Hidalgo Ruz et al., 2012; Law, 2016). As a result, our data more comprehensively capture the "micro" plastic range in the Great Lakes, knowledge of which is critical to our assessments of environmental risk. Smaller plastic particles stay at the water surface longer than larger particles of the same composition and shape (Khatmullina and Isachenko, 2016; Kowalski et al., 2016) and are more readily consumed by smaller organisms in aquatic food webs, increasing the chances of biomagnified effects due to predation (Wagner et al., 2014). Further, the larger surface area to volume ratios of these small particles increases their potential as vectors of adsorbing contaminants (Barnes et al., 2009; Teuten et al., 2009). Future studies should continue to probe this small size class, as well as develop innovative high-throughput solutions to capture and quantify particles below 106 μm and into the nanoscale, where risk may be highest due to subcellular effects (Syberg et al., 2015).

Secondary Plastics (Fragments) Were the Most Common Plastic Type

Fragments were the most abundant plastic shape class across the dataset (**Figure 6**). This finding is consistent with other recent studies that used comparable analytical methods, including a survey of 59 stations in Lake Michigan (79% fragments, 14% fibers; Mason et al., 2016), and even a study in remote Lake Hovsgol, Mongolia (40% fragments, 20% fibers and lines; Free et al., 2014). Rivers and urban effluent (e.g., WWTP) are thought to be major contributors of plastic to freshwater water systems. Notably, studies of sources of plastic to the Great Lakes have documented fibers to dominate, not fragments. An analysis of 29 Great Lakes tributaries (Baldwin et al., 2016) found total debris comprised of 71% fibers and 17% fragments. Similarly, anthropogenic litter in the effluent of a high capacity wastewater treatment plant that discharges directly to the Great Lakes was found to be 61% fibers and 33% fragments (Michielssen et al., 2016).

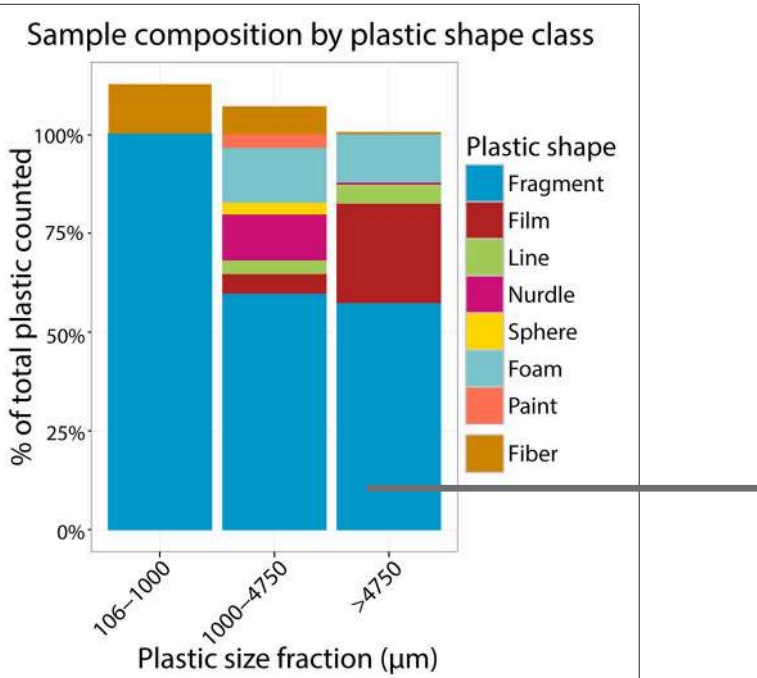

FIGURE 6 | Stacked barplot depicting the relative abundance of different shape classes amongst plastic from each size fraction. The bar to 100% for each size class represent the relative abundance of different shape classes when fibers were not included in the total counts and the portion above 100% represents the relative abundance of fibers in the total counts.

This difference may be due to the fact that typically fibers are comprised of polymers that are denser than water, e.g., nylon, polyester, acrylic. As such, in a stable water body (e.g., large lakes, ocean gyres) they are expected to sink, while in the flow of turbulent mixing systems (e.g., streams, rivers, WWTP effluent, tidal inlets) these fibers may remain mixed and in the seston (Baldwin et al., 2016). Fragments are primarily secondary

plastic debris and are likely to be composed of more positively buoyant polymers (e.g., polyethylene and polypropylene, as demonstrated in a study in Lake Michigan; Mason et al., 2016) that float at the lake surface. Alternatively, fibers may be drastically underestimated in surface aquatic environments owing to difficulties collecting fiber data, as discussed below.

When station type was considered, the relative abundances of fragments, foam, and (for the largest size class) film were high in urban and river plume samples—the latter of which were all coincidentally urban, as well (Supplementary Figure 2). Similarly, this trend was observed in river samples, where "litter-related plastic" (the collective class of fragments, foam, and film) was significantly more highly represented in Great Lakes tributaries of watersheds with urban attributes (Baldwin et al., 2016). This may be attributed to proximity to land-based plastic sources, such as, recreation on populated beaches and litter in urban areas and suggests that curbing mismanaged waste in urban centers could reduce the load of plastic in waterways.

Assessing Confidence in Plastic Count Data

Though recommendations (Ryan et al., 2009) and protocols (Masura et al., 2015) have been put forth for sample collection, processing, and quantification, standardized sampling methodology, and reporting are critically lacking (Hidalgo Ruz et al., 2012; Law, 2016). The reasons for these inconsistencies are multifaceted. This is a relatively young field of research with many newly recruited researchers from broad disciplines, e.g., environmental science, biology, chemistry, engineering, physics, oceanography, ecology, bringing diverse backgrounds to a common problem. Each study contributes new insights, but also highlights the Achilles' heel of their given approach. This process is necessary to arrive ultimately at a unified approach. In the present study, the greatest uncertainty arose in the treatment of fiber count data, as well as our ability to visually and chemically discern plastic particles from non-plastic in the smallest size class.

Confidence in fiber count data depends on size class and sorting effort

Fibers were identified in all size classes, yet the degree of certainty in the fiber count data depended on the size class, oxidative treatment of sample, and effort of the sample sorter. First, it is likely that fiber counts from field samples were underestimated because the sampled material was so heterogeneous causing fibers to be missed and unaccounted for. This was especially likely in the larger two size classes (1,000–4,750 μm and >4,750 μm), where WPO treatment was impractical at the volumes needed to be effective and thus could not be used to eliminate bulk non-plastic organic matter. In these fractions, the fibers, which are much less rigid than other plastic morphologies and more prone to "stick" to other objects when wet, were deeply enmeshed in the crevices of or entwined in natural fibers of non-plastic items (e.g., leaves, sticks, bark, feather, etc.) during sieving and sorting. As a result, fibers were difficult to separate from the non-plastic organic matter co-sampled from the lake surfaces, much of which was naturally fibrous (**Figures 2B–E**). This increased difficulty in acquiring fiber counts also required greater effort and vigilance by the person visually sorting, given the enmeshed fibers would be much thinner than other items the sorter was looking for. These issues were much less apparent in the smallest size class, where most non-plastic organic matter was removed chemically and fibers were more obvious with little surrounding or overlapping material. Thus, it is difficult to compare fiber abundance across size classes, as the "sorting effort" required varied widely. Second, owing to their small width and surface area, we could not use the same sensory data that we relied upon to discern plastic fragments from non-plastic particles under the microscope (e.g., squeezing, pinching, scratching, etc.). The small size of fibers also prohibited the controlled physical manipulation needed to perform chemical analysis via SEM-EDS—though we cannot predict whether this led to an over- or underestimate of fiber counts. Notably, these issues did not influence our ability to detect and report concentrations of plastic line. Lines were more discernible and behaved very differently when manipulated owing to their greater length, thickness, and consequent rigidity (**Figures 2A,H,J**).

Finally, fibers were the plastic type most likely to contaminate a sample during processing in this study. All but one of the 126 particles introduced to the blank controls were fibers (Supplementary Table 3). For instance, the 1,000–4,750 μm fraction of a single blank control contained 33 fibers, whereas the maximum raw number of fibers counted in the same size class was 33 and the average across all trawls was 24 (Supplementary Table 3). Further contributing to the underestimate of fibers in field samples relative to sample counts was that blank samples were pristine and easy to see, whereas fibers in field samples were often complex conglomerations of suspected natural and plastic fibers (**Figure 2E**). Though anecdotal evidence derived from observations during processing suggest that the environmental samples contained more fibers than the blanks, the possibility of contamination of samples by fibers could not be ruled out. Fiber contamination during sample processing has been reported previously (Foekema et al., 2013; Dekiff et al., 2014; McCormick et al., 2014; Woodall et al., 2015). A comparison of numbers of fibers introduced using different protocols suggested fiber contamination was introduced primarily as a result of sample sieving and moving from one holding vessel to another (unpublished data; BW Locke, RN Cable). We recommend taking precautions to reduce the number of times a sample is transferred, sieved, or filtered from the beginning of sample collection, in addition to reducing the amount of time a sample is exposed to open air outside of a fume or laminar hood.

It is paramount that the field overcomes the limitations and uncertainties related to the quantification of plastic fibers. Evidence is mounting that fibers are a dominant form of plastic pollution in many aquatic ecosystems—especially fluvial (McCormick et al., 2014; Zhao et al., 2014; Dris et al., 2015; Baldwin et al., 2016), but also in marine beaches and sediment (Browne et al., 2011; Claessens et al., 2011; Woodall et al., 2014; Fischer et al., 2015; Naidoo et al., 2015; Van Cauwenberghe et al., 2015). The ecological implications of these fibers remain to be shown, but plastic fibers are increasingly found in the stomachs and tissues of aquatic wildlife, many of which are consumed by larger animals, including humans (Neves et al., 2015; Rochman et al., 2015a; Vandermeersch et al., 2015; Li et al., 2016). Direct

human health impacts have been reported, as well: when inhaled, microplastic fibers are retained the lung tissues and can become associated with malignant tumors (Pauly et al., 1998). We must develop an accurate assessment of the sources, abundances, and impacts of synthetic fibers in our environment so that informed mitigation practices can be put into place, if deemed necessary.

Visual discrimination of plastics is confirmed by analytical methods

While most studies rely on visual inspection alone (reviewed in Hidalgo Ruz et al., 2012; Law, 2016), such human sensory-based observations can be error-prone. First, misidentification can occur due to the similarities in appearances of plastic and non-plastic particles (Filella, 2015). Second, the reliability of visual identification decreases with decreasing particle size. In the smallest size class, we used SEM-EDS analysis to test and reduce our rate of incorrectly differentiating plastic from non-plastic via visual and tactile inspection alone. EDS spectra and SEM images representative of plastic, inorganic, and non-plastic organic particles were highlighted (**Figure 7**). EDS spectra are summarized in Supplementary Data Sheet 2; EDS spectra and SEM microscopic data files are included in Supplementary Image 1.

To address erroneous counts caused by misidentification while sorting, we built a diverse library of standards (described in Supplementary Data Sheet 2). This library was used to train our classification efforts prior to analyzing sample spectra. Among the qualitative anecdotes resulting from the analysis of this library, we learned that microbeads from personal care products all contained the elements C (primary peak), N, Si, and, all but one, O (Supplementary Data Sheet 2). One personal care product (PCP) bead standard had a large Si peak relative to the other

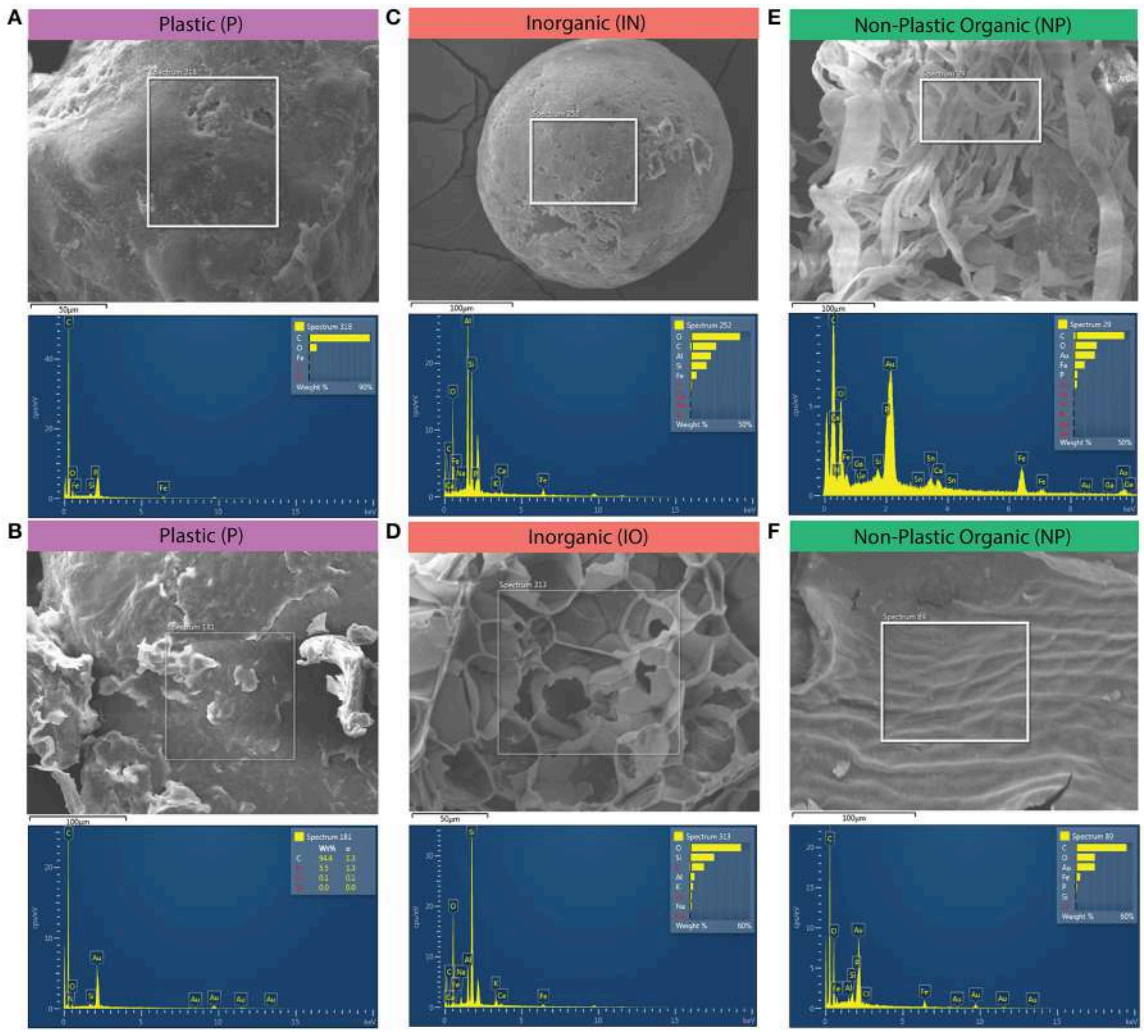

FIGURE 7 | Examples of SEM-EDS spectra and microscopic images representative of the three compositional classes: plastic (P), inorganic (IO), and non-plastic organic (O). **(A)** plastic fragment. **(B)** Flaking, jagged, "crumbly" bead from a personal care product that served as a positive control. **(C)** Coal fly ash from a Lake Erie sample. **(D)** Piece of silica foam from Lake Erie sample. **(E)** Stringy, fibrous organic matter particle from Lake Erie sample. **(F)** Non-plastic organic matter control depicting diagnostic shallow surface veining; likely a leaf or other vegetation.

elements. We attributed this composition to the particle being mica or previously having been in close association with mica. Indeed, sparkling "beads" from PCPs that crumbled upon touch were found often, which we presumed were mica particles, after finding it listed as an inactive ingredient in PCP. Further, all organic matter standards contained Fe (in the presence of O), as did the nylon mesh net that had been used to filter organic material, whereas no Fe was found in pristine virgin polymers. This pattern held until environmental samples were analyzed. As opposed to pristine standards, Fe was detected in nearly all particle types (plastic, non-plastic organic, and mineral) that had been exposed to the environment.

Physical features of the particle surface further informed our classification decisions between plastic and non-plastic organic. Plastic tended to have deep and clean fractures, and smooth surfaces with shallow flakes (e.g., **Figures 7A,B**); though this could be obscured as particles oxidized with age and appeared brittle. Particles with relatively simple elemental spectra consisting of a large primary C peak, frequently with a smaller O peak, were classified as plastic (P; **Figures 7A,B**). Inorganic (IO) particles were best characterized by the presence of a large primary peak of the element Si (**Figures 7C,D**; Supplementary Data Sheet 2). One IO particle (of 47 total) that lacked Si instead contained Ti (Supplementary Data Sheet 2). Many of the IO particles were round spheres suspected to be coal fly ash (**Figure 7C**), a positively buoyant byproduct of coal combustion that has been reported previously in Great Lakes surface waters (Eriksen et al., 2013). Some IO particles physically resembled styrofoam balls but were confirmed to be puffed silica foam, having contained prominent mineral elements (e.g., **Figure 7D**). Non-plastic organic matter (NP) was physically characterized by stringy fibers of irregular width or shallow-relief surface patterns typical of leaf veining (**Figures 7C,F**, respectively) and chemically characterized by more complex elemental signatures with several smaller peaks rather than a single dominant C peak.

To assess our tendency to accurately classify plastic from non-plastic, we compared our initial visual classifications with those based on EDS-SEM analysis (**Figure 8**; Supplementary Data Sheet 2; Supplementary Image 1; Supplementary Table 1). Of all pieces visually identified as plastic, 76% were confirmed as P, 2% were NP, 12% could not be identified as P or NP, and 10% were IO. Of all pieces visually identified as non-plastic, 46% were confirmed as NP, 35% were IO, 11% couldn't be identified as P or NP, and 7% were plastic (**Figure 8**). A chi-squared test of independence confirms that the EDS-SEM-based plastic (P) calls occur most often in the visually-determined plastic category, followed by the P-NP class, and the EDS-SEM-based non-plastic (NP) calls occur most often in the visually-determined non-plastic category, followed by the inorganic (IO), and NP-IO ($\chi^2 = 112.63$, $p = 2.003\text{e-}23$, **Table 2**). These findings provided confidence in the visual discrimination between plastic and non-plastic particles in the smallest size class, and that rates of false-positives in both categories are similar enough that there was no need for adjustments to plastic abundances.

Lake Erie Plastic Transport Model

To develop a more holistic view of plastic transport dynamics than is possible based on discrete field collections and assess

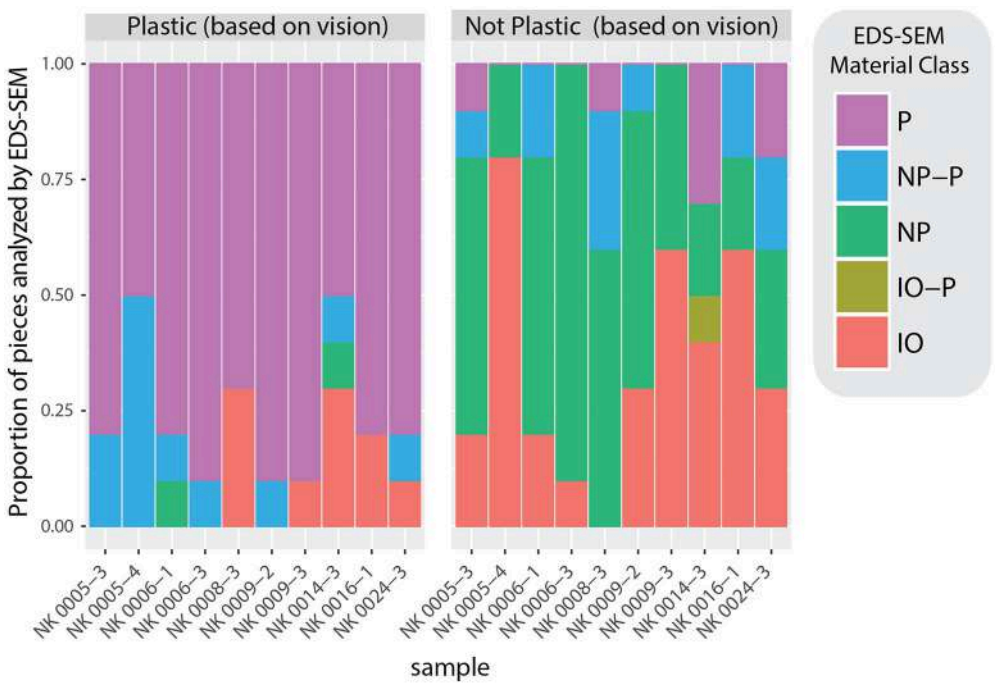

FIGURE 8 | Barplots representing the agreement between visually categorized fragments (plastic vs. non-plastic) and SEM-EDS analytically categorized fragments. SEM-EDS-based classifications fall along a spectrum of three discrete categories: plastic (P), inorganic (IO), and non-plastic organic (NP). This is a visual representation of the contingency table used in the chi-square test of independence (Supplementary Table 1).

the possibility of predicting plastic distributions, we modeled the transport of plastic and tested the effect of plastic buoyancy on the resident times in Lake Erie. Lake Erie is the smallest and shallowest of the Great Lakes, but is disproportionately surrounded by highly populated areas and used heavily for shipping and fishery industries.

No Lake Erie "Garbage Patch," but Prominent Longshore Transport Highlights at-Risk Coastal Areas

For decades, studies have described the presence of an oceanic "garbage patch" (coined in Moore et al., 2001), an amalgam of human-generated trash caught-up in the North Pacific Central Gyre that results from the convergence of floating debris in the anticyclonic eddy of the gyre's high pressure cell (Day and Shaw, 1987; Law et al., 2014). Similar anticyclonic currents form in Lake Erie in summer months (Beletsky et al., 2012) and the high concentrations of plastic in Lake Erie's eastern basin have been attributed to this feature (Eriksen et al., 2013; Driedger et al., 2015). Yet, our plastic transport model did not predict a permanent plastic "garbage patch" in Lake Erie (**Figures 9**, **10A**). This lack of a "garbage patch" may be explained by less intense convergence of surface lake currents or by the less persistent lake currents that last on the order of only weeks to months. Comparatively, stable anticyclonic circulation persists in the oceans for much longer time periods.

Results of monthly drift in summer (June, July, and August, each run over 6 years) illustrated the variability of spread due to changing current patterns (**Figure 9**). In early summer, the model generally predicted the eastward drift of neutrally buoyant particles. This was especially pronounced along both the northern and southern coasts in June, the month the majority of our field survey took place. Later in the season, the large-scale anticyclonic circulation that typically develops in mid and late summer (Beletsky et al., 2012) influenced the movement of plastics. Due to that circulation feature,

TABLE 2 | Residuals of chi-squared test of independence performed on the contingency table (Supplementary Table 3) that related the number of samples visually deemed as plastic and not plastic vs. their SEM-EDS-based classification into plastic (P), non-plastic organic (NP), and inorganic (IO) particles.

Visual-based class	SEM-EDS-based class				
	P	P-NP	NP	IO-P	IO
Plastic	5.3554386	0.147442	−4.4907312	−0.7071068	−2.6352314
Not plastic	−5.3554386	−0.147442	4.4907312	0.7071068	2.6352314

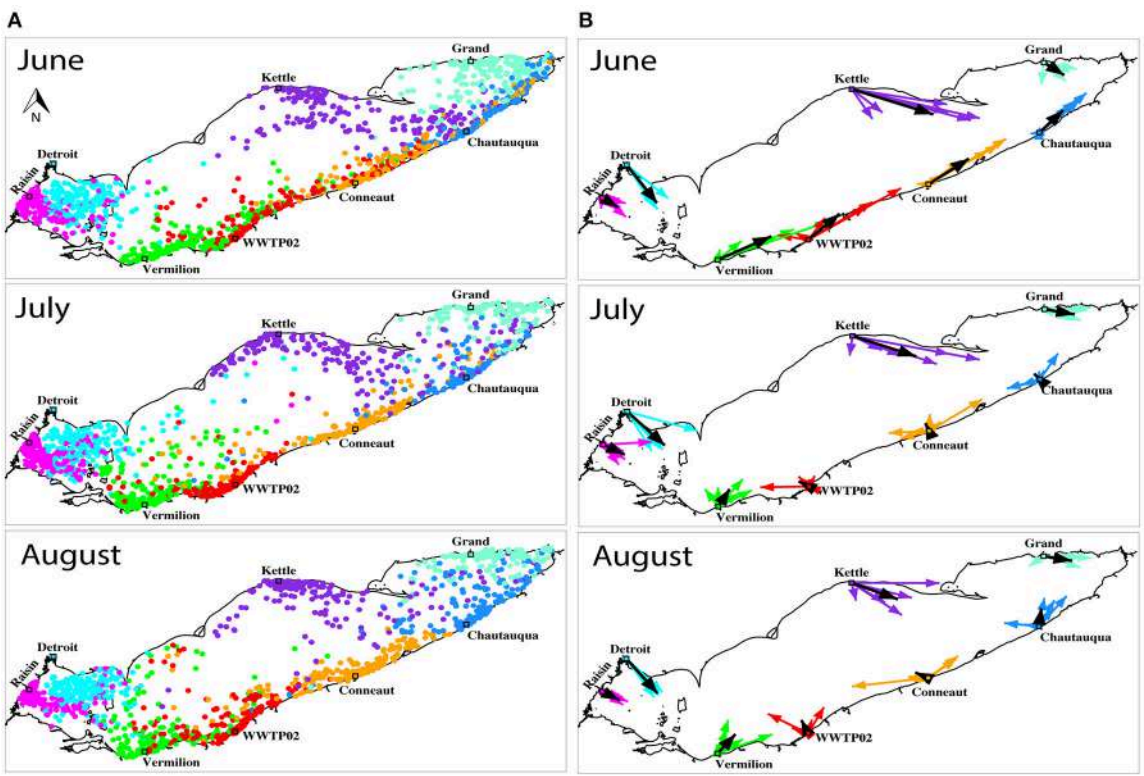

FIGURE 9 | (A) The distribution of neutrally buoyant particles at the end of month-long transport in June, July, and August for 6 years. For visual simplicity, 8 of the 29 sources (influents) are depicted: the Raisin Rv. (magenta), Detroit Rv. (cyan), Kettle Rv. (purple), Grand Rv. (turquoise), Chautauqua Rv. (blue), Conneaut Rv. (orange), Cleveland WWTP (red), and Vermillion Rv. (green). **(B)** Mean transport vectors summarizing the positions of all particles at the end of month at each of the same eight representative sources (similarly colored coded). The six vectors per source represent mean transport for each of the 6 years. The 6-year mean vector is shown in black at each input.

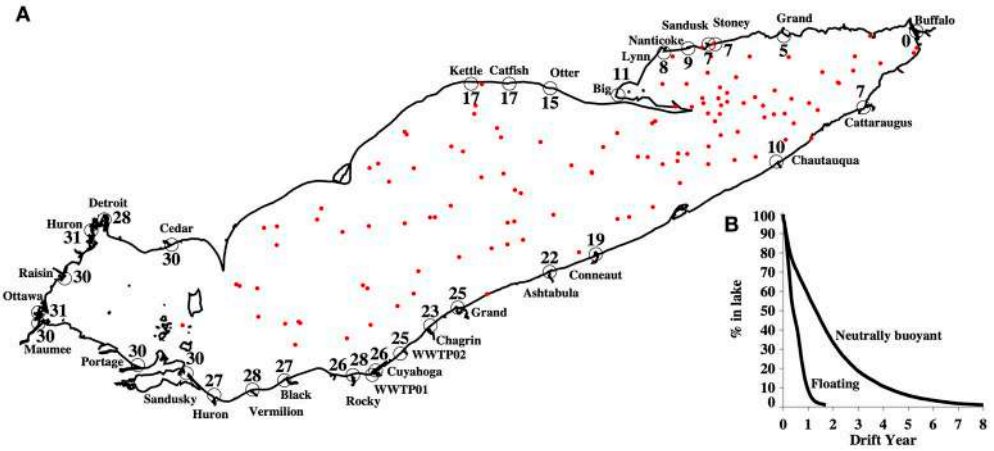

FIGURE 10 | (A) Mean residence time (months) for each source of neutrally buoyant particles. Particles were released daily for 1 year and tracked for 8 years (time for 99% of particles to leave the lake). Red dots represent the particles that remain in the lake after 8 years of drift. **(B)** Percent of particles remaining as a function of time for the neutrally buoyant (right curve) and floating (left curve) models; based on same run conditions as **(A)**.

particles released along the southern coast east of Cleveland were often transported westward (**Figure 9**). During that time, temporary patches (lasting for a few days) formed in the floating particles model. In this case, particle aggregation due to current convergence *is* expected. For example, in mid-August 2010, floating particles aggregated in a large anticyclonic gyre developed in the central basin and two smaller anticyclonic gyres in the eastern basin (Supplementary Figure 4). Overall, particles in both neutrally buoyant and floating cases exhibited general eastward drift and flushed quickly from the western basin by the Detroit River flow (**Figure 10A**). Recirculation in the central and eastern basins was especially pronounced in the summer. Neutrally buoyant particles drifted more slowly than floating particles because of reduction of current speed with depth.

Our model did not predict elevated concentrations of plastic in Lake Erie's eastern basin relative to the central basin, as seen in both our field survey (**Figure 3D**) and that of a prior study in this lake (Eriksen et al., 2013). Notably, this pattern was absent in a recent Great Lakes particle model, as well (Hoffman and Hittinger, 2017). This is despite the fact that the forcing used in the particle model presented here has superior temporal resolution (e.g., hourly vs. three-hourly) and more accurately predicts observed Lake Erie circulation patterns (Beletsky et al., 2013). For example, the winds used in the Hoffman and Hittinger particle model (NOAAs Great Lakes Coastal Forecast System model output) typically produce cyclonic circulation patterns in summer, rather than the anticyclonic patterns observed in summer (Beletsky et al., 2013). We hypothesize that model discrepancy can be either due to a temporary patch in both observational surveys or due to an elevated input near or in the eastern basin that was not accounted for in our model (e.g., Baldwin et al., 2016 documented a peak in microplastic concentration at Ashtabula, OH).

According to the neutrally buoyant particle model predictions, habitats along the southern coast of Lake Erie were predicted to be most affected by plastic pollution (**Figure 9**). The higher concentration of rivers along the southern coast led to more particles released in that area in model runs. The eastward drift of particles from upstream sources (e.g., the Detroit River and other rivers in the western basin) led to higher concentration of particles (**Figure 9**; particle release points identified by open circles and are listed in Supplementary Table 2). This interpretation is consistent with the recognition that rivers are major sources of plastics to inland water bodies (Wagner et al., 2014), including the Great Lakes (Baldwin et al., 2016). In most months, rather than moving offshore, the model predicted longshore transport from coastal sources. This model indicates that future plastic pollution mitigation and management efforts in Lake Erie should focus on its southern shore and downstream of urbanized areas. Extending this plastic transport model to the other four Great Lakes will similarly inform future efforts across this critical watershed.

Plastic Density Drastically Impacts Residence Time in the Lake

The buoyancy of modeled particles had a strong effect on residence time in the lake; floating particles flush from the lake in 1.7 years—nearly 5 times faster than neutrally buoyant particles (8.1 years; **Figure 10B**). In fact, the modeled flushing time for neutrally buoyant particles in Lake Erie substantially exceeds hydraulic residence time estimates (2.7 years; Bolsenga and Herdendorf, 1993). However, the residence time is not uniform across the lake. Average residence times of neutrally buoyant particles released at different sources show a west-east gradient (**Figure 10A**), with the shortest residence times for the particles released at the Buffalo River (less than a month) and longest for those released at the Ottawa and Huron Rivers in the western basin (over 30 months, **Figure 10A**).

Most surveys of environmental plastic pollution tend to collect samples at the water surface, capturing floating plastic only. According to this model, most of the floating plastics

sampled in the western and central basin would have been in Lake Erie for <2 years. However, while most virgin plastic used in consumer products—especially one-time use plastic (PlasticsEurope: Association of Plastics Manufacturers, 2015)—is predicted to be positively buoyant, plastic litter is readily found in sediment (Corcoran et al., 2015; Van Cauwenberghe et al., 2015; Ballent et al., 2016). This can be attributed to denser polymer types sinking, but there are other dynamic changes in the buoyant density that plastics are likely to undergo once in the environment, e.g., oxidation or biofouling. These changes are poorly described, but our results indicate the need to resolve these phenomena to effectively model the loads and fluxes of environmental plastic pollution in freshwater and marine systems alike.

CONCLUSION

This study has improved our understanding of the distribution, transport, and fate of plastics in four lakes of the Great Lakes system. As the largest freshwater system on the planet, these critical lakes hold 20% of the world's fresh water. Plastic pollution was documented down to the smallest size class yet reported, shedding light on the magnitude of plastics in a small size class (106–333 μm) that is missing from most existing reports (Hidalgo Ruz et al., 2012; Law, 2016). This led to load estimates of nearly 2 million particles km^{-2}, the highest reported levels in the Great Lakes and possibly any surface water ecosystem. These high numbers can be attributed to the high nearshore population density, a feature unique to inland waterways that does not similarly influence remote ocean basins, and the long hydraulic residence time of some of the Great Lakes (3–100s of years, depending on the lake). Given this time and the recalcitrance of plastic to degradation, fragments of some of the first plastic ever produced for the consumer market are certainly present in the Great Lakes still today. This scenario is likely representative of lakes worldwide, which account for 87% of the planet's freshwater and have an average residence time of 50–100 years[4]—indeed spanning the introduction of plastics to the consumer market.

Data describing the abundance of plastic pollution in the Great Lakes are sparse and will continue to be. Field-based quantification surveys are time-consuming, expensive, and low-throughput. As a result, there is insufficient spatial and temporal resolution of plastic debris in the Great Lakes and other aquatic ecosystems. In addition, detailed data on plastic loads (e.g., from rivers and WWTPs) are needed to determine the plastic budget and to inform future models. Integrating the modeling approach developed here will guide targeted research surveys, experiments, and technological innovation for improved understanding of the ecosystem and public health risks plastic pollution pose to freshwater systems. These are the steps needed to develop a global plastic mass balance transport model to effectively inform the policy, mitigation, and prevention initiatives needed to protect our vital freshwater resources.

Research was conducted in the absence of any commercial or financial relationships that could be construed as a potential conflict of interest.

[4]https://scied.ucar.edu/longcontent/water-cycle

AUTHOR CONTRIBUTIONS

MD, DB, and KW: conceived the study. MD, RC, and BL: performed field sampling, sample processing, and plastic count data collection and analyzed data. DB and RB: developed and ran the transport model and analyzed data. MD, RC, DB, and KW: wrote the manuscript.

FUNDING

This work was supported by the University of Michigan Water Center, a center of the Graham Sustainability Institute. The Water Center is supported by funds from the Fred A. and Barbara M. Erb Family Foundation and the University of Michigan. Additional funding for DB and RB was provided by NOAA GLERL. Funding was awarded to Cooperative Institute for Limnology and Ecosystems Research (CILER) through the NOAA Cooperative Agreement with the University of Michigan (NA12OAR4320071). Additional funding was provided by the NSF grant 1039043.

ACKNOWLEDGMENTS

We wish to acknowledge David Brooks for providing and operating the research vessel, Nancy *K*, for funding its operation, and for providing additional engineering and logistical support during the 2014 campaign. We thank Steve Ruberg (NOAA GLERL) and the captain and crew of R5501 for sampling in the Detroit River and the Cleveland area. Gregory Boehm, Sarah Halpern, Kat Wiles, Kaitie Benedeck, Scott Koenigbauer, Naomi Huntley, Shibhum Sidhar, Payton Watt, Andrew Wong, Emma Borjigin-Wang, Marlies Michielssen, and Elien Michielssen assisted in the massive effort of sample collection in the field and processing in the lab. Larissa Sano, Allen Burton, Jeanne Hankett, Zhan Chen, and Lorena Rios Mendoza supported project thematic development. We thank Will Bender for technical assistance with SEM-EDS. This is CIGLR 1113 and NOAA GLERL contribution 1858.

SUPPLEMENTARY MATERIAL

The Supplementary Material for this article can be found online at: http://journal.frontiersin.org/article/10.3389/fenvs.2017.00045/full#supplementary-material

REFERENCES

Baldwin, A. K., Corsi, S. R., and Mason, S. A. (2016). Plastic debris in 29 great lakes tributaries: relations to watershed attributes and hydrology. *Environ. Sci. Technol.* 50, 10377–10385. doi: 10.1021/acs.est.6b02917

Ballent, A., Corcoran, P. L., Madden, O., Helm, P. A., and Longstaffe, F. J. (2016). Sources and sinks of microplastics in Canadian Lake Ontario nearshore, tributary and beach sediments. *Mar. Pollut. Bull.* 110, 383–395. doi: 10.1016/j.marpolbul.2016.06.037

Barnes, D. K., Galgani, F., Thompson, R. C., and Barlaz, M. (2009). Accumulation and fragmentation of plastic debris in global environments. *Philos. Trans. R. Soc. Lond. B. Biol. Sci.* 364, 1985–1998. doi: 10.1098/rstb.2008.0205

Beletsky, D., Beletsky, R., Rutherford, E. S., Sieracki, J. L., Bossenbroek, J. M., Chadderton, W. L., et al. (2017). Predicting spread of aquatic invasive species by lake currents. *J. Great Lakes Res.* 43, 14–32. doi: 10.1016/j.jglr.2017.02.001

Beletsky, D., Hawley, N., and Rao, Y. R. (2013). Modeling summer circulation and thermal structure of Lake Erie. *J. Geophys. Res. Oceans* 118, 6238–6252. doi: 10.1002/2013JC008854

Beletsky, D., Hawley, N., Rao, Y. R., Vanderploeg, H. A., Beletsky, R., Schwab, D. J., et al. (2012). Summer thermal structure and anticyclonic circulation of Lake Erie. *Geophys. Res. Lett.* 39:L06605. doi: 10.1029/2012GL051002

Bennett, J. R., and Clites, A. H. (1987). Accuracy of trajectory calculation in a finite-difference circulation model. *J. Comput. Phys.* 68, 272–282. doi: 10.1016/0021-9991(87)90058-1

Besseling, E., Wegner, A., Foekema, E. M., Van Den Heuvel-Greve, M. J., and Koelmans, A. A. (2012). Effects of microplastic on fitness and PCB bioaccumulation by the lugworm *Arenicola marina* (L.). *Environ. Sci. Technol.* 47, 593–600. doi: 10.1021/es302763x

Blumberg, A. F., and Mellor, G. L. (1987). "A description of a three-dimensional coastal ocean circulation model," in *Three-Dimensional Coastal Ocean Models*, ed N. S. Heaps (Washington, DC: American Geophysical Union; Wiley Online Library), 1–16. doi: 10.1029/CO004p0001

Boerger, C. M., Lattin, G. L., Moore, S. L., and Moore, C. J. (2010). Plastic ingestion by planktivorous fishes in the North Pacific central gyre. *Mar. Pollut. Bull.* 60, 2275–2278. doi: 10.1016/j.marpolbul.2010.08.007

Bolsenga, S. J., and Herdendorf, C. E. (1993). *Lake Erie and Lake St. Clair Handbook*. Detroit, MI: Wayne State University Press.

Browne, M. A., Crump, P., Niven, S. J., Teuten, E., Tonkin, A., Galloway, T., et al. (2011). Accumulation of microplastic on shorelines woldwide: sources and sinks. *Environ. Sci. Technol.* 45, 9175–9179. doi: 10.1021/es201811s

Carpenter, E. J., and Smith, K. L. (1972). Plastics on the Sargasso sea surface. *Science* 175, 1240–1241. doi: 10.1126/science.175.4027.1240

Castañeda, R. A., Avlijas, S., Simard, M. A., and Ricciardi, A. (2014). Microplastic pollution in st. Lawrence river sediments. *Can. J. Fish. Aquat. Sci.* 71, 1767–1771. doi: 10.1139/cjfas-2014-0281

Claessens, M., De Meester, S., Van Landuyt, L., De Clerck, K., and Janssen, C. R. (2011). Occurrence and distribution of microplastics in marine sediments along the Belgian coast. *Mar. Pollut. Bull.* 62, 2199–2204. doi: 10.1016/j.marpolbul.2011.06.030

Colton, J. B., Knapp, F. D., and Burns, B. R. (1974). Plastic particles in surface waters of the northwestern Atlantic. *Science* 185, 491–497. doi: 10.1126/science.185.4150.491

Corcoran, P. L., Norris, T., Ceccanese, T., Walzak, M. J., Helm, P. A., and Marvin, C. H. (2015). Hidden plastics of Lake Ontario, Canada and their potential preservation in the sediment record. *Environ. Pollut.* 204, 17–25. doi: 10.1016/j.envpol.2015.04.009

Cózar, A., Echevarría, F., González-Gordillo, J. I., Irigoien, X., Ubeda, B., Hernández-León, S., et al. (2014). Plastic debris in the open ocean. *Proc. Natl. Acad. Sci. U.S.A.* 111, 10239–10244. doi: 10.1073/pnas.1314705111

Day, R. H., and Shaw, D. G. (1987). Patterns in the abundance of pelagic plastic and tar in the North Pacific ocean, 1976–1985. *Mar. Pollut. Bull.* 18, 311–316. doi: 10.1016/S0025-326X(87)80017-6

Dekiff, J. H., Remy, D., Klasmeier, J., and Fries, E. (2014). Occurrence and spatial distribution of microplastics in sediments from Norderney. *Environ. Pollut.* 186, 248–256. doi: 10.1016/j.envpol.2013.11.019

Driedger, A. G., Dürr, H. H., Mitchell, K., and Van Cappellen, P. (2015). Plastic debris in the Laurentian great lakes: a review. *J. Great Lakes Res.* 41, 9–19. doi: 10.1016/j.jglr.2014.12.020

Dris, R., Imhof, H., Sanchez, W., Gasperi, J., Galgani, F., Tassin, B., et al. (2015). Beyond the ocean: contamination of freshwater ecosystems with (micro-) plastic particles. *Environ. Chem.* 12, 539–550. doi: 10.1071/EN14172

Eerkes-Medrano, D., Thompson, R. C., and Aldridge, D. C. (2015). Microplastics in freshwater systems: a review of the emerging threats, identification of knowledge gaps and prioritisation of research needs. *Water Res.* 75, 63–82. doi: 10.1016/j.watres.2015.02.012

Eriksen, M., Lebreton, L. C., Carson, H. S., Thiel, M., Moore, C. J., Borerro, J. C., et al. (2014). Plastic pollution in the world's oceans: more than 5 trillion plastic pieces weighing over 250,000 tons afloat at sea. *PLoS ONE* 9:e111913. doi: 10.1371/journal.pone.0111913

Eriksen, M., Mason, S., Wilson, S., Box, C., Zellers, A., Edwards, W., et al. (2013). Microplastic pollution in the surface waters of the laurentian great lakes. *Mar. Pollut. Bull.* 77, 177–182. doi: 10.1016/j.marpolbul.2013.10.007

Filella, M. (2015). Questions of size and numbers in environmental research on microplastics: methodological and conceptual aspects. *Environ. Chem.* 12, 527–538. doi: 10.1071/EN15012

Fischer, V., Elsner, N. O., Brenke, N., Schwabe, E., and Brandt, A. (2015). Plastic pollution of the Kuril–Kamchatka trench area (NW pacific). *Deep Sea Res. II Top. Stud. Oceanogr.* 111, 399–405. doi: 10.1016/j.dsr2.2014.08.012

Foekema, E. M., De Gruijter, C., Mergia, M. T., van Franeker, J. A., Murk, A. J., and Koelmans, A. A. (2013). Plastic in North Sea fish. *Environ. Sci. Technol.* 47, 8818–8824. doi: 10.1021/es400931b

Fraker, M. E., Anderson, E. J., May, C. J., Chen, K.-Y., Davis, J. J., DeVanna, K. M., et al. (2015). Stock-specific advection of larval walleye (*Sander vitreus*) in western Lake Erie: implications for larval growth, mixing, and stock discrimination. *J. Great Lakes Res.* 41, 830–845. doi: 10.1016/j.jglr.2015.04.008

Free, C. M., Jensen, O. P., Mason, S. A., Eriksen, M., Williamson, N. J., and Boldgiv, B. (2014). High-levels of microplastic pollution in a large, remote, mountain lake. *Mar. Pollut. Bull.* 85, 156–163. doi: 10.1016/j.marpolbul.2014.06.001

Frère, L., Paul-Pont, I., Rinnert, E., Petton, S., Jaffré, J., Bihannic, I., et al. (2017). Influence of environmental and anthropogenic factors on the composition, concentration and spatial distribution of microplastics: a case study of the Bay of Brest (Brittany, France). *Environ. Pollut.* 225, 211–222. doi: 10.1016/j.envpol.2017.03.023

GESAMP: IMO/FAO/UNESCO-IOC/UNIDO/WMO/IAEA/UN/UNEP Joint Group of Experts on the Scientific Aspects of Marine Environmental Protection (2010). "GESAMP reports and studies," in *Proceedings of the GESAMP International Workshop on Microplastic Particles as a Vector in Transporting Persistent, bio-Accumulating and Toxic Sub-Stances in the Ocean*, Vol. 82 (Paris), 1–68.

Goldstein, M. C., Titmus, A. J., and Ford, M. (2013). Scales of spatial heterogeneity of plastic marine debris in the northeast Pacific Ocean. *PLoS ONE* 8:e80020. doi: 10.1371/journal.pone.0080020

Hankett, J. M., Collin, W. R., Yang, P., Chen, Z., and Duhaime, M. B. (2016). Low-volatility model demonstrates humidity affects environmental toxin deposition on plastics at a molecular level. *Environ. Sci. Technol.* 50, 1304–1305. doi: 10.1021/acs.est.5b05598

Hidalgo Ruz, V., Gutow, L., Thompson, R. C., and Thiel, M. (2012). Microplastics in the marine environment: a review of the methods used for identification and quantification. *Environ. Sci. Technol.* 46, 3060–3075. doi: 10.1021/es2031505

Hoellein, T., Rojas, M., Pink, A., Gasior, J., and Kelly, J. (2014). Anthropogenic litter in urban freshwater ecosystems: distribution and microbial interactions. *PLoS ONE* 9:e98485. doi: 10.1371/journal.pone.0098485

Hoffman, M., and Hittinger, E. (2017). Inventory and transport of plastic debris in the Laurentian Great Lakes. *Mar. Pollut. Bull.* 115, 273–281. doi: 10.1016/j.marpolbul.2016.11.061

Imhof, H. K., Laforsch, C., Wiesheu, A. C., Schmid, J., Anger, P. M., Niessner, R., et al. (2016). Pigments and plastic in limnetic ecosystems: a qualitative and quantitative study on microparticles of different size classes. *Water Res.* 98, 64–74. doi: 10.1016/j.watres.2016.03.015

IPCC (2012). *Managing the Risks of Extreme Events and Disasters to Advance Climate Change Adaptation.* A Special Report of Working Groups I and II of the Intergovernmental Panel on Climate Change, Edited by C. B. Field, V. Barros, T. F. Stocker, D. Qin, D. J. Dokken, K. L. Ebi, M. D. Mastrandrea, K. J. Mach,

G.-K. Plattner, S. K. Allen, M. Tignor, and P. M. Midgley. Cambridge University Press.

Jambeck, J. R., Geyer, R., Wilcox, C., Siegler, T. R., Perryman, M., Andrady, A., et al. (2015). Marine pollution. Plastic waste inputs from land into the ocean. *Science* 347, 768–771. doi: 10.1126/science.1260352

Kang, J. H., Kwon, O. Y., Lee, K. W., Song, Y. K., and Shim, W. J. (2015). Marine neustonic microplastics around the southeastern coast of Korea. *Mar. Pollut. Bull.* 96, 304–312. doi: 10.1016/j.marpolbul.2015.04.054

Khatmullina, L., and Isachenko, I. (2016). Settling velocity of microplastic particles of regular shapes. *Mar. Poll. Bull.* 114, 871–880. doi: 10.1016/j.marpolbul.2016.11.024

Koelmans, A. A., Bakir, A., Burton, G. A., and Janssen, C. R. (2016). Microplastic as a vector for chemicals in the aquatic environment: critical review and model-supported reinterpretation of empirical studies. *Environ. Sci. Technol.* 50, 3315–3326. doi: 10.1021/acs.est.5b06069

Kowalski, N., Reichardt, A. M., and Waniek, J. J. (2016). Sinking rates of microplastics and potential implications of their alteration by physical, biological, and chemical factors. *Mar. Pollut. Bull.* 109, 310–319. doi: 10.1016/j.marpolbul.2016.05.064

Law, K. L. (2016). Plastics in the marine environment. *Ann. Rev. Mar. Sci.* 9, 205–229. doi: 10.1146/annurev-marine-010816-060409

Law, K. L., More t-Ferguson, S. E., Goodwin, D. S., Zettler, E. R., DeForce, E., Kukulka, T., et al. (2014). Distribution of surface plastic debris in the Eastern pacific ocean from an 11-year data set. *Environ. Sci. Technol.* 48, 4732–4738. doi: 10.1021/es4053076

Law, K. L., Morét-Ferguson, S., Maximenko, N. A., Proskurowski, G., Peacock, E. E., Hafner, J., et al. (2010). Plastic accumulation in the North Atlantic subtropical gyre. *Science* 329, 1185–1188. doi: 10.1126/science.1192321

Lechner, A., Keckeis, H., Lumesberger-Loisl, F., Zens, B., Krusch, R., Tritthart, M., et al. (2014). The Danube so colourful: a potpourri of plastic litter outnumbers fish larvae in Europe's second largest river. *Environ. Pollut.* 188, 177–181. doi: 10.1016/j.envpol.2014.02.006

Li, J., Qu, X., Su, L., Zhang, W., Yang, D., Kolandhasamy, P., et al. (2016). Microplastics in mussels along the coastal waters of China. *Environ. Pollut.* 214, 177–184. doi: 10.1016/j.envpol.2016.04.012

Lima, A. R., Costa, M. F., and Barletta, M. (2014). Distribution patterns of microplastics within the plankton of a tropical estuary. *Environ. Res.* 132, 146–155. doi: 10.1016/j.envres.2014.03.031

Löder, M. G., and Gerdts, G. (2015). "Methodology used for the detection and identification of microplastics-A critical appraisal," in *Marine Anthropogenic Litter*, eds M. Bergmann, L. Gutow, and M. Klages (Cham; Heidelberg; New York, NY; Dordrecht; London: Springer), 201–227. doi: 10.1007/978-3-319-16510-3_8

Lorenz, C. (2014). *Detection of Microplastics in Marine Sediments of the German Coast via FT-IR Spectroscopy*. Master's thesis, University of Rostock, Rostock.

Lynch, D. R., Greenberg, D. A., Bilgili, A., McGillicuddy, D. J. Jr., Manning, J. P., and Aretxabaleta, A. L. (2014). *Particles in the Coastal Ocean: Theory and Applications*. New York, NY: Cambridge University Press.

Mani, T., Hauk, A., Walter, U., and Burkhardt-Holm, P. (2015). Microplastics profile along the Rhine River. *Sci. Rep.* 5:17988. doi: 10.1038/srep17988

Mason, S. A., Kammin, L., Eriksen, M., Aleid, G., Wilson, S., Box, C., et al. (2016). Pelagic plastic pollution within the surface waters of Lake Michigan, USA. *J. Great Lakes Res.* 42, 753–759. doi: 10.1016/j.jglr.2016.05.009

Masura, J., Baker, J. E., Foster, G., Arthur, C., and Herring, C. (2015). *Laboratory Methods for the Analysis of Microplastics in the Marine Environment: Recommendations for Quantifying Synthetic Particles in Waters and Sediments*. NOAA Technical Memorandum NOS-OR and R-48, 1–31.

McCormick, A., Hoellein, T. J., Mason, S. A., Schluep, J., and Kelly, J. J. (2014). Microplastic is an abundant and distinct microbial habitat in an urban river. *Environ. Sci. Technol.* 48, 11863–11871. doi: 10.1021/es503610r

Michalak, A. M., Anderson, E. J., Beletsky, D., Boland, S., Bosch, N. S., Bridgeman, T. B., et al. (2013). Record-setting algal bloom in Lake Erie caused by agricultural and meteorological trends consistent with expected future conditions. *Proc. Natl. Acad. Sci. U.S.A.* 110, 6448–6452. doi: 10.1073/pnas.1216006110

Michielssen, M., Michielssen, E., Ni, J., and Duhaime, M. (2016). Fate of microplastics and other small anthropogenic litter (SAL) in wastewater treatment plants depends on unit processes employed. *Environ. Sci Water Res. Technol.* 2, 1064–1073. doi: 10.1039/C6EW00207B

Moore, C. J., Moore, S. L., Leecaster, M. K., and Weisberg, S. B. (2001). A comparison of plastic and plankton in the North Pacific central gyre. *Mar. Pollut. Bull.* 42, 1297–1300. doi: 10.1016/S0025-326X(01)00114-X

Naidoo, T., Glassom, D., and Smit, A. J. (2015). Plastic pollution in five urban estuaries of KwaZulu-Natal, South Africa. *Mar. Pollut. Bull.* 101, 473–480. doi: 10.1016/j.marpolbul.2015.09.044

Neves, D., Sobral, P., Ferreira, J. L., and Pereira, T. (2015). Ingestion of microplastics by commercial fish off the Portuguese coast. *Mar. Pollut. Bull.* 101, 119–126. doi: 10.1016/j.marpolbul.2015.11.008

Nizzetto, L., Bussi, G., Futter, M. N., Butterfield, D., and Whitehead, P. G. (2016). A theoretical assessment of microplastic transport in river catchments and their retention by soils and river sediments. *Environ. Sci. Process Impacts* 18, 1050–1059. doi: 10.1039/C6EM00206D

O'Connor, I. A., Golsteijn, L., and Hendriks, A. J. (2016). Review of the partitioning of chemicals into different plastics: consequences for the risk assessment of marine plastic debris. *Mar. Pollut. Bull.* 113, 17–24. doi: 10.1016/j.marpolbul.2016.07.021

Pauly, J. L., Stegmeier, S. J., Allaart, H. A., Cheney, R. T., Zhang, P. J., Mayer, A. G., et al. (1998). Inhaled cellulosic and plastic fibers found in human lung tissue. *Cancer Epidemiol. Biomarkers Prev.* 7, 419–428.

PlasticsEurope: Association of Plastics Manufacturers (2015). *Plastics-the Facts 2014/2015*.

QGIS Development Team (2016). *QGIS Geographic Information system*. Open source geospatial foundation project. Available online at: http://www.qgis.org/

Rochman, C. M., Browne, M. A., Underwood, A. J., van Franeker, J. A., Thompson, R. C., and Amaral-Zettler, L. A. (2016). The ecological impacts of marine debris: Unraveling the demonstrated evidence from what is perceived. *Ecology* 97, 302–312. doi: 10.1890/14-2070.1

Rochman, C. M., Hoh, E., Kurobe, T., and Teh, S. J. (2013). Ingested plastic transfers hazardous chemicals to fish and induces hepatic stress. *Sci. Rep.* 3:3263. doi: 10.1038/srep03263

Rochman, C. M., Kross, S. M., Armstrong, J. B., Bogan, M. T., Darling, E. S., Green, S. J., et al. (2015a). Scientific evidence supports a ban on microbeads. *Environ. Sci. Technol.* 49, 10759–10761. doi: 10.1021/acs.est.5b03909

Rochman, C. M., Tahir, A., Williams, S. L., Baxa, D. V., Lam, R., Miller, J. T., et al. (2015b). Anthropogenic debris in seafood: plastic debris and fibers from textiles in fish and bivalves sold for human consumption. *Sci. Rep.* 5:14340. doi: 10.1038/srep14340

Ryan, P. G., Moore, C. J., van Franeker, J. A., and Moloney, C. L. (2009). Monitoring the abundance of plastic debris in the marine environment. *Philos. Trans. R. Soc. Lond. B Biol. Sci.* 364, 1999–2012. doi: 10.1098/rstb.2008.0207

Schwab, D. J., Beletsky, D., DePinto, J., and Dolan, D. M. (2009). A hydrodynamic approach to modeling phosphorus distribution in Lake Erie. *J. Great Lakes Res.* 35, 50–60. doi: 10.1016/j.jglr.2008.09.003

Smagorinsky, J. (1963). General circulation experiments with the primitive equations: I. The basic experiment. *Mon. Weather Rev.* 91, 99–164. doi: 10.1175/1520-0493(1963)091<0099:GCEWTP>2.3.CO;2

Song, Y. K., Hong, S. H., Jang, M., Han, G. M., Rani, M., Lee, J., et al. (2015). A comparison of microscopic and spectroscopic identification methods for analysis of microplastics in environmental samples. *Mar. Pollut. Bull.* 93, 202–209. doi: 10.1016/j.marpolbul.2015.01.015

Syberg, K., Khan, F. R., Selck, H., Palmqvist, A., Banta, G. T., Daley, J., et al. (2015). Microplastics: addressing ecological risk through lessons learned. *Environ. Toxicol. Chem.* 34, 945–953. doi: 10.1002/etc.2914

Team, R. C. (2014). *R: A Language and Environment for Statistical Computing*. Vienna: R Foundation for Statistical Computing. Available online at: http://www.R-project.org/

Teuten, E. L., Saquing, J. M., Knappe, D. R., Barlaz, M. A., Jonsson, S., Björn, A., et al. (2009). Transport and release of chemicals from plastics to the environment and to wildlife. *Philos. Trans. R. Soc. Lond. B Biol. Sci.* 364, 2027–2045. doi: 10.1098/rstb.2008.0284

Thompson, R. C., Olsen, Y., Mitchell, R. P., Davis, A., Rowland, S. J., John, A. W. G., et al. (2004). Lost at sea: where is all the plastic? *Science* 304, 838–838. doi: 10.1126/science.1094559

UNEP (2016). *Marine Plastic Debris and Microplastics – Global Lessons and Research to Inspire action and Guide Policy Change*. Nairobi: United Nations Environment Programme.

Van Cauwenberghe, L., Devriese, L., Galgani, F., Robbens, J., and Janssen, C. R. (2015). Microplastics in sediments: a review of techniques, occurrence and effects. *Mar. Environ. Res.* 111, 5–17. doi: 10.1016/j.marenvres.2015.06.007

Van Cauwenberghe, L., and Janssen, C. R. (2014). Microplastics in bivalves cultured for human consumption. *Environ. Pollut.* 193, 65–70. doi: 10.1016/j.envpol.2014.06.010

Vandermeersch, G., Van Cauwenberghe, L., Janssen, C. R., Marques, A., Granby, K., Fait, G., et al. (2015). A critical view on microplastic quantification in aquatic organisms. *Environ. Res.* 143, 46–55. doi: 10.1016/j.envres.2015.07.016

van Sebille, E., Wilcox, C., Lebreton, L., Maximenko, N., Hardesty, B. D., van Franeker, J. A., et al. (2015). A global inventory of small floating plastic debris. *Environ. Res. Lett.* 10:124006. doi: 10.1088/1748-9326/10/12/124006

Wagner, M., Scherer, C., Alvarez-Mu-oz, D., Brennholt, N., Bourrain, X., Buchinger, S., et al. (2014). Microplastics in freshwater ecosystems: what we know and what we need to know. *Environ. Sci. Eur.* 26, 1–9. doi: 10.1186/s12302-014-0012-7

Wang, W., Wairimu Ndungu, A., Li, Z., and Wang, J. (2017). Microplastics pollution in inland freshwaters of China: a case study in urban surface waters of Wuhan, China. *Sci. Tot. Environ.* 1369–1374. doi: 10.1016/j.scitotenv.2016.09.213

Wong, C. S., Green, D. R., and Cretney, W. J. (1974). Quantitative tar and plastic waste distributions in the Pacific Ocean. *Nature* 247, 30–32. doi: 10.1038/247030a0

Woodall, L. C., Gwinnett, C., Packer, M., Thompson, R. C., Robinson, L. F., and Paterson, G. L. (2015). Using a forensic science approach to minimize environmental contamination and to identify microfibres in marine sediments. *Mar. Pollut. Bull.* 95, 40–46. doi: 10.1016/j.marpolbul.2015.04.044

Woodall, L. C., Sanchez-Vidal, A., Canals, M., Paterson, G. L., Coppock, R., Sleight, V., et al. (2014). The deep sea is a major sink for microplastic debris. *R. Soc. Open Sci.* 1:140317. doi: 10.1098/rsos.140317

Wright, S. L., Thompson, R. C., and Galloway, T. S. (2013). The physical impacts of microplastics on marine organisms: a review. *Environ. Pollut.* 178, 483–492. doi: 10.1016/j.envpol.2013.02.031

Yonkos, L. T., Friedel, E. A., Perez-Reyes, A. C., Ghosal, S., and Arthur, C. D. (2014). Microplastics in four estuarine rivers in the Chesapeake Bay, U.S.A. *Environ. Sci. Technol.* 48, 14195–14202. doi: 10.1021/es5036317

Zbyszewski, M., and Corcoran, P. L. (2011). Distribution and degradation of fresh water plastic particles along the beaches of Lake Huron, Canada. *Water Air Soil Pollut.* 220, 365–372. doi: 10.1007/s11270-011-0760-6

Zbyszewski, M., Corcoran, P. L., and Hockin, A. (2014). Comparison of the distribution and degradation of plastic debris along shorelines of the Great Lakes, North America. *J. Great Lakes Res.* 40, 288–299. doi: 10.1016/j.jglr.2014.02.012

Zhang, K., Xiong, X., Hu, H., Wu, C., Bi, Y., Wu, Y., et al. (2017). Occurrence and characteristics of microplastic pollution in Xiangxi bay of three Gorges Reservoir, China. *Environ. Sci. Technol.* 51, 3794–3801. doi: 10.1021/acs.est.7b00369

Zhao, S., Zhu, L., Wang, T., and Li, D. (2014). Suspended microplastics in the surface water of the Yangtze estuary system, China: first observations on occurrence, distribution. *Mar. Pollut. Bull.* 86, 562–568. doi: 10.1016/j.marpolbul.2014.06.032

Conflict of Interest Statement: The authors declare that the research was conducted in the absence of any commercial or financial relationships that could be construed as a potential conflict of interest.

Advantages of publishing in Frontiers

OPEN ACCESS
Articles are free to read, for greatest visibility

COLLABORATIVE PEER-REVIEW
Designed to be rigorous – yet also collaborative, fair and constructive

FAST PUBLICATION
Average 85 days from submission to publication (across all journals)

COPYRIGHT TO AUTHORS
No limit to article distribution and re-use

TRANSPARENT
Editors and reviewers acknowledged by name on published articles

SUPPORT
By our Swiss-based editorial team

IMPACT METRICS
Advanced metrics track your article's impact

GLOBAL SPREAD
5'100'000+ monthly article views and downloads

LOOP RESEARCH NETWORK
Our network increases readership for your article

Frontiers
EPFL Innovation Park, Building I • 1015 Lausanne • Switzerland
Tel +41 21 510 17 00 • Fax +41 21 510 17 01 • info@frontiersin.org
www.frontiersin.org

Find us on